The CHAIN_2D Code for Simulating Two-Dimensional Movement of Water, Heat, and Multiple Solutes in Variably-Saturated Porous Media

Version 1.1

Research Report No. 136

October, 1994

U. S. SALINITY LABORATORY
AGRICULTURAL RESEARCH SERVICE
U. S. DEPARTMENT OF AGRICULTURE
RIVERSIDE, CALIFORNIA

The CHAIN_2D Code for Simulating Two-Dimensional Movement of Water, Heat, and Multiple Solutes in Variably-Saturated Porous Media

Version 1.1

by

J. Šimůnek and M. Th. van Genuchten

Research Report No. 136

October, 1994

U. S. SALINITY LABORATORY
AGRICULTURAL RESEARCH SERVICE
U. S. DEPARTMENT OF AGRICULTURE
RIVERSIDE, CALIFORNIA

DISCLAIMER

This report documents the CHAIN_2D computer program for simulating two-dimensional variably-saturated water flow, heat movement, and the transport of solutes involved in sequential first-order decay reactions. CHAIN_2D is a public domain code, and as such may be used and copied freely. The code has been verified against a large number of test cases. However, no warranty is given that the program is completely error-free. If you do encounter problems with the code, find errors, or have suggestions for improvement, please contact one of the authors at

U. S. Salinity Laboratory
USDA, ARS
450 Big Springs Road
Riverside, CA 92507

Tel. 909-369-4846
Fax. 909-369-4818

ABSTRACT

Šimůnek, J. and M. Th. van Genuchten. 1994. The CHAIN_2D Code for Simulating Two-Dimensional Movement of Water, Heat, and Multiple Solutes in Variably-Saturated Porous Media, Version 1.1. Research Report No. 136, U. S. Salinity Laboratory, USDA, ARS, Riverside, California.

This report documents the CHAIN_2D computer program for simulating two-dimensional variably saturated water flow, heat transport, and the movement of solutes involved in sequential first-order decay reactions. The program numerically solves the Richards' equation for saturated-unsaturated water flow and the convection-dispersion equation for heat and solute transport. The flow equation incorporates a sink term to account for water uptake by plant roots. The water flow part of the model can deal with prescribed head, gradient, and flux boundaries, as well as boundaries controlled by atmospheric conditions. Free drainage boundary condition and a simplified representation of nodal drains using results of electric analog experiments is also included. The heat transport equation considers transport due to conduction and convection with flowing water. The solute transport equations consider convective-dispersive transport in the liquid phase, as well as diffusion in the gaseous phase. The transport equations also include provisions for nonlinear nonequilibrium reactions between the solid and liquid phases, linear equilibrium reactions between the liquid and gaseous phases, zero-order production, and two first-order degradation reactions: one which is independent of other solutes, and one which provides the coupling between solutes involved in the sequential first-order decay reactions. The program may be used to analyze water and solute movement in unsaturated, partially saturated, or fully saturated porous media. CHAIN_2D can handle flow regions delineated by irregular boundaries. The flow region itself may be composed of nonuniform soils having an arbitrary degree of local anisotropy. Flow and transport can occur in the vertical plane, the horizontal plane, or in a three-dimensional region exhibiting radial symmetry about the vertical axis.

The governing flow and transport equations are solved numerically using Galerkin-

type linear finite element schemes. Depending upon the size of the problem, the matrix equations resulting from discretization of the governing equations are solved using either Gaussian elimination for banded matrices or the conjugate gradient method for symmetric matrices, or the ORTHOMIN method for asymmetric matrices. The program is written in ANSI standard FORTRAN 77. Computer memory is a function of the problem definition. This report serves as both a user manual and reference document. Detailed instructions are given for data input preparation. Example input and selected output files are also provided.

TABLE OF CONTENTS

LIST OF FIGURES

LIST OF TABLES

LIST OF VARIABLES

a	ion activity in soil solution [-]
a_r	dimensionless water stress response function [-]
a_v	air content [L^3L^{-3}]
$\bar{a}$	ion activity on the exchange surfaces [-]
A	amplitude of temperature sine wave [K]
A_e	area of a triangular element [L^2]
A_{qh}	parameter in equation (7.1) [LT^{-1}]
$[A]$	coefficient matrix in the global matrix equation for water flow, [LT^{-1}] or [L^2T^{-1}]†
b	normalized root water uptake distribution, [L^{-2}] or [L^{-3}]†
b'	arbitrary root water uptake distribution, [L^{-2}] or [L^{-3}]†
b_i, c_i	geometrical shape factors [L]
b_1, b_2, b_3	empirical parameters to calculate thermal conductivity λ_0 [$MLT^{-3}K^{-1}$](e.g.$Wm^{-1}K^{-1}$)
B_{qh}	parameter in equation (7.1) [L^{-1}]
$\{B\}$	vector in the global matrix equation for water flow, [L^2T^{-1}] or [L^3T^{-1}]†
c	solution concentration [ML^{-3}]
c'	finite element approximation of c [ML^{-3}]
c_i	initial solution concentration [ML^{-3}]
c_n	value of the concentration at node n [ML^{-3}]
c_r	concentration of the sink term [ML^{-3}]
c_0	prescribed concentration boundary condition [ML^{-3}]
C	volumetric heat capacity of porous medium [$ML^{-1}T^{-2}K^{-1}$] (e.g. $Jm^{-3}K^{-1}$)
C_d	factor used to adjust the hydraulic conductivity of elements in the vicinity of drains [-]
C_g	volumetric heat capacity of gas phase [$ML^{-1}T^{-2}K^{-1}$] (e.g. $Jm^{-3}K^{-1}$)
C_n	volumetric heat capacity of solid phase [$ML^{-1}T^{-2}K^{-1}$] (e.g. $Jm^{-3}K^{-1}$)
C_o	volumetric heat capacity of organic matter [$ML^{-1}T^{-2}K^{-1}$] (e.g. $Jm^{-3}K^{-1}$)
C_T	total solution concentration [ML^{-3}] ($mmol_c l^{-1}$)
C_w	volumetric heat capacity of liquid phase [$ML^{-1}T^{-2}K^{-1}$] (e.g. $Jm^{-3}K^{-1}$)

Cr_i^e	local Courant number [-]
d	thickness of stagnant boundary layer [L]
d_e	effective drain diameter [L]
D	side length of the square in the finite element mesh surrounding a drain (elements have adjusted hydraulic conductivities) [L]
D_g	ionic or molecular diffusion coefficient in the gas phase [L^2T^{-1}]
D_{ij}	effective dispersion coefficient tensor in the soil matrix [L^2T^{-1}]
D_{ij}^g	diffusion coefficient tensor for the gas phase [L^2T^{-1}]
D_{ij}^w	dispersion coefficient tensor for the liquid phase [L^2T^{-1}]
D_L	longitudinal dispersivity [L]
D_T	transverse dispersivity [L]
D_w	ionic or molecular diffusion coefficient in free water [L^2T^{-1}]
$\{D\}$	vector in the global matrix equation for water flow, [L^2T^{-1}] or [L^3T^{-1}]†
e_n	subelements which contain node n [-]
E	maximum (potential) rate of infiltration or evaporation under the prevailing atmospheric conditions [LT^{-1}]
E_a	activation energy of a reaction or process [$ML^2T^{-2}M^{-1}$] ($m^2s^{-2}mol^{-1}$)
f	fraction of exchange sites assumed to be at equilibrium with the solution concentration [-]
$\{f\}$	vector in the global matrix equation for solute transport, [$MT^{-1}L^{-1}$] or [MT^{-1}]†
$[F]$	coefficient matrix in the global matrix equation for water flow, [L^2] or [L^3]†
g	gas concentration [ML^{-3}]
g_{atm}	gas concentration above the stagnant boundary layer [ML^{-3}]
$\{g\}$	vector in the global matrix equation for solute transport, [$MT^{-1}L^{-1}$] or [MT^{-1}]†
$[G]$	coefficient matrix in the global matrix equation for solute transport, [L^2T^{-1}] or [L^3T^{-1}]†
h	pressure head [L]
h^*	scaled pressure head [L]
h'	finite element approximation of h [L]
h_A	minimum pressure head allowed at the soil surface [L]
h_n	nodal values of the pressure head [L]

h_{ref} pressure head at reference temperature T_{ref} [L]

h_s air-entry value in the soil water retention function [L]

h_S maximum pressure head allowed at the soil surface [L]

h_T pressure head at soil temperature T [L]

h_0 initial condition for the pressure head [L]

k kth chain number [-]

k_g empirical constant relating the solution and gas concentrations [-]

k_s empirical constant relating the solution and adsorbed concentrations [L^3M^{-1}]

K unsaturated hydraulic conductivity [LT^{-1}]

K^* scaled unsaturated hydraulic conductivity [LT^{-1}]

$\mathbf{K}^A$ dimensionless anisotropy tensor for the unsaturated hydraulic conductivity K [-]

K_{drain} adjusted hydraulic conductivity in the elements surrounding a drain [LT^{-1}]

K_{ex} dimensionless thermodynamic equilibrium constant [-]

K_H Henry's Law constant [$MT^2M^{-1}L^{-2}$]

K_{ij}^A components of the dimensionless anisotropy tensor $\mathbf{K}^A$ [-]

K_k measured value of the unsaturated hydraulic conductivity at θ_k [LT^{-1}]

K_r relative hydraulic conductivity [-]

K_{ref} hydraulic conductivity at reference temperature T_{ref} [LT^{-1}]

K_s saturated hydraulic conductivity [LT^{-1}]

K_T hydraulic conductivity at soil temperature T [LT^{-1}]

K_v Vanselow selectivity coefficient [-]

K_{12} selectivity coefficient [-]

L length of the side of an element [L]

L_i local coordinate [-]

L_n length of a boundary segment [L]

L_t width of soil surface associated with transpiration, [L] or [L^2]†

L_x width of the root zone [L]

L_z depth of the root zone [L]

m parameter in the soil water retention function [-]

M^0 cumulative amount of solute removed from the flow region by zero-order reactions, $[ML^{-1}]$ or $[M]^{\dagger}$

M^1 cumulative amount of solute removed from the flow region by first-order reactions, $[ML^{-1}]$ or $[M]^{\dagger}$

M_r cumulative amount of solute removed from the flow region by root water uptake, $[ML^{-1}]$ or $[M]^{\dagger}$

M_t amount of solute in the flow region at time t, $[ML^{-1}]$ or $[M]^{\dagger}$

M_t^e amount of solute in element e at time t, $[ML^{-1}]$ or $[M]^{\dagger}$

M_0 amount of solute in the flow region at the beginning of the simulation, $[ML^{-1}]$ or $[M]^{\dagger}$

M_0^e amount of solute in element e at the beginning of the simulation, $[ML^{-1}]$ or $[M]^{\dagger}$

n exponent in the soil water retention function [-]

n_i components of the outward unit vector normal to boundary Γ_N or Γ_G [-]

n_s number of solutes involved in the chain reaction [-]

N total number of nodes [-]

N_e number of subelements e_n which contain node n [-]

O actual rate of inflow/outflow to/from a subregion, $[L^2T^{-1}]$ or $[L^3T^{-1}]^{\dagger}$

Pe_i^e local Peclet number [-]

q_i components of the Darcian fluid flux density $[LT^{-1}]$

Q_n^A convective solute flux at node n, $[MT^{-1}L^{-1}]$ or $[MT^{-1}]^{\dagger}$

Q_n^D dispersive solute flux at node n, $[MT^{-1}L^{-1}]$ or $[MT^{-1}]^{\dagger}$

Q_n^T total solute flux at node n, $[MT^{-1}L^{-1}]$ or $[MT^{-1}]^{\dagger}$

$\{Q\}$ vector in the global matrix equation for water flow, $[L^2T^{-1}]$ or $[L^3T^{-1}]^{\dagger}$

$[Q]$ coefficient matrix in the global matrix equation for solute transport, $[L^2]$ or $[L^3]^{\dagger}$

R retardation factor [-]

R_u universal gas constant $[ML^2T^{-2}K^{-1}M^{-1}]$ ($=8.314 kg\ m^2s^{-2}K^{-1}mol^{-1}$)

s adsorbed solute concentration [-]

S sink term $[T^{-1}]$

S_e degree of saturation [-]

S_{ek} degree of saturation at θ_k [-]

S_p spatial distribution of the potential transpiration rate $[T^{-1}]$

S_T	cation exchange capacity [MM^{-1}] ($mmol_c kg^{-1}$)
$[S]$	coefficient matrix in the global matrix equation for solute transport, [L^2T^{-1}] or [L^3T^{-1}]†
t	time [T]
t^*	local time within the time period t_p [T]
t_p	period of time covering one complete cycle of the temperature sine wave [T]
T	temperature [K]
T_a	actual transpiration rate per unit surface length [LT^{-1}]
$\bar{T}$	average temperature at soil surface during period t_p [K]
T^A	absolute temperature [K]
T_i	initial temperature [K]
T_p	potential transpiration rate [LT^{-1}]
T_r^A	reference absolute temperature [K] (293.15K=20°C)
T_0	prescribed temperature boundary condition [K]
v	average pore-water velocity [LT^{-1}]
V	volume of water in each subregion, [L^2] or [L^3]†
V_{new}	volume of water in each subregion at the new time level, [L^2] or [L^3]†
V_{old}	volume of water in each subregion at the previous time level, [L^2] or [L^3]†
V_t	volume of water in the flow domain at time t, [L^2] or [L^3]†
V_t^e	volume of water in element e at time t, [L^2] or [L^3]†
V_0	volume of water in the flow domain at time zero, [L^2] or [L^3]†
V_0^e	volume of water in element e at time zero, [L^2] or [L^3]†
W	total amount of energy in the flow region, [MLT^{-2}] or [ML^2T^{-2}]†
x_i	spatial coordinates (i=1,2) [L]
Z_0	characteristic impedance of a transmission line analog to drain
Z_0'	characteristic impedance of free space (≈376.7 ohms)
α	coefficient in the soil water retention function [L^{-1}]
α^w	weighing factor [-]
α_h	scaling factor for the pressure head [-]
α_h^*	temperature scaling factor for the pressure head [-]

α_K scaling factor for the hydraulic conductivity [-]

α_K^* temperature scaling factor for the hydraulic conductivity [-]

α_θ scaling factor for the water content [-]

β empirical constant in adsorption isotherm [-]

γ_g zero-order rate constant for solutes in the gas phase [$ML^{-3}T^{-1}$]

γ_i activity coefficient in soil solution [L^3M^{-1}] (1 mol^{-1})

γ_s zero-order rate constant for solutes adsorbed onto the solid phase [T^{-1}]

γ_w zero-order rate constants for solutes in the liquid phase [$ML^{-3}T^{-1}$]

Γ_e boundary segments connected to node n

Γ_D part of flow domain boundary where Dirichlet type conditions are specified

Γ_G part of flow domain boundary where gradient type conditions are specified

Γ_N part of flow domain boundary where Neumann type conditions are specified

Γ_C part of flow domain boundary where Cauchy type conditions are specified

δ_{ij} Kronecker delta [-]

Δt time increment [T]

Δt_{max} maximum permitted time increment [T]

Δt_{min} minimum permitted time increment [T]

ϵ temporal weighing factor [-]

ϵ_a^c absolute error in the solute mass balance, [ML^{-1}] or [M]†

ϵ_a^w absolute error in the water mass balance, [L^2] or [L^3]†

ϵ_r^c relative error in the solute mass balance [%]

ϵ_r^w relative error in the water mass balance [%]

ϵ_0 permittivity of free space (used in electric analog representation of drains)

η empirical constant in adsorption isotherm [L^3M^{-3}]

θ volumetric water content [L^3L^{-3}]

θ^* scaled volumetric water content [L^3L^{-3}]

θ_a parameter in the soil water retention function [L^3L^{-3}]

θ_k volumetric water content corresponding to K_k [L^3L^{-3}]

θ_m parameter in the soil water retention function [L^3L^{-3}]

θ_n volumetric solid phase fraction [L^3L^{-3}]

θ_o volumetric organic matter fraction [L^3L^{-3}]

θ_r residual soil water content [L^3L^{-3}]

θ_s saturated soil water content [L^3L^{-3}]

κ parameter which depends on the type of flow being analyzed, [-] or [L]†

λ first-order rate constant [T^{-1}]

λ_{ij} apparent thermal conductivity tensor of the soil [$MLT^{-3}K^{-1}$] (e.g. $Wm^{-1}K^{-1}$)

λ_L longitudinal thermal dispersivity [L]

λ_T transverse thermal dispersivity [L]

λ_0 thermal conductivity of porous medium in the absence of flow [$MLT^{-3}K^{-1}$] (e.g. $Wm^{-1}K^{-1}$)

μ_g first-order rate constant for solutes in the gas phase [T^{-1}]

μ_{ref} dynamic viscosity at reference temperature T_{ref} [$MT^{-1}L^{-1}$]

μ_s first-order rate constant for solutes adsorbed onto the solid phase [T^{-1}]

μ_T dynamic viscosity at temperature T [$MT^{-1}L^{-1}$]

μ_w first-order rate constant for solutes in the liquid phase [T^{-1}]

μ_g' first-order rate constant for chain solutes in the gas phase [T^{-1}]

μ_s' first-order rate constant for chain solutes adsorbed onto the solid phase [T^{-1}]

μ_w' first-order rate constant for chain solutes in the liquid phase [T^{-1}]

ξ_i activity coefficient on the exchange surfaces [MM^{-1}] (kg mol^{-1})

ρ bulk density of porous medium [ML^{-3}]

ρ_d dimensionless ratio between the side of the square in the finite element mesh surrounding the drain, D, and the effective diameter of a drain, d_e [-]

ρ_{ref} density of soil water at reference temperature T_{ref} [ML^{-3}]

ρ_T density of soil water at temperature T [ML^{-3}]

σ_{ref} surface tension at reference temperature T_{ref} [MT^{-2}]

σ_T surface tension at temperature T [MT^{-2}]

σ_1 prescribed flux boundary condition at boundary Γ_N [LT^{-1}]

σ_2 prescribed gradient boundary condition at boundary Γ_G [-]

τ_a tortuosity factor in the gas phase [-]

τ_w	tortuosity factor in the liquid phase [-]
ϕ_n	linear basis functions [-]
ϕ_n^u	upstream weighted basis functions [-]
ψ	prescribed pressure head boundary condition at boundary Γ_D [L]
ω	first-order adsorption rate constant [T^{-1}]
ω_a	angle between principal direction of K_1^A and the x-axis of the global coordinate system [-]
ω_s	performance index used as a criterion to minimize or eliminate numerical oscillations [-]
Ω	flow region
Ω_e	domain occupied by element e
Ω_R	region occupied by the root zone

† for plane and axisymmetric flow, respectively

1. INTRODUCTION

The importance of the unsaturated zone as an integral part of the hydrological cycle has long been recognized. The zone plays an inextricable role in many aspects of hydrology, including infiltration, soil moisture storage, evaporation, plant water uptake, groundwater recharge, runoff and erosion. Initial studies of the unsaturated (vadose) zone focused primarily on water supply studies, inspired in part by attempts to optimally manage the root zone of agricultural soils for maximum crop production. Interest in the unsaturated zone has dramatically increased in recent years because of growing concern that the quality of the subsurface environment is being adversely affected by agricultural, industrial and municipal activities. Federal, state and local action and planning agencies, as well as the public at large, are now scrutinizing the intentional or accidental release of surface-applied and soil-incorporated chemicals into the environment. Fertilizers and pesticides applied to agricultural lands inevitably move below the soil root zone and may contaminate underlying groundwater reservoirs. Chemicals migrating from municipal and industrial disposal sites also represent environmental hazards. The same is true for radionuclides emanating from energy waste disposal facilities.

The past several decades has seen considerable progress in the conceptual understanding and mathematical description of water flow and solute transport processes in the unsaturated zone. A variety of analytical and numerical models are now available to predict water and/or solute transfer processes between the soil surface and the groundwater table. The most popular models remain the Richards' equation for variably saturated flow, and the Fickian-based convection-dispersion equation for solute transport. Deterministic solutions of these classical equations have been used, and likely will continue to be used in the near future, for predicting water and solute movement in the vadose zone, and for analyzing specific laboratory or field experiments involving unsaturated water flow and/or solute transport. These models are also helpful tools for extrapolating information from a limited number of field experiments to different soil, crop and climatic conditions, as well as to different tillage and water management schemes.

Once released into the subsurface environment, industrial and agricultural chemicals

are generally subjected to a large number of simultaneous physical, chemical, and biological processes, including sorption-desorption, volatilization, photolysis, and biodegradation, as well as their kinetics. The extent of degradation, sorption and volatilization largely determines the persistence of a pollutant in the subsurface [*Chiou*, 1989]. For example, the fate of organic chemicals in soils is known to be strongly affected by the kinetics of biological degradation. *Alexander and Scow* [1989] gave a review of some of the equations used to represent the kinetics of biodegradation. These equations include zero-order, half-order, first-order, three-half-order, mixed-order, logistic, logarithmic, Michaelis-Menton, and Monod type (with or without growth) expressions. While most of these expressions have a theoretical bases, they are commonly used only in an empirical fashion by fitting the equations to observed data. Zero- and first-order kinetic equations remain the most popular for describing biodegradation of organic compounds, mostly because of their simplicity and the ease in which they can be incorporated in solute transport models. Conditions for the application of these two equations are described by *Alexander and Scow* [1989].

One special group of degradation reactions involves decay chains in which solutes are subject to sequential (or consecutive) decay reactions. Problems of solute transport involving sequential first-order decay reactions frequently occur in soil and groundwater systems. Examples are the migration of various radionuclides [*Lester et al.*, 1975; *Rogers*, 1978; *Gureghian*, 1981; *Gureghian and Jansen*, 1983], the simultaneous movement of interacting nitrogen species [*Cho*, 1971; *Misra et al.*, 1974; *Wagenet et al.*, 1976; *Tillotson et al.*, 1980], organic phosphate transport [*Castro and Rolston*, 1977], and the transport of certain pesticides and their metabolites [*Bromilow and Leistra*, 1980; *Wagenet and Hutson*, 1987].

While in the past most pesticides were regarded as involatile, volatilization is now increasingly recognized as an important process affecting the fate of pesticides in field soils [*Glotfelty and Schomburg*, 1989; *Spencer*, 1991]. Another process affecting pesticide fate and transport is the relative reactivity of solutes in the sorbed and solution phases. Several processes such as gaseous and liquid molecular diffusion, and convective-dispersive transport, act only on solutes that are not adsorbed. Degradation of organic compounds

likely occurs mainly, or even exclusively, in the liquid phase [*Pignatello*, 1989]. On the other side, radioactive decay takes place equally in the solution and adsorbed phases, while other reactions may occur only in the sorbed phase.

Several analytical solutions have been published for simplified transport systems involving consecutive decay reactions [*Cho*, 1971; *Wagenet et al.*, 1976; *Harada et al.*, 1980; *Higashi and Pigford*, 1980; *van Genuchten*, 1985]. Unfortunately, analytical solutions for more complex situations, such as for transient water flow or the nonequilibrium solute transport with nonlinear reactions, are not available and/or cannot be derived, in which case numerical models must be employed. To be useful, such numerical models must allow for different reaction rates to take place in the solid, liquid, and gaseous phases, as well as for a correct distribution of the solutes among the different phases.

The purpose of this report is to document the CHAIN_2D computer program for simulating two-dimensional variably-saturated water flow, heat movement, and the transport of solutes involved in sequential first-order decay reactions. The program numerically solves the Richards' equation for saturated-unsaturated water flow and the convection-dispersion equation for heat and solute transport. The water flow equation incorporates a sink term to account for water uptake by plant roots. The heat transport equation considers movement by conduction as well as convection with flowing water. The governing convection-dispersion solute transport equations are written in a very general form by including provisions for nonlinear nonequilibrium reactions between the solid and liquid phases, and linear equilibrium reaction between liquid and gaseous phases. Hence, both adsorbed and volatile solutes such as pesticides can be considered. The solute transport equations also incorporate the effects of zero-order production, first-order degradation independent of other solutes, and first-order decay/production that provides the required coupling between the solutes involved in the sequential first-order reactions. The transport models also account for convection and dispersion in the liquid phase, as well as for diffusion in the gas phase, thus permitting one to simulate solute transport simultaneously in both the liquid and gaseous phases. CHAIN_2D at present considers up to six solutes which can be either coupled in a unidirectional chain or may move independent of each other.

The CHAIN_2D code may be used to analyze water and solute movement in unsaturated, partially saturated, or fully saturated porous media. The program can handle flow domains delineated by irregular boundaries. The flow region itself may be composed of nonuniform soils having an arbitrary degree of local anisotropy. Flow and transport can occur in the vertical plane, the horizontal plane, or in a three-dimensional region exhibiting radial symmetry about a vertical axis. The water flow part of the model considers prescribed head and flux boundaries, as well as boundaries controlled by atmospheric conditions or free drainage. A simplified representation of nodal drains using results of electric analog experiments is also included. The first and third-type boundary conditions can be prescribe in the solute and heat transport part of the model.

The governing flow and transport equations are solved numerically using Galerkin-type linear finite element schemes. Depending upon the size of the problem, the matrix equations resulting from discretization of the governing equations are solved using either Gaussian elimination for banded matrices or the conjugate gradient method for symmetric matrices, and the ORTHOMIN method for asymmetric matrices [*Mendoza et al.*, 1991]. The program is an extension of the SWMS_2D code for simulating water flow and solute transport in two-dimensional variably saturated media [*Šimůnek et al.*, 1992], which in turn was based in part on the variably saturated flow code SWMII of *Vogel* [1987] and early numerical work by Neuman and colleagues [*Neuman*, 1972, 1973, *Neuman et al.*, 1974; *Neuman*, 1975; *Davis and Neuman*, 1983]. Experience obtained with a model simulating two-dimensional heat transport and two-phase transport of carbon dioxide [*Šimůnek and Suarez*, 1993b] was used in developing CHAIN_2D. The code is written in ANSI standard FORTRAN 77, and hence can be compiled, linked and run on any standard micro-, mini-, or mainframe system, as well as on personal computers. The source code was developed and tested on a PC 486 using the Microsoft's Fortran PowerStation compiler.

This report serves as both a user manual and reference document. Detailed instructions are given for data input preparation. Example input and selected output files are also provided. Two 3½ or 5¼ inch floppy diskettes containing the input and output files of seven examples discussed in this report, as well as the source code, are available upon request from the authors.

2. VARIABLY SATURATED WATER FLOW

2.1. *Governing Flow Equation*

Consider two-dimensional isothermal Darcian flow of water in a variably saturated rigid porous medium and assume that the air phase plays an insignificant role in the liquid flow process. The governing flow equation for these conditions is given by the following modified form of the Richards' equation:

$$\frac{\partial \theta}{\partial t} = \frac{\partial}{\partial x_i}[K(K_{ij}^A \frac{\partial h}{\partial x_j} + K_{iz}^A)] - S \qquad (2.1)$$

where θ is the volumetric water content [L^3L^{-3}], h is the pressure head [L], S is a sink term [T^{-1}], x_i (i=1,2) are the spatial coordinates [L] , t is time [T], K_{ij}^A are components of a dimensionless anisotropy tensor $\mathbf{K}^A$, and K is the unsaturated hydraulic conductivity function [LT^{-1}] given by

$$K(h,x,z) = K_s(x,z)\, K_r(h,x,z) \qquad (2.2)$$

where K_r is the relative hydraulic conductivity and K_s the saturated hydraulic conductivity [LT^{-1}]. The anisotropy tensor K_{ij}^A in (2.1) is used to account for an anisotropic medium. The diagonal entries of K_{ij}^A equal one and the off-diagonal entries zero for an isotropic medium. If (2.1) is applied to planar flow in a vertical cross-section, x_1=x is the horizontal coordinate and x_2=z is the vertical coordinate, the latter taken to be positive upward. Einstein's summation convention is used in (2.1) and throughout this report. Hence, when an index appears twice in an algebraic term, this particular term must be summed over all possible values of the index.

2.2. *Root Water Uptake*

The sink term, S, in (2.1) represents the volume of water removed per unit time from a unit volume of soil due to plant water uptake. *Feddes et al.* [1978] defined S as

$$S(h) = a_r(h) S_p \tag{2.3}$$

where the water stress response function $a_r(h)$ is a prescribed dimensionless function (Fig. 2.1) of the soil water pressure head ($0 \le a_r \le 1$), and S_p is the potential water uptake rate [T^{-1}]. Figure 2.1. gives a schematic plot of the stress response function as used by *Feddes et al.* [1978]. Notice that water uptake is assumed to be zero close to saturation (i.e., wetter than some arbitrary "anaerobiosis point", h_1). For $h < h_4$ (the wilting point pressure head), water uptake is also assumed to be zero. Water uptake is considered optimal between pressure heads h_2 and h_3, whereas for pressure head between h_3 and h_4 (or h_1 and h_2), water uptake decreases (or increases) linearly with h. S_p is equal to the water uptake rate during periods of no water stress when $a_r(h) = 1$.

When the potential water uptake rate is equally distributed over a two-dimensional rectangular root domain, S_p becomes

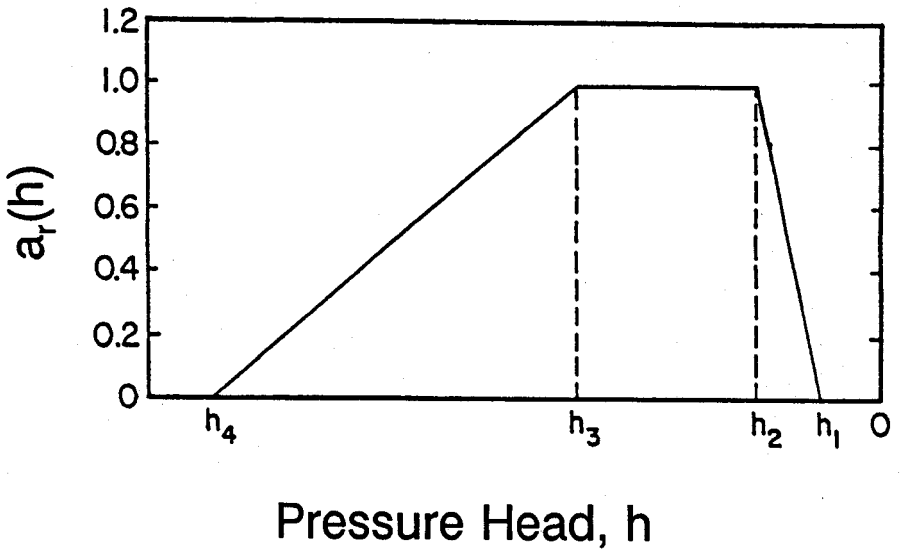

Fig. 2.1. Schematic of the plant water stress response function, $a_r(h)$, as used by *Feddes et al.* [1978].

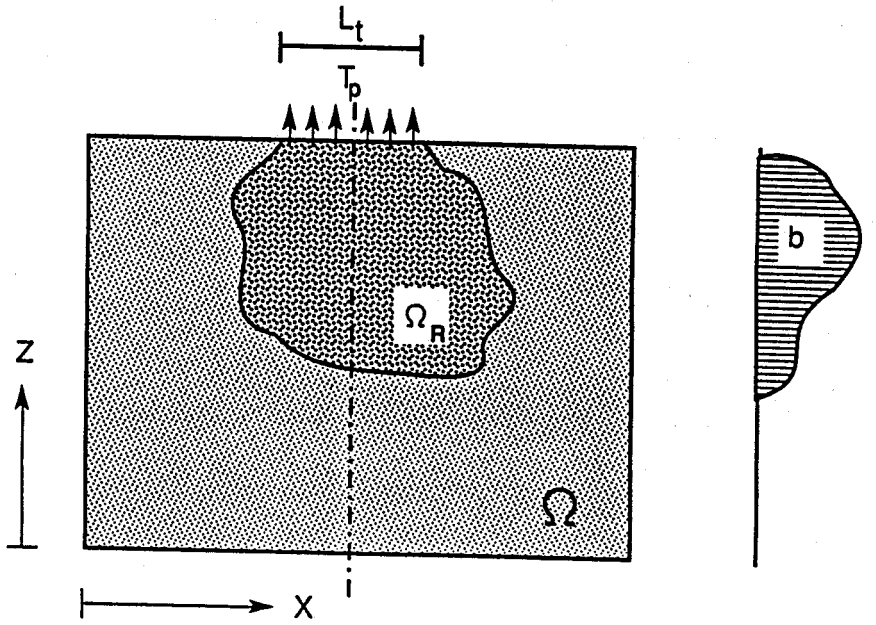

Fig. 2.2. Schematic of the potential water uptake distribution function, $b(x,z)$, in the soil root zone.

$$S_p = \frac{1}{L_x L_z} L_t T_p \tag{2.4}$$

where T_p is the potential transpiration rate [LT^{-1}], L_z is the depth [L] of the root zone, L_x is the width [L] of the root zone, and L_t is the width [L] of the soil surface associated with the transpiration process. Notice that S_p reduces to T_p/L_z when $L_t=L_x$.

Equation (2.4) may be generalized by introducing a non-uniform distribution of the potential water uptake rate over a root zone of arbitrary shape [*Vogel*, 1987]:

$$S_p = b(x,z) L_t T_p \tag{2.5}$$

where $b(x,z)$ is the normalized water uptake distribution [L^{-2}]. This function describes the spatial variation of the potential extraction term, S_p, over the root zone (Fig. 2.2), and is obtained from $b'(x,z)$ as follows

$$b(x,z) = \frac{b'(x,z)}{\int_{\Omega_R} b'(x,z)\,d\Omega} \tag{2.6}$$

where Ω_R is the region occupied by the root zone, and $b'(x,z)$ is an arbitrarily prescribed distribution function. Normalizing the uptake distribution ensures that $b(x,z)$ integrates to unity over the flow domain, i.e.,

$$\int_{\Omega_R} b(x,z)\,d\Omega = 1 \tag{2.7}$$

From (2.5) and (2.7) it follows that S_p is related to T_p by the expression

$$\frac{1}{L_t}\int_{\Omega_R} S_p\,d\Omega = T_p \tag{2.8}$$

The actual water uptake distribution is obtained by substituting (2.5) into (2.3):

$$S(h,x,z) = a_r(h,x,z)\,b(x,z)\,L_t\,T_p \tag{2.9}$$

whereas the actual transpiration rate, T_a, is obtained by integrating (2.9) as follows

$$T_a = \frac{1}{L_t}\int_{\Omega_R} S\,d\Omega = T_p \int_{\Omega_R} a_r(h,x,z)\,b(x,z)\,d\Omega \tag{2.10}$$

2.3. *The Unsaturated Soil Hydraulic Properties*

The unsaturated soil hydraulic properties in the CHAIN_2D code are described by a set of closed-form equations resembling those of *van Genuchten* [1980] who used the statistical pore-size distribution model of *Mualem* [1976] to obtain a predictive equation for the unsaturated hydraulic conductivity function. The original van Genuchten equations were modified to add extra flexibility in the description of the hydraulic properties near saturation [*Šír et al.*, 1985; *Vogel and Císlerová*, 1988]. The soil water retention, $\theta(h)$, and hydraulic conductivity, $K(h)$, functions in CHAIN_2D are given by

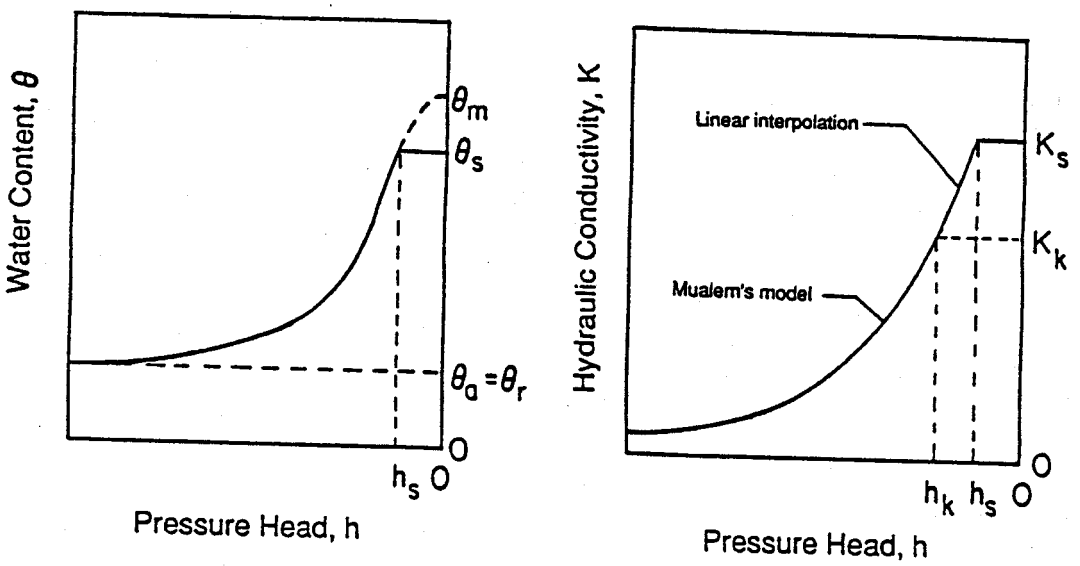

Fig. 2.3. Schematics of the soil water retention (a) and hydraulic conductivity (b) functions as given by equations (2.11) and (2.12), respectively.

function were replaced by the fictitious (extrapolated) parameters $\theta_a \le \theta_r$ and $\theta_m \ge \theta_s$ as shown in Fig. 2.3. The approach maintains the physical meaning of θ_r and θ_s as measurable quantities. Equation (2.13) assumes that the predicted hydraulic conductivity function is matched to a measured value of the hydraulic conductivity, $K_k = K(\theta_k)$, at some water content, θ_k, less that or equal to the saturated water content, i.e., $\theta_k \le \theta_s$ and $K_k \le K_s$ [*Vogel and Císlerová*, 1988; *Luckner et al.*, 1989].

Inspection of (2.11) through (2.17) shows that the hydraulic characteristics contain 9 unknown parameters: θ_r, θ_s, θ_a, θ_m, α, n, K_s, K_k, and θ_k. When $\theta_a = \theta_r$, $\theta_m = \theta_k = \theta_s$ and $K_k = K_s$, the soil hydraulic functions reduce to the original expressions of *van Genuchten* [1980]:

$$\theta(h) = \begin{cases} \theta_r + \dfrac{\theta_s - \theta_r}{[1 + |\alpha h|^n]^m} & h < 0 \\ \theta_s & h \ge 0 \end{cases} \qquad (2.18)$$

$$\theta(h) = \begin{cases} \theta_a + \dfrac{\theta_m - \theta_a}{(1 + |\alpha h|^n)^m} & h < h_s \\ \theta_s & h \geq h_s \end{cases} \tag{2.11}$$

and

$$K(h) = \begin{cases} K_s K_r(h) & h \leq h_k \\ K_k + \dfrac{(h - h_k)(K_s - K_k)}{h_s - h_k} & h_k < h < h_s \\ K_s & h \geq h_s \end{cases} \tag{2.12}$$

respectively, where

$$K_r = \frac{K_k}{K_s} \left[\frac{S_e}{S_{ek}} \right]^{1/2} \left[\frac{F(\theta_r) - F(\theta)}{F(\theta_r) - F(\theta_k)} \right]^2 \tag{2.13}$$

$$F(\theta) = \left[1 - \left[\frac{\theta - \theta_a}{\theta_m - \theta_a} \right]^{1/m} \right]^m \tag{2.14}$$

$$m = 1 - 1/n \quad , \qquad n > 1 \tag{2.15}$$

$$S_e = \frac{\theta - \theta_r}{\theta_s - \theta_r} \tag{2.16}$$

$$S_{ek} = \frac{\theta_k - \theta_r}{\theta_s - \theta_r} \tag{2.17}$$

in which θ_r and θ_s denote the residual and saturated water contents, respectively, and K_s is the saturated hydraulic conductivity. To increase the flexibility of the analytical expressions, and to allow for a non-zero air-entry value, h_s, the parameters θ_r and θ_s in the retention

$$K(h) = \begin{cases} K_s K_r(h) & h < 0 \\ K_s & h \geq 0 \end{cases} \tag{2.19}$$

where

$$K_r = S_e^{1/2}[1 - (1 - S_e^{1/m})^m]^2 \tag{2.20}$$

2.4. *Scaling of the Soil Hydraulic Functions*

2.4.1. *Spatial variability of the Soil Hydraulic Functions*

CHAIN_2D implements a scaling procedure designed to simplify the description of the spatial variability of the unsaturated soil hydraulic properties in the flow domain. The code assumes that the hydraulic variability in a given area can be approximated by means of a set of linear scaling transformations which relate the individual soil hydraulic characteristics $\theta(h)$ and $K(h)$ to reference characteristics $\theta^*(h^*)$ and $K^*(h^*)$. The technique is based on the similar media concept introduced by *Miller and Miller* [1956] for porous media which differ only in the scale of their internal geometry. The concept was extended by *Simmons et al.* [1979] to materials which differ in morphological properties, but which exhibit 'scale-similar' soil hydraulic functions. Three independent scaling factors are embodied in CHAIN_2D. These three scaling parameters may be used to define a linear model of the actual spatial variability in the soil hydraulic properties as follows [*Vogel et al.*, 1991]:

$$\begin{aligned} K(h) &= \alpha_K K^*(h^*) \\ \theta(h) &= \theta_r + \alpha_\theta[\theta^*(h^*) - \theta_r^*] \\ h &= \alpha_h h^* \end{aligned} \tag{2.21}$$

in which, for the most general case, α_θ, α_h and α_K are mutually independent scaling factors

for the water content, the pressure head and the hydraulic conductivity, respectively. Less general scaling methods arise by invoking certain relationships between α_θ, α_h and/or α_K. For example, the original Miller-Miller scaling procedure is obtained by assuming $\alpha_\theta=1$ (with $\theta_r^* = \theta_r$), and $\alpha_K=\alpha_h^{-2}$. A detailed discussion of the scaling relationships given by (2.21), and their application to the hydraulic description of heterogeneous soil profiles, is given by *Vogel et al.* [1991].

2.4.2. *Temperature Dependence of the Soil Hydraulic Functions*

A similar scaling technique as described above is used to express the temperature dependence of the soil hydraulic functions. Based on capillary theory that assumes that the influence of temperature on the soil water pressure head can be quantitatively predicted from the influence of temperature on surface tension, *Philip and de Vries* [1957] derived following equation

$$\frac{dh}{dT} = \frac{h}{\sigma}\frac{d\sigma}{dT} \tag{2.22}$$

where T is temperature [K] and σ is the surface tension at the air-water interface [MT^{-2}]. From (2.22) it follows that

$$h_T = \frac{\sigma_T}{\sigma_{ref}} h_{ref} = \alpha_h^* h_{ref} \tag{2.23}$$

where h_T and h_{ref} (σ_T and σ_{ref}) are pressure heads (surface tensions) at temperature T and reference temperature T_{ref}, respectively; and α_h^* is the temperature scaling factor for the pressure head.

Following *Constantz* [1982], the temperature dependence of the hydraulic conductivity can be expressed as

$$K_T(\theta) = \frac{\mu_{ref}}{\mu_T}\frac{\rho_T}{\rho_{ref}} K_{ref}(\theta) = \alpha_K^* K_{ref}(\theta) \qquad (2.24)$$

where K_{ref} and K_T denote hydraulic conductivities at the reference temperature T_{ref} and soil temperature T, respectively; μ_{ref} and μ_T (ρ_{ref} and ρ_T) similarly represent the dynamic viscosity [$ML^{-1}T^{-1}$] (density of soil water [ML^{-3}]) at temperatures T_{ref} and T, respectively; and α_K^* is the temperature scaling factor for the hydraulic conductivity.

2.5. *Initial and Boundary Conditions*

The solution of Eq. (2.1) requires knowledge of the initial distribution of the pressure head within the flow domain, Ω:

$$h(x,z,t) = h_0(x,z) \qquad for\ t = 0 \qquad (2.25)$$

where h_0 is a prescribed function of x and z.

CHAIN_2D implements three types of conditions to describe system-independent interactions along the boundaries of the flow region. These conditions are specified pressure head (Dirichlet type) boundary conditions of the form

$$h(x,z,t) = \psi\,(x,z,t) \qquad for\ (x,z) \in \Gamma_D \qquad (2.26)$$

specified flux (Neumann type) boundary conditions given by

$$-[K(K_{ij}^A \frac{\partial h}{\partial x_j} + K_{iz}^A)]n_i = \sigma_1(x,z,t) \qquad for\ (x,z) \in \Gamma_N \qquad (2.27)$$

and specified gradient boundary conditions

$$(K_{ij}^A \frac{\partial h}{\partial x_j} + K_{iz}^A)n_i = \sigma_2(x,z,t) \qquad for\ (x,z) \in \Gamma_G \qquad (2.28)$$

where Γ_D, Γ_N, and Γ_G indicate Dirichlet, Neumann, and gradient type boundary segments, respectively; ψ [L], σ_1 [LT^{-1}], and σ_2 [-] are prescribed functions of x, z and t; and n_i are the

components of the outward unit vector normal to boundary Γ_N or Γ_G. As pointed out by *McCord* [1991], the use of the term "Neumann type boundary condition" for the flux boundary is not very appropriate since this term should hold for a gradient type condition (see also Section 3.2 for solute transport). However, since the use of the Neumann condition is standard in the hydrologic literature [*Neuman*, 1972; *Neuman et al.*, 1974], we shall also use this term to indicate flux boundaries throughout this report. CHAIN_2D implements the gradient boundary condition only in terms of a unit vertical hydraulic gradient simulating free drainage from a relatively deep soil profile. This situation is often observed in field studies of water flow and drainage in the vadose zone [*Sisson*, 1987; *McCord*, 1991]. *McCord* [1991] states that the most pertinent application of (2.28) is its use as a bottom outflow boundary condition for situations where the water table lies far below the domain of interest.

In addition to the system-independent boundary conditions given by (2.26), (2.27) and (2.28), CHAIN_2D considers two different types of system-dependent boundary conditions which cannot be defined a priori. One of these involves soil-air interfaces which are exposed to atmospheric conditions. The potential fluid flux across these interfaces is controlled exclusively by external conditions. However, the actual flux depends also on the prevailing (transient) soil moisture conditions. Soil surface boundary conditions may change from prescribed flux to prescribed head type conditions (and vice-versa). In the absence of surface ponding, the numerical solution of (2.1) is obtained by limiting the absolute value of the flux by the following two conditions [*Neuman et al.*, 1974]:

$$| K(K_{ij}^A \frac{\partial h}{\partial x_j} + K_{iz}^A) n_i | \leq E \tag{2.29}$$

and

$$h_A \leq h \leq h_S \tag{2.30}$$

where E is the maximum potential rate of infiltration or evaporation under the current atmospheric conditions, h is the pressure head at the soil surface, and h_A and h_S are, respectively, minimum and maximum pressure heads allowed under the prevailing soil

conditions. The value for h_A is determined from the equilibrium conditions between soil water and atmospheric water vapor, whereas h_S is usually set equal to zero. CHAIN_2D assumes that any excess water on the soil surface is immediately removed. When one of the end points of (2.30) is reached, a prescribed head boundary condition will be used to calculate the actual surface flux. Methods of calculating E and h_A on the basis of atmospheric data have been discussed by *Feddes et al.* [1974].

A second type of system-dependent boundary conditions considered in CHAIN_2D is a seepage face through which water leaves the saturated part of the flow domain. In this case, the length of the seepage face is not known a priori. CHAIN_2D assumes that the pressure head is always uniformly equal to zero along a seepage face. Additionally, the code assumes that water leaving the saturated zone across a seepage face is immediately removed by overland flow or some other removal process.

3. NONEQUILIBRIUM TRANSPORT OF SOLUTES INVOLVED IN SEQUENTIAL FIRST-ORDER DECAY REACTIONS

3.1. *Governing Solute Transport Equations*

We assume that solutes can exist in all three phases (liquid, solid, and gaseous) and that the decay and production processes can be different in each phase. Interactions between the solid and liquid phases may be described by nonlinear nonequilibrium equations, while interactions between the liquid and gaseous phases are assumed to be linear and instantaneous. We further assume that the solutes are transported by convection and dispersion in the liquid phase, as well as by diffusion in the gas phase. A general structure of the system of first-order decay reactions for three solutes (A, B and C) is as follows:

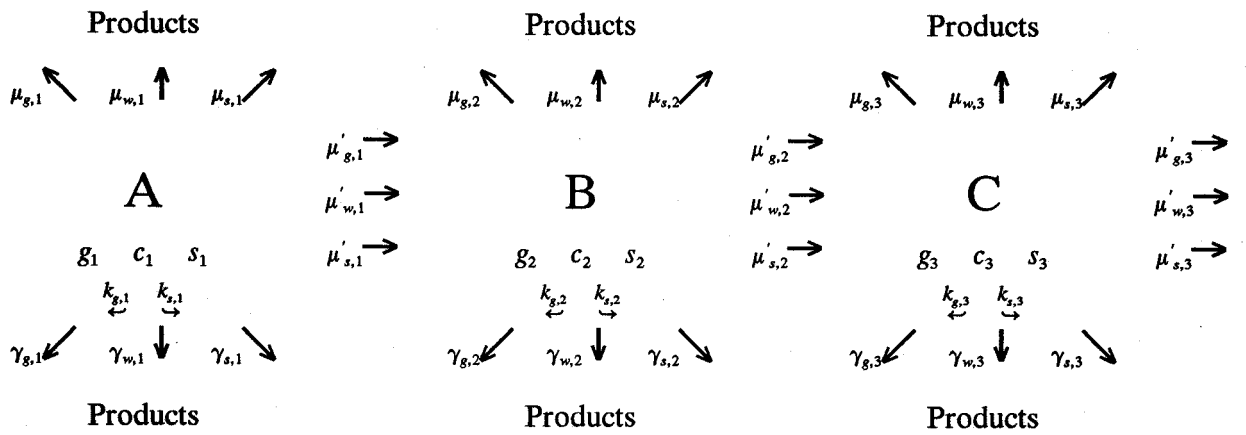

where c, s, and g represent concentrations in the liquid, solid, and gaseous phases, respectively; the subscripts s, w, and g refer to solid, liquid and gaseous phases, respectively; straight arrows represent the different zero-order (γ) and first-order (μ, μ') rate reactions, and circular arrows (k_g, k_s) indicate equilibrium distribution coefficients between phases.

Typical examples of sequential first-order decay chains are:

1. Radionuclides [*van Genuchten*, 1985]

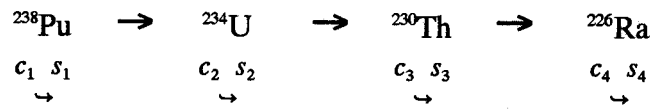

2. Nitrogen [*Tillotson et al.*, 1980]

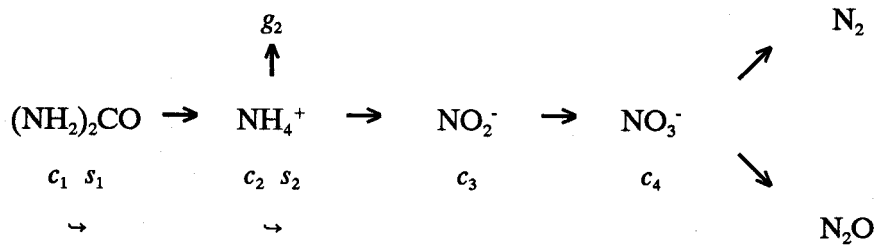

3. Pesticides [*Wagenet and Hutson*, 1987]:

   a) Uninterrupted chain - one reaction path:

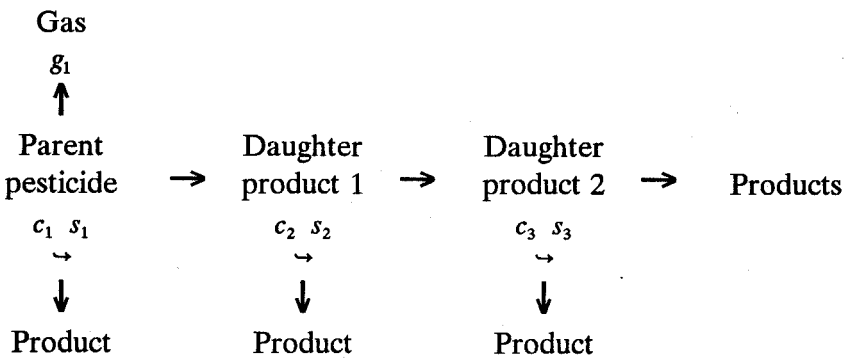

   b) Interrupted chain - two independent reaction paths:

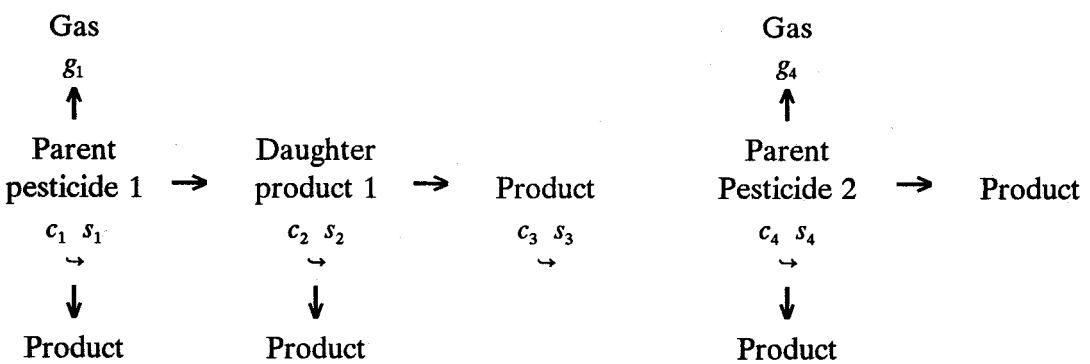

CHAIN_2D at present considers up to six solutes which can be either coupled in a unidirectional chain or may move independently of each other.

The partial differential equations governing two-dimensional nonequilibrium chemical transport of solutes involved in a sequential first-order decay chain during transient water flow in a variably saturated rigid porous medium are taken as

$$\frac{\partial \theta c_1}{\partial t} + \frac{\partial \rho s_1}{\partial t} + \frac{\partial a_v g_1}{\partial t} = \frac{\partial}{\partial x_i}(\theta D_{ij,1}^{w} \frac{\partial c_1}{\partial x_j}) + \frac{\partial}{\partial x_i}(a_v D_{ij,1}^{g} \frac{\partial g_1}{\partial x_j}) - \frac{\partial q_i c_1}{\partial x_i} - Sc_{r,1} -$$
$$-(\mu_{w,1} + \mu'_{w,1})\theta c_1 - (\mu_{s,1} + \mu'_{s,1})\rho s_1 - (\mu_{g,1} + \mu'_{g,1}) a_v g_1 + \gamma_{w,1}\theta + \gamma_{s,1}\rho + \gamma_{g,1} a_v \qquad (3.1)$$

$$\frac{\partial \theta c_k}{\partial t} + \frac{\partial \rho s_k}{\partial t} + \frac{\partial a_v g_k}{\partial t} = \frac{\partial}{\partial x_i}(\theta D_{ij,k}^{w} \frac{\partial c_k}{\partial x_j}) + \frac{\partial}{\partial x_i}(a_v D_{ij,k}^{g} \frac{\partial g_k}{\partial x_j}) - \frac{\partial q_i c_k}{\partial x_i} -$$
$$-(\mu_{w,k} + \mu'_{w,k})\theta c_k - (\mu_{s,k} + \mu'_{s,k})\rho s_k - (\mu_{g,k} + \mu_{g,k}) a_v g_k + \mu'_{w,k-1}\theta c_{k-1} \qquad (3.2)$$
$$+\mu'_{s,k-1}\rho s_{k-1} + \mu'_{g,k-1} a_v g_{k-1} + \gamma_{w,k}\theta + \gamma_{s,k}\rho + \gamma_{g,k} a_v - Sc_{r,k} \qquad k \in (2, n_s)$$

where c, s, and g are solute concentrations in the liquid [ML^{-3}], solid [MM^{-1}], and gaseous [ML^{-3}], phases, respectively; q_i is the i-th component of the volumetric flux density [LT^{-1}], μ_w, μ_s, and μ_g are first-order rate constants for solutes in the liquid, solid, and gas phases [T^{-1}], respectively; μ_w', μ_s', and μ_g' are similar first-order rate constants providing connections between individual chain species, γ_w, γ_s, and γ_g are zero-order rate constants for the liquid [$ML^{-3}T^{-1}$], solid [T^{-1}], and gas [$ML^{-3}T^{-1}$] phases, respectively; ρ is the soil bulk density [$M L^{-3}$], a_v is the air content [L^3L^{-3}], S is the sink term in the water flow equation (2.1), c_r is the concentration of the sink term [ML^{-3}], D_{ij}^{w} is the dispersion coefficient tensor [L^2T^{-1}] for the liquid phase, and D_{ij}^{g} is the diffusion coefficient tensor [L^2T^{-1}] for the gas phase. As before, the subscripts w, s, and g correspond with the liquid, solid and gas phases, respectively; while the subscript k represents the kth chain number, and n_s is the number of solutes involved in the chain reaction. The indicial notation used in this report assumes summations over indices i and j (i,j = 1,2), but not over index k. The nine zero- and first-order rate constants in (3.1) and (3.2) may be used to represent a variety of reactions or transformations

including biodegradation, volatilization, and precipitation. Note the differences in the signs of the first-order rate constants in comparison with the SWMS_2D code.

CHAIN_2D assumes nonequilibrium interaction between the solution (c) and adsorbed (s) concentrations, and equilibrium interaction between the solution (c) and gas (g) concentrations of the solute in the soil system. The adsorption isotherm relating s_k and c_k is described by a generalized nonlinear equation of the form

$$s_k = \frac{k_{s,k} c_k^{\beta_k}}{1 + \eta_k c_k^{\beta_k}} \qquad k \epsilon (1, n_s) \tag{3.3}$$

$$\frac{\partial s_k}{\partial t} = \frac{k_{s,k}\beta_k c_k^{\beta_k - 1}}{(1 + \eta_k c_k^{\beta_k})^2} \frac{\partial c_k}{\partial t} + \frac{c_k^{\beta_k}}{1 + \eta_k c_k^{\beta_k}} \frac{\partial k_{s,k}}{\partial t} - \frac{k_{s,k} c_k^{2\beta_k}}{(1 + \eta_k c_k^{\beta_k})^2} \frac{\partial \eta_k}{\partial t} + \frac{k_{s,k} c_k^{\beta_k} \ln c_k}{(1 + \eta_k c_k^{\beta_k})^2} \frac{\partial \beta_k}{\partial t}$$

where $k_{s,k}$ [L^3M^{-1}], β_k [-] and η_k [L^3M^{-1}] are empirical coefficients. The Freundlich, Langmuir, and linear adsorption equations are special cases of equation (3.3). When β_k=1, equation (3.3) becomes the Langmuir equation, when η_k=0, equation (3.3) becomes the Freundlich equation, and when both β_k=1 and η_k=0, equation (3.3) leads to a linear adsorption isotherm. Solute transport without adsorption is described with $k_{s,k}$=0. While the coefficients $k_{s,k}$, β_k, and η_k in equation (3.3) are assumed to be independent of concentration, they are permitted to change as a function of time through their dependency on temperature. This feature will be discussed later.

The concept of two-site sorption [*Selim et al.*, 1977; *van Genuchten and Wagenet*, 1989] is implemented in CHAIN_2D to permit consideration of nonequilibrium adsorption-desorption reactions. The two-site sorption concept assumes that the sorption sites can be divided into two fractions:

$$s_k = s_k^e + s_k^k \qquad k \epsilon (1, n_s) \tag{3.4}$$

Sorption, s_k^e [MM^{-1}], on one fraction of the sites (the type-1 sites) is assumed to be instantaneous, while sorption, s_k^k [MM^{-1}], on the remaining (type-2) sites is considered to be time-dependent. At equilibrium we have for the type-1 (equilibrium) and type-2 (kinetic)

sites, respectively

$$s_k^e = f s_k \qquad k \in (1, n_s) \tag{3.5}$$

$$s_k^k = (1-f) s_k \qquad k \in (1, n_s) \tag{3.6}$$

where f is the fraction of exchange sites assumed to be in equilibrium with the solution phase [-]. Because type-1 sorption sites are always at equilibrium, differentiation of (3.5) gives immediately the sorption rate for the type-1 equilibrium sites:

$$\frac{\partial s_k^e}{\partial t} = f \frac{\partial s_k}{\partial t} \qquad k \in (1, n_s) \tag{3.7}$$

Sorption on the type-2 nonequilibrium sites is assumed to be a first-order kinetic rate process. Following *Toride et al.* [1993], the mass balance equation for the type-2 sites in the presence of production and degradation is given by

$$\frac{\partial s_k^k}{\partial t} = \omega_k \left[(1-f) \frac{k_{s,k} c_k^{\beta_k}}{1 + \eta_k c_k^{\beta_k}} - s_k^k \right] - (\mu_{s,k} + \mu'_{s,k}) s_k^k + (1-f) \gamma_{s,k} \qquad k \in (1, n_s) \tag{3.8}$$

where ω_k is the first-order rate constant for the kth solute [T^{-1}].

The concentrations g_k and c_k are related by a linear expression of the form

$$g_k = k_{g,k} c_k \qquad k \in (1, n_s) \tag{3.9}$$

where $k_{g,k}$ is an empirical constant [-] equal to $(K_H R_u T^A)^{-1}$ [*Stumm and Morgan*, 1981] in which K_H is Henry's Law constant [$MT^2M^{-1}L^{-2}$], R_u is the universal gas constant [$ML^2T^{-2}K^{-1}M^{-1}$] and T^A is absolute temperature [K].

Substituting (3.3) through (3.9) into (3.1) and (3.2), and using the continuity equation describing the isothermal Darcian flow of water in a variably saturated porous medium, i.e.,

$$\frac{\partial \theta}{\partial t} = -\frac{\partial q_i}{\partial x_i} - S \tag{3.10}$$

leads to the following equation

$$-\theta R_k \frac{\partial c_k}{\partial t} - q_i \frac{\partial c_k}{\partial x_i} + \frac{\partial}{\partial x_i}(\theta D_{ij,k} \frac{\partial c_k}{\partial x_j}) + F_k c_k + G_k = 0 \qquad k \epsilon (1, n_s) \tag{3.11}$$

in which D_{ij} [L^2T^{-1}] is an effective dispersion coefficient tensor given by

$$\theta D_{ij,k} = \theta D^{w}_{ij,k} + a_v D^{g}_{ij,k} k_{g,k} \qquad k \epsilon (1, n_s) \tag{3.12}$$

The coefficients F_k and G_k in (3.11) are defined as

$$\begin{aligned} F_k(c_k) = &-(\mu_{w,k} + \mu'_{w,k})\theta - (\mu_{s,k} + \mu'_{s,k})\rho f \frac{k_{s,k} c_k^{\beta_k - 1}}{1 + \eta_k c_k^{\beta_k}} - (\mu_{g,k} + \mu'_{g,k}) a_v k_{g,k} + \\ &+ S + k_{g,k} \frac{\partial \theta}{\partial t} - a_v \frac{\partial k_{g,k}}{\partial t} - \omega_k \rho \frac{(1-f) k_{s,k} c_k^{\beta_k - 1}}{1 + \eta_k c_k^{\beta_k}} - g_k(c_k) \quad k \epsilon (1, n_s) \end{aligned} \tag{3.13}$$

$$\begin{aligned} G_1(c_1) &= \gamma_{w,1}\theta + \gamma_{s,1} f \rho + \gamma_{g,1} a_v - S c_{r,1} + \omega_1 \rho s_1^k \\ G_k(c_k) &= (\mu'_{w,k-1}\theta + \mu'_{s,k-1} f \rho \frac{k_{s,k-1} c_{k-1}^{\beta_{k-1} - 1}}{1 + \eta_{k-1} c_{k-1}^{\beta_{k-1}}} + \mu_{g,k-1} a_v k_{g,k-1}) c_{k-1} + \\ &+ \mu'_{s,k-1} \rho s_{k-1}^k + \gamma_{w,k}\theta + \gamma_{s,k} f \rho + \gamma_{g,k} a_v - S c_{r,k} + \omega_k \rho s_k^k \qquad k \epsilon (2, n_s) \end{aligned} \tag{3.14}$$

where the variable g_k accounts for possible changes in the adsorption parameters caused by temperature changes in the system as follows (see also section 3.4):

$$g_k(c_k) = \rho f \left[\frac{c_k^{\beta_k - 1}}{1 + \eta_k c_k^{\beta_k}} \frac{\partial k_{s,k}}{\partial t} - \frac{k_{s,k} c_k^{2\beta_k - 1}}{(1 + \eta_k c_k^{\beta_k})^2} \frac{\partial \eta_k}{\partial t} + \frac{k_{s,k} \ln c_k c_k^{\beta_k - 1}}{(1 + \eta_k c_k^{\beta_k})^2} \frac{\partial \beta_k}{\partial t} \right] \quad k \epsilon (1, n_s) \tag{3.15}$$

The retardation factor R_k [-] in (3.11) is given by

$$R_k(c_k) = 1 + \frac{\rho}{\theta}\frac{f k_{s,k}\beta_k c_k^{\beta_k - 1}}{(1+\eta_k c_k^{\beta_k})^2} + \frac{a_v k_{g,k}}{\theta} \qquad k\epsilon(1,n_s) \tag{3.16}$$

Equation (3.11) has the same form as equation (3.4) of *Šimůnek et al.* [1992], except that the coefficients R_k, F_k, and G_k are now nonlinear in c_k because of the consideration of the nonlinear sorption. Because of this similarity, the development of the numerical solution of (3.11) is largely the same as that followed by *Šimůnek et al.* [1992] for the SWMS_2D code. In order to solve equation (3.11), it is necessary to know the water content θ and the volumetric flux q_i. Both variables are obtained from solutions of the Richards' equation. Assuming that μ_w', μ_s', μ_g', η_k, and k_g are zero, and f and β_k are equal to one, the entire system of equations (3.1) through (3.16) simplifies into a system of mutually independent solutes as described in SWMS_2D [*Šimůnek et al.*, 1992].

3.2. *Initial and Boundary Conditions*

The solution of (3.11) requires knowledge of the initial concentration within the flow region, Ω, i.e.,

$$\begin{aligned} c(x,z,0) &= c_i(x,z) \\ s^k(x,z,0) &= s_i^k(x,z) \end{aligned} \tag{3.17}$$

where c_i [ML^{-3}] and s_i^k [-] are prescribed functions of x and z. The initial condition for s_i^k must be specified only when nonequilibrium adsorption is considered. The subscript k is dropped in (3.17) and throughout the remainder of this report, thus assuming that the transport-related equations in the theoretical development and numerical solution apply to each of the solutes in the decay chain.

Two types of boundary conditions (Dirichlet and Cauchy type conditions) can be specified along the boundary of Ω. First-type (or Dirichlet type) boundary conditions prescribe the concentration along a boundary segment Γ_D:

$$c(x,z,t) = c_0(x,z,t) \qquad for\ (x,z) \in \Gamma_D \tag{3.18}$$

whereas third-type (Cauchy type) boundary conditions may be used to prescribe the concentration flux along a boundary segment Γ_C as follows:

$$-\theta D_{ij}\frac{\partial c}{\partial x_j}n_i + q_i n_i c = q_i n_i c_0 \qquad for\ (x,z) \in \Gamma_C \tag{3.19}$$

in which $q_i n_i$ represents the outward fluid flux, n_i is the outward unit normal vector and c_0 is the concentration of the incoming fluid [ML^{-3}]. In some cases, for example when Γ_C is an impermeable boundary ($q_i n_i = 0$) or when water flow is directed out of the region, (3.19) reduces to a second-type (Neumann type) boundary condition of the form:

$$\theta D_{ij}\frac{\partial c}{\partial x_j}n_i = 0 \qquad for\ (x,z) \in \Gamma_N \tag{3.20}$$

A different type of boundary condition is needed for volatile solutes when they are present in both the liquid and gas phases. This situation requires a third-type boundary condition which has on the right-hand side an additional term to account for gas diffusion through a stagnant boundary layer of thickness d [L] on the soil surface. The additional solute flux is proportional to the difference in gas concentrations above and below this boundary layer [*Jury et al.*, 1983]. This modified boundary condition has the form

$$-\theta D_{ij}\frac{\partial c}{\partial x_j}n_i + q_i n_i c = q_i n_i c_0 + \frac{D_g}{d}(k_g c - g_{atm}) \qquad for\ (x,z) \in \Gamma_C \tag{3.21}$$

where D_g is the molecular diffusion coefficient in the gas phase [L^2T^{-1}] and g_{atm} is the gas concentration above the stagnant boundary layer [ML^{-3}] (*Jury et al.* [1983] assumed g_{atm} to be zero). Similarly as for (3.19), (3.21) reduces to a second-type (Neumann type) boundary condition when water flow is zero or directed out of the region:

$$-\theta D_{ij}\frac{\partial c}{\partial x_j}n_i = \frac{D_g}{d}(k_g c - g_{atm}) \qquad for\ (x,z) \in \Gamma_N \tag{3.22}$$

Equations (3.21) and (3.22) can only be used when the additional gas diffusion flux is

positive. *Jury et al.* [1983] discussed how to estimate the thickness of the boundary layer, d, and recommended $d=0.5$ cm as a good average value for a bare surface.

3.3. *Effective Dispersion Coefficient*

The components of the dispersion tensor in the liquid phase, D_{ij}^{w}, are given by [*Bear*, 1972]

$$\theta D_{ij}^{w} = D_T |q| \delta_{ij} + (D_L - D_T)\frac{q_j q_i}{|q|} + \theta D_w \tau_w \delta_{ij} \tag{3.23}$$

where D_w is the molecular diffusion coefficient in free water [L^2T^{-1}], τ_w is a tortuosity factor in the liquid phase [-], $|q|$ is the absolute value of the Darcian fluid flux density [LT^{-1}], δ_{ij} is the Kronecker delta function ($\delta_{ij}=1$ if $i=j$, and $\delta_{ij}=0$ if $i\neq j$), and D_L and D_T are the longitudinal and transverse dispersivities, respectively [L]. After adding the diffusion contribution from the gas phase, the individual components of the effective dispersion tensor in the soil matrix for two-dimensional transport are as follows:

$$\begin{aligned}
\theta D_{xx} &= D_L\frac{q_x^2}{|q|} + D_T\frac{q_z^2}{|q|} + \theta D_w \tau_w + a_v D_g k_g \tau_g \\
\theta D_{zz} &= D_L\frac{q_z^2}{|q|} + D_T\frac{q_x^2}{|q|} + \theta D_w \tau_w + a_v D_g k_g \tau_g \\
\theta D_{xz} &= (D_L - D_T)\frac{q_x q_z}{|q|}
\end{aligned} \tag{3.24}$$

where D_g is the molecular diffusion coefficient in the gas phase [L^2T^{-1}] and τ_g is a tortuosity factor in the gas phase [-].

The tortuosity factors for both phases are evaluated in CHAIN_2D as a function of the water and gas contents using the relationship of *Millington and Quirk* [1961]:

$$\tau_w = \frac{\theta^{7/3}}{\theta_s^2}$$
$$\tau_g = \frac{a_v^{7/3}}{\theta_s^2} \qquad (3.25)$$

3.4. *Temperature Dependence of Transport and Reaction Coefficients*

Several of the diffusion (D_w, D_g), zero-order production (γ_w, γ_s, γ_g), first-order degradation (μ_w', μ_s', μ_g', μ_w, μ_s, and μ_g), and adsorption (k_s, k_g, β, η, ω) coefficients may be strongly dependent upon temperature. CHAIN_2D assumes that this dependency can be expressed by the Arrhenius equation [*Stumm and Morgan*, 1981]. After some modification, this equation can be expressed in the general form [*Šimůnek and Suarez*, 1993a]

$$a_T = a_r \exp\left[\frac{E_a(T^A - T_r^A)}{R_u T^A T_r^A}\right] \qquad (3.26)$$

where a_r and a_T are the values of the coefficient being considered at a reference absolute temperature T_r^A and absolute temperature T^A, respectively; R_u is the universal gas constant, and E_a [$ML^2T^{-2}M^{-1}$] is the activation energy of the particular reaction or process being modeled.

4. HEAT TRANSPORT

4.1. *Governing Heat Transport Equations*

Neglecting the effects of water vapor diffusion, two-dimensional heat transport can be described as [*Sophocleous*, 1979]:

$$C(\theta)\frac{\partial T}{\partial t} = \frac{\partial}{\partial x_i}[\lambda_{ij}(\theta)\frac{\partial T}{\partial x_j}] - C_w q_i \frac{\partial T}{\partial x_i} \tag{4.1}$$

where $\lambda_{ij}(\theta)$ is the apparent thermal conductivity of the soil [$MLT^{-3}K^{-1}$] (e.g. $Wm^{-1}K^{-1}$) and $C(\theta)$ and C_w are the volumetric heat capacities [$ML^{-1}T^{-2}K^{-1}$] (e.g. $Jm^{-3}K^{-1}$) of the porous medium and the liquid phase, respectively. Volumetric heat capacity is defined as the product of the bulk density and gravimetric heat capacity. The first term on the right-hand side of (4.1) represents heat flow due to conduction and the second term accounts for heat being transported by flowing water. We do not consider the transfer of latent heat by vapor movement. According to *de Vries* [1963] the volumetric heat capacity can be expressed as

$$C(\theta) = C_n\theta_n + C_o\theta_o + C_w\theta + C_g a_v \approx (1.92\,\theta_n + 2.51\,\theta_o + 4.18\,\theta)\,10^6 \quad [\mathrm{J\,m^{-3}K^{-1}}] \tag{4.2}$$

where θ refers to a volumetric fraction [L^3L^{-3}], and subscripts *n, o, g, w* represent solid phase, organic matter, gas phase and liquid phase, respectively.

4.2. *Apparent Thermal Conductivity Coefficient*

The apparent thermal conductivity, $\lambda_{ij}(\theta)$, combines the thermal conductivity $\lambda_0(\theta)$ of the porous medium (solid plus water) in the absence of flow, and the macrodispersivity which is assumed to be a linear function of the velocity [*de Marsily*, 1986]. In analogy with the dispersion coefficient for solute transport, the apparent thermal conductivity $\lambda_{ij}(\theta)$ is given by [*Šimůnek and Suarez*, 1993b]

$$\lambda_{ij}(\theta) = \lambda_T C_w |q| \delta_{ij} + (\lambda_L - \lambda_T) C_w \frac{q_j q_i}{|q|} + \lambda_0(\theta)\delta_{ij} \tag{4.3}$$

where $|q|$ is the absolute value of the Darcian fluid flux density [LT^{-1}], δ_{ij} is the Kronecker delta function as before, and λ_L and λ_T are the longitudinal and transverse thermal dispersivities [L], respectively. The individual components of the thermal conductivity tensor for two-dimensional transport are as follows:

$$\begin{aligned}
\lambda_{xx} &= \lambda_L C_w \frac{q_x^2}{|q|} + \lambda_T C_w \frac{q_z^2}{|q|} + \lambda_0 \\
\lambda_{zz} &= \lambda_L C_w \frac{q_z^2}{|q|} + \lambda_T C_w \frac{q_x^2}{|q|} + \lambda_0 \\
\lambda_{xz} &= (\lambda_L - \lambda_T) C_w \frac{q_x q_z}{|q|}
\end{aligned} \tag{4.4}$$

The volumetric heat capacity of the liquid phase is included here in the definition of the thermal conductivity in order to have the dimensions of the thermal dispersivities in the length units [*de Marsily*, 1986]. The thermal conductivity, $\lambda_0(\theta)$, accounts for the tortuosity of the porous medium, and is described with the simple equation [*Chung and Horton*, 1987]

$$\lambda_0(\theta) = b_1 + b_2\theta_w + b_3\theta_w^{0.5} \tag{4.5}$$

where b_1, b_2 and b_3 are empirical parameters [$MLT^{-3}K^{-1}$] (e.g. $Wm^{-1}K^{-1}$).

4.3. *Initial and Boundary Conditions*

Equation (4.1) will be solved subject to the general initial condition

$$T(x,z,0) = T_i(x,z) \tag{4.6}$$

where T_i is a prescribed function of x and z.

Two types of boundary conditions (Dirichlet and Cauchy type conditions) can again be specified along the boundary of Ω. First-type (or Dirichlet type) boundary conditions

prescribe the temperature along a boundary segment Γ_D:

$$T(x,z,t) = T_0(x,z,t) \qquad for\ (x,z) \in \Gamma_D \tag{4.7}$$

whereas third-type (Cauchy type) boundary conditions prescribe the heat flux along a boundary segment Γ_C as follows

$$-\lambda_{ij}\frac{\partial T}{\partial x_j}n_i + TC_w q_i n_i = T_0 C_w q_i n_i \qquad for\ (x,z) \in \Gamma_C \tag{4.8}$$

in which $q_i n_i$ represents the outward fluid flux, n_i is the outward unit normal vector and T_0 is the temperature of the incoming fluid. When Γ_C is an impermeable boundary ($q_i n_i = 0$) or when water flow is directed out of the region, (4.8) reduces to a second-type (Neumann type) boundary condition of the form:

$$\lambda_{ij}\frac{\partial T}{\partial x_j}n_i = 0 \qquad for\ (x,z) \in \Gamma_N \tag{4.9}$$

The atmospheric boundary condition for soil temperature is assumed to be given by a sine function as follows [*Kirkham and Powers*, 1972]:

$$T_0 = \bar{T} + A\sin\left(\frac{2\pi t^*}{t_p} - \frac{7\pi}{12}\right) \tag{4.10}$$

where t_p is the period of time [T] necessary to complete one cycle of the sine wave (taken to be 1 day), $\bar{T}$ is the average temperature at the soil surface [K] during period t_p, A is the amplitude of the sine wave [K], and t^* is the local time [T] within the period t_p. The second term within the argument of the sine function is included to allow the highest temperature to occur at 1 p.m.

5. NUMERICAL SOLUTION OF THE WATER FLOW EQUATION

The Galerkin finite element method with linear basis functions is used to obtain a solution of the flow equation (2.1) subject to the imposed initial and boundary conditions. Since the Galerkin method is relatively standard and has been covered in detail elsewhere [*Neuman*, 1975; *Zienkiewicz*, 1977; *Pinder and Gray*, 1977], only the most pertinent steps in the solution process are given here. The development given here is the same as in the SWMS_2D manual [*Šimůnek et al.*, 1992].

5.1. *Space Discretization*

The flow region is divided into a network of triangular elements. The corners of these elements are taken to be the nodal points. The dependent variable, the pressure head function $h(x,z,t)$, is approximated by a function $h'(x,z,t)$ as follows

$$h'(x,z,t) = \sum_{n=1}^{N} \phi_n(x,z)\, h_n(t) \tag{5.1}$$

where ϕ_n are piecewise linear basis functions satisfying the condition $\phi_n(x_m,z_m)=\delta_{nm}$, h_n are unknown coefficients representing the solution of (2.1) at the nodal points, and N is the total number of nodal points.

The Galerkin method postulates that the differential operator associated with the Richards' equation (2.1) is orthogonal to each of the N basis functions, i.e.,

$$\int_{\Omega} \{ \frac{\partial \theta}{\partial t} - \frac{\partial}{\partial x_i}[K(K_{ij}^A \frac{\partial h}{\partial x_j} + K_{iz}^A)] + S \}\, \phi_n d\Omega = 0 \tag{5.2}$$

Applying Green's first identity to (5.2), and replacing h by h', leads to

$$\sum_e \int_{\Omega_e} \left(\frac{\partial \theta}{\partial t}\phi_n + KK_{ij}^A \frac{\partial h'}{\partial x_j}\frac{\partial \phi_n}{\partial x_i}\right) d\Omega =$$

$$\sum_e \int_{\Gamma_e} K\left(K_{ij}^A \frac{\partial h'}{\partial x_j} + K_{iz}^A\right) n_i \phi_n d\Gamma + \sum_e \int_{\Omega_e} \left(-KK_{iz}^A \frac{\partial \phi_n}{\partial x_i} - S\phi_n\right) d\Omega \tag{5.3}$$

where Ω_e represents the domain occupied by element e, and Γ_e is a boundary segment of element e. Natural flux-type (Neumann) and gradient type boundary conditions can be immediately incorporated into the numerical scheme by specifying the line integral in equation (5.3).

After imposing additional simplifying assumptions to be discussed later, and performing integration over the elements, the procedure leads to a system of time-dependent ordinary differential equations with nonlinear coefficients. In matrix form, these equations are given by

$$[F]\frac{d\{\theta\}}{dt} + [A]\{h\} = \{Q\} - \{B\} - \{D\} \tag{5.4}$$

where

$$\begin{aligned} A_{nm} &= \sum_e K_l K_{ij}^A \int_{\Omega_e} \phi_l \frac{\partial \phi_n}{\partial x_i}\frac{\partial \phi_m}{\partial x_j} d\Omega \\ &= \sum_e \frac{K}{4A_e} \bar{K} \left[K_{xx}^A b_m b_n + K_{xz}^A (c_m b_n + b_m c_n) + K_{zz}^A c_n c_m\right] \end{aligned} \tag{5.5}$$

$$B_n = \sum_e K_l K_{iz}^A \int_{\Omega_e} \phi_l \frac{\partial \phi_n}{\partial x_i} d\Omega = \sum_e \frac{K}{2} \bar{K} \left(K_{xz}^A b_n + K_{zz}^A c_n\right) \tag{5.6}$$

$$F_{nm} = \delta_{nm} \sum_e \int_{\Omega_e} \phi_n d\Omega = \delta_{nm} \sum_e \frac{\kappa}{3} A_e \tag{5.7}$$

$$Q_n = -\sum_e \sigma_{1_l} \int_{\Gamma_e} \phi_l \phi_n d\Gamma = -\sum_e \sigma_{1_n} \lambda_n \tag{5.8}$$

$$D_n = \sum_e S_l \int_{\Omega_e} \phi_l \phi_n d\Omega = \sum_e \frac{\kappa}{12} A_e (3\bar{S} + S_n) \tag{5.9}$$

where the overlined variables represent average values over an element e, the subscripts i and j are space direction indices (i,j = 1,2), and

$$l = 1,2,...,N \quad m = 1,2,...,N \quad n = 1,2,...,N$$

$$\begin{aligned} b_i &= z_j - z_k & c_i &= x_k - x_j \\ b_j &= z_k - z_i & c_j &= x_i - x_k \\ b_k &= z_i - z_j & c_k &= x_j - x_i \end{aligned} \tag{5.10}$$

$$A_e = \frac{c_k b_j - c_j b_k}{2} \qquad \bar{K} = \frac{K_i + K_j + K_k}{3} \qquad \bar{S} = \frac{S_i + S_j + S_k}{3}$$

Equation (5.8) is valid for a flux-type boundary condition. For a gradient-type boundary condition the variable σ_1 in (5.8) must be replaced by the product of the hydraulic conductivity K and the prescribed gradient σ_2 (=1). Equations (5.5) through (5.9) hold for flow in a two-dimensional Cartesian (x,z) domain, as well as for flow in an axisymmetric (x,z) system in which x is used as the radial coordinate. For plane flow we have

$$\kappa = 1 \qquad \lambda_n = \frac{L_n}{2} \tag{5.11}$$

while for axisymmetric flow

$$\kappa = 2\pi \frac{x_i + x_j + x_k}{3} \qquad \lambda_n = L_n \pi \frac{x'_n + 2x_n}{3} \tag{5.12}$$

The subscripts i, j and k in equations (5.10) and (5.12) represent the three corners of a triangular element e. A_e is the area of element e, $\bar{K}$ and $\bar{S}$ are the average hydraulic conductivity and root water extraction values over element e, L_n is the length of the boundary segment connected to node n, and x'_n is the x-coordinate of a boundary node adjacent to node n. The symbol σ_n in equation (5.8) stands for the flux [LT^{-1}] across the boundary in the vicinity of boundary node n (positive when directed outward of the system). The boundary flux is assumed to be uniform over each boundary segment. The entries of the vector Q_n are zero at all internal nodes which do not act as sources or sinks for water.

The numerical procedure leading to (5.4) incorporates two important assumptions in addition to those related to the Galerkin finite element approach. One assumption concerns the time derivatives of the nodal values of the water content in (5.4). These time derivatives were weighted according to

$$\frac{d\theta_n}{dt} = \frac{\sum_e \int_{\Omega_e} \frac{\partial \theta}{\partial t} \phi_n d\Omega}{\sum_e \int_{\Omega_e} \phi_n d\Omega} \tag{5.13}$$

This assumption implements mass-lumping which has been shown to improve the rate of convergence of the iterative solution process [e.g., *Neuman*, 1973].

A second assumption in the numerical scheme is related to the anisotropy tensor $\mathbf{K}^A$ which is taken to be constant over each element. By contrast, the water content θ, the hydraulic conductivity K, the soil water capacity C, and the root water extraction rate S, at a given point in time are assumed to vary linearly over each element, e. For example, the water content is expanded over each element as follows:

$$\theta(x,z) = \sum_{n=1}^{3} \theta(x_n,z_n)\,\phi_n(x,z) \qquad for\ (x,z) \in \Omega_e \tag{5.14}$$

where n stands for the corners of element e. The advantage of linear interpolation is that no numerical integration is needed to evaluate the coefficients in (5.4).

5.2. *Time Discretization*

Integration of (5.4) in time is achieved by discretizing the time domain into a sequence of finite intervals and replacing the time derivatives by finite differences. An implicit (backward) finite difference scheme is used for both saturated and unsaturated conditions:

$$[F]\frac{\{\theta\}_{j+1} - \{\theta\}_j}{\Delta t_j} + [A]_{j+1}\{h\}_{j+1} = \{Q\}_j - \{B\}_{j+1} - \{D\}_j \tag{5.15}$$

where $j+1$ denotes the current time level at which the solution is being considered, j refers to the previous time level, and $\Delta t_j = t_{j+1} - t_j$. Equation (5.15) represents the final set of algebraic equations to be solved. Since the coefficients θ, A, B, D, and Q (Q for only gradient-type boundary conditions) are functions of h, the set of equations is generally highly nonlinear. Note that the vectors D and Q are evaluated at the old time level.

5.3. *Numerical Solution Strategy*

5.3.1. *Iterative Process*

Because of the nonlinear nature of (5.15), an iterative process must be used to obtain solutions of the global matrix equation at each new time step. For each iteration a system of linearized algebraic equations is first derived from (5.15) which, after incorporation of the boundary conditions, is solved using either Gaussian elimination or the conjugate gradient method (see Section 7.5). The Gaussian elimination process takes advantage of

the banded and symmetric features of the coefficient matrices in (5.15). After inversion, the coefficients in (5.15) are re-evaluated using the first solution, and the new equations are again solved. The iterative process continues until a satisfactory degree of convergence is obtained, i.e., until at all nodes in the saturated (or unsaturated) region the absolute change in pressure head (or water content) between two successive iterations becomes less than some small value determined by the imposed absolute pressure head (or water content) tolerance [*Šimůnek and Suarez*, 1993b]. The first estimate (at zero iteration) of the unknown pressure heads at each time step is obtained by extrapolation from the pressure head values at the previous two time levels.

5.3.2. *Treatment of the Water Capacity Term*

The iteration process is extremely sensitive to the method used for evaluating the water content term ($\Delta\theta/\Delta t$) in equation (5.15). The present version of CHAIN_2D code uses the "mass-conservative" method proposed by *Celia et al.* [1990]. Their method has been shown to provide excellent results in terms of minimizing the mass balance error. The mass-conservative method proceeds by separating the water content term into two parts:

$$[F]\frac{\{\theta\}_{j+1}-\{\theta\}_j}{\Delta t_j}=[F]\frac{\{\theta\}_{j+1}^{k+1}-\{\theta\}_{j+1}^{k}}{\Delta t_j}+[F]\frac{\{\theta\}_{j+1}^{k}-\{\theta\}_j}{\Delta t_j} \tag{5.16}$$

where $k+1$ and k denote the current and previous iteration levels, respectively; and $j+1$ and j the current and previous time levels, respectively. Notice that the second term on the right hand side of (5.16) is known prior to the current iteration. The first term on the right hand side can be expressed in terms of the pressure head, so that (5.16) becomes

$$[F]\frac{\{\theta\}_{j+1}-\{\theta\}_j}{\Delta t_j}=[F][C]_{j+1}\frac{\{h\}_{j+1}^{k+1}-\{h\}_{j+1}^{k}}{\Delta t_j}+[F]\frac{\{\theta\}_{j+1}^{k}-\{\theta\}_j}{\Delta t_j} \tag{5.17}$$

where $C_{nm}=\delta_{nm}C_n$, in which C_n represents the nodal value of the soil water capacity. The first term on the right hand side of (5.17) should vanish at the end of the iteration process if the numerical solution converges. This particular feature guarantees relatively small mass

balance errors in the solution.

5.3.3. *Time Control*

Three different time discretizations are introduced in CHAIN_2D: (1) time discretizations associated with the numerical solution, (2) time discretizations associated with the implementation of boundary conditions, and (3) time discretizations which provide printed output of the simulation results (e.g., nodal values of dependent variables, water and solute mass balance components, and other information about the flow regime).

Discretizations 2 and 3 are mutually independent; they generally involve variable time steps as described in the input data file. Discretization 1 starts with a prescribed initial time increment, Δt. This time increment is automatically adjusted at each time level according to the following rules [*Mls*, 1982; *Vogel*, 1987]:

a. Discretization 1 must coincide with time values resulting from discretizations 2 and 3.
b. Time increments cannot become less than a preselected minimum time step, Δt_{min}, nor exceed a maximum time step, Δt_{max} (i.e., $\Delta t_{min} \leq \Delta t \leq \Delta t_{max}$).
c. If, during a particular time step, the number of iterations necessary to reach convergence is ≤ 3, the time increment for the next time step is increased by multiplying Δt by a predetermined constant >1 (usually between 1.1 and 1.5). If the number of iterations is ≥ 7, Δt for the next time level is multiplied by a constant <1 (usually between 0.3 and 0.9).
d. If, during a particular time step, the number of iterations at any time level becomes greater than a prescribed maximum (usually between 10 and 50), the iterative process for that time level is terminated. The time step is subsequently reset to $\Delta t/3$, and the iterative process restarted.

The selection of optimal time steps, Δt, is also influenced by the solution scheme for solute transport (see Section 6.3.6).

5.3.4. *Treatment of Pressure Head Boundary Conditions*

Finite element equations corresponding to Dirichlet nodes where the pressure head is prescribed can, at least in principle, be eliminated from the global matrix equation. An alternative and numerically simpler approach is to replace the Dirichlet finite element equations by dummy expressions of the form [*Neuman*, 1974]

$$\delta_{nm} h_m = \psi_n \tag{5.18}$$

where δ_{nm} is the Kronecker delta and ψ_n is the prescribed value of the pressure head at node n. The values of h_n in all other equations are set equal to ψ_n and the appropriate entries containing ψ_n in the left hand side matrix are incorporated into the known vector on the right-hand side of the global matrix equation. When done properly, this rearrangement will preserve symmetry in the matrix equation. This procedure is applied only when Gaussian elimination is used to solve the matrix equations. When the conjugate gradient solver is used, then the finite element equation representing the Dirichlet node is modified as follows. The right hand side of this equation is set equal to the prescribed pressure head multiplied by a large number (10^{30}), and entry on the left hand side representing the Dirichlet node is set equal to this large number. After solving for all pressure heads, the value of the flux Q_n can be calculated explicitly and accurately from the original finite element equation associated with node n [e.g., *Lynch*, 1984].

5.3.5. *Flux and Gradient Boundary Conditions*

The values of the fluxes Q_n at nodal points along prescribed flux and gradient boundaries are computed according to equation (5.8). Internal nodes which act as Neumann type sources or sinks have values of Q_n equal to the imposed fluid injection or extraction rate.

5.3.6. *Atmospheric Boundary Conditions and Seepage Faces*

Atmospheric boundaries are simulated by applying either prescribed head or prescribed flux boundary conditions depending upon whether equation (2.29) or (2.30) is satisfied [*Neuman*, 1974]. If (2.30) is not satisfied, node n becomes a prescribed head boundary. If, at any point in time during the computations, the calculated flux exceeds the specified potential flux in (2.29), the node will be assigned a flux equal to the potential value and treated again as a prescribed flux boundary.

All nodes expected to be part of a seepage face during code execution must be identified a priori. During each iteration, the saturated part of a potential seepage face is treated as a prescribed pressure head boundary with $h=0$, while the unsaturated part is treated as a prescribed flux boundary with $Q=0$. The lengths of the two surface segments are continually adjusted [*Neuman*, 1974] during the iterative process until the calculated values of Q (equation (5.8)) along the saturated part, and the calculated values of h along the unsaturated part, are all negative, thus indicating that water is leaving the flow region through the saturated part of the surface boundary only.

4.3.7. *Tile Drains as Boundary Conditions*

The representation of tile drains as boundary conditions is based on studies by *Vimoke et al.* [1963] and *Fipps et al.* [1986]. The approach uses results of electric analog experiments conducted by *Vimoke and Taylor* [1962] who reasoned that drains can be represented by nodal points in a regular finite element mesh, provided adjustments are made in the hydraulic conductivity, K, of neighboring elements. The adjustments should correspond to changes in the electric resistance of conducting paper as follows

$$K_{drain} = K C_d \tag{5.19}$$

where K_{drain} is the adjusted conductivity [LT^{-1}], and C_d is the correction factor [-]. C_d is determined from the ratio of the effective radius, d_e [L], of the drain to the side length, D

[L], of the square formed by finite elements surrounding the drain node [*Vimoke at al.*, 1962]:

$$C_d = \frac{Z_0'}{Z_0} \approx \frac{\sqrt{\mu_0 / \epsilon_0}}{138 \log_{10}\rho_d + 6.48 - 2.34A - 0.48B - 0.12C} \tag{5.20}$$

where Z_0' is the characteristic impedance of free space ($\approx$376.7 ohms), μ_0 is the permeability of free space, ϵ_0 is the permittivity of free space, and Z_0 is the characteristic impedance of a transmission line analog of the drain. The coefficients in (5.20) are given by

$$\rho_d = \frac{D}{d_e} \qquad A = \frac{1 + 0.405\rho_d^{-4}}{1 - 0.405\rho_d^{-4}}$$

$$B = \frac{1 + 0.163\rho_d^{-8}}{1 - 0.163\rho_d^{-8}} \qquad C = \frac{1 + 0.067\rho_d^{-12}}{1 - 0.067\rho_d^{-12}} \tag{5.21}$$

where d_e is the effective drain diameter to be calculated from the number and size of small openings in the drain tube [*Mohammad and Skaggs*, 1984], and D is the size of the square in the finite element mesh surrounding the drain having adjusted hydraulic conductivities. The approach above assumes that the node representing a drain must be surrounded by finite elements (either triangular or quadrilateral) which form a square whose hydraulic conductivities are adjusted according to (5.19). This method of implementing drains by means of a boundary condition gives an efficient, yet relatively accurate, prediction of the hydraulic head in the immediate vicinity of the drain, as well as of the drain flow rate [*Fipps et al.*, 1986]. More recent studies have shown that the correction factor, C_d, could be further reduced by a factor of 2 [*Rogers and Fouss*, 1989] or 4 [*Tseng*, 1994, personal communication]. These two studies compared numerical simulations of the flow of ponded water into a tile drain system with an analytical solution given by *Kirkham* [1949]. Pressure head contours calculated numerically with the original correction factor C_d (5.20), as well as with the additionally reduced correction factor $C_d/4$, were compared with the analytical results in *Šimůnek et al.* [1994].

5.3.8. *Water Balance Computations*

The CHAIN_2D code performs water balance computations at prescribed times for several preselected subregions of the flow domain. The water balance information for each subregion consists of the actual volume of water, V, in that subregion, and the rate, O, of inflow or outflow to or from the subregion. V and O are given by

$$V = \sum_e \kappa A_e \frac{\theta_i + \theta_j + \theta_k}{3} \tag{5.22}$$

and

$$O = \frac{V_{new} - V_{old}}{\Delta t} \tag{5.23}$$

respectively, where θ_i, θ_j, and θ_k are water contents evaluated at the corner nodes of element e, and where V_{new} and V_{old} are volumes of water in the subregion computed at the current and previous time levels, respectively. The summation in (5.22) is taken over all elements within the subregion.

The absolute error in the mass balance is calculated as

$$\epsilon_a^w = V_t - V_0 + L_t \int_0^t T_a dt - \int_0^t \sum_{n_r} Q_n dt \tag{5.24}$$

where V_t and V_0 are the volumes of water in the flow domain at time t and zero, respectively, as calculated with (5.22). The third term on the right-hand side represents the cumulative root water uptake amount, while the fourth term gives the cumulative flux through nodes, n_r, located along the boundary of the flow domain or at internal source and sink nodes.

The accuracy of the numerical solution is evaluated in terms of the relative error, ϵ_r^w [%], in the water mass balance as follows:

$$\epsilon_r^w = \frac{|\epsilon_a^w|}{\max\left[\sum_e |V_t^e - V_0^e|,\ L_t \int_0^t T_a dt + \int_0^t \sum_{n_r} |Q_n| dt\right]} 100 \qquad (5.25)$$

where V_t^e and V_0^e are the volumes of water in element e at times t and zero, respectively. Note that CHAIN_2D does not relate the absolute error to the volume of water in the flow domain, but instead to the maximum value of two quantities. The first quantity represents the sum of the absolute changes in water content over all elements, whereas the second quantity is the sum of the absolute values of all fluxes in and out of the flow domain. This criterion is much more strict than the usual criterion involving the total volume of water in the flow domain. This is because cumulative boundary fluxes are often much smaller than the volume in the domain, especially at the beginning of the simulation.

5.3.9. *Computation of Nodal Fluxes*

Components of the Darcian flux are computed at each time level during the simulation only when the water flow and solute transport equations are solved simultaneously. When the flow equation is being solved alone, the flux components are calculated only at selected print times. The x- and z-components of the nodal fluxes are computed for each node n according to:

$$q_x = -\frac{K_n}{N_e}\sum_{e_n}\left[\frac{\gamma_i^x h_i + \gamma_j^x h_j + \gamma_k^x h_k}{2A_e} + K_{xz}^A\right]$$

$$q_z = -\frac{K_n}{N_e}\sum_{e_n}\left[\frac{\gamma_i^z h_i + \gamma_j^z h_j + \gamma_k^z h_k}{2A_e} + K_{zz}^A\right] \qquad (5.26)$$

$$\gamma_n^x = K_{xx}^A b_n + K_{xz}^A c_n$$

$$\gamma_n^z = K_{xz}^A b_n + K_{zz}^A c_n$$

where N_e is the number of sub-elements e_n adjacent to node n. Einstein's summation

convention is not used in (5.26).

5.3.10. *Water Uptake by Plant Roots*

CHAIN_2D considers the root zone to consist of all nodes, n, for which the potential root water uptake distribution, b (see Section 2.2), is greater than zero. The root water extraction rate is assumed to vary linearly over each element; this leads to approximation (5.9) for the root water extraction term D_n in the global matrix equation. The values of the actual root extraction rate S_n in (5.9) are evaluated with (2.9). In order to speed up the calculations, the extraction rates S_n are calculated at the old time level and are not updated during the iterative solution process at a given time step. CHAIN_2D calculates the total rate of transpiration per unit soil surface length using the equation

$$T_a = \frac{1}{L_t} \sum_e \kappa A_e \bar{S} \tag{5.27}$$

in which the summation takes place over all elements within the root zone.

5.3.11. *Evaluation of the Soil Hydraulic Properties*

At the beginning of a numerical simulation, CHAIN_2D generates for each soil type in the flow domain a table of water contents, hydraulic conductivities, and specific water capacities from the specified set of hydraulic parameters. The values of θ_i, K_i and C_i in the table are evaluated at prescribed pressure heads h_i within a specified interval (h_a, h_b). The entries in the table are generated such that

$$\frac{h_{i+1}}{h_i} = constant \tag{5.28}$$

which means that the spacing between two consecutive pressure head values increases in a logarithmic fashion. Values for the hydraulic properties, $\theta(h)$, $K(h)$ and $C(h)$, are computed

during the iterative solution process using linear interpolation between the entries in the table. If an argument h falls outside the prescribed interval (h_a, h_b), the hydraulic characteristics are evaluated directly from the hydraulic functions, i.e., without interpolation. The above interpolation technique was found to be much faster computationally than direct evaluation of the hydraulic functions over the entire range of pressure heads, except when very simple hydraulic models were used.

5.3.12. *Implementation of Hydraulic Conductivity Anisotropy*

Since the hydraulic conductivity anisotropy tensor, $\mathbf{K}^A$, is assumed to be symmetric, it is possible to define at any point in the flow domain a local coordinate system for which the tensor $\mathbf{K}^A$ is diagonal (i.e., having zeroes everywhere except on the diagonal). The diagonal entries K_1^A and K_2^A of $\mathbf{K}^A$ are referred to as the principal components of $\mathbf{K}^A$.

The CHAIN_2D code permits one to vary the orientation of the local principal directions from element to element. For this purpose, the local coordinate axes are subjected to a rotation such that they coincide with the principal directions of the tensor $\mathbf{K}^A$. The principal components K_1^A and K_2^A, together with the angle ω_a between the principal direction of K_1^A and the x-axis of the global coordinate system, are specified for each element. Each locally determined tensor $\mathbf{K}^A$ is transformed to the global (x,z) coordinate system at the beginning of the simulation using the following rules:

$$\begin{aligned} K_{xx}^A &= K_1^A \cos^2\omega_a + K_2^A \sin^2\omega_a \\ K_{zz}^A &= K_1^A \sin^2\omega_a + K_2^A \cos^2\omega_a \\ K_{xz}^A &= (K_2^A - K_1^A)\sin\omega_a \cos\omega_a \end{aligned} \tag{5.29}$$

5.3.13. *Steady-State Analysis*

All transient flow problems are solved by time marching until a prescribed time is

reached. The steady-state problem can be solved in the same way, i.e., by time marching until two successive solutions differ less than some prescribed pressure head tolerance. CHAIN_2D implements a faster way of obtaining the steady-state solution without having to go through a large number of time steps. The steady-state solution for a set of imposed boundary conditions is obtained directly during one set of iterations at the first time step by equating the time derivative term in the Richards' equation (2.1) to zero.

6. NUMERICAL SOLUTION OF THE SOLUTE TRANSPORT EQUATION

The Galerkin finite element method is also used to solve the solute and heat transport equations (equations (3.11) and (4.1), respectively) subject to appropriate initial and boundary conditions. Since the heat transport equation (4.1) has the same mathematical form as the (linearized) solute transport equation (3.11), the numerical solution will be given here only for solute transport. The solution procedure largely parallels the approach used in Section 5 for the flow equation.

6.1. *Space Discretization*

The dependent variable, the concentration function $c(x,z,t)$, is approximated by a finite series $c'(x,z,t)$ of the form

$$c'(x,z,t) = \sum_{n=1}^{N} \phi_n(x,z)\, c_n(t) \tag{6.1}$$

where ϕ_n are the selected linear basis functions, c_n are the unknown time dependent coefficients which represent solutions of (3.11) at the finite element nodal points and, as before, N is the total number of nodal points. Application of the standard Galerkin method leads to the following set of N equations

$$\int_{\Omega} [-\theta R \frac{\partial c}{\partial t} - q_i \frac{\partial c}{\partial x_i} + \frac{\partial}{\partial x_i}(\theta D_{ij} \frac{\partial c}{\partial x_j}) + Fc + G]\phi_n d\Omega = 0 \tag{6.2}$$

Application of Green's theorem to the second derivatives in (6.2) and substitution of c by c' results in the following system of time-dependent differential equations

$$\begin{aligned} \sum_e \int_{\Omega_e} [(-\theta R \frac{\partial c'}{\partial t} - q_i \frac{\partial c'}{\partial x_i} + Fc' + G)\phi_n - \theta D_{ij} \frac{\partial c'}{\partial x_j} \frac{\partial \phi_n}{\partial x_i}] d\Omega \\ + \sum_e \int_{\Gamma_e} \theta D_{ij} \frac{\partial c'}{\partial x_j} n_i \phi_n d\Gamma = 0 \end{aligned} \tag{6.3}$$

or in matrix form:

$$[Q]\frac{d\{c\}}{dt} + [S]\{c\} + \{f\} = -\{Q^D\} \tag{6.4}$$

where

$$Q_{nm} = \delta_{nm}\sum_e (-\theta R)_l \int_{\Omega_e} \phi_l \phi_n d\Omega = -\sum_e \frac{\kappa A_e}{12}(3\overline{\theta R} + \theta_n R_n)\delta_{nm} \tag{6.5}$$

$$\begin{aligned} S_{nm} &= \sum_e [(-q_i)_l \int_{\Omega_e} \phi_l \phi_n \frac{\partial \phi_m}{\partial x_i} d\Omega - (\theta D_{ij})_l \int_{\Omega_e} \phi_l \frac{\partial \phi_n}{\partial x_i}\frac{\partial \phi_m}{\partial x_j} d\Omega + F_l \int_{\Omega_e} \phi_l \phi_n \phi_m d\Omega] = \\ &= \sum_e \{-\frac{\kappa b_m}{24}(3\overline{q_x} + q_{xn}) - \frac{\kappa c_m}{24}(3\overline{q_z} + q_{zn}) + \frac{\kappa A_e}{60}(3\bar{F} + F_n + F_m)(1+\delta_{nm}) \\ &\quad - \frac{\kappa}{4A_e}[b_m b_n \theta\overline{D_{xx}} + (b_m c_n + c_m b_n)\theta\overline{D_{xz}} + c_m c_n \theta\overline{D_{zz}})\} \end{aligned} \tag{6.6}$$

$$f_n = \sum_e G_l \int_{\Omega_e} \phi_l \phi_n d\Omega = \sum_e \frac{\kappa A_e}{12}(3\bar{G} + G_n) \tag{6.7}$$

in which the overlined variables represent average values over a given element *e*. The notation in the above equations is similar as in (5.10). The boundary integral in (6.3) represents the dispersive flux, Q_n^D, across the boundary and will be discussed later in Section 6.3.4.

The derivation of equations (6.5) through (6.7) invoked several important assumptions in addition to those involved in the Galerkin finite element approach [*Huyakorn and Pinder*, 1983; *van Genuchten*, 1978]. First, the different coefficients under the integral signs (θR, q_i, θD_{ij}, F, G) were expanded linearly over each element, similarly as for the dependent variable, i.e., in terms of their nodal values and associated basis functions. Second, mass lumping was invoked by redefining the nodal values of the time derivative in (6.4) as weighted averages over the entire flow region:

$$\frac{dc_n}{dt} = \frac{\sum_e \int_{\Omega_e} \theta R \frac{\partial c'}{\partial t} \phi_n d\Omega}{\sum_e \int_{\Omega_e} \theta R \phi_n d\Omega} \tag{6.8}$$

6.2. *Time Discretization*

The Galerkin method is used only for approximating the spatial derivatives while the time derivatives are discretized by means of finite differences. A first-order approximation of the time derivatives leads to the following set of algebraic equations:

$$[Q]_{j+\epsilon} \frac{\{c\}_{j+1} - \{c\}_j}{\Delta t} + \epsilon[S]_{j+1}\{c\}_{j+1} + (1-\epsilon)[S]_j\{c\}_j + \epsilon\{f\}_{j+1} + (1-\epsilon)\{f\}_j = 0 \tag{6.9}$$

where j and $j+1$ denote the previous and current time levels, respectively; Δt is the time increment, and ϵ is a time weighing factor. The incorporation of the dispersion flux, Q_n^D, into matrix $[Q]$ and vector $\{f\}$ is discussed in Section 6.3.4. The coefficient matrix $[Q]_{j+\epsilon}$ is evaluated using weighted averages of the current and previous nodal values of θ and R. Equation (6.9) can be rewritten in the form:

$$[G]\{c\}_{j+1} = \{g\} \tag{6.10}$$

where

$$\begin{aligned} [G] &= \frac{1}{\Delta t}[Q]_{j+\epsilon} + \epsilon[S]_{j+1} \\ \{g\} &= \frac{1}{\Delta t}[Q]_{j+\epsilon}\{c\}_j - (1-\epsilon)[S]_j\{c\}_j - \epsilon\{f\}_{j+1} - (1-\epsilon)\{f\}_j \end{aligned} \tag{6.11}$$

Higher-order approximations for the time derivative in the transport equation were derived by *van Genuchten* [1976, 1978]. The higher-order effects may be incorporated into

the transport equation by introducing time-dependent dispersion corrections as follows

$$D_{ij}^{-} = D_{ij} - \frac{q_i q_j \Delta t}{6\theta^2 R}$$
$$D_{ij}^{+} = D_{ij} + \frac{q_i q_j \Delta t}{6\theta^2 R} \qquad (6.12)$$

where the superscripts + and - indicate evaluation at the old and new time levels, respectively.

6.3. *Numerical Solution Strategy*

6.3.1. *Solution Process*

The solution process at each time step proceeds as follows. First, an iterative procedure is used to obtain the solution of the Richards' equation (2.1) (see Section 5.3.1). After achieving convergence, the solution of the transport equation (6.10) is implemented. This is done by first determining the nodal values of the fluid flux from nodal values of the pressure head by applying Darcy's law. Nodal values of the water content and the fluid flux at the previous time level are already known from the solution at the previous time step. Values for the water content and the fluid flux are subsequently used as input to the transport equations (first for heat transport and then for solute transport), leading to the system of linear algebraic equations given by (6.10). The structure of the final set of equations depends upon the value of the temporal weighing factor, ϵ. The explicit ($\epsilon=0$) and fully implicit ($\epsilon=1$) schemes require that the global matrix $[G]$ and the vector $\{g\}$ be evaluated at only one time level (the previous or current time level). All other schemes require evaluation at both time levels. Also, all schemes except for the explicit formulation ($\epsilon=0$) lead to an asymmetric banded matrix $[G]$. The associated set of algebraic equations is solved using either a standard asymmetric matrix equation solver [e.g., *Neuman*, 1972], or the ORTHOMIN method [*Mendoza et al.*, 1991], depending upon the size of final matrix. By contrast, the explicit scheme leads to a diagonal matrix $[G]$ which is much easier to solve

(but generally requires smaller time steps).

Since the heat transport equation is linear, there is no need for an iterative solution process for heat flow. The same is true for the transport of solutes undergoing only linear sorption reactions. On the other hand, iteration is needed when a nonlinear reaction between the solid and liquid phase is considered. The iteration procedure for solute transport is very similar to that for water flow. The coefficients in (6.10) are re-evaluated using each iteration, and the new equations are again solved using results of the previous iteration. The iterative process continues until a satisfactory degree of convergence is obtained, i.e., until at all nodes the absolute change in concentration between two successive iterations becomes less than some small value determined by the imposed relative and absolute concentration tolerances.

6.3.2. *Upstream Weighted Formulation*

Upstream weighing is provided as an option in the CHAIN_2D to minimize some of the problems with numerical oscillations when relatively steep concentration fronts are being simulated. For this purpose the second (flux) term of equation (6.3) is not weighted by regular linear basis functions ϕ_n, but instead using the nonlinear functions ϕ_n^u [*Yeh and Tripathi*, 1990]

$$\begin{aligned}
\phi_1^u &= L_1 - 3\alpha_3^w L_2 L_1 + 3\alpha_2^w L_3 L_1 \\
\phi_2^u &= L_2 - 3\alpha_1^w L_3 L_2 + 3\alpha_3^w L_1 L_2 \\
\phi_3^u &= L_3 - 3\alpha_2^w L_1 L_3 + 3\alpha_1^w L_2 L_3
\end{aligned} \tag{6.13}$$

where α_i^w is a weighing factor associated with the length of the element size opposite to node i, and L_i are the local coordinates. The weighing factors are evaluated using the equation of *Christie et al.* [1976]:

$$\alpha_i^w = \coth\left(\frac{uL}{2D}\right) - \frac{2D}{uL} \tag{6.14}$$

where u, D and L are the flow velocity, dispersion coefficient and length associated with side i. The weighing functions ϕ^u ensure that relatively more weight is placed on the flow velocities of nodes located at the upstream side of an element. Evaluating the integrals in (6.3) shows that the following additional terms must be added to the entries of the global matrix S_{nm} in equation (6.6):

$$\begin{aligned} S_{1j}^{e'} = S_{1j}^{e} &- \frac{b_j}{40}\left[2q_{x1}(\alpha_2^w - \alpha_3^w) + q_{x2}(\alpha_2^w - 2\alpha_3^w) + q_{x3}(2\alpha_2^w - \alpha_3^w)\right] \\ &- \frac{c_j}{40}\left[2q_{z1}(\alpha_2^w - \alpha_3^w) + q_{z2}(\alpha_2^w - 2\alpha_3^w) + q_{z3}(2\alpha_2^w - \alpha_3^w)\right] \end{aligned} \tag{6.15}$$

$$\begin{aligned} S_{2j}^{e'} = S_{2j}^{e} &- \frac{b_j}{40}\left[q_{x1}(2\alpha_3^w - \alpha_1^w) + 2q_{x2}(\alpha_3^w - \alpha_1^w) + q_{x3}(\alpha_3^w - 2\alpha_1^w)\right] \\ &- \frac{c_j}{40}\left[q_{z1}(2\alpha_3^w - \alpha_1^w) + 2q_{z2}(\alpha_3^w - \alpha_1^w) + q_{z3}(\alpha_3^w - 2\alpha_1^w)\right] \end{aligned} \tag{6.16}$$

and

$$\begin{aligned} S_{3j}^{e'} = S_{3j}^{e} &- \frac{b_j}{40}\left[q_{x1}(\alpha_1^w - 2\alpha_2^w) + q_{x2}(2\alpha_1^w - \alpha_2^w) + 2q_{x3}(\alpha_1^w - \alpha_2^w)\right] \\ &- \frac{c_j}{40}\left[q_{z1}(\alpha_1^w - 2\alpha_2^w) + q_{z2}(2\alpha_1^w - \alpha_2^w) + 2q_{z3}(\alpha_1^w - \alpha_2^w)\right] \end{aligned} \tag{6.17}$$

The weighing factors are applied only to those element sides that are inclined within 10 degrees from the flow direction.

6.3.3. *Implementation of First-Type Boundary Conditions*

Individual equations in the global matrix equation which correspond to nodes at which the concentration is prescribed are replaced by new equations:

$$\delta_{nm} c_m = c_{n0} \tag{6.18}$$

where c_{n0} is the prescribed value of the concentration at node n. This is done only when Gaussian elimination is used to solve the matrix equation. A similar procedure as for water flow (described in Section 5.3.4) is applied when the ORTHOMIN method is used. Because of asymmetry of the global matrix [G], no additional manipulations are needed in the resulting system of equations as was the case for the water flow solution.

The total material flux, Q_n^T, through a boundary at node n consists of the dispersive flux, Q_n^D, and the convective flux, Q_n^A:

$$Q_n^T = Q_n^D + Q_n^A \tag{6.19}$$

The dispersive boundary nodal flux is not known explicitly but must be calculated from equation (6.4). Hence, the dispersion flux, Q_n^D, for node n can be calculated as

$$Q_n^D = -[\epsilon S_{nm}^{j+1} + (1-\epsilon) S_{nm}^j] c_m^j - \epsilon f_n^{j+1} - (1-\epsilon) f_n^j - Q_{nn}^{j+\epsilon} \frac{c_n^{j+1} - c_n^j}{\Delta t} \tag{6.20}$$

The convective flux is evaluated as

$$Q_n^A = Q_n c_n \tag{6.21}$$

where the fluid flux Q_n is known from the solution of the water flow equation.

6.3.4. *Implementation of Third-Type Boundary Conditions*

Equation (3.19) is rewritten as follows

$$\theta D_{ij} \frac{\partial c'}{\partial x_j} n_i = q_i n_i (c - c_0) \tag{6.22}$$

When substituted into the last term of (6.3), the boundary integral becomes

$$\sum_e \int_{\Gamma_e} \theta D_{ij} \frac{\partial c'}{\partial x_j} n_i \phi_n d\Gamma = Q_n c_n - Q_n c_{n0} \tag{6.23}$$

The first term on the right-hand side of (6.23) represents the convective flux. This term is incorporated into the coefficient matrix [*S*] of (6.4). The last term of (6.23) represents the total material flux, which is added to the known vector {*f*}.

At nodes where free outflow of water and its dissolved solutes takes place, the exit concentration c_0 is equal to the local (nodal) concentration c_n. In this case the dispersive flux becomes zero and the total material flux through the boundary is evaluated as

$$Q_n^T = Q_n c_n \tag{6.24}$$

The Cauchy boundary condition for volatile solutes is treated in a similar way. Equation (3.21) is rewritten as follows

$$\theta D_{ij} \frac{\partial c}{\partial x_j} n_i = q_i n_i (c - c_0) - \frac{D_g}{d} (k_g c - g_{atm}) \tag{6.25}$$

Again, when substituted into the last term of (6.3), the boundary integral becomes

$$\sum_e \int_{\Gamma_e} \theta D_{ij} \frac{\partial c'}{\partial x_j} n_i \phi_n d\Gamma = Q_n c_n - Q_n c_{n0} - \frac{D_g \Delta L}{d} (k_g c_n - g_{atm}) \tag{6.26}$$

where ΔL is the length of the boundary associated with node n. The last term of (6.26) representing the gas diffusion flux through the stagnant boundary layer at the soil surface is directly added to the vector {*f*} in equation (6.9), whereas the term containing k_g and unknown concentration c_n is incorporated into the coefficient matrix [*S*]. The other terms on the right-hand side of (6.26) are treated in the same way as described above for equation (6.23).

6.3.5. *Mass Balance Calculations*

The total amount of mass in the entire flow domain, or in a preselected subregion, is given by

$$M = \sum_e \int_{\Omega_e} (\theta c + a_v g + \rho s) d\Omega = \sum_e \int_{\Omega_e} [(\theta + a_v k_g + \rho f \frac{k_s c^{\beta-1}}{1 + \eta c^{\beta}}) c + \rho s^k] d\Omega \quad (6.27)$$

The summation is taken over all elements within the specified region.

The cumulative amounts M^0 and M^1 of solute removed from the flow region by zero- and first-order reactions, respectively, are calculated as follows

$$M_1^0 = -\int_0^t \sum_e \int_{\Omega_e} (\gamma_{w,1}\theta + \gamma_{s,1}\rho + \gamma_{g,1}a_v) d\Omega\, dt$$

$$M_k^0 = -\int_0^t \sum_e \int_{\Omega_e} [(\mu'_{w,k-1}\theta + \mu'_{s,k-1}\rho f \frac{k_{s,k-1} c_{k-1}^{\beta_{k-1}-1}}{1 + \eta_{k-1} c_{k-1}^{\beta_{k-1}}} + \mu'_{g,k-1} a_v k_{g,k-1}) c_{k-1} + \quad (6.28)$$

$$+ \mu'_{s,k-1}\rho s_{k-1}^k + \gamma_{w,k}\theta + \gamma_{s,k}\rho + \gamma_{g,k}a_v] d\Omega\, dt \qquad k \in (2, n_s)$$

$$M^1 = \int_0^t \sum_e \int_{\Omega_e} \{[(\mu_w + \mu'_w)\theta + (\mu_s + \mu'_s)\rho f \frac{k_s c^{\beta-1}}{1 + \eta c^{\beta}} + (\mu_g + \mu'_g) a_v k_g] c + \quad (6.29)$$

$$+ (\mu_s + \mu'_s)\rho s^k\} d\Omega\, dt$$

whereas the cumulative amount M_r of solute taken up by plant roots is given by

$$M_r = \int_0^t \sum_{e_R} \int_{\Omega_e} S c_r d\Omega\, dt \quad (6.30)$$

where e_R represents the elements making up the root zone.

Finally, when all boundary material fluxes, decay reactions, and root uptake mass fluxes have been computed, the following mass balance should hold for the flow domain as

a whole:

$$M_t - M_0 = + \int_0^t \sum_{n_\Gamma} Q_n^T dt - M^0 - M^1 - M_r \tag{6.31}$$

where M_t and M_0 are the amounts of solute in the flow region at times t and zero, respectively, as calculated with (6.27), and n_Γ represents nodes located along the boundary of the flow domain or at internal sinks and/or sources. The difference between the left- and right-hand sides of (6.31) represents the absolute error, ϵ_a^c, in the solute mass balance. Similarly as for water flow, the accuracy of the numerical solution for solute transport is evaluated by using the relative error, ϵ_r^c [%], in the solute mass balance as follows

$$\epsilon_r^c = \frac{100 \mid \epsilon_a^c \mid}{\max \left(\sum_e |M_t^e - M_0^e|, \quad |M^0| + |M^1| + |M_r| + \int_0^t \sum_{n_\Gamma} |Q_n^T| dt \right)} \tag{6.32}$$

where M_0^e and M_t^e are the amounts of solute in element e at times 0 and t, respectively. Note again that CHAIN_2D does not relate the absolute error to the total amount of mass in the flow region. Instead, the program uses as a reference the maximum value of (1) the absolute change in element concentrations as summed over all elements, and (2) the sum of the absolute values of all cumulative solute fluxes across the flow boundaries including those resulting from sources and sinks in the flow domain.

The total amount of heat energy in the entire flow domain, or in a preselected subregion, is given by

$$W = \sum_e \int_{\Omega_e} (C_n \theta_n + C_o \theta_o + C_w \theta + C_g a_v) T^A d\Omega \tag{6.33}$$

where T^A is the absolute temperature [K]. The summation is taken over all elements within the specified region.

6.3.6. *Oscillatory Behavior*

Numerical solutions of the transport equation often exhibit oscillatory behavior and/or excessive numerical dispersion near relatively sharp concentration fronts. These problems can be especially serious for convection-dominated transport characterized by small dispersivities. One way to partially circumvent numerical oscillations is to use upstream weighing as discussed in Section 6.3.2. Undesired oscillations can often be prevented also by selecting an appropriate combination of space and time discretizations. Two dimensionless numbers may be used to characterize the space and time discretizations. One of these is the grid Peclet number, Pe_i^e, which defines the predominant type of the solute transport (notably the ratio of the convective and dispersive transport terms) in relation to coarseness of the finite element grid:

$$Pe_i^e = \frac{q_i \Delta x_i}{\theta D_{ii}} \tag{6.34}$$

where Δx_i is the characteristic length of a finite element. The Peclet number increases when the convective part of the transport equation dominates the dispersive part, i.e., when a relatively steep concentration front is present. To achieve acceptable numerical results, the spatial discretization must be kept relatively fine to maintain a low Peclet number. Numerical oscillation can be virtually eliminated when the local Peclet numbers do not exceed about 5. However, acceptably small oscillations may be obtained with local Peclet numbers as high as 10 [*Huyakorn and Pinder*, 1983]. Undesired oscillation for higher Peclet numbers can be effectively eliminated by using upstream weighing (see Section 6.3.2).

A second dimensionless number which characterizes the relative extent of numerical oscillations is the Courant number, Cr_i^e. The Courant number is associated with the time discretization as follows

$$Cr_i^e = \frac{q_i \Delta t}{\theta R \Delta x_i} \tag{6.35}$$

Three stabilizing options are used in CHAIN_2D to avoid oscillations in the

numerical solution of the solute transport equation [*Šimůnek and Suarez*, 1993b]. One option is upstream weighing (see Section 6.3.2), which effectively eliminates undesired oscillations at relatively high Peclet numbers. A second option for minimizing or eliminating numerical oscillations uses the criterion developed by *Perrochet and Berod* [1993]

$$Pe \cdot Cr \leq \omega_s \quad (=2) \tag{6.36}$$

where ω_s is the performance index [-]. This criterion indicates that convection-dominated transport problems having large *Pe* numbers can be safely simulated provided *Cr* is reduced according to (6.36) [*Perrochet and Berod*, 1993]. When small oscillations in the solution can be tolerated, ω_s can be increased to about 5 or 10.

A third stabilization option implemented in CHAIN_2D also utilizes criterion (6.36). However, instead of decreasing *Cr* to satisfy equation (6.36), this option introduces artificial dispersion to decrease the Peclet number. The amount of additional longitudinal dispersion, $\bar{D}_L$ [L], is given by [*Perrochet and Berod*, 1993]

$$\bar{D}_L = \frac{|q|\Delta t}{R\theta\omega_s} - D_L - \frac{\theta D_w \tau}{|q|} \tag{6.37}$$

The maximum permitted time step is calculated for all three options, as well as with the additional requirement that the Courant number must remain less than or equal to 1. The time step calculated in this way is subsequently used as one of the time discretization rules (rule No. B) discussed in section 5.3.3.

7. PROBLEM DEFINITION

7.1. *Construction of Finite Element Mesh*

The finite element mesh is constructed by dividing the flow region into quadrilateral and/or triangular elements whose shapes are defined by the coordinates of the nodes that form the element corners. The program automatically subdivides the quadrilaterals into triangles which are then treated as subelements.

Transverse lines [*Neuman*, 1974] formed by element boundaries must transect the mesh along the general direction of its shortest dimension. These transverse lines should be continuous and non-intersecting, but need not be straight. The nodes are numbered sequentially from 1 to *NumNP* (total number of nodes) by proceeding along each transverse line in the same direction. Elements are numbered in a similar manner. The maximum number of nodes on any transverse line, *IJ*, is used to determine the effective size of the finite element matrix (i.e., its band width). To minimize memory and time requirements, *IJ* should be kept as small as possible. The above rules for defining the finite element mesh apply only when Gaussian elimination is used to solve the matrix equations. Iterative methods (such as the conjugate gradient and ORTHOMIN methods) are not so restrictive since only non-zero entries in the coefficient matrix are stored in memory, and since the computational efficiency is less dependent upon the bandwidth of the matrix as compared to direct equation solvers.

The finite element dimensions must be adjusted to a particular problem. They should be made relatively small in directions where large hydraulic gradients are expected. Region with sharp gradients are usually located in the vicinity of the internal sources or sinks, or close to the soil surface where highly variable meteorological factors can cause fast changes in pressure head. Hence, we recommend to normally use relatively small elements at and near the soil surface. The size of elements can gradually increase with depth to reflect the generally much slower changes in pressure heads at deeper depths. The element dimensions should also depend upon the soil hydraulic properties. For example, coarse-

textured soils having relatively high n-values and small α-values (see Eqs. (2.11) and (2.18)) generally require a finer discretization than fine-textured soils. We also recommend using elements having approximately equal sizes to decrease numerical errors. For axisymmetric three-dimensional flow systems, the vertical axis must coincide with, or be to the left of, the left boundary of the mesh. No special restrictions are necessary to facilitate the soil root zone.

7.2. *Coding of Soil Types and Subregions*

Soil Types - An integer code beginning with 1 and ending with *NMat* (the total number of soil materials) is assigned to each soil type in the flow region. The appropriate material code is subsequently assigned to each nodal point n of the finite element mesh.

Interior material interfaces do not coincide with element boundaries. When different material numbers are assigned to the corner nodes of a certain element, material properties of this element will be averaged automatically by the finite element algorithm. This procedure will somewhat smooth soil interfaces.

A set of soil hydraulic parameters and solute transport characteristics must be specified for each soil material. Also, the user must define for each element the principal components of the conductivity anisotropy tensor, as well as the angle between the local and global coordinate systems.

As explained in Section 2.3, one additional way of changing the unsaturated soil hydraulic properties in the flow domain is to introduce scaling factors associated with the water content, the pressure head and the hydraulic conductivity. The scaling factors are assigned to each nodal point n in the flow region.

Subregions - Water and solute mass balances are computed separately for each specified subregion. The subregions may or may not coincide with the material regions. Subregions are characterized by an integer code which runs from 1 to *NLay* (the total number of subregions). A subregion code is assigned to each element in the flow domain.

7.3. *Coding of Boundary Conditions*

Flow boundary conditions were programmed in a fairly similar way as done in the UNSAT1 and UNSAT2 models of *Neuman* [1972] and *Neuman et al.* [1974], and in the SWMS_2D code [*Šimůnek et al.*, 1992]. Unit vertical hydraulic gradient boundary conditions simulating free drainage are implemented in CHAIN_2D, in addition to the boundary conditions used in SWMS_2D. A boundary code, $Kode(n)$, must be assigned to each node, n. If node n is to have a prescribed pressure head during a time step (Dirichlet boundary condition), $Kode(n)$ must be set positive during that time step. If the volumetric flux of water entering or leaving the system at node n is prescribed during a time step (Neumann boundary condition), $Kode(n)$ must be negative or zero.

Constant Boundary Conditions - The values of constant boundary conditions for a particular node, n, are given by the initial values of the pressure head, $h(n)$, in case of Dirichlet boundary conditions, or by the initial values of the recharge/discharge flux, $Q(n)$, in case of Neumann boundary conditions. Table 7.1 summarizes the use of the variables $Kode(n)$, $Q(n)$ and $h(n)$ for various types of nodes.

Table 7.1. Initial settings of $Kode(n)$, $Q(n)$, and $h(n)$ for constant boundary conditions.

Node Type	$Kode(n)$	$Q(n)$	$h(n)$
Internal; not sink/source	0	0.0	Initial Value
Internal; sink/source (Dirichlet condition)	1	0.0	Prescribed
Internal; sink/source (Neumann condition)	-1	Prescribed	Initial Value
Impermeable Boundary	0	0.0	Initial Value
Specified Head Boundary	1†	0.0	Prescribed
Specified Flux Boundary	-1‡	Prescribed	Initial Value

† 5 and/or 6 may also be used
‡ -5 and/or -6 may also be used

Variable Boundary Conditions - Three types of variable boundary conditions can be imposed:

1. Atmospheric boundary conditions for which $Kode(n) = \pm 4$,
2. Variable pressure head boundary conditions for which $Kode(n) = +3$, and
3. Variable flux boundary conditions for which $Kode(n) = -3$.

These conditions can be specified along any part of the boundary. It is not possible to specify more than one time-dependent boundary condition for each type. Initial settings of the variables $Kode(n)$, $Q(n)$ and $h(n)$ for the time-dependent boundary conditions are given in Table 7.2.

Table 7.2. Initial settings of $Kode(n)$, $Q(n)$, and $h(n)$ for variable boundary conditions.

Node Type	$Kode(n)$	$Q(n)$	$h(n)$
Atmospheric Boundary	–4	0.0	Initial Value
Variable Head Boundary	+3	0.0	Initial Value
Variable Flux Boundary	–3	0.0	Initial Value

Atmospheric boundary conditions are implemented when $Kode(n) = \pm 4$, in which case time-dependent input data for the precipitation, *Prec*, and evaporation, *rSoil*, rates must be specified in the input file ATMOSPH.IN. The potential fluid flux across the soil surface is determined by *rAtm* = *rSoil-Prec*. The actual surface flux is calculated internally by the program. Two limiting values of surface pressure head must also be provided: *hCritS* which specifies the maximum allowed pressure head at the soil surface (usually 0.0), and *hCritA* which specifies the minimum allowed surface pressure head (defined from equilibrium conditions between soil water and atmospheric vapor). The program automatically switches the value of $Kode(n)$ from -4 to +4 if one of these two limiting points is reached. Table 7.3 summarizes the use of the variables *rAtm*, *hCritS* and *hCritA* during program execution. $Width(n)$ in the table denotes the length of the boundary segment associated with node n.

Table 7.3. Definition of the variables *Kode*(*n*), *Q*(*n*) and *h*(*n*) when an atmospheric boundary condition is applied.

Kode(*n*)	*Q*(*n*)	*h*(*n*)	Event
–4	*-Width*(*n*)**rAtm*	Unknown	*rAtm=rSoil-Prec*
+4	Unknown	*hCritA*	Evaporation capacity is exceeded
+4	Unknown	*hCritS*	Infiltration capacity is exceeded

Variable head and flux boundary conditions along a certain part of the boundary are implemented when *Kode*(*n*) = +3 and -3, respectively. In that case, the input file ATMOSPH.IN must contain the prescribed time-dependent values of the pressure head, *ht*, or the flux, *rt*, imposed along the boundary. The values of *ht* or *rt* are assigned to particular nodes at specified times according to rules given in Table 7.4.

Table 7.4. Definition of the variables *Kode*(*n*), *Q*(*n*) and *h*(*n*) when variable head or flux boundary conditions are applied.

Node Type	*Kode*(*n*)	*Q*(*n*)	*h*(*n*)
Variable Head Boundary	+3	Unknown	*ht*
Variable Flux Boundary	–3	*-Width*(*n*)**rt*	Unknown

Water Uptake by Plant Roots - The program calculates the rate at which plants extract water from the soil root zone by evaluating the term *D* (equation (5.9)) in the finite element formulation. The code requires that *Kode*(*n*) be set equal to 0 or negative for all nodes in the root zone. Values of the potential transpiration rate, *rRoot*, must be specified at preselected times in the input file ATMOSPH.IN. Actual transpiration rates are calculated internally by the program as discussed in Section 2.2. The root uptake parameters are taken

from an input file SELECTOR.IN. Values of the function *Beta*(n), which describes the potential water uptake distribution over the root zone (equation (2.5)), must be specified for each node in the flow domain (see the description of input Block I in Table 9.9 of Section 9). All parts of the flow region where *Beta*(n)>0 are treated as the soil root zone.

Deep Drainage from the Soil Profile - Vertical drainage, $q(h)$, across the lower boundary of the soil profile is sometimes approximated by a flux which depends on the position of groundwater level (e.g., *Hopmans and Stricker*, 1989). If available, such a relationship can be implemented in the form of a variable flux boundary condition for which *Kode*(n)=-3. This boundary condition is implemented in CHAIN_2D by setting the logical variable *qGWLF* in the input file ATMOSPH.IN equal to ".true.". The discharge rate $Q(n)$ assigned to node n is determined by the program as $Q(n)$=-*Width*(n)*$q(h)$ where h is the local value of the pressure head, and $q(h)$ is given by

$$q(h) = -A_{qh}\exp(B_{qh}|h - GWL0L|) \tag{7.1}$$

where A_{qh} and B_{qh} are empirical parameters which must be specified in the input file ATMOSPH.IN, together with *GWL0L* which represents the reference position of the groundwater level (usually set equal to the z-coordinate of the soil surface).

Free Drainage - Unit vertical hydraulic gradient boundary conditions can be implemented in the form of a variable flux boundary condition for which *Kode*(n)=-3. This boundary condition is implemented in CHAIN_2D by setting the logical variable *FreeD* in the input file SELECTOR.IN equal to ".true.". The program determines the discharge rate $Q(n)$ assigned to node n as $Q(n)$=-*Width*(n)*$K(h)$, where h is the local value of the pressure head, and $K(h)$ is the hydraulic conductivity corresponding to this pressure head.

Seepage Faces - The initial settings of the variables *Kode*(n), $Q(n)$ and $h(n)$ for nodes along a seepage face are summarized in Table 7.5. All potential seepage faces must be identified before starting the numerical simulation. This is done by providing a list of nodes

along each potential seepage face (see input Block E as defined in Table 9.5 of Section 9).

Table 7.5. Initial setting of *Kode*(n), $Q(n)$, and $h(n)$ for seepage faces.

Node Type	*Kode*(n)	$Q(n)$	$h(n)$
Seepage Face (initially saturated)	+2	0.0	0.0
Seepage Face (initially unsaturated)	−2	0.0	Initial Value

Drains - Table 7.6 summarizes the initial settings of the variables *Kode*(n), $Q(n)$ and $h(n)$ for nodes representing drains. All drains must be identified before starting the numerical simulation. This is done by providing a list of nodes representing drains, together with a list of elements around each drain whose hydraulic conductivities are to be adjusted according to discussion in Section 5.3.7 (see also input Block F as defined in Table 9.6 of Section 9).

Table 7.6. Initial setting of *Kode*(n), $Q(n)$, and $h(n)$ for drains.

Node Type	*Kode*(n)	$Q(n)$	$h(n)$
Drain (initially saturated)	+5	0.0	0.0
Drain (initially unsaturated)	−5	0.0	Initial Value

Solute and Heat Transport Boundary Conditions - The original version 1.1. of SWMS_2D [*Šimůnek et al.*, 1992] assumed a strict relationship between the boundary conditions for water flow and solute transport. A first-type boundary condition for water flow forced the boundary condition for solute transport also to be of the first-type.

Similarly, a second-type boundary condition for water flow induced a second- or third-type boundary condition for solute transport depending upon direction of the water flux. These strict relationships between the boundary conditions for water flow and solute transport have been abandoned in CHAIN_2D. Selection of the type of boundary condition for the solute transport is now much more independent of the boundary condition implemented for water flow. The type of boundary condition to be invoked for solute or heat transport is specified by the input variable *KodCB* or *KodTB*, respectively. A positive sign of this variable means that a first-type boundary condition will be used. When *KodCB* (*KodTB*) is negative, CHAIN_2D selects a third-type boundary condition when the calculated water flux is directed into the region, or a second-type boundary condition when the water flux is zero or directed out of the region. One exception to these rules occurs for atmospheric boundary conditions when $Kode(n) = \pm 4$ and $Q(n) < 0$. CHAIN_2D assumes that solutes can leave the flow region across atmospheric boundaries only by gas diffusion. The solute flux in this situation becomes zero, i.e., $c_0 = 0$ in equation (6.22). Cauchy and Neumann boundary conditions are automatically applied to internal sinks/sources depending upon the direction of water flow. The dependence or independence of the solute and heat boundary conditions on time or the system is still defined through the variable $Kode(n)$ as discussed above.

Although CHAIN_2D can implement first-type boundary conditions, we recommend users to invoke third-type conditions where possible. This is because third-type conditions, in general, are physically more realistic and preserve solute mass in the simulated system (e.g., *van Genuchten and Parker* [1984]; *Leij et al.* [1991]).

7.4. *Program Memory Requirements*

One single parameter statement is used at the beginning of the code to define the problem dimensions. All major arrays in the program are adjusted automatically according to these dimensions. This feature makes it possible to change the dimensions of the problem to be simulated without having to recompile all program subroutines. Different problems can be investigated by changing the dimensions in the parameter statement at the

beginning of the main program, and subsequently linking all previously compiled subroutines with the main program when creating an executable file. Table 7.7 lists the array dimensions which must be defined in the parameter statement.

Table 7.7. List of array dimensions in CHAIN_2D.

Dimension	Description
NumNPD	Maximum number of nodes in finite element mesh
NumElD	Maximum number of elements in finite element mesh
MBandD	Maximum dimension of the bandwidth of matrix A when Gaussian elimination is used. Maximum number of nodes adjacent to a particular node, including itself, when iterative matrix solvers are used.
NumBPD	Maximum number of boundary nodes for which $Kode(n) \neq 0$
NSeepD	Maximum number of seepage faces
NumSPD	Maximum number of nodes along a seepage face
NDrD	Maximum number of drains
NElDrD	Maximum number of elements surrounding a drain
NMatD	Maximum number of materials
NTabD	Maximum number of items in the table of hydraulic properties generated by the program for each soil material
NumKD	Maximum number of available code number values (equals 6 in present version)
NSD	Maximum number of solutes (equals 6 in present version)
NObsD	Maximum number of observation nodes for which the pressure head, the water content, temperature and concentration are printed at each time level
MNorth	Maximum number of orthogonalizations performed when iterative solvers are used

7.5. *Matrix Equation Solvers*

Discretization of the governing partial differential equations for water flow (2.1), solute transport (3.11) and heat movement (4.1) leads to the system of linear equations

$$[A]\{x\} = \{b\} \tag{7.2}$$

in which matrix $[A]$ is symmetric for water flow and asymmetric for solute and heat transport.

The original version of SWMS_2D [*Šimůnek et al.*, 1992] uses Gaussian elimination to solve both systems of linear algebraic equations. The invoked solvers took advantage of the banded nature of the coefficient matrices and, in the case of water flow, of the symmetric properties of the matrix. Such direct solution methods have several disadvantages as compared to iterative methods. Direct methods require a fixed number of operations (depending upon the size of the matrix) which increases approximately by the square of the number of nodes [*Mendoza et al.*, 1991]. Iterative methods, on the other hand, require a variable number of repeated steps which increases at a much smaller rate (about 1.5) with the size of a problem [*Mendoza et al.*, 1991]. A similar reduction also holds for the memory requirement since iterative methods do not require one to store non-zero matrix elements. Memory requirements, therefore, increase at a much smaller rate with the size of the problem when iterative solvers are used [*Mendoza et al.*, 1991]. Round-off errors also represent less of a problem for iterative methods as compared to direct methods. This is because round-off errors in iterative methods are self-correcting [*Letniowski*, 1989]. Finally, for time-dependent problems, a reasonable approximation of the solution (i.e., the solution at the previous time step) exists for iterative methods, but not for direct methods [*Letniowski*, 1989]. In general, direct methods are more appropriate for relatively small problems, while iterative methods are more suitable for larger problems.

Many iterative methods have been used in the past for handling large sparse matrix equations. These methods include Jacobi, Gauss-Seidel, alternating direction implicit (ADI), block successive over-relaxation (BSSOR), successive line over-relaxation (SLOR), and

strongly implicit procedures (SIP), among others [*Letniowski*, 1989]. More powerful preconditioned accelerated iterative methods, such as the preconditioned conjugate gradient method (PCG) [*Behie and Vinsome*, 1982], were introduced more recently. *Sudicky and Huyakorn* [1991] gave three advantages of the PCG procedure as compared to other iterative methods: PCG can be readily modified for finite element methods with irregular grids, the method does not require iterative parameters, and PCG usually outperforms its iterative counterparts for situations involving relatively stiff matrix conditions.

CHAIN_2D implements both direct and iterative methods for solving the system of linear algebraic equations given by (7.2). Depending upon the size of matrix [A], we use either direct Gaussian elimination or the preconditioned conjugate gradient method [*Mendoza et al.*, 1991] for water flow and the ORTHOMIN (preconditioned conjugate gradient squared) procedure [*Mendoza et al.*, 1991] for solute transport. Gaussian elimination is used if either the bandwidth of matrix [A] is smaller than 20, or the total number of nodes is smaller than 500. The iterative methods used in CHAIN_2D were adopted from the ORTHOFEM software package of *Mendoza et al.* [1991].

The preconditioned conjugate gradient and ORTHOMIN methods consist of two essential parts: initial preconditioning, and the iterative solution with either conjugate gradient or ORTHOMIN acceleration [*Mendoza et al.*, 1991]. Incomplete lower-upper (ILU) preconditioning is used in ORTHOFEM when matrix [A] is factorized into lower and upper triangular matrices by partial Gaussian elimination. The preconditioned matrix is subsequently repeatedly inverted using updated solution estimates to provide a new approximation of the solution. The orthogonalization-minimization acceleration technique is used to update the solution estimate. This technique insures that the search direction for each new solution is orthogonal to the previous approximate solution, and that either the norm of the residuals (for conjugate gradient acceleration [*Meijerink and van der Vorst*, 1981]) or the sum of the squares of the residuals (for ORTHOMIN [*Behie and Vinsome*, 1982]) is minimized. More details about the two methods is given in the user's guide of ORTHOFEM [*Mendoza et al.*, 1991] or in *Letniowski* [1989]. *Letniowski* [1989] also gives a comprehensive review of accelerated iterative methods, as well as of the preconditional

techniques.

8. EXAMPLE PROBLEMS

Seven example problems are presented in this section. The first three examples are identical to those presented with the first version of SWMS_2D [*Šimůnek et al.*, 1992]. The other four examples in this section were included mainly for mathematical verification purposes, and for demonstrating new features of CHAIN_2D, i.e., non-equilibrium and nonlinear adsorption, sequential first-order decay reactions, solute diffusion in the gas phase, and heat transport.

Examples 1 and 2 provide comparisons of the water flow part of CHAIN_2D code with results from both the UNSAT2 code of *Neuman* [1974] and the SWATRE code of *Belmans et al.* [1983]. Example 3 serves to verify the accuracy of the solute transport part of CHAIN_2D by comparing numerical results against those obtained with a two-dimensional analytical solution during steady-state groundwater flow. The results obtained with CHAIN_2D code for these three examples are identical to the results obtained with SWMS_2D. Example 4 serves to verify the accuracy of CHAIN_2D by comparing numerical results for a problem with three solutes involved in a sequential first-order decay reaction against results obtained with an analytical solution during one-dimensional steady-state water flow [*van Genuchten*, 1985]. Example 5 considers one-dimensional transport of a solute undergoing nonlinear cation adsorption. Numerical results are compared with experimental data and previous numerical solutions obtained with the MONOC code of *Selim et al.* [1987] and the HYDRUS code of *Kool and van Genuchten* [1991]. Example 6 serves to verify the accuracy of CHAIN_2D in describing non-equilibrium adsorption by comparing numerical results against experimental data and previous numerical predictions during one-dimensional steady-state water flow [*van Genuchten*, 1981]. Example 7 demonstrates numerical results for a field infiltration experiment involving a two-layered axisymmetric three-dimensional flow domain. The infiltrating water was assumed to have a higher temperature than the soil, and to contain an organic compound (parent pesticide) which in the soil profile degraded into two sequential daughter products. The selected input and output files of the examples are listed at the end of Sections 9 and 10, respectively.

8.1. *Example 1 - Column Infiltration Test*

This example simulates a one-dimensional laboratory infiltration experiment discussed by *Skaggs et al.* [1970]. The example was used later by *Davis and Neuman* [1983] as a test problem for the UNSAT2 code. Hence, the example provides a means of comparing results obtained with the CHAIN_2D and UNSAT2 codes.

Figure 8.1 gives a graphical representation of the soil column and the finite element mesh used for the numerical simulations. The soil water retention and relative hydraulic conductivity functions of the sandy soil are presented in Figure 8.2. The sand was assumed to be at an initial pressure head of -150 cm. The soil hydraulic properties were assumed to

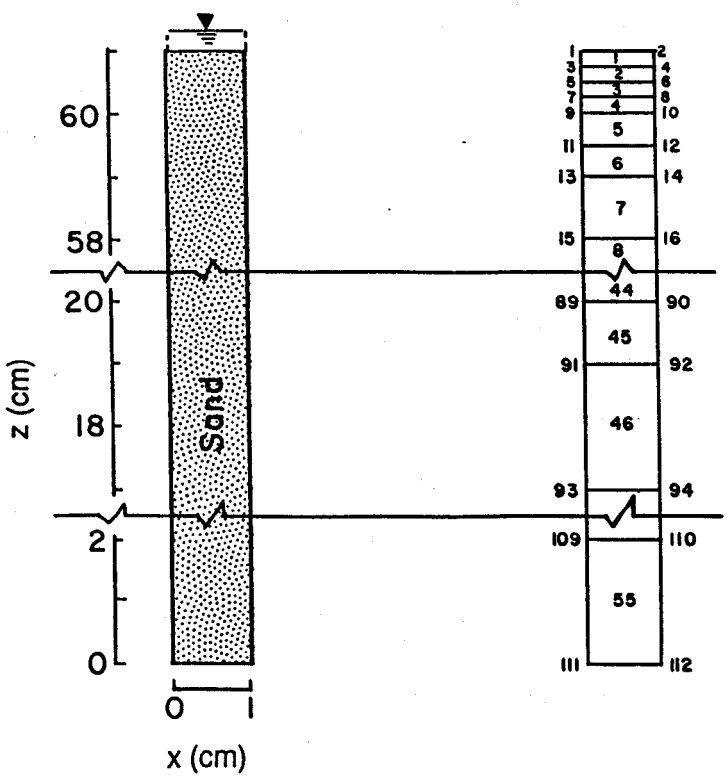

Fig. 8.1. Flow system and finite element mesh for example 1.

be homogenous and isotropic with a saturated hydraulic conductivity of 0.0433 cm/min. The column was subjected to ponded infiltration (a Dirichlet boundary condition) at the soil surface, resulting in one-dimensional vertical water flow. The open bottom boundary of the soil column was simulated by implementing a no-flow boundary condition during unsaturated flow ($h<0$), and a seepage face with $h=0$ when the bottom boundary becomes saturated (this last condition was not reached during the simulation). The impervious sides of the column were simulated by imposing no-flow boundary conditions.

The simulation was carried out for 90 min, which corresponds to the total time duration of the experiment. Figure 8.3 shows the calculated instantaneous (q_0) and cumulative (I_0) infiltration rates simulated with CHAIN_2D. The calculated results agree closely with those obtained by *Davis and Neuman* [1983] using their UNSAT2 code.

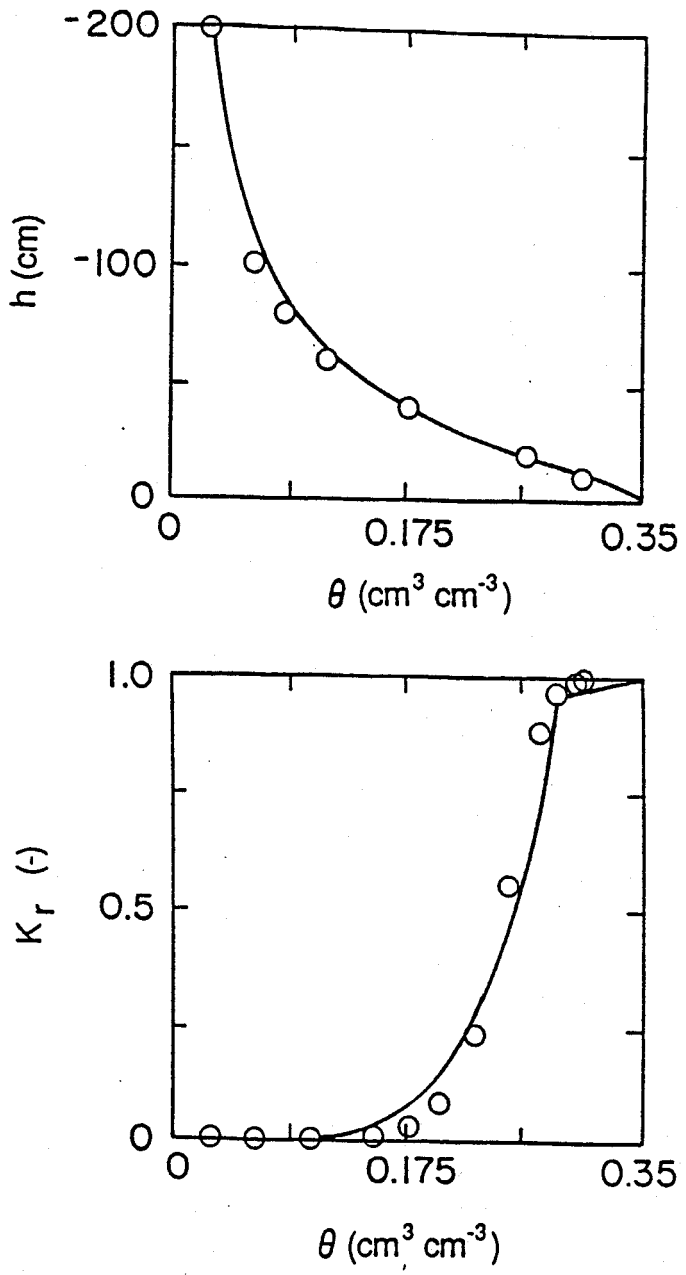

Fig. 8.2. Retention and relative hydraulic conductivity functions for example 1. The open circles are UNSAT2 input data [*Davis and Neuman*, 1983].

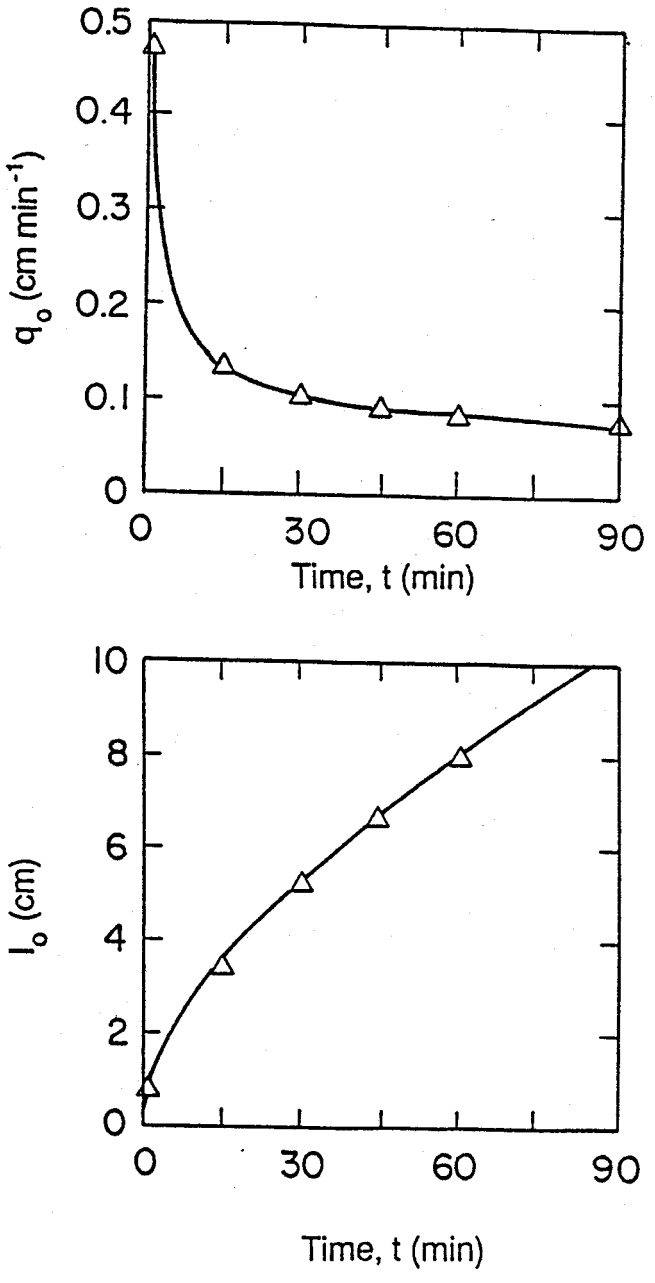

Fig. 8.3. Instantaneous, q_0, and cumulative, I_0, infiltration rates simulated with the CHAIN_2D (solid lines) and UNSAT2 (triangles) codes for example 1.

8.2. *Example 2 - Water Flow in a Field Soil Profile Under Grass*

This example considers one-dimensional water flow in a field profile of the Hupselse Beek watershed in the Netherlands. Atmospheric data and observed ground water levels provided the required boundary conditions for the numerical model. Calculations were performed for the period of April 1 to September 30 of the relatively dry year 1982. Simulation results obtained with CHAIN_2D will be compared with those generated with the SWATRE computer program [*Feddes et al.*, 1978, *Belmans et al.*, 1983].

The soil profile (Fig. 8.4) consisted of two layers: a 40-cm thick A-horizon, and a B/C-horizon which extended to a depth of about 300 cm. The depth of the root zone was 30 cm. The mean scaled hydraulic functions of the two soil layers in the Hupselse Beek area [*Císlerová*, 1987; *Hopmans and Stricker*, 1989] are presented in Figure 8.5.

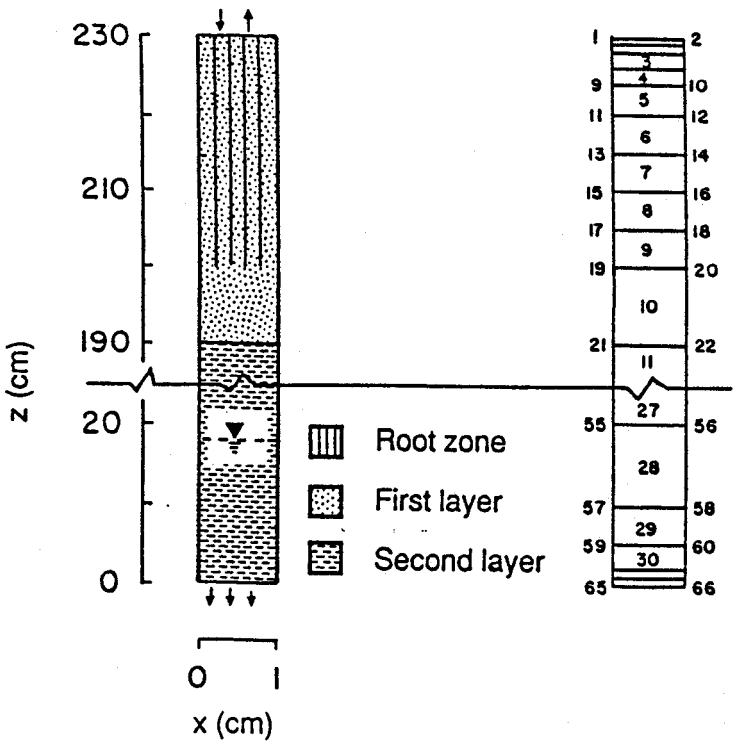

Fig. 8.4. Flow system and finite element mesh for example 2.

The soil surface boundary conditions involved actual precipitation and potential transpiration rates for a grass cover. The surface fluxes were incorporated by using average daily rates distributed uniformly over each day. The bottom boundary condition consisted of a prescribed drainage flux - groundwater level relationship, $q(h)$, as given by equation (7.1). The groundwater level was initially set at 55 cm below the soil surface. The initial moisture profile was taken to be in equilibrium with the initial ground water level.

Figure 8.6 presents input values of the precipitation and potential transpiration rates. Calculated cumulative transpiration and cumulative drainage amounts as obtained with the CHAIN_2D and SWATRE codes are shown in Figure 8.7. The pressure head at the soil surface and the arithmetic mean pressure head of the root zone during the simulated season are presented in Figure 8.8. Finally, Figure 8.9 shows variations in the calculated groundwater level with time.

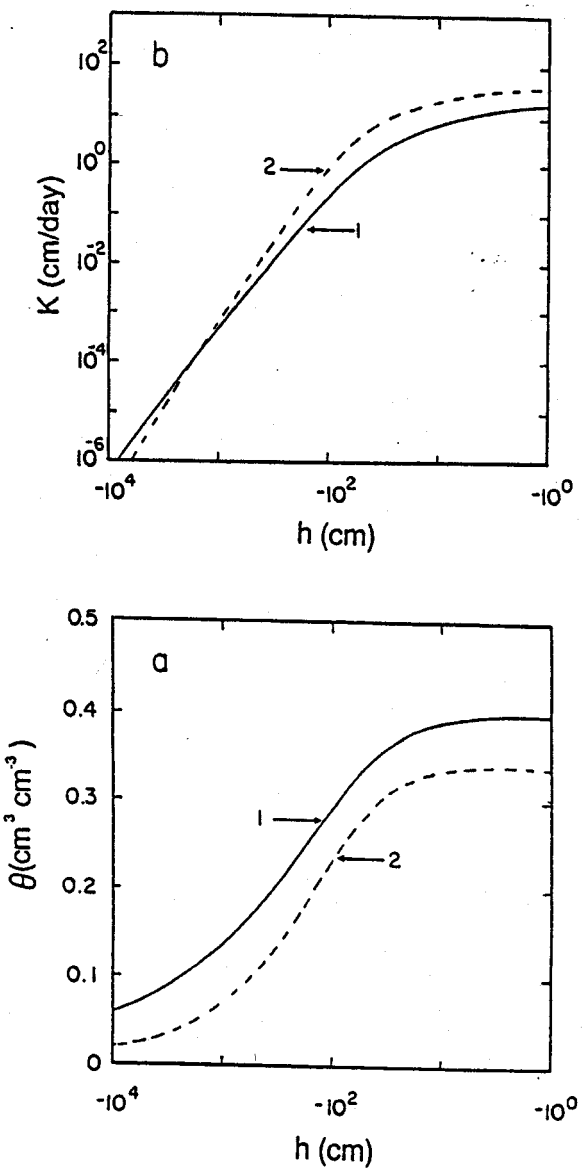

Fig. 8.5. Unsaturated hydraulic properties of the first and second soil layers for example 2.

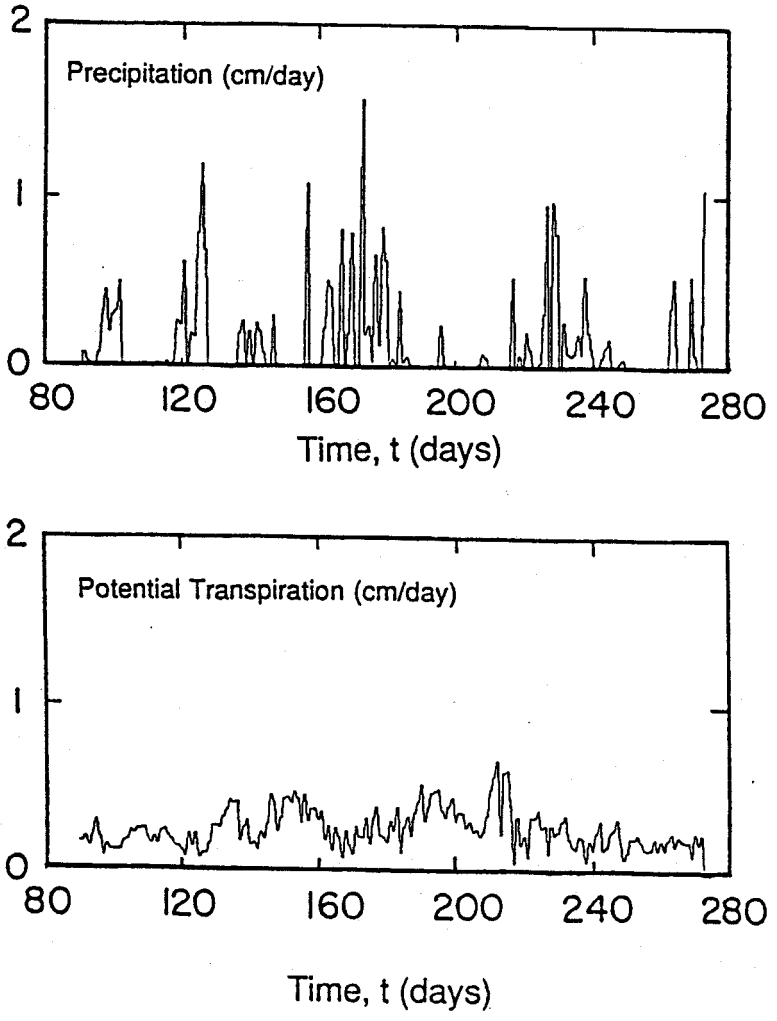

Fig. 8.6. Precipitation and potential transpiration rates for example 2.

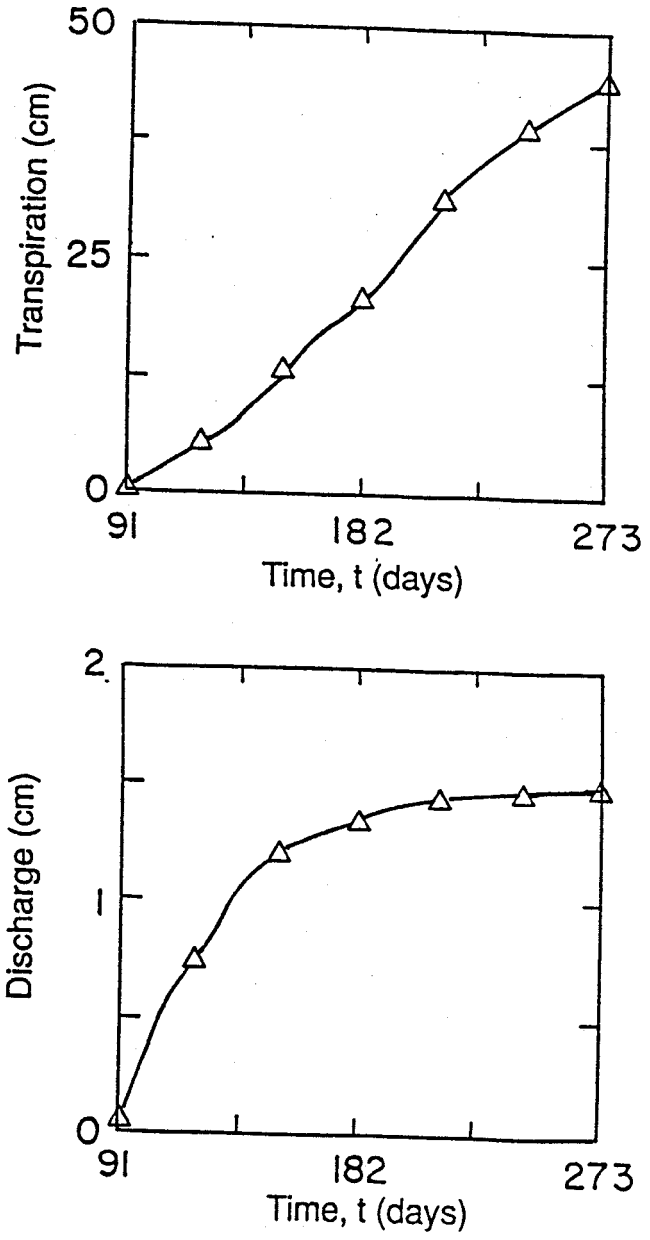

Fig. 8.7. Cumulative values for the actual transpiration and bottom discharge rates for example 2 as simulated with CHAIN_2D (solid line) and SWATRE (triangles).

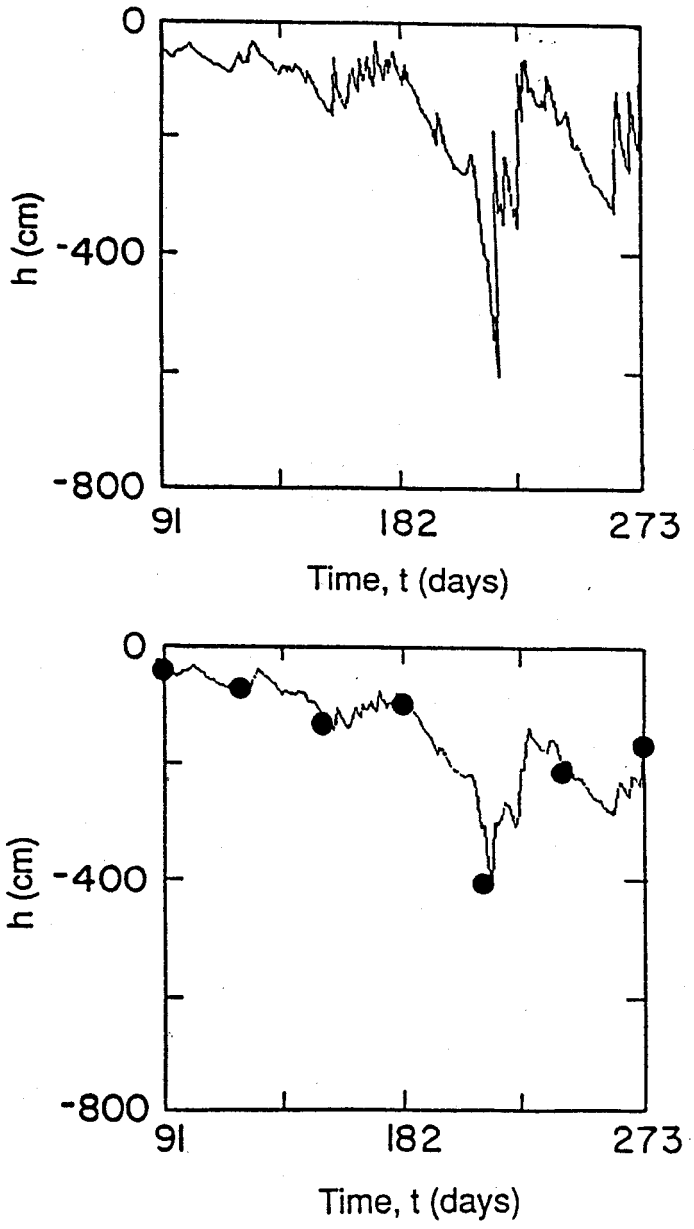

Fig. 8.8. Pressure head at the soil surface and mean pressure head of the root zone for example 2 as simulated with CHAIN_2D (solid lines) and SWATRE (solid circles).

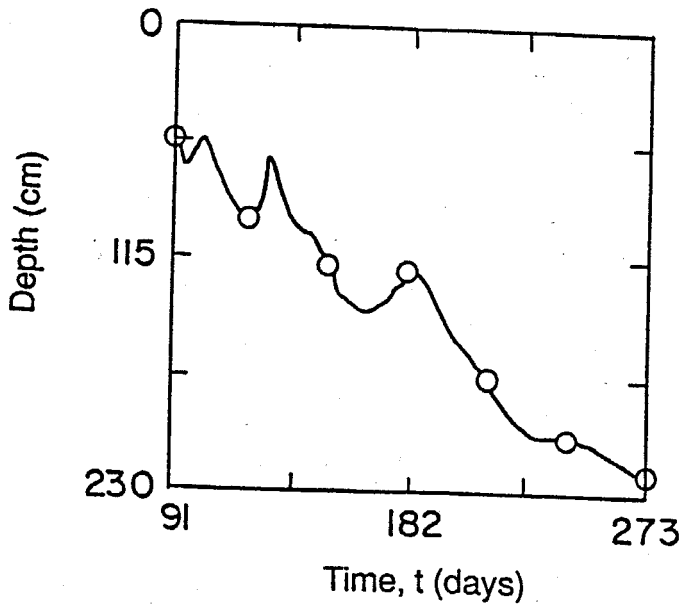

Fig. 8.9. Location of the groundwater table versus time for example 2 as simulated with the CHAIN_2D (solid line) and SWATRE (open circles) computer programs.

8.3. *Example 3 - Two-Dimensional Solute Transport*

This example was used to verify the mathematical accuracy of the solute transport part of CHAIN_2D. *Cleary and Ungs* [1978] published several analytical solutions for two-dimensional dispersion problems. One of these solutions holds for solute transport in a homogeneous, isotropic porous medium during steady-state unidirectional groundwater flow. The solute transport equation (3.11) for this situation reduces to

$$D_T \frac{\partial^2 c}{\partial x^2} + D_L \frac{\partial^2 c}{\partial z^2} - v \frac{\partial c}{\partial z} - \lambda R c = R \frac{\partial c}{\partial t} \qquad (8.1)$$

where λ is a first-order degradation constant, D_L and D_T are the longitudinal and transverse dispersion coefficients, respectively; v is the average pore water velocity (q_z/θ) in the flow direction, and z and x are the spatial coordinates parallel and perpendicular to the direction

of flow. The initially solute-free medium is subjected to a solute source, c_0, of unit concentration. The source covers a length $2a$ along the inlet boundary at $z=0$, and is located symmetrically about the coordinate $x=0$. The transport region of interest is the half-plane ($z \geq 0$; $-\infty \leq x \leq \infty$). The boundary conditions may be written as:

$$\begin{aligned} & c(x,0,t) = c_0 \qquad -a \leq x \leq a \\ & c(x,0,t) = 0 \qquad \textit{other values of } x \\ & \lim_{z \to \infty} \frac{\partial c}{\partial z} = 0 \\ & \lim_{x \to \pm\infty} \frac{\partial c}{\partial x} = 0 \end{aligned} \tag{8.2}$$

The analytical solution of the above transport problem is [*Javandel et al.*, 1984, *Leij and Bradford*, 1994]

$$\begin{aligned} c(x,z,t) = & \frac{c_0 z}{4(\pi D_L)^{1/2}} \exp\left(\frac{vz}{2D_L}\right) \int_0^{t/R} \exp\left[-\left(\lambda R + \frac{v^2}{4D_L}\right)\tau - \frac{z^2}{4D_L\tau}\right] \tau^{-3/2} \\ & \cdot \left[erf\left(\frac{a-x}{2(D_T\tau)^{1/2}}\right) + erf\left(\frac{a+x}{2(D_T\tau)^{1/2}}\right)\right] d\tau \end{aligned} \tag{8.3}$$

The input transport parameters for two simulations are listed in Table 8.1. The width of the source was assumed to be 100 m. Because of symmetry, calculations were carried out only for the quarter plane where $x \geq 0$ and $z \geq 0$.

Figure 8.10 shows the calculated concentration front (taken at a concentration of 0.1) at selected times for the first set of transport parameters in Table 8.1. Note the close agreement between the analytical and numerical results. Excellent agreement is also obtained for the calculated concentration distributions after 365 days at the end of the simulation (Fig. 8.11). Figures 8.12 and 8.13 show similar results for the second set of transport parameters listed in Table 8.1.

Table 8.1. Input parameters for example 3.

Parameter	Example 3a	Example 3b
v [m/day]	0.1	1.0
D_T [m^2/day]	1.0	0.5
D_L [m^2/day]	1.0	1.0
λ [day^{-1}]	0.0	0.01
R [-]	1.0	3.0
c_0 [-]	1.0	1.0

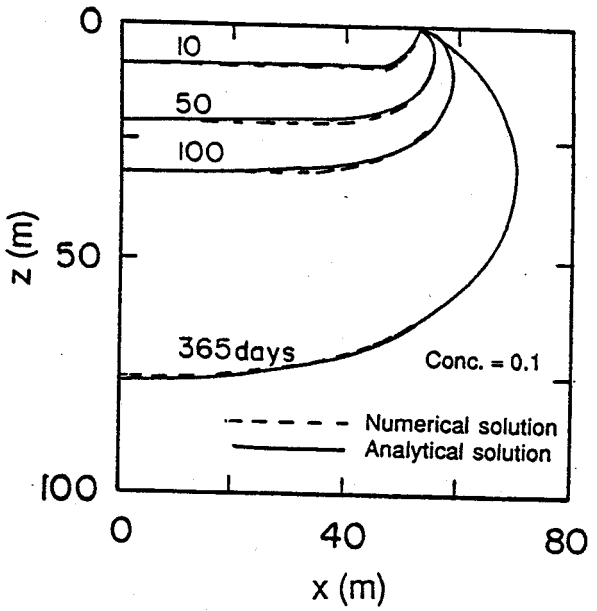

Fig. 8.10. Advancement of the concentration front (c=0.1) for example 3a as calculated with CHAIN_2D (dotted lines) and the analytical solution (solid lines).

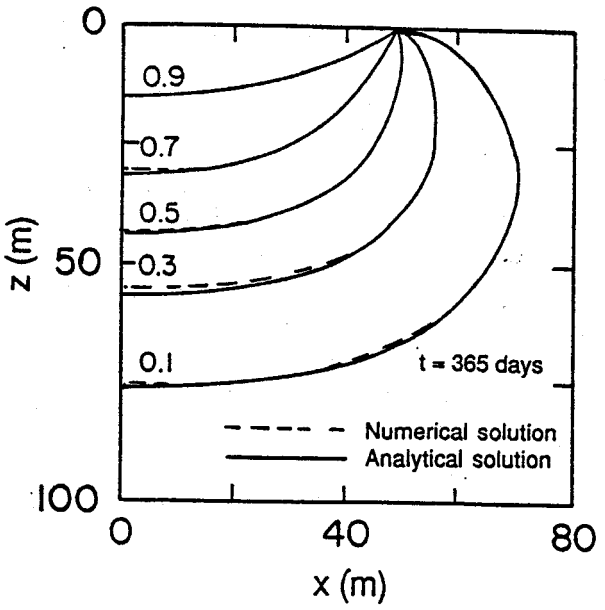

Fig. 8.11. Concentration profile at the end of the simulation (t=365 days) for example 3a calculated with CHAIN_2D (dotted lines) and the analytical solution (solid lines).

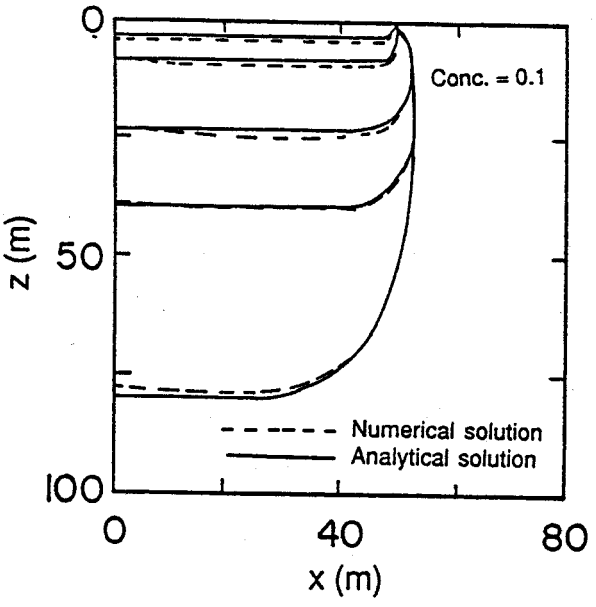

Fig. 8.12. Advancement of the concentration front (c=0.1) for example 3b as calculated with CHAIN_2D (dotted lines) and the analytical solution (solid lines).

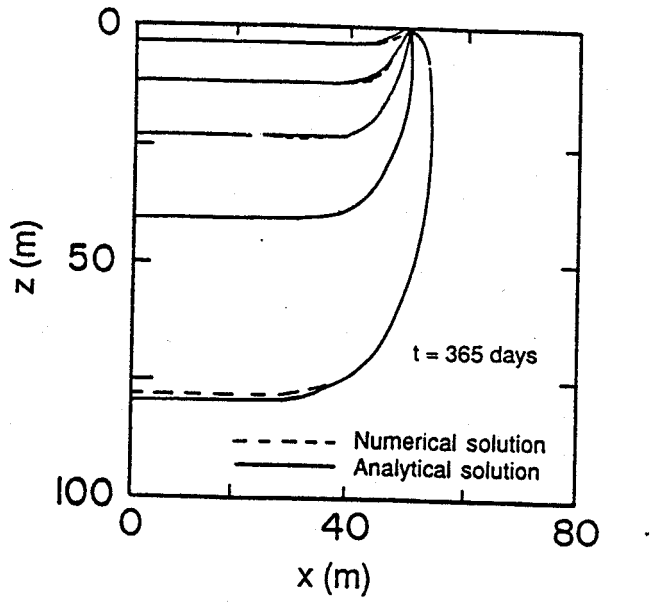

Fig. 8.13. Concentration profile at the end of the simulation (t=365 days) for example 3b as calculated with CHAIN_2D (dotted lines) and the analytical solution (solid lines).

8.4. *Example 4 - One-Dimensional Solute Transport with Nitrification Chain*

This example was used to verify in part the mathematical accuracy of the solute transport part of CHAIN_2D. Numerical results will be compared with results generated with an analytical solution published by *van Genuchten* [1985] for one-dimensional convective-dispersive transport of solutes involved in sequential first-order decay reactions. The analytical solution holds for solute transport in a homogeneous, isotropic porous medium during steady-state unidirectional groundwater flow. Solute transport equations (3.1) and (3.2) for this situation reduce to

$$R_1 \frac{\partial c_1}{\partial t} = D \frac{\partial^2 c_1}{\partial x^2} - v \frac{\partial c_1}{\partial x} - \mu_1 R_1 c_1 \qquad (8.4)$$

$$R_i \frac{\partial c_i}{\partial t} = D \frac{\partial^2 c_i}{\partial x^2} - v \frac{\partial c_i}{\partial x} + \mu_{i-1} R_{i-1} c_{i-1} - \mu_i R_i c_i \qquad i = 2,3 \tag{8.5}$$

where μ is a first-order degradation constant, D is the dispersion coefficient, v is the average pore water velocity (q_x/θ) in the flow direction, x is the spatial coordinate in the direction of flow, and where it is assumed that 3 solutes participate in the decay chain. The specific example used here applies to the three-species nitrification chain

$$NH_4^+ \rightarrow NO_2^- \rightarrow NO_3^- \tag{8.6}$$

and is the same as described by *van Genuchten* [1985], and earlier by *Cho* [1971]. The boundary conditions may be written as:

$$\begin{aligned}
&\left[-D \frac{\partial c_1}{\partial x} + v c_1 \right] = v c_{0,1}(0,t) \\
&\left[-D \frac{\partial c_i}{\partial x} + v c_i \right] = 0 \qquad i = 2,3 \\
&\lim_{x \to \infty} \frac{\partial c_i}{\partial x} = 0 \qquad i = 1,2,3
\end{aligned} \tag{8.7}$$

The experiment involves the application of a NH_4^+ solution to an initially solute-free medium (c_i = 0). The input transport parameters for the simulation are listed in Table 8.2.

Figure 8.14 shows concentration profiles for all three solutes at time 200 hours, calculated both numerically with CHAIN_2D and analytically with the CHAIN code of *van Genuchten* [1985]. Figure 8.15 shows the concentration profiles at three different times (50, 100, and 200 hours) for NH_4^+, NO_2^-, and NO_3^-, respectively. The numerical results in each case duplicated the analytical results.

Table 8.2. Input parameters for example 4.

Parameter	Value
v [cm/hour]	1.0
D [cm^2/hour]	0.18
μ_1 [hour^{-1}]	0.005
μ_2 [hour^{-1}]	0.1
μ_3 [hour^{-1}]	0.0
R_1 [-]	2.0
R_2 [-]	1.0
R_3 [-]	1.0
c_i [-]	0.0
$c_{0,1}$ [-]	1.0

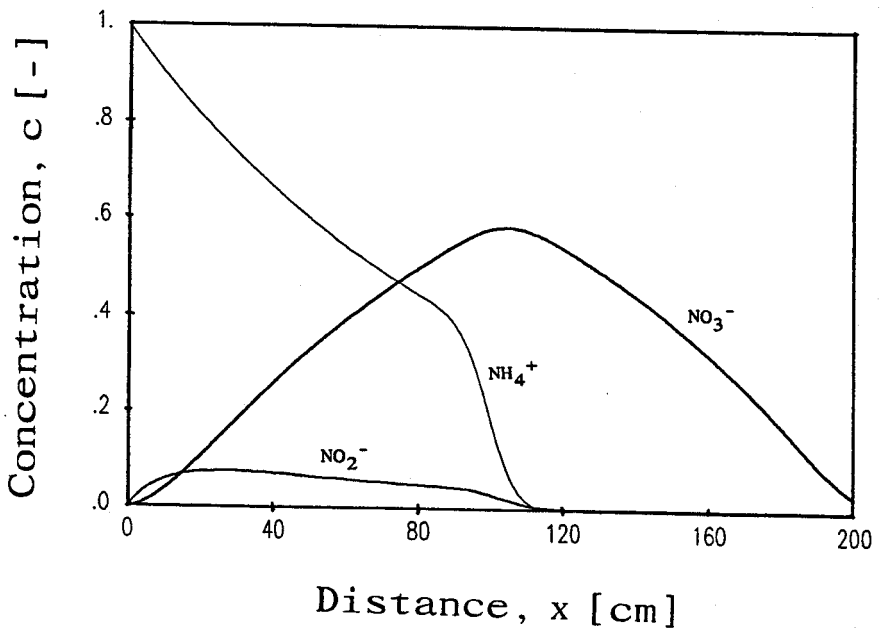

Fig. 8.14. Analytically and numerically calculated concentration profiles for NH_4^+, NO_2^-, and NO_3^- after 200 hours for example 4.

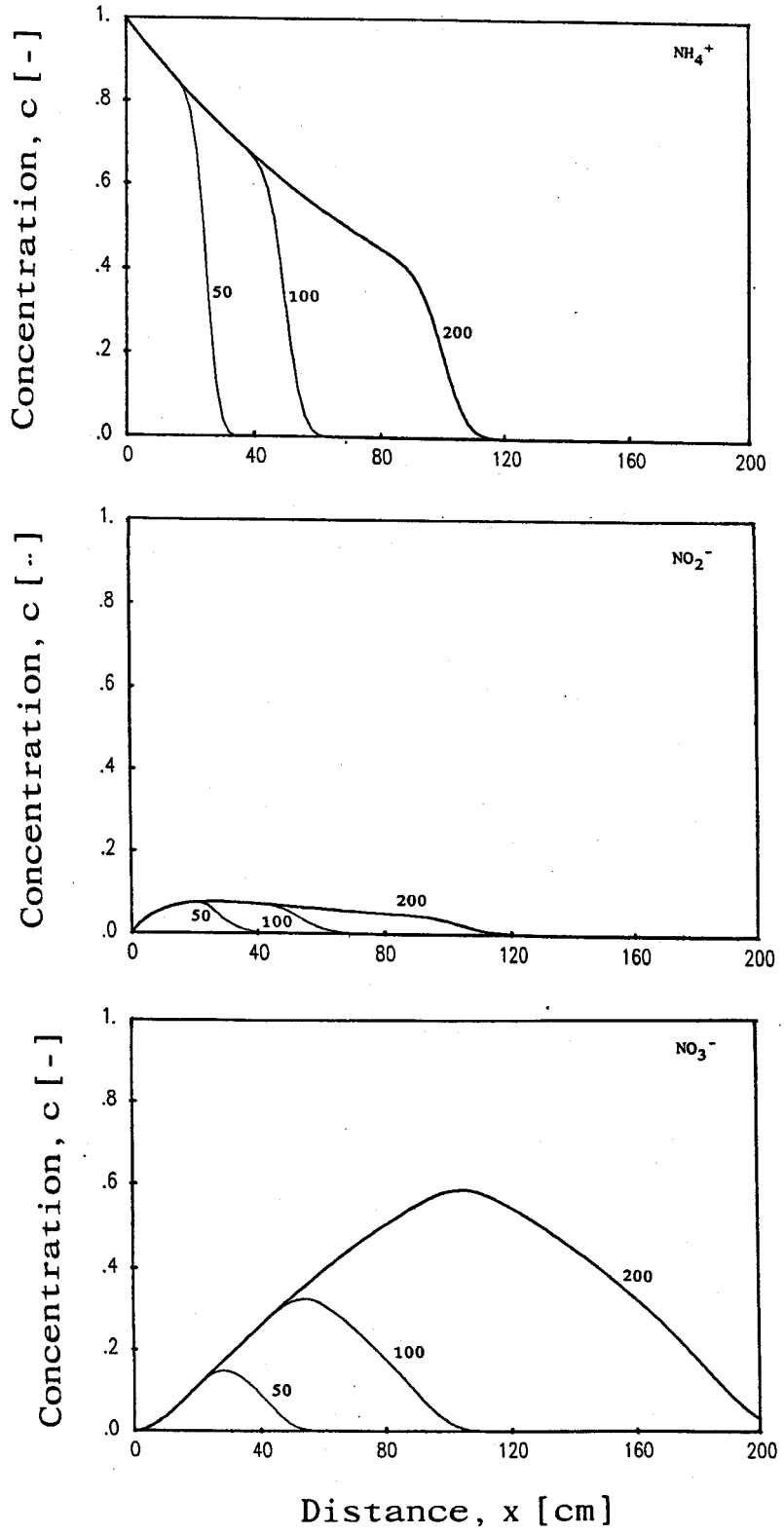

Fig. 8.15. Analytically and numerically calculated concentration profiles for NH_4^+ (top), NO_2^- (middle), NO_3^- (bottom) after 50, 100, and 200 hours for example 4.

8.5. *Example 5 - One-Dimensional Solute Transport with Nonlinear Cation Adsorption*

The experiment discussed in this example was conducted by *Selim et al.* [1987], and used later for validation of the HYDRUS code [*Kool and van Genuchten*, 1991]. The soil in this experiment was Abist loam. A 10.75-cm long soil column was first saturated with a 10 $mmol_c L^{-1}$ $CaCl_2$ solution. The experiment consisted of applying a 14.26 pore volume pulse (t=358.05 hours) of 10 $mmol_c L^{-1}$ $MgCl_2$ solution, followed by the original $CaCl_2$ solution. The adsorption isotherm was determined with the help of batch experiments [*Selim et al.*, 1987], and fitted with the Freundlich equation (3.3) [*Kool and van Genuchten*, 1991]. The Freundlich isotherm parameters, as well as other transport parameters for this problem, are listed in Table 8.3. First- and second-type boundary conditions were applied at the top and bottom of the soil column, respectively.

The observed Mg breakthrough curve is shown in Figure 8.16, together with simulated breakthrough curves obtained with CHAIN_2D, the MONOC code of *Selim et al.* [1987] and the HYDRUS code of *Kool and van Genuchten* [1991]. The results indicate a reasonable prediction of the measured breakthrough curve using CHAIN_2D, and close correspondence between the simulated results obtained with the CHAIN_2D and MONOC models. The CHAIN_2D results became identical to those generated with HYDRUS when a third-type boundary condition was invoked at the top of the soil column.

Table 8.3. Input parameters for example 5.

Parameter	Value
q [cm/hour]	0.271
D [cm^2/hour]	1.167
ρ [g/cm^3]	0.884
θ [-]	0.633
c_0 [$mmol_c/L$]	10.0
k_s [cm^3/g]	1.687
β [-]	1.615

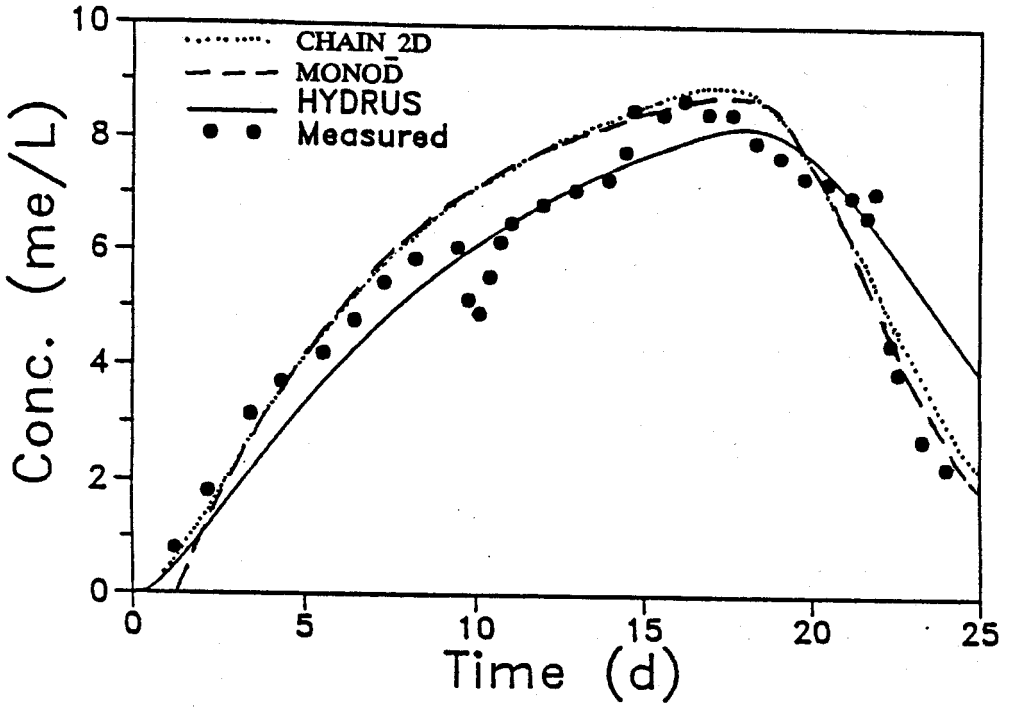

Fig. 8.16. Mg breakthrough curves for Abist loam calculated with the MONOD, HYDRUS, and CHAIN_2D codes (data points from *Selim et al.* [1978]).

The Langmuir adsorption isotherm can also be used to model the exchange of homovalent ions. Parameters in the Langmuir adsorption isotherm for homovalent ion exchange may be derived as follows. Ion exchange for two ions with valences n and m can be expressed in a generalized form as [*Sposito*, 1981]

$$K_{ex} = \left[\frac{\bar{a}_1}{a_1}\right]^m \left[\frac{a_2}{\bar{a}_2}\right]^n \tag{8.8}$$

where K_{ex} is the dimensionless thermodynamic equilibrium constant, and a and $\bar{a}$ denote the ion activities in the soil solution and on the exchange surfaces [-], respectively:

$$a_i = \gamma_i c_i \qquad i = 1,2$$
$$\bar{a}_i = \xi_i s_i \qquad i = 1,2 \tag{8.9}$$

where c_i [ML^{-3}] (mmol/l) and s_i [MM^{-1}] (mmol/kg) are solution and exchangeable concentrations, respectively, and γ_i and ξ_i are activity coefficients in the soil solution [L^3M^{-1}] (l/mmol) and on the exchange surfaces [MM^{-1}] (kg/mmol), respectively. Substituting (8.9) into (8.8) gives

$$K_{12} = K_v \frac{\gamma_1^{\,m}}{\gamma_2^{\,n}} = K_{ex} \frac{\xi_2^{\,n}}{\xi_1^{\,m}} \frac{\gamma_1^{\,m}}{\gamma_2^{\,n}} = \frac{s_1^{\,m}}{s_2^{\,n}} \frac{c_2^{\,n}}{c_1^{\,m}} \tag{8.10}$$

where K_v denotes the Vanselow selectivity coefficient [-], while K_{12} will be simply referred to as the selectivity coefficient [-]. Assuming that both the total solution concentration, C_T [ML^{-3}] ($mmol_c$/l), and the cation exchange capacity, S_T [MM^{-1}] ($mmol_c$/kg), are time invariant, i.e.,

$$nc_1 + mc_2 = C_T$$
$$ns_1 + ms_2 = S_T \tag{8.11}$$

the Langmuir parameters k_s and η in (3.3) for the incoming solute become

$$k_s = \frac{K_{12} S_T}{C_T}$$
$$\eta = \frac{\vartheta (K_{12} - 1)}{C_T} \tag{8.12}$$

whereas for the solute initially in the soil column:

$$k_s = \frac{S_T}{K_{12} C_T}$$

$$\eta = \frac{\vartheta(1 - K_{12})}{K_{12} C_T} \tag{8.13}$$

The parameter ϑ in (8.12) and (8.13) equals 1 for monovalent ions, and 2 for divalent ions.

The selectivity coefficient K_{12} for example 5 was measured by *Selim et al.* [1987] (K_{12}=0.51). From the total solution concentration (C_T=10 mmol$_c$/l) and the known cation exchange capacity (S_T=62 mmol$_c$/kg), it follows that the parameters in the Langmuir adsorption isotherm for the incoming solute (Mg) are k_s=3.126 and η=-0.098, while those for the solute initially in the soil profile (Ca) the parameters are k_s=12.157 and η=0.192. The observed Ca breakthrough curve is shown in Figure 8.17, together with the simulated breakthrough curves obtained with the CHAIN_2D and MONOC codes [*Selim et al.*, 1987]. Note the closed agreement between the numerical results and the experimental data.

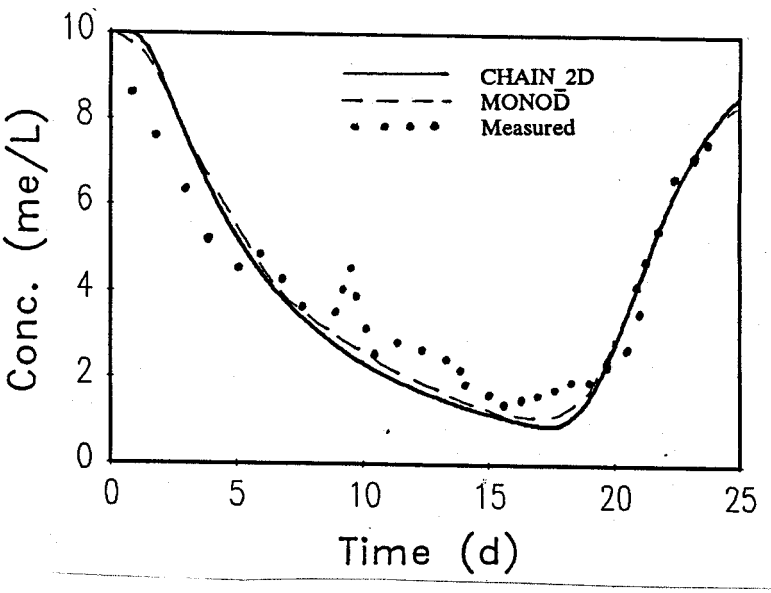

Fig. 8.17. Ca breakthrough curves for Abist loam calculated with the MONOD and CHAIN_2D codes (data points from *Selim et al.* [1978]) (example 5).

8.6. *Example 6 - One-Dimensional Solute Transport with Nonequilibrium Adsorption*

This example considers the movement of a boron (H_3BO_4) pulse through Glendale clay loam [*van Genuchten*, 1981]. The numerical simulation uses solute transport parameters that were fitted to the breakthrough curve with the CFITIM parameter estimation model [*van Genuchten*, 1981] assuming a two-site chemical nonequilibrium sorption model analogous to the formulation discussed in Section 3, but for steady-state water flow. Input parameters for example 6 are listed in Table 8.4. Figure 8.18 compares CHAIN_2D numerical results with the experimental data, and with a numerical simulation assuming physical non-equilibrium and nonlinear adsorption [*van Genuchten*, 1981].

Table 8.4. Input parameters for example 6.

Parameter	Value
q [cm/day]	17.12
D [cm^2/day]	49.0
θ [-]	0.445
ρ [g/cm$_3$]	1.222
c_0 [mmol$_c$/L]	20.0
k_s [cm^3/g]	1.14
β [-]	1.0
η [-]	0.0
f [-]	0.47
ω [1/day]	0.320
t_p [day]	5.06

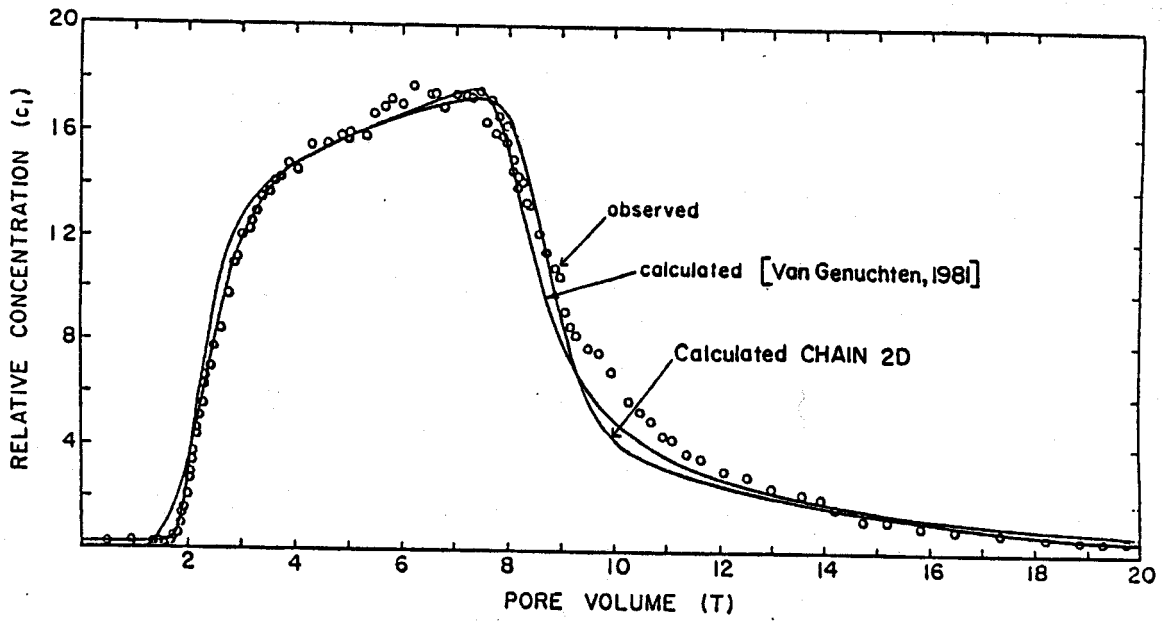

Fig. 8.18. Observed and calculated effluent curves for Boron movement through Glendale clay (data points from *van Genuchten* [1981]) (example 6).

8.7. *Example 7 - Water and Solute Infiltration Test*

This example corresponds to example 4 in the SWMS_2D manual [*Šimůnek et al.*, 1992]. The example concerns the movement of water and a dissolved solute from a single-ring infiltrometer into the soil profile consisting of two layers: a 40-cm thick A-horizon, and an underlying B/C-horizon. The hydraulic functions of the two soil layers are the same as those used in Example 2. The axisymmetric flow system and associated finite element mesh for the ponded infiltration experiment are shown in Figure 8.19. The soil profile had an initial temperature of 20°C, whereas the infiltrated water had a temperature of 30°C and contained an organic (parent) compound (the pesticide aldicarb) which is known to degrade by oxidation into two sequential daughter products (sulfone and sulfoxide) [*Ou et al.*, 1988]. Each of the three solutes also undergoes hydrolytical first-order decay that leads to products which are not simulated or monitored during their subsequent transport (i.e., oxime, sulfone oxime, and sulfoxide oxime) [*Ou et al.*, 1988]. All major solutes adsorb onto the solid phase, and volatilization is considered for the first and the third solutes. The reaction pathway is schematically given by:

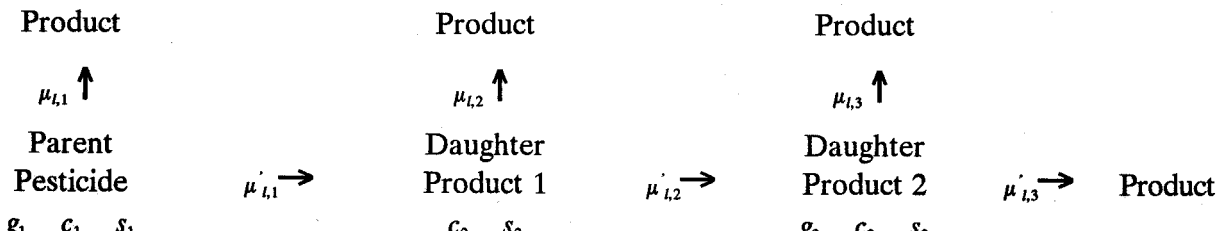

The example is used here to illustrate variably-saturated water flow, heat movement, and solute transport in a layered and radially symmetric three-dimensional soil profile.

Calculations were carried out over a period of 10 days. The pressure head profile obtained in example problem 2 at the beginning of June 1982 was taken as the initial condition for the water flow equation, similarly as in example 4 of *Šimůnek et al.* [1992]. The soil profile was assumed to be initially free of any solutes. All sides of the flow region were considered to be impervious, except for a small portion around the origin at the

surface (the ponded surface inside the ring infiltrometer) where constant pressure head and concentration flux boundary conditions were imposed, as well as the lower right corner where the groundwater level was kept constant. The concentration of the infiltrating water was free of any solute except for the first five days of the simulation during which time the infiltrating water contained the parent solute of unit concentration. Boundary condition (3.22) was used for the non-ponded part of the soil surface, thereby assuming the existence of a stagnant boundary layer of thickness d at the soil surface through which volatile solutes moved to the atmosphere by gas diffusion only. Water and solute extraction by plant roots was not considered.

Tables 8.5, 8.6, and 8.7 list the unsaturated soil hydraulic, heat and solute transport parameters, respectively. The solute and heat transport parameters were assumed to be the same for the two soil layers. The heat transport parameters b_1, b_2, b_3, C_n, C_o, and C_w in Table 8.6 were taken from *Chung and Horton* [1987]. The solute parameters k_s, k_g, μ_w, μ'_w, and D_g in Table 8.7 were taken from *Wagenet and Hutson* [1987].

Figure 8.20 presents the initial and steady-state pressure head profiles. The steady-state profile for water flow was reached after approximately 2 or 3 days. Temperature profiles at times 1 and 10 days are shown in Figure 8.21. The heat front moved relatively slowly into the soil profile in comparison with the solute front (shown later) because of the high volumetric heat capacity of the relatively wet soil. Figures 8.22, 8.23, and 8.24 show concentration profiles for all three solutes at times 2.5, 5, 7.5, and 10 days. After its application in the infiltrating water during the first five days of the simulation (Fig. 8.22a, b), the first (parent) solute is transported further by water flow and gaseous diffusion, as well as is being degraded by two first-order decay reactions, such that the soil profile is practically free of this solute after 10 days (Fig. 8.22c, d). The second solute exists exclusively because of first-order degradation of the first solute. Hence, the second solute initially corresponds mainly with the first solute, but subsequently moves faster through the soil profile because of less sorption. Note that the highest concentrations of the second solute were reached after complete application of the first solute (Fig. 8.23c, d). Similar features as for the second solute also apply to the third solute. In particular, notice that the soil profile is almost free of this solute after 2.5 days (Fig. 8.24a), and that the highest

concentrations of the third solute (while being much smaller than those for the first two solutes) were reached at the end of the simulation (Fig. 8.24d).

Table 8.5. Hydraulic input parameters for example 7.

Parameter	1st layer	2nd layer
$\theta_s=\theta_m=\theta_k$	0.399	0.339
$\theta_r=\theta_a$	0.000	0.000
$K_s=K_k$ [m/day]	0.298	0.454
α [1/m]	1.74	1.39
n [-]	1.38	1.60

Table 8.6. Heat transport input parameters for example 7.

Parameter	Value
θ_n [-]	0.600† (0.660‡)
θ_o [-]	0.001
λ_L [m]	0.005
λ_T [m]	0.001
b_1 [$Wm^{-1}K^{-1}$]	0.243
b_2 [$Wm^{-1}K^{-1}$]	0.393
b_3 [$Wm^{-1}K^{-1}$]	1.534
C_n [$Jm^{-3}K^{-1}$]	$1.92*10^6$
C_o [$Jm^{-3}K^{-1}$]	$2.51*10^6$
C_w [$Jm^{-3}K^{-1}$]	$4.18*10^6$
T_i [°C]	20
T_0 [°C]	30

† for the first layer
‡ for the second layer

Table 8.7. Solute transport input parameters for example 7.

Parameter	Value
ρ [kg/m^3]	1300
D_w [m^2/day]	0.00374
D_g [m^2/day]	0.432
D_L [m]	0.005
D_T [m]	0.001
$k_{s,1}$ [m^3/kg]	0.0001
$k_{s,2}$ [m^3/kg]	0.00005
$k_{s,3}$ [m^3/kg]	0.0002
$k_{g,1}$ [-]	$1.33*10^{-7}$
$k_{g,2}$ [-]	0.0
$k_{g,3}$ [-]	$1.33*10^{-3}$
$\mu_{w,1}$ [1/day]	0.2
$\mu_{w,2}$ [1/day]	0.01
$\mu_{w,3}$ [1/day]	0.005
$\mu'_{w,1}$ [1/day]	0.36
$\mu'_{w,2}$ [1/day]	0.024
$\mu'_{w,3}$ [1/day]	0.0024
$c_{0,1}$ [-]	1.0
$c_{0,2}$ [-]	0.0
$c_{0,3}$ [-]	0.0
d [m]	0.005

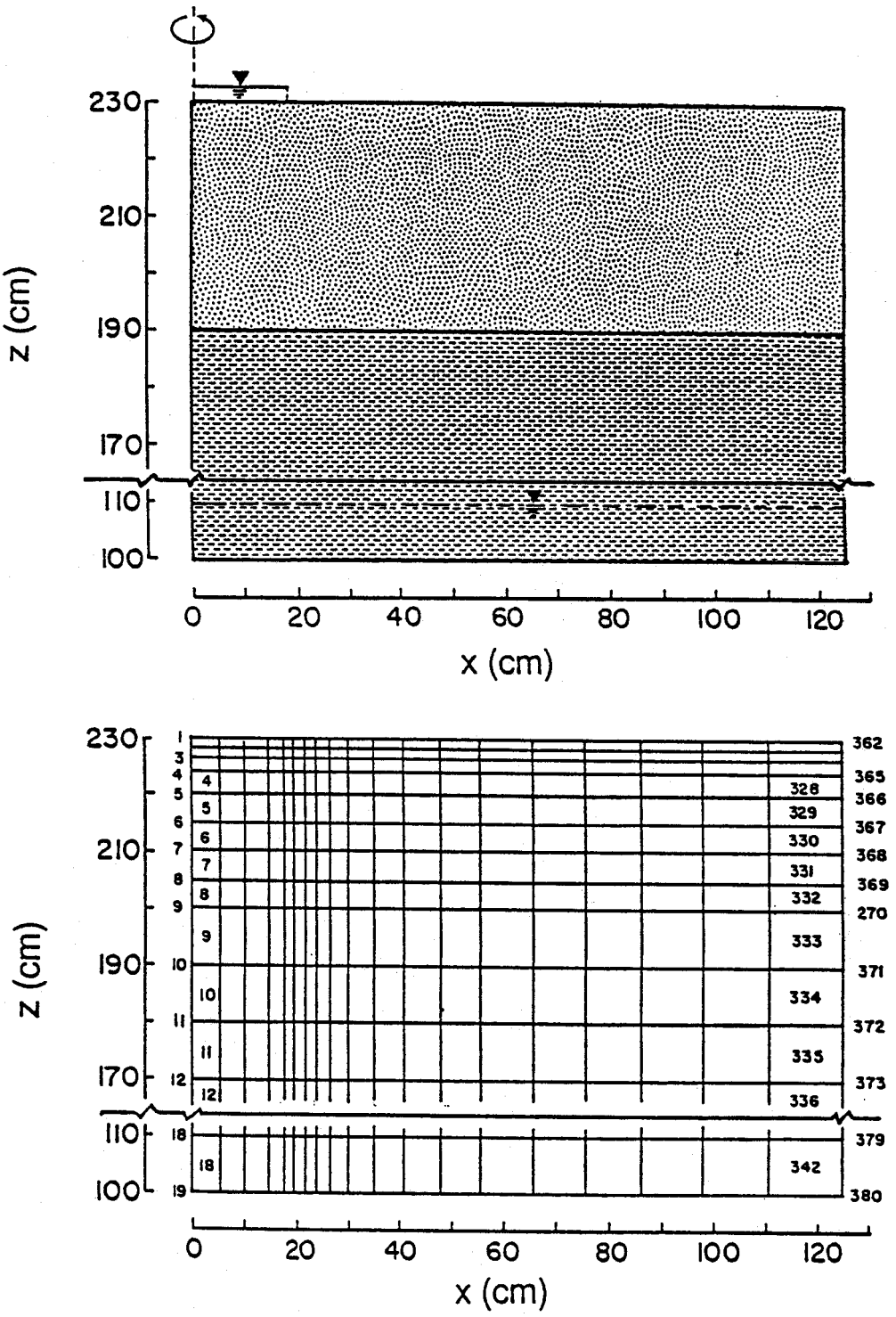

Fig. 8.19. Flow system and finite element mesh for example 7.

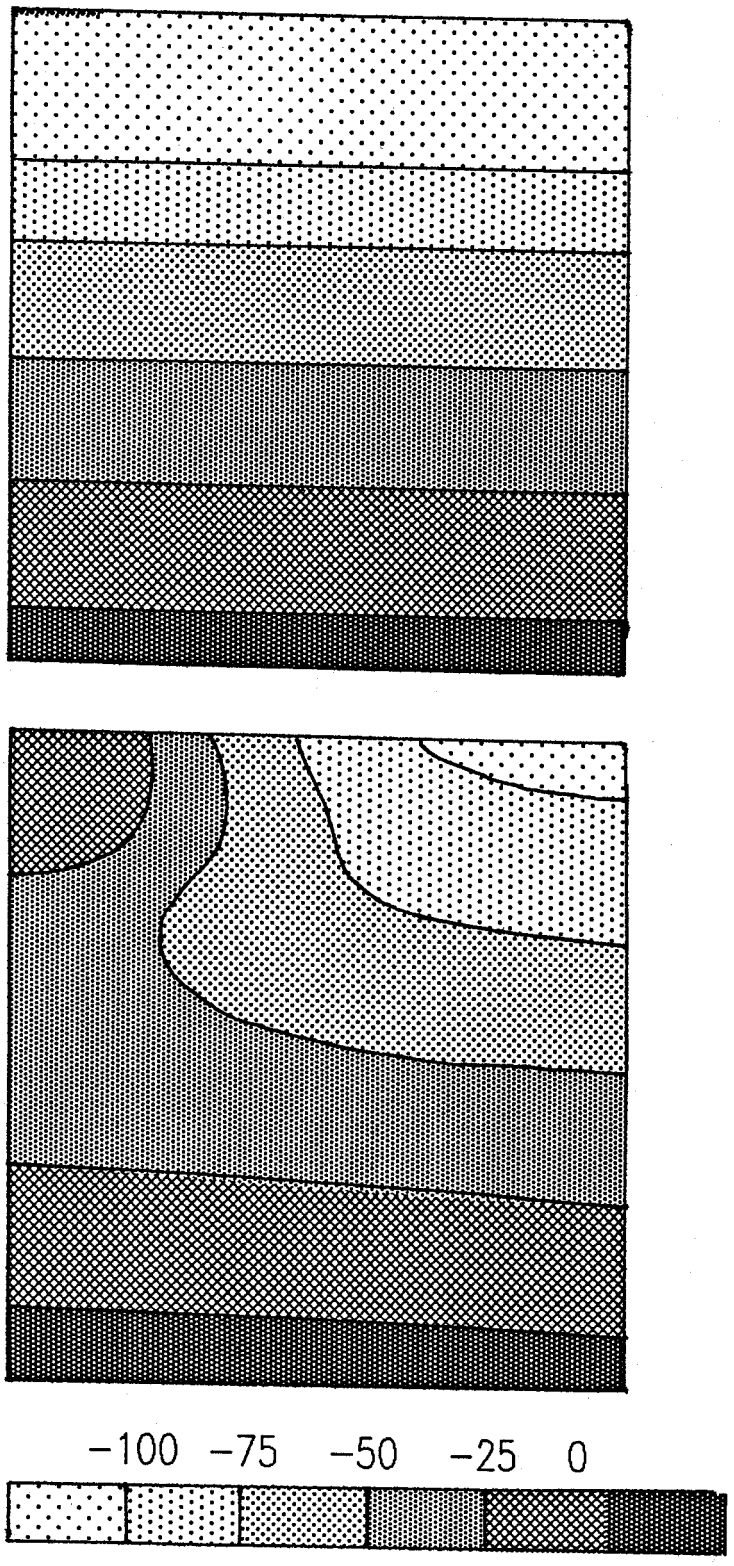

Fig. 8.20. Initial (top) and steady state (bottom) pressure head profiles for example 7.

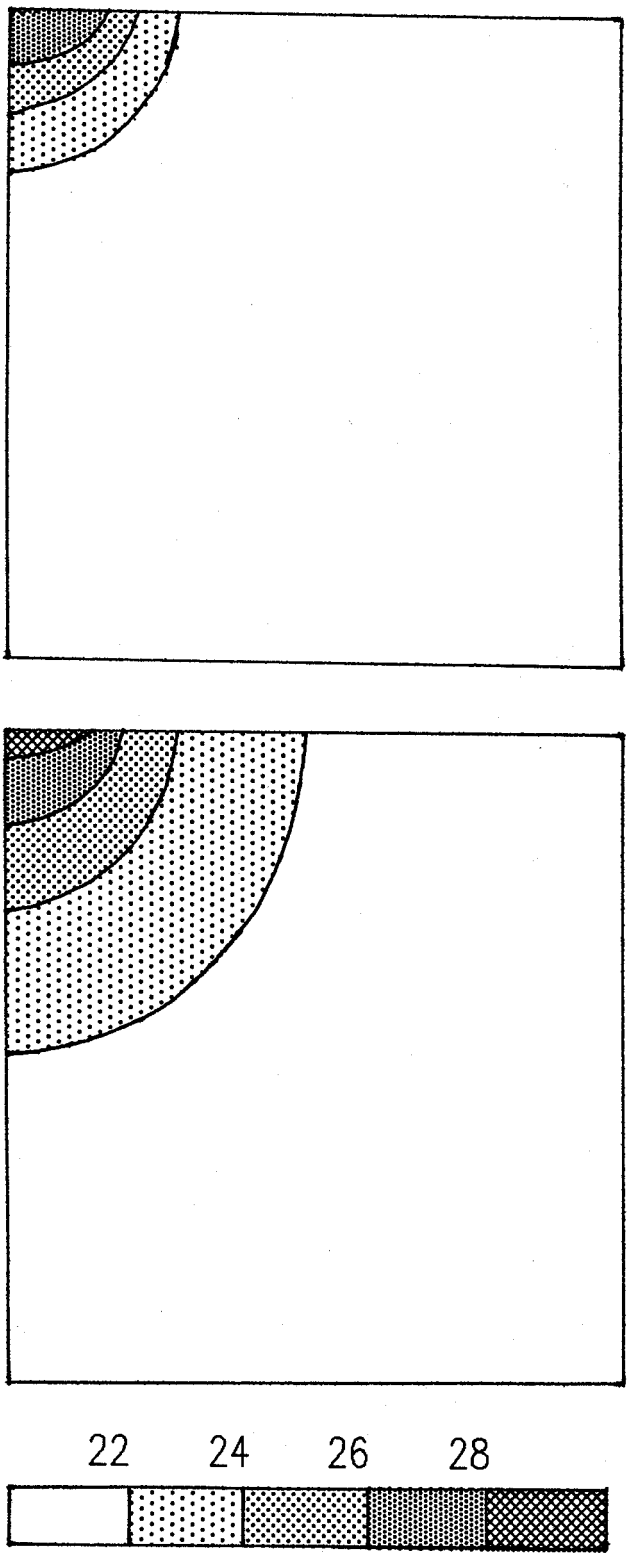

Fig. 8.21. Temperature profiles after 1 (top) and 10 days (bottom) for example 7.

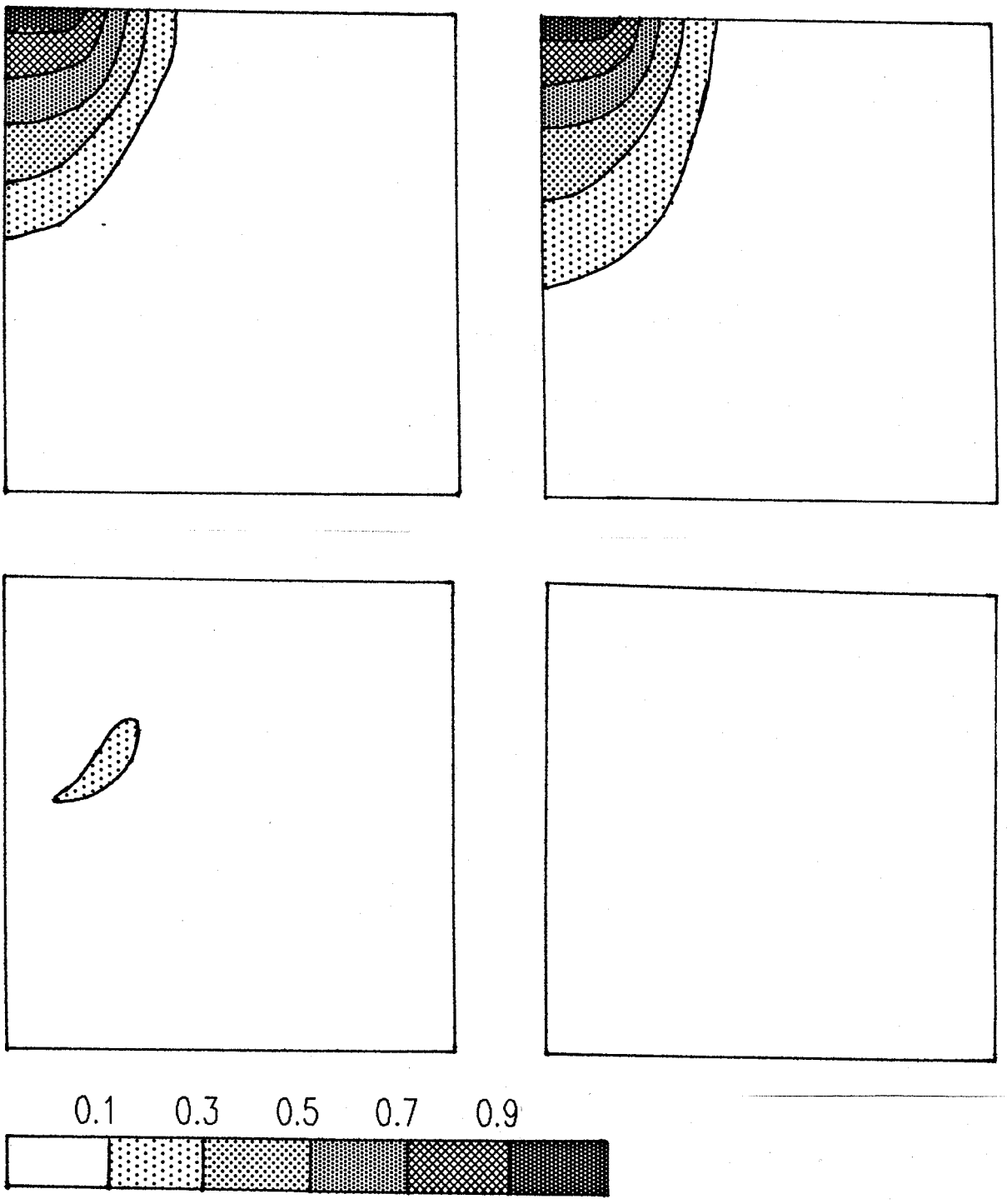

Fig. 8.22. Concentration profiles for the first solute after 2.5, 5, 7.5, and 10 days for example 7.

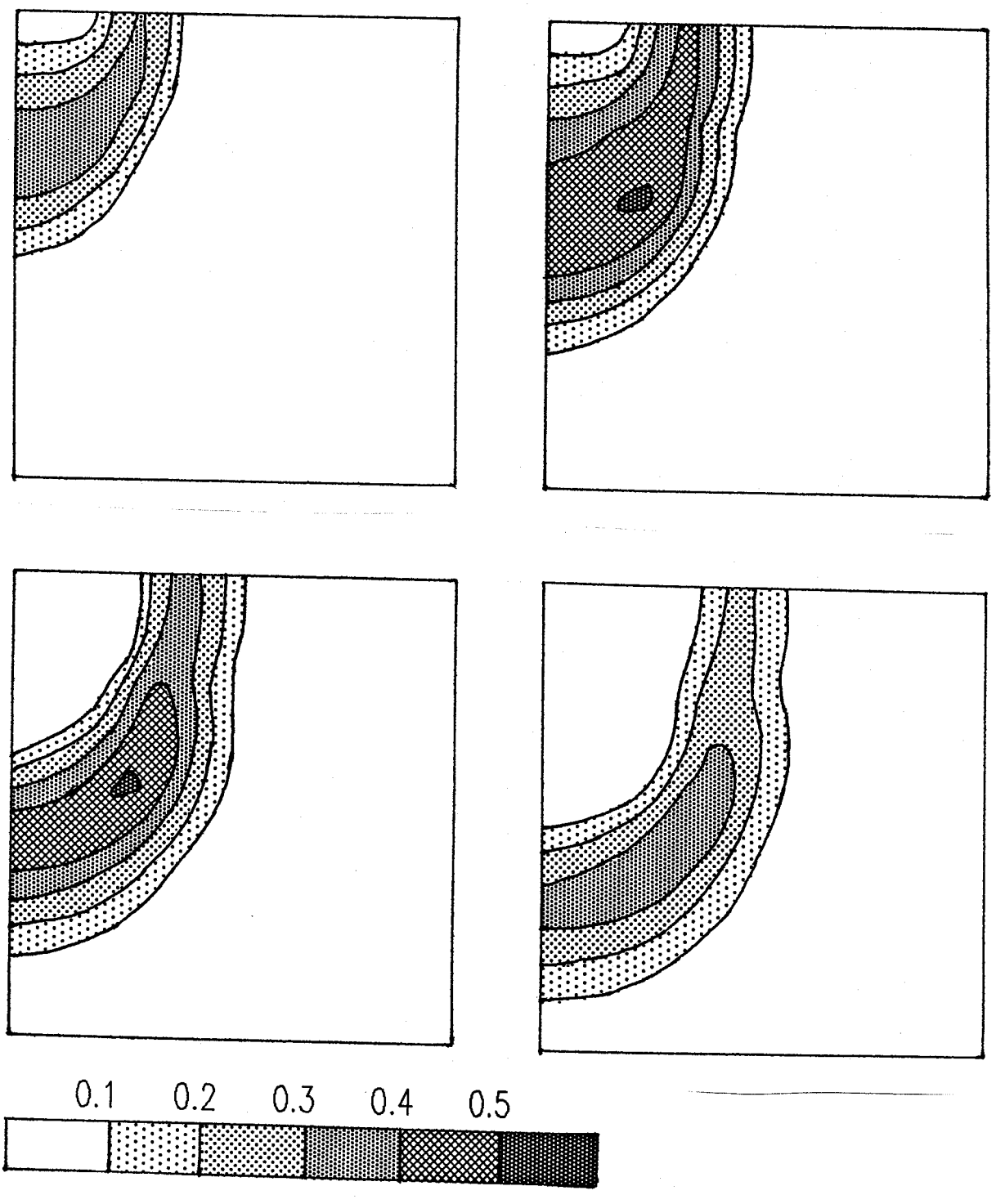

Fig. 8.23. Concentration profiles for the second solute after 2.5, 5, 7.5, and 10 days for example 7.

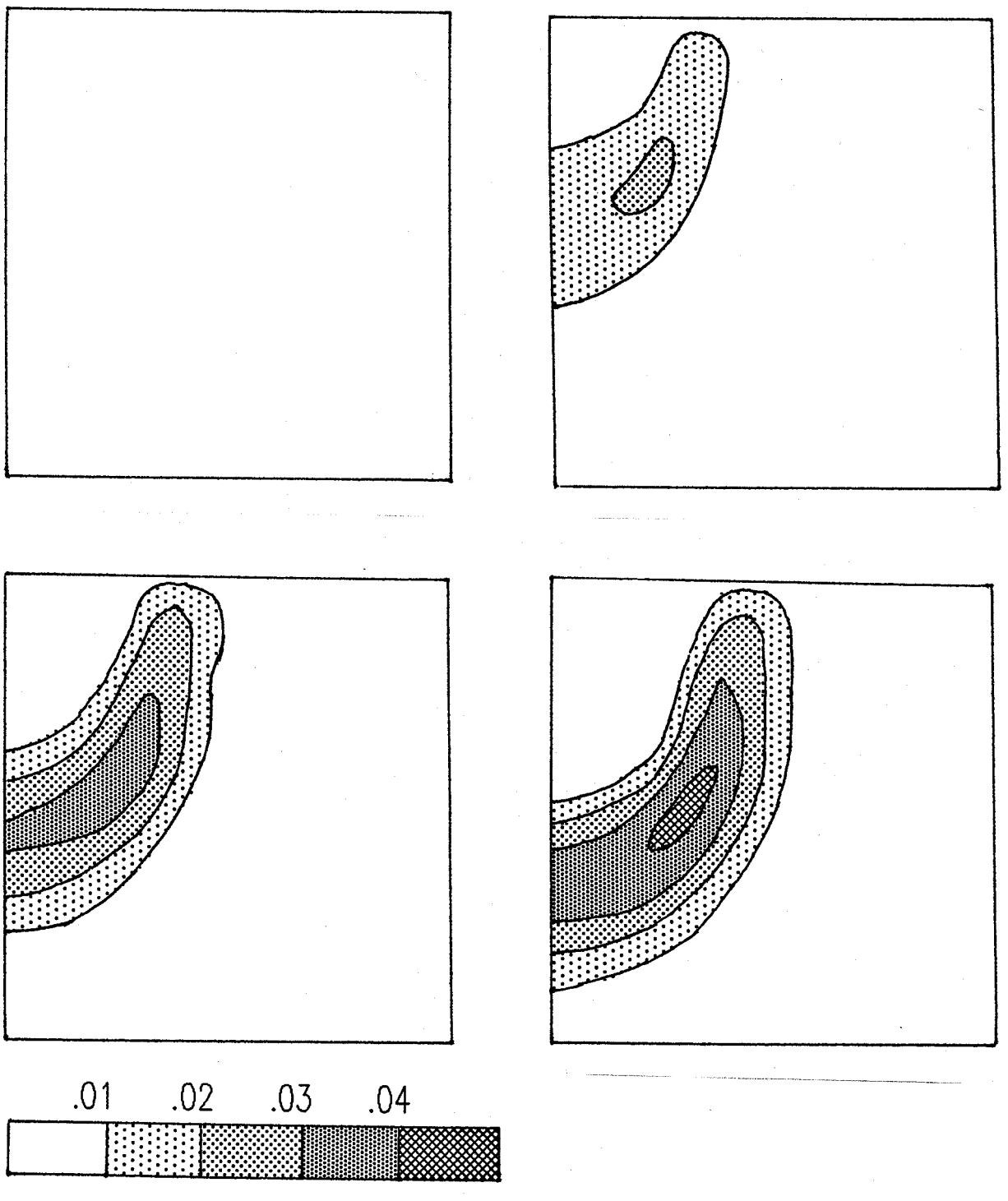

Fig. 8.24. Concentration profiles for the third solute after 2.5, 5, 7.5, and 10 days for example 7.

9. INPUT DATA

The input data for CHAIN_2D are given in three separate input files. These input files consist of one or more input blocks identified by the letters from A through L. The input files and blocks must be arranged as follows:

SELECTOR.IN
- A. Basic Information
- B. Material Information
- C. Time Information
- D. Root Water Uptake Information
- E. Seepage Face Information
- F. Drainage Information
- G. Solute Transport Information
- H. Heat Transport Information

GRID.IN
- I. Nodal Information
- J. Element Information
- K. Boundary Geometry Information

ATMOSPH.IN
- L. Atmospheric Information

The various input blocks are described in detail in Section 9.1, while Section 9.2 lists the actual input files for examples 1 through 7 discussed in Section 8. The output files for these examples are discussed in Section 10.

9.1. *Description of Data Input Blocks*

Tables 9.1 through 9.12 describe the data required for each input block. All data are read in using list-directed formatting (free format). Comment lines are provided at the beginning of, and within, each input block to facilitate, among other things, proper identification of the function of the block and the input variables. The comment lines are ignored during program execution; hence, they may be left blank but should not be omitted. All input files must be placed in the directory CHAIN_2D.IN. The program assumes that

all input data are specified in a consistent set of units for mass M, length L, and time T. The values of temperature should be specified in degrees Celsius.

Most of the information in Tables 9.1 through 9.12 should be self-explanatory. Table 9.9 (Block I) is used to define, among other things, the nodal coordinates and initial conditions for the pressure head, temperature and solute concentrations. One short-cut may be used when generating the nodal coordinates. The short-cut is possible when two nodes (e.g., N_1 and N_2), not adjacent to each other, are located along a transverse line such that N_2 is greater than N_1+1. The program will automatically generate nodes between N_1 and N_2, provided all of the following conditions are met simultaneously: (1) all nodes along the transverse line between nodes N_1 and N_2 are spaced at equal intervals, (2) values of the input variables *hNew*(n), *Beta*(n), *Axz*(n), *Bxz*(n), *Dxz*(n), *Temp*(n), and *Conc*(1,n) through *Conc*(*NS*,n) vary linearly between nodes N_1 and N_2, and (3) values of *Kode*(n), *Q*(n) and *MatNum*(n) are the same for all $n = N_1, N_1+1,..., N_2-1$ (see Table 9.9).

A similar short-cut is possible when generating the elements in Block J (Table 9.10). Consider two elements, E_1 and E_2, between two transverse lines such that E_2 is greater than E_1. The program requires input data only for element E_1 (i.e., data for elements E_1+1 through E_2 may be omitted), provided the following two conditions are met simultaneously: (1) all elements between E_1 and E_2 are quadrilaterals, including E_1 and E_2, and (2) all elements, $E_1,...., E_2$, are assigned the same values of *Angle*(e), *ConA*1(e), *ConA*2(e), and *LayNum*(e) as defined in Table 9.10.

Table 9.1. Block A - Basic information.

Record	Type	Variable	Description
1,2	-	-	Comment lines.
3	Char	*Hed*	Heading.
4	-	-	Comment line.
5	Char	*LUnit*	Length unit (e.g., 'cm').
5	Char	*TUnit*	Time unit (e.g., 'min').
5	Char	*MUnit*	Mass unit for concentration (e.g., 'g', 'mol', '-').
6	-	-	Comment line.
7	Integer	*Kat*	Type of flow system to be analyzed: 0 for a horizontal (areal) system 1 for axisymmetric flow 2 for vertical flow in a cross-section
8	-	-	Comment line.
9	Integer	*MaxIt*	Maximum number of iterations allowed during any time step (usually 20).
9	Real	*TolTh*	Absolute water content tolerance for nodes in the unsaturated part of the flow region [-] (its recommended value is 0.0001). *TolTh* represents the maximum desired absolute change in the value of the water content, θ, between two successive iterations during a particular time step.
9	Real	*TolH*	Absolute pressure head tolerance for nodes in the saturated part of the flow region [L] (its recommended value is 0.1 cm). *TolH* represents the maximum desired absolute change in the value of the pressure head, h, between two successive iterations during a particular time step.
10	-	-	Comment line.
11	Logical	*lWat*	Set this logical variable equal to **.true.** when transient water flow is considered. Set this logical variable equal to **.false.** when steady-state water flow is to be calculated.
11	Logical	*lChem*	Set this logical variable equal to **.true.** if solute transport is to be considered.
11	Logical	*CheckF*	Set this logical variable equal to **.true.** if the grid input data are to be printed for checking.
11	Logical	*ShortF*	**.true.** if information is to be printed only at preselected times, but not at each time step (T-level information, see Section 10.1), **.false.** if information is to be printed at each time step.
11	Logical	*FluxF*	**.true.** if detailed information about the element fluxes and discharge/recharge rates is to be printed.

Table 9.1. (continued)

Record	Type	Variable	Description
11	Logical	*AtmInf*	**.true.** if atmospheric boundary conditions are supplied via the input file ATMOSPH.IN, **.false.** if the file ATMOSPH.IN is not provided (i.e., in case of time independent boundary conditions).
11	Logical	*SeepF*	**.true.** if one or more seepage faces is to be considered.
11	Logical	*DrainF*	Set this logical variable equal to **.true.** if a drain is to be simulated by means of a boundary condition. Otherwise set equal to **.false.** . Section 4.3.7 explains how tile drains can be represented as boundary conditions in a regular finite element mesh.
11	Logical	*FreeD*	Set this variable equal to **.true.** if a unit vertical hydraulic gradient boundary condition (free drainage) is used at the bottom boundary. Otherwise set equal to **.false.** .
11	Logical	*lTemp*	Set this logical variable equal to **.true.** if heat transport is to be considered.
11	Logical	*lWDep*	**.true.** if hydraulic properties are to be considered as temperature dependent. **.false.** otherwise (see Section 2.4.2).
11	Logical	*lEquil*	**.true.** if equilibrium or no adsorption is considered in the solute transport equation. **.false.** if nonequilibrium adsorption is considered for at least one solute species.

Table 9.2. Block B - Material information.

Record	Type	Variable	Description
1,2	-	-	Comment lines.
3	Integer	*NMat*	Number of soil materials. Materials are identified by the material number, *MatNum*, specified in Block I.
3	Integer	*NLay*	Number of subregions for which separate water balances are being computed. Subregions are identified by the subregion number, *LayNum*, specified in Block J.
3	Real	*ha*	Absolute value of the upper limit [L] of the pressure head interval below which a table of hydraulic properties will be generated internally for each material (h_a must be greater than 0.0; e.g. 0.001 cm) (see Section 5.3.11).
3	Real	*hb*	Absolute value of the lower limit [L] of the pressure head interval for which a table of hydraulic properties will be generated internally for each material (e.g. 1000 m). One may assign to h_b the highest (absolute) expected pressure head to be expected during a simulation. If the absolute value of the pressure head during program execution lies outside of the interval $[h_a, h_b]$, then appropriate values for the hydraulic properties are computed directly from the hydraulic functions (i.e., without interpolation in the table).
3	Integer	*NPar*	Number of parameters specified for each material (i.e., 9 in case of the modified van Genuchten model). If the original van Genuchten model is to be used, then set $\theta_a=\theta_r$, $\theta_m=\theta_k=\theta_s$ and $K_k=K_s$ (see Section 2.3 for the description of unsaturated soil hydraulic properties).
4	-	-	Comment line.
5	Real	*Par*(1,*M*)	Parameter θ_r for material M [-].
5	Real	*Par*(2,*M*)	Parameter θ_s for material M [-].
5	Real	*Par*(3,*M*)	Parameter θ_a for material M [-].
5	Real	*Par*(4,*M*)	Parameter θ_m for material M [-].
5	Real	*Par*(5,*M*)	Parameter α for material M [L^{-1}].
5	Real	*Par*(6,*M*)	Parameter n for material M [-].
5	Real	*Par*(7,*M*)	Parameter K_s for material M [LT^{-1}].
5	Real	*Par*(8,*M*)	Parameter K_k for material M [LT^{-1}].
5	Real	*Par*(9,*M*)	Parameter θ_k for material M [-].
			Record 5 information is provided for each material M (from 1 to *NMat*). If *lWDep*=**.true.** (Block A) then the parameters of the soil hydraulic properties *Par*(*i*,*M*) must be specified at reference temperature T_{ref}=20°C.

Table 9.3. Block C - Time information.

Record	Type	Variable	Description
1,2	-	-	Comment lines.
3	Real	*dt*	Initial time increment, Δt [T]. Initial time step should be estimated in dependence on the problem solved. For problems with high pressure gradients (e.g. infiltration into an initially dry soil), Δt should be relatively small.
3	Real	*dtMin*	Minimum permitted time increment, Δt_{min} [T].
3	Real	*dtMax*	Maximum permitted time increment, Δt_{max} [T].
3	Real	*dMul*	If the number of required iterations at a particular time step is less than or equal to 3, then Δt for the next time step is multiplied by a dimensionless number *dMul* $\geq$ 1.0 (its value is recommended not to exceed 1.3).
3	Real	*dMul2*	If the number of required iterations at a particular time step is greater than or equal to 7, then Δt for the next time step is multiplied by *dMul2* $\leq$ 1.0 (e.g. 0.33).
3	Integer	*MPL*	Number of specified print-times at which detailed information about the pressure head, water content, flux, temperature, concentrations, and the water and solute balances will be printed.
4	-	-	Comment line.
5	Real	*TPrint*(1)	First specified print-time [T].
5	Real	*TPrint*(2)	Second specified print-time [T].
.	.	.	.
.	.	.	.
5	Real	*TPrint*(*MPL*)	Last specified print-time [T].

Table 9.4. Block D - Root water uptake information.†

Record	Type	Variable	Description
1,2	-	-	Comment lines.
3	Real	*P0*	Value of the pressure head, h_1 (Fig. 2.1), below which roots start to extract water from the soil.
3	Real	*P2H*	Value of the limiting pressure head, h_3, below which the roots cannot extract water at the maximum rate (assuming a potential transpiration rate of *r2H*).
3	Real	*P2L*	As above, but for a potential transpiration rate of *r2L*.
3	Real	*P3*	Value of the pressure head, h_4, below which root water uptake ceases (usually equal to the wilting point).
3	Real	*r2H*	Potential transpiration rate [LT^{-1}] (currently set at 0.5 cm/day).
3	Real	*r2L*	Potential transpiration rate [LT^{-1}] (currently set at 0.1 cm/day).
			The above input parameters permit one to make the variable h_3 a function of the potential transpiration rate, T_p (h_3 presumably decreases at higher transpiration rates). CHAIN_2D currently implements the same linear interpolation scheme as used in several versions of the SWATRE code (e.g., *Wesseling and Brandyk* [1985]) and in the code SWMS_2D [*Šimůnek et al.*, 1992]. The scheme is based on the following interpolation: $$h_3 = P2H + \frac{P2L - P2H}{r2H - r2L}(r2H - T_p) \qquad for\ r2L < T_p < r2H$$ $$h_3 = P2L \qquad for\ T_a \le r2L$$ $$h_3 = P2H \qquad for\ T_a \ge r2H$$
4	-	-	Comment line.
5	Real	*POptm*(1)	Value of the pressure head, h_2, below which roots start to extract water at the maximum possible rate (material number 1).
5	Real	*POptm*(2)	As above (material number 2).
.	.	.	.
.	.	.	.
5	Real	*POptm*(*NMat*)	As above (for material number *NMat*).

† Block D is not read in if the logical variable *SinkF* (Block L) is set equal to **.false.** .

Table 9.5. Block E - Seepage face information.†

Record	Type	Variable	Description
1,2	-	-	Comment lines.
3	Integer	*NSeep*	Number of seepage faces expected to develop.
4	-	-	Comment line.
5	Integer	*NSP*(1)	Number of nodes on the first seepage face.
5	Integer	*NSP*(2)	Number of nodes on the second seepage face.
.	.	.	.
.	.	.	.
5	Integer	*NSP*(*NSeep*)	Number of nodes on the last seepage face.
6	-	-	Comment line.
7	Integer	*NP*(1,1)	Sequential global number of the first node on the first seepage face.
7	Integer	*NP*(1,2)	Sequential global number of the second node on the first seepage face.
.	.	.	.
.	.	.	.
7	Integer	*NP*(1,*NSP*(1))	Sequential global number of the last node on the first seepage face.
			Record 7 information is provided for each seepage face.

† Block E is not read in if the logical variable *SeepF* (Block A) is set equal to **.false.** .

Table 9.6. Block F - Drainage information.†

Record	Type	Variable	Description
1,2	-	-	Comment lines.
3	Integer	*NDr*	Number of drains. See Section 5.3.7 for a discussion on how tile drains can be represented as boundary conditions in a regular finite element mesh.
3	Real	*DrCorr*	Additional reduction in the correction factor C_d (See Section 5.3.7).
4	-	-	Comment line.
5	Integer	*ND*(1)	Global number of the first drain.
5	Integer	*ND*(2)	Global number of the second drain.
.	.	.	.
.	.	.	.
5	Integer	*ND*(*NDr*)	Global number of the last drain.
6	-	-	Comment line.
7	Integer	*NElD*(1)	Number of elements surrounding the first drain.
7	Integer	*NElD*(2)	Number of elements surrounding the second drain.
.	.	.	.
.	.	.	.
7	Integer	*NElD*(*NDr*)	Number of elements surrounding the last drain.
8	-	-	Comment line.
9	Real	*EfDim*(1,1)	Effective diameter of the first drain, d_e [L] (see Section 5.3.7).
9	Real	*EfDim*(2,1)	Dimension of the square in finite element mesh representing the first drain, D [L] (see Section 5.3.7).
			Record 9 information is provided for each drain.
10	-	-	Comment line.
11	Integer	*KElDr*(1,1)	Global number of the first element surrounding the first drain.
11	Integer	*KElDr*(1,2)	Global number of the second element surrounding the first drain.
.	.	.	.
.	.	.	.
11	Integer	*KElDr*(1,*NElD*(1))	Global number of the last element surrounding the first drain.
			Record 11 information is provided for each drain.

† Block F is not read in if the logical variable *DrainF* (Block A) is set equal to .false. .

Table 9.7. Block G - Solute transport information.†

Record	Type	Variable	Description
1,2	-	-	Comment lines.
3	Real	*Epsi*	Temporal weighing coefficient. =0.0 for an explicit scheme. =0.5 for a Crank-Nicholson implicit scheme. =1.0 for a fully implicit scheme.
3	Logical	*lUpW*	**.true.** if upstream weighing formulation is to be used. **.false.** if the original Galerkin formulation is to be used.
3	Logical	*lArtD*	**.true.** if artificial dispersion is to be added in order to fulfill the stability criterion *PeCr* (see Section 6.3.6). **.false.** otherwise.
3	Logical	*lTDep*	**.true.** if at least one transport or reaction coefficient (*ChPar*) is temperature dependent. **.false.** otherwise. If *lTDep*=**.true.**, then all values of *ChPar(i,M)* should be specified at a reference temperature T_r=20°C.
3	Real	*cTolA*	Absolute concentration tolerance [ML^{-3}], the value is dependent on the units used (set equal to zero if nonlinear adsorption is not considered).
3	Real	*cTolR*	Relative concentration tolerance [-] (set equal to zero if nonlinear adsorption is not considered).
3	Integer	*MaxItC*	Maximum number of iterations allowed during any time step for solute transport - usually 20 (set equal to zero if nonlinear adsorption is not considered).
3	Real	*PeCr*	Stability criteria (see Section 6.3.6). Set equal to zero when *lUpW* is equal to **.true.**.
4	-	-	Comment line.
5	Real	*ChPar*(1,*M*)	Bulk density of material *M*, ρ [ML^{-3}].
5	Real	*ChPar*(2,*M*)	Longitudinal dispersivity for material type *M*, D_L [L].
5	Real	*ChPar*(3,*M*)	Transverse dispersivity for material type *M*, D_T [L].
5	Real	*ChPar*(4,*M*)	Dimensionless fraction of the adsorption sites classified as type-1, i.e., sites with instantaneous sorption. Set equal to 1 if equilibrium transport is to be considered. Record 5 information is provided for each material *M* (from 1 to *NMat*).
6	-	-	Comment line.
7	Real	*ChPar*(5,*M*)	Ionic or molecular diffusion coefficient in free water, D_w [L^2T^{-1}].
7	Real	*ChPar*(6,*M*)	Ionic or molecular diffusion coefficient in gas phase, D_g [L^2T^{-1}].
8	-	-	Comment line.

Table 9.7. (continued)

Record	Type	Variable	Description
9	Real	*ChPar*(7,*M*)	Adsorption isotherm coefficient, k_s, for material type *M* [L^3M^{-1}]. Set equal to zero if no adsorption is to be considered.
9	Real	*ChPar*(8,*M*)	Adsorption isotherm coefficient, η, for material type M [L^3M^{-1}]. Set equal to zero if Langmuir adsorption isotherm is not to be considered.
9	Real	*ChPar*(9,*M*)	Adsorption isotherm coefficient, β, for material type M [-]. Set equal to one if Freundlich adsorption isotherm is not to be considered.
9	Real	*ChPar*(10,*M*)	Equilibrium distribution constant between liquid and gas phases, k_g, material type *M* [-].
9	Real	*ChPar*(11,*M*)	First-order rate constant for dissolved phase, μ_w, material type *M* [T^{-1}].
9	Real	*ChPar*(12,*M*)	First-order rate constant for solid phase, μ_s, material type *M* [T^{-1}].
9	Real	*ChPar*(13,*M*)	First-order rate constant for gas phase, μ_g, material type *M* [T^{-1}].
9	Real	*ChPar*(14,*M*)	Rate constant, μ_w', representing a first-order decay for the first solute and zero-order production for the second solute in the dissolved phase, material type *M* [T^{-1}].
9	Real	*ChPar*(15,*M*)	Same as above for the solid phase, μ_s', material type *M* [T^{-1}].
9	Real	*ChPar*(16,*M*)	Same as above for the gas phase, μ_g', material type *M* [T^{-1}].
9	Real	*ChPar*(17,*M*)	Zero-order rate constant for dissolved phase, γ_w, material type *M* [$ML^{-3}T^{-1}$].
9	Real	*ChPar*(18,*M*)	Zero-order rate constant for solid phase, γ_s, material type *M* [T^{-1}].
9	Real	*ChPar*(19,*M*)	Zero-order rate constant for gas phase, γ_g, material type *M* [$ML^{-3}T^{-1}$].
9	Real	*ChPar*(20,*M*)	First-order mass transfer coefficient for nonequilibrium adsorption, ω, material type M [T^{-1}].
			Record 9 information is provided for each material *M* (from 1 to *NMat*).
			Record 6 through 9 informations are provided for each solute (from 1 to *NS*).
10,11	-	-	Comment lines.
12	Real	*TDep*(5)	Activation energy for parameter *ChPar*(5,*M*) [$ML^2T^{-2}M^{-1}$] (See Section 3.4). This parameter should be specified in J mol^{-1}. Set equal to 0 if *ChPar*(5,*M*) is temperature independent.
12	Real	*TDep*(6)	Same for parameter *ChPar*(6,*M*) [$ML^2T^{-2}M^{-1}$].
13	-	-	Comment line.
14	Real	*TDep*(7)	Same for parameter *ChPar*(7,*M*) [$ML^2T^{-2}M^{-1}$].
.	.	.	.
.	.	.	.
14	Real	*TDep*(20)	Same for parameter *ChPar*(20,*M*) [$ML^2T^{-2}M^{-1}$].
			Records 11 through 14 information is provided only when the logical variable *lTDep* of record 3 is set equal to **.true.**.
15	-	-	Comment line.

Table 9.7. (continued)

Record	Type	Variable	Description
16	Integer	*KodCB*(1)	Code specifying the type of boundary condition for solute transport applied to a particular node. Positive and negative signs indicate that first-, or second- or third- (depending upon the calculated water flux Q), type boundary conditions are implemented, respectively. In case of time-independent boundary conditions (*Kode*(1) = $\pm 1, \pm 2, \pm 5$, or ± 6; See Block I), *KodCB*(1) also refers to the field *cBound* for the value of the solute transport BC. *cBound*(*i*,abs(*KodCB*(1))) is the value of the boundary condition for node *KXB*(1) (the first of a set of sequentially numbered boundary nodes for which *Kode*(*N*) is not equal to zero). Permissible values are $\pm 1, \pm 2, ..., \pm 5, \pm 6$,-7. When *KodCB*(1) equals -7, a special type of boundary condition for volatile solutes described by equations (3.21) and (3.22) is applied.
16	Integer	*KodCB*(2)	Same as above for the second boundary node.
.	.	.	.
.	.	.	.
16	Integer	*KodCB*(*NumBP*)	Same as above for the last boundary node.
17	-	-	Comment line.
18	Real	*cBound*(1,1)	Value of the concentration for the first time-independent BC [ML^{-3}]. Set equal to zero if no *KodCB*(n) = ± 1 is specified.
18	Real	*cBound*(1,2)	Value of the concentration for the second time-independent BC [ML^{-3}]. Set equal to zero if no *KodCB*(n) = ± 2 is specified.
.	.	.	.
.	.	.	.
18	Real	*cBound*(1,5)	Value of the concentration for the fifth time-independent BC [ML^{-3}]. If water uptake is specified, then *cBound*(1,5) is automatically used for the concentration of water removed from the flow region by root water uptake [ML^{-3}]. Set equal to zero if no *KodCB*(n) = ± 5 and no root solute uptake is specified.
18	Real	*cBound*(1,6)	Value of the concentration for the sixth time-independent BC [ML^{-3}]. If internal sources are specified, then *cBound*(1,6) is automatically used for the concentration of water injected into the flow region through internal sources [ML^{-3}]. Set equal to zero if no *KodCB*(n) = ± 6 and no internal sources are specified.
18	Real	*cBound*(1,7)	Concentration of the incoming fluid in equation (3.21) [ML^{-3}]. Set equal to zero if no *KodCB*(n) = -7 is specified.
18	Real	*cBound*(1,8)	Concentration above the stagnant boundary layer, g_{atm} (see equation (3.21)) [ML^{-3}]. Set equal to zero if no *KodCB*(n) = -7 is specified.
18	Real	*cBound*(1,9)	Thickness of the stagnant boundary layer, d [L] (see equation (3.21)). Set equal to zero if no *KodCB*(n) = -7 is specified.
			Record 18 information is provided for each solute (from 1 to *NS*).

Table 9.7. (continued)

Record	Type	Variable	Description
19	-	-	Comment line.
20	Real	*tPulse*	Time duration of the concentration pulse [T].

†Block G is not needed when the logical variable *lChem* in Block A is set equal to **.false.** .

Table 9.8. Block H - Heat transport information.†

Record	Type	Symbol	Description
1,2	-	-	Comment lines.
3	Real	*TPar*(1,*M*)	Volumetric solid phase fraction of material *M*, θ_n [-].
3	Real	*TPar*(2,*M*)	Volumetric organic matter fraction of material *M*, θ_o [-].
3	Real	*TPar*(3,*M*)	Longitudinal thermal dispersivity of material *M*, λ_L [L].
3	Real	*TPar*(4,*M*)	Transverse thermal dispersivity of material *M*, λ_T [L].
3	Real	*TPar*(5,*M*)	Coefficient b_1 in the thermal conductivity function [$MLT^{-3}K^{-1}$] (e.g.$Wm^{-1}K^{-1}$) (see equation (4.5)).
3	Real	*TPar*(6,*M*)	Coefficient b_2 in the thermal conductivity function [$MLT^{-3}K^{-1}$] (e.g.$Wm^{-1}K^{-1}$) (see equation (4.5)).
3	Real	*TPar*(7,*M*)	Coefficient b_3 in the thermal conductivity function [$MLT^{-3}K^{-1}$] (e.g.$Wm^{-1}K^{-1}$) (see equation (4.5)).
3	Real	*TPar*(8,*M*)	Volumetric heat capacity of solid phase of material *M*, C_n [$ML^{-1}T^{-2}K^{-1}$] (e.g. $Jm^{-3}K^{-1}$).
3	Real	*TPar*(9,*M*)	Volumetric heat capacity of organic matter of material *M*, C_o [$ML^{-1}T^{-2}K^{-1}$] (e.g. $Jm^{-3}K^{-1}$).
3	Real	*TPar*(10,*M*)	Volumetric heat capacity of liquid phase of material *M*, C_w [$ML^{-1}T^{-2}K^{-1}$] (e.g. $Jm^{-3}K^{-1}$).
			Record 3 is required for each soil material *M* (from 1 to *NMat*).
4	-	-	Comment line.
5	Integer	*KodTB*(1)	Code specifying the type of boundary condition for heat transport applied to a particular node. Positive and negative signs mean that first-, or second- or third- (depending upon the calculated water flux *Q*) type boundary conditions will be implemented, respectively. In case of time-independent boundary conditions (*Kode*(1) = $\pm$1, $\pm$2, $\pm$5, or $\pm$6; See Block I), *KodTB*(1) refers to the vector *TBound* for the value of the heat transport BC. *TBound*(abs(*KodTB*(1))) is the value of the boundary condition for node *KXB*(1) (the first of a set of sequentially numbered boundary nodes for which *Kode*(*N*) is not equal to zero). Permissible values are $\pm$1,...,$\pm$6.
5	Integer	*KodTB*(2)	Same as above for the second boundary node.
.	.	.	.
.	.	.	.
5	Integer	*KodTB*(*NumBP*)	Same as above for the last boundary node.
6	-	-	Comment line.
7	Real	*TBound*(1)	Value of the first time-independent thermal boundary condition [^{0}C]. Set equal to zero if no *KodTB*(*n*) = $\pm$1 is specified.
7	Integer	*TBound*(2)	Value of the second time-independent thermal boundary condition [^{0}C]. Set equal to zero if no *KodTB*(*n*) = $\pm$2 is specified.
.	.	.	.
.	.	.	.

Table 9.8. (continued)

Record	Type	Variable	Description
7	Integer	*TBound*(6)	Value of the sixth time-independent thermal boundary condition [°C]. Set equal to zero if no $KodTB(n) = \pm 6$ is specified. If internal sources are specified, then *TBound*(6) is automatically used for the temperature of water injected into the flow region through internal source.
8	-	-	Comment line.
9	Real	*Ampl*	Temperature amplitude at the soil surface [K] prescribed for nodes where $Kode(n) = \pm 4$. Set equal to zero when no $Kode(n) = \pm 4$ is specified.
9	Real	*tPeriod*	Time interval for the completion of one temperature cycle (usually 1 day) [T].

† Block H need not be supplied if logical variables *lTemp* (Block A) is set equal to **.false.**

Table 9.9. Block I - Nodal information.

Record	Type	Variable	Description
1,2	-	-	Comment lines.
3	Integer	*NumNP*	Number of nodal points.
3	Integer	*NumEl*	Number of elements (quadrilaterals and/or triangles).
3	Integer	*IJ*	Maximum number of nodes on any transverse line. Set equal to zero if *IJ* > 10.
3	Integer	*NumBP*	Number of boundary nodes for which *Kode(N)* is not equal to 0.
3	Integer	*NS*	Number of solutes in a chain reaction.
3	Integer	*NObs*	Number of observation nodes for which values of the pressure head, the water content, temperature (for *lTemp* = .true.), and the solution and sorbed concentrations (for *lChem* = .true.) are printed at each time level.
4	-	-	Comment line.
5	Integer	*n*	Nodal number.
5	Integer	*Kode(n)*	Code specifying the type of boundary condition applied to a particular node. Permissible values are $0, \pm 1, \pm 2, \pm 3, \pm 4, ..., \pm NumKD$ (see Section 7.3).
5	Real	*x(n)*	*x*-coordinate of node *n* [L] (always a horizontal coordinate).
5	Real	*z(n)*	*z*-coordinate of node *n* [L]. *z* is the vertical coordinate for problems involving vertical planar or axisymmetric flow. For axisymmetric flow, *z* coincides with the vertical axis of symmetry.
5	Real	*hNew(n)*	Initial value of the pressure head at node *n* [L]. If *lWat* = **.false.** in Block A, then *hNew(n)* represents the initial guess of the pressure head for steady state conditions.
5	Real	*Q(n)*	Prescribed recharge/discharge rate at node *n*; [L^2T^{-1}] for planar flow, [L^3T^{-1}] for axisymmetric flow. *Q(n)* is negative when directed out of the system. When no value for *Q(n)* is needed, set *Q(n)* equal to zero.
5	Integer	*MatNum(n)*	Index for material whose hydraulic and transport properties are assigned to node *n*.
5	Real	*Beta(n)*	Value of the water uptake distribution, $b(x,z)$ [L^{-2}], in the soil root zone at node *n*. Set *Beta(n)* equal to zero if node *n* lies outside the root zone.
5	Real	*Axz(n)*	Nodal value of the dimensionless scaling factor α_h [-] associated with the pressure head.
5	Real	*Bxz(n)*	Nodal value of the dimensionless scaling factor α_K [-] associated with the saturated hydraulic conductivity.
5	Real	*Dxz(n)*	Nodal value of the dimensionless scaling factor α_θ [-] associated with the water content.

Table 9.9. (continued)

Record	Type	Variable	Description
5	Real	*Temp*(*n*)	Initial value of temperature at node *n* [°C] (if *lTemp* = **.false.** then set equal to 0 or any initial value, which is to be used with temperature dependent water flow and solute transport).
5	Real	*Conc*(1,*n*)	Initial value of the concentration of the first solute at node *n* [ML^{-3}] (do not have to be specified if *lChem* = **.false.**).
5	Real	*Conc*(2,*n*)	Initial value of concentration of the second solute at node *n* [ML^{-3}] (must not be specified if *lChem* = **.true.** and *NS* < 2).
.	.	.	.
.	.	.	.
5	Real	*Conc*(*i*,*n*)	Initial value of the concentration of the last solute at node *n* [ML^{-3}] (must not be specified if *lChem* = **.true.** and *NS* < *i*)..
5	Real	*Sorb*(1,*n*)	Initial value of the adsorbed concentration on type-2 sites of the first solute at node *n* [ML^{-3}]. This variable does not have to be specified if *lChem* = **.false.**. or *lEquil* = **.true.** .
5	Real	*Sorb*(2,*n*)	Initial value of the adsorbed concentration on type-2 sites of the second solute at node *n* [ML^{-3}]. This variable does not have to be specified if *lChem* = **.false.** or *lEquil* = **.true.** or *NS* < 2.
.	.	.	.
.	.	.	.
5	Real	*Sorb*(*NS*,*n*)	Initial value of the adsorbed concentration on type-2 sites of the *NS*th solute at node *n* [ML^{-3}]. This variable does not have to be specified if *lChem* = **.false.** or *lEquil* = **.true.** .
			In general, record 5 information is required for each node *n*, starting with *n* = 1 and continuing sequentially until *n* = *NumNP*. Record 5 information for certain nodes may be skipped if several conditions are satisfied (see beginning of this section).

Table 9.10. Block J - Element information.

Record	Type	Variable	Description
1,2	-	-	Comment lines.
3	Integer	e	Element number.
3	Integer	$KX(e,1)$	Global nodal number of corner node i.
3	Integer	$KX(e,2)$	Global nodal number of corner node j.
3	Integer	$KX(e,3)$	Global nodal number of corner node k.
3	Integer	$KX(e,4)$	Global nodal number of corner node l. Indices i, j, k, and l, refer to the corner nodes of an element e taken in a counter-clockwise direction. For triangular elements $KX(e,4)$ must be equal to $KX(e,3)$.
3	Real	$Angle(e)$	Angle in degrees between K_1^A and the x-coordinate axis assigned to each element e.
3	Real	$ConA1(e)$	First principal component, K_1^A, of the dimensionless tensor $\mathbf{K}^A$ which describes the local anisotropy of the hydraulic conductivity assigned to element e.
3	Real	$ConA2(e)$	Second principal component, K_2^A.
3	Integer	$LayNum(e)$	Subregion number assigned to element e.
			In general, record 3 information is required for each element e, starting with $e=1$ and continuing sequentially until $e=NumEl$. Record 3 information for certain elements may be skipped if several conditions are satisfied (see beginning of this section).

Table 9.11. Block K - Boundary geometry information.

Record	Type	Variable	Description
1,2	-	-	Comment lines.
3	Integer	*KXB*(1)	Global node number of the first of a set of sequentially numbered boundary nodes for which *Kode*(*n*) is not equal to zero.
3	Integer	*KXB*(2)	As above for the second boundary node.
.	.	.	.
.	.	.	.
3	Integer	*KXB*(*NumBP*)	As above for the last boundary node.
4	-	-	Comment line.
5	Real	*Width*(1)	Width of the boundary [L] associated with boundary node *KXB*(1). *Width*(*n*) includes half the boundary length of each element connected to node *KXB*(*n*) along the boundary. The type of boundary condition assigned to *KXB*(*n*) is determined by the value of *Kode*(*n*). In case of axisymmetric flow, *Width*(*n*) represents the area of the boundary strip [L^2] associated with node *KXB*(*n*), and along a horizontal boundary should be calculated as $$Width(j) = \frac{\pi}{3}[(x_{j-1} + 2x_j)(x_j - x_{j-1}) + (x_{j+1} + 2x_j)(x_{j+1} - x_j)]$$ If a unit vertical hydraulic gradient or a deep drainage boundary condition is specified at node *n*, then *Width*(*n*) represents only the horizontal component of the boundary.
5	Real	*Width*(2)	As above for node *KXB*(2).
.	.	.	.
.	.	.	.
5	Real	*Width*(*NumBP*)	As above for node *KXB*(*NumBP*).
6	-	-	Comment line.
7	Real	*rLen*	Width of soil surface associated with transpiration [L]; represents surface area [L^2] in case of axisymmetrical flow. Set *rLen* equal to zero for problems without transpiration.
8	-	-	Comment line.
9	Integer	*Node*(1)	Global node number of the first observation node for which values of the pressure head, the water content, temperature (for *lTemp* = .true.), and the solution and sorbed concentrations (for *lChem* = .true.) are printed at each time level. It does not have to be specified if *NObs* = 0.
9	Integer	*Node*(2)	Same as above for the second observation node. It does not have to be specified if *NObs* < 2.
.	.	.	.
.	.	.	.
9	Integer	*Node*(*NObs*)	Same as above for the last observation node.

Table 9.12. Block L - Atmospheric information.†

Record	Type	Variable	Description
1,2,3,4	-	-	Comment lines.
5	Logical	*SinkF*	Set this variable equal to **.true.** if water extraction from the root zone is imposed.
5	Logical	*qGWLF*	Set this variable equal to **.true.** if the discharge-groundwater level relationship $q(GWL)$ given by equation (7.1) is used as the bottom boundary condition; $GWL = h - GWL0L$, where h is the pressure head at the boundary.
6	-	-	Comment line.
7	Real	*GWL0L*	Reference position of groundwater table (usually the z-coordinate of the soil surface).
7	Real	*Aqh*	Value of the parameter A_{qh} [LT^{-1}] in the $q(GWL)$-relationship (equation (7.1)); set to zero if *qGWLF* = **.false.**
7	Real	*Bqh*	Value of the parameter B_{qh} [L^{-1}] in the $q(GWL)$-relationship (equation (7.1)); set to zero if *qGWLF* = **.false.**
8	-	-	Comment line.
9	Real	*tInit*	Starting time [T] of the simulation.
9	Integer	*MaxAl*	Number of atmospheric data records.
10	-	-	Comment line.
11	Real	*hCritS*	Maximum allowed pressure head at the soil surface [L].
12	-	-	Comment line.
13	Real	*tAtm(i)*	Time for which the i-th data record is provided [T].
13	Real	*Prec(i)*	Precipitation [LT^{-1}] (in absolute value).
13	Real	*rSoil(i)*	Potential evaporation rate [LT^{-1}] (in absolute value).
13	Real	*rRoot(i)*	Potential transpiration rate [LT^{-1}] (in absolute value).
13	Real	*hCritA(i)*	Absolute value of the minimum allowed pressure head at the soil surface [L].
13	Real	*rGWL(i)*	Drainage flux [LT^{-1}] across the bottom boundary, or other time-dependent prescribed flux boundary condition (positive when water leaves the flow region), for nodes where $Kode(n) = -3$; set to zero when no $Kode(n) = -3$ boundary condition is specified.
13	Real	*GWL(i)*	Groundwater level [L] (usually negative), or other time-dependent prescribed head boundary condition, for nodes where $Kode(n) = +3$; set equal to zero when no $Kode(n) = +3$ is specified. The prescribed value of the pressure head is $h = GWL + GWL0L$.

Table 9.12. (continued)

Record	Type	Variable	Description
13	Real	*Th3(i)*	Time-dependent temperature [K] prescribed for nodes where $Kode(n) = \pm 3$ (must not be specified if *lTemp* = **.false.** and *lChem* = **.true.**; set equal to zero when no $Kode(n) = \pm 3$ or when the flux *rGWL(i)* is directed out of the flow domain).
13	Real	*Th4(i)*	Time-dependent temperature [K] prescribed for nodes where $Kode(n) = \pm 4$ (must not be specified if *lTemp* = **.false.** and *lChem* = **.true.**; set equal to zero when no $Kode(n) = \pm 4$).
13	Real	*cPrec(1,i)*	Solute concentration of rainfall water [ML^{-3}] (does not need to be specified if *lChem* = **.false.**).
13	Real	*crt(1,i)*	Time-dependent concentration of the drainage flux [ML^{-3}], or some other time-dependent prescribed flux, for nodes where $Kode(n) = \pm 3$ and $KodCB(n) < 0$ (does not need to be specified if *lChem* = **.false.**; set equal to zero when no $Kode(n) = \pm 3$ and $KodCB(n) < 0$, or when the flux *rGWL(i)* is directed out of the flow domain).
13	Real	*cht(1,i)*	Time-dependent concentration [ML^{-3}] for the first-type boundary condition prescribed for nodes for which $Kode(n) = \pm 3$ and $KodCB(n) > 0$ (does not need to be specified if *lChem* = **.false.**; set equal to zero when no $Kode(n) = \pm 3$ and $KodCB(n) > 0$).
13	Real	*cPrec(2,i)*	Same as *cPrec(1,i)* for the second solute (does not need to be specified if *lChem* = **.false.** or NS < 2).
13	Real	*crt(2,i)*	Same as *crt(1,i)* for the second solute (does not need to be specified if *lChem* = **.false.** or NS < 2).
13	Real	*cht(2,i)*	Same as *cht(1,i)* for the second solute (does not need to be specified if *lChem* = **.false.** or NS < 2).
			The last three entries are entered for each solute from 1 to *NS*.
			The total number of atmospheric data records is *MaxAl* (i=1,2, ..,*MaxAl*).

† Block L is not read in if the logical variable *AtmInf* (Block A) is set equal to **.false.** .

Table 9.13. Input data for example 1 (input file 'SELECTOR.IN').

```
*** BLOCK A: BASIC INFORMATION ****************************************
Heading
'Example 1 - Column Test'
LUnit  TUnit  MUnit            (units are obligatory for all input data)
'cm'   'sec'  '-'
Kat (0:horizontal plane, 1:axisymmetric vertical flow, 2:vertical plane)
  2
MaxIt   TolTh    TolH (max. number of iteration and precision tolerance)
  20    .0001    .1
lWat   lChem Check Short Flux AtmIn SeepF Drain FreeD lTemp lWDep lEquil
 t      f     f     t     t    f     t     f     f     f     f     f
*** BLOCK B: MATERIAL INFORMATION ***************************************
NMat    NLay    hTab1   hTabN   NPar
  1      1      .001    200.     9
thr     ths     tha     thm     Alfa    n       Ks      Kk      thk
 .02    .350    .02     .350    .0410   1.964  .000722 .000695 .2875
*** BLOCK C: TIME INFORMATION *****************************************
dt      dtMin   dtMax   DMul    DMul2   MPL
 1.     .01     60.     1.1     .33     6
TPrint(1),TPrint(2),...,TPrint(MPL)                  (print-time array)
 60 900 1800 2700 3600 5400
*** BLOCK E: SEEPAGE INFORMATION (only if SeepF =.true.) ***************
NSeep                                          (number of seepage faces)
  1
NSP(1),NSP(2),.......,NSP(NSeep)          (number of nodes in each s.f.)
  2
NP(i,1),NP(i,2),.....,NP(i,NSP(i))     (nodal number array of i-th s.f.)
  111     112
*** END OF INPUT FILE 'SELECTOR.IN' ************************************
```

Table 9.14. Input data for example 1 (input file 'GRID.IN').

```
*** BLOCK I: NODAL INFORMATION ***********************************************
      NumNP      NumEl         IJ      NumBP         NS       NObs
        112         55          2          4          0          0
   n  Code     x        z         h          Q        M    B     Axz    Bxz    Dxz     Temp
   1     1    0.00    61.00      0.75   0.00E+00    1   0.00   1.00   1.00   1.00    0.00
   2     1    1.00    61.00      0.75   0.00E+00    1   0.00   1.00   1.00   1.00    0.00
   3     0    0.00    60.75   -150.00   0.00E+00    1   0.00   1.00   1.00   1.00    0.00
   4     0    1.00    60.75   -150.00   0.00E+00    1   0.00   1.00   1.00   1.00    0.00
   5     0    0.00    60.50   -150.00   0.00E+00    1   0.00   1.00   1.00   1.00    0.00
   6     0    1.00    60.50   -150.00   0.00E+00    1   0.00   1.00   1.00   1.00    0.00
   7     0    0.00    60.25   -150.00   0.00E+00    1   0.00   1.00   1.00   1.00    0.00
   8     0    1.00    60.25   -150.00   0.00E+00    1   0.00   1.00   1.00   1.00    0.00
   9     0    0.00    60.00   -150.00   0.00E+00    1   0.00   1.00   1.00   1.00    0.00
  10     0    1.00    60.00   -150.00   0.00E+00    1   0.00   1.00   1.00   1.00    0.00
  11     0    0.00    59.50   -150.00   0.00E+00    1   0.00   1.00   1.00   1.00    0.00
  12     0    1.00    59.50   -150.00   0.00E+00    1   0.00   1.00   1.00   1.00    0.00
  13     0    0.00    59.00   -150.00   0.00E+00    1   0.00   1.00   1.00   1.00    0.00
  14     0    1.00    59.00   -150.00   0.00E+00    1   0.00   1.00   1.00   1.00    0.00
   .     .      .       .         .          .       .     .      .      .      .       .
   .     .      .       .         .          .       .     .      .      .      .       .
   .     .      .       .         .          .       .     .      .      .      .       .
 103     0    0.00    8.00   -150.00   0.00E+00    1   0.00   1.00   1.00   1.00    0.00
 104     0    1.00    8.00   -150.00   0.00E+00    1   0.00   1.00   1.00   1.00    0.00
 105     0    0.00    6.00   -150.00   0.00E+00    1   0.00   1.00   1.00   1.00    0.00
 106     0    1.00    6.00   -150.00   0.00E+00    1   0.00   1.00   1.00   1.00    0.00
 107     0    0.00    4.00   -150.00   0.00E+00    1   0.00   1.00   1.00   1.00    0.00
 108     0    1.00    4.00   -150.00   0.00E+00    1   0.00   1.00   1.00   1.00    0.00
 109     0    0.00    2.00   -150.00   0.00E+00    1   0.00   1.00   1.00   1.00    0.00
 110     0    1.00    2.00   -150.00   0.00E+00    1   0.00   1.00   1.00   1.00    0.00
 111    -2    0.00    0.00   -150.00   0.00E+00    1   0.00   1.00   1.00   1.00    0.00
 112    -2    1.00    0.00   -150.00   0.00E+00    1   0.00   1.00   1.00   1.00    0.00
*** BLOCK J: ELEMENT INFORMATION *********************************************
    e     i     j     k     l   Angle   Aniz1   Aniz2 LayNum
    1     1     3     4     2    0.00    1.00    1.00   1
    2     3     5     6     4    0.00    1.00    1.00   1
    3     5     7     8     6    0.00    1.00    1.00   1
    4     7     9    10     8    0.00    1.00    1.00   1
    5     9    11    12    10    0.00    1.00    1.00   1
    6    11    13    14    12    0.00    1.00    1.00   1
    7    13    15    16    14    0.00    1.00    1.00   1
    8    15    17    18    16    0.00    1.00    1.00   1
    9    17    19    20    18    0.00    1.00    1.00   1
   10    19    21    22    20    0.00    1.00    1.00   1
    .     .     .     .     .
    .     .     .     .     .
    .     .     .     .     .
   48    95    97    98    96    0.00    1.00    1.00   1
   49    97    99   100    98    0.00    1.00    1.00   1
   50    99   101   102   100    0.00    1.00    1.00   1
   51   101   103   104   102    0.00    1.00    1.00   1
   52   103   105   106   104    0.00    1.00    1.00   1
   53   105   107   108   106    0.00    1.00    1.00   1
   54   107   109   110   108    0.00    1.00    1.00   1
   55   109   111   112   110    0.00    1.00    1.00   1
*** BLOCK K: BOUNDARY GEOMETRY INFORMATION ************************************
 Node number array:
        1         2       111       112
 Width array:
     0.50      0.50      0.50      0.50
 Length:
     0.00
*** END OF INPUT FILE 'GRID.IN' **********************************************
```

Table 9.15. Input data for example 2 (input file 'SELECTOR.IN').

```
*** BLOCK A: BASIC INFORMATION ****************************************
Heading
'Example 2 - Grass Field Problem (Hupselse Beek 1982)'
LUnit  TUnit  MUnit  (indicated units are obligatory for all input data)
'cm'   'day'  '-'
Kat (0:horizontal plane, 1:axisymmetric vertical flow, 2:vertical plane)
  2
MaxIt   TolTh   TolH (max. number of iteration and precision tolerances)
  20    .0001     .1
lWat   lChem Check Short Flux AtmIn SeepF Drain FreeD lTemp lWDep lEquil
 t      f     f     t     t    t     f     f     f      f     f     t
*** BLOCK B: MATERIAL INFORMATION ***************************************
NMat    NLay    hTab1   hTabN   NPar
  2      2      .001    1000.    9
thr     ths     tha     thm     Alfa    n       Ks      Kk      thk
.0001   .399    .0001   .399    .0174   1.3757  29.75   29.75   .399
.0001   .339    .0001   .339    .0139   1.6024  45.34   45.34   .339
*** BLOCK C: TIME INFORMATION ******************************************
dt      dtMin   dtMax   DMul    DMul2   MPL
 .02    1e-10   0.50    1.3     .3      6
TPrint(1),TPrint(2),...,TPrint(MPL)                  (print-time array)
 120 151 181 212 243 273
*** BLOCK D: SINK INFORMATION ******************************************
P0      P2H     P2L     P3      r2H     r2L
 -10.   -200.   -800.   -8000.  0.5     0.1
POptm(1),POptm(2),...,POptm(NMat)
 -25.   -25.
*** END OF INPUT FILE 'SELECTOR.IN' ************************************
```

Table 9.16. Input data for example 2 (input file 'ATMOSPH.IN').

```
*** BLOCK L: ATMOSPHERIC INFORMATION  ***********************************
*** Hupselse Beek 1982                ***********************************
*****************************************************************************
SinkF   qGWLF
 t       t
GWLOL   Aqh      Bqh                              (if qGWLF=f then Aqh=Bqh=0)
 230    -.1687  -.02674
tInit   MaxAL                 (MaxAL = number of atmospheric data-records)
 90.     183
hCritS                  (max. allowed pressure head at the soil surface)
 1.e30
    tAtm     Prec    rSoil     rRoot     hCritA      rt      ht
      91        0        0      0.16    1000000       0       0
      92     0.07        0      0.18    1000000       0       0
      93     0.02        0      0.13    1000000       0       0
      94        0        0      0.20    1000000       0       0
      95        0        0      0.28    1000000       0       0
      96     0.07        0      0.18    1000000       0       0
      97     0.29        0      0.08    1000000       0       0
      98     0.44        0      0.14    1000000       0       0
      99     0.20        0      0.11    1000000       0       0
     100     0.29        0      0.11    1000000       0       0
     101     0.32        0      0.11    1000000       0       0
     102     0.49        0      0.11    1000000       0       0
     103     0.01        0      0.16    1000000       0       0
     104        0        0      0.17    1000000       0       0
     105        0        0      0.22    1000000       0       0
     106        0        0      0.21    1000000       0       0
     107        0        0      0.23    1000000       0       0
     108        0        0      0.23    1000000       0       0
     109        0        0      0.24    1000000       0       0
     110        0        0      0.18    1000000       0       0
     111        0        0      0.15    1000000       0       0
     112        0        0      0.19    1000000       0       0
     113     0.01        0      0.15    1000000       0       0
     114     0.01        0      0.22    1000000       0       0
     115        0        0      0.23    1000000       0       0
     116     0.02        0      0.20    1000000       0       0
     117        0        0      0.17    1000000       0       0
     118     0.02        0      0.14    1000000       0       0
     119     0.26        0      0.13    1000000       0       0
     120     0.24        0      0.11    1000000       0       0
       .        .        .         .          .       .       .
       .        .        .         .          .       .       .
       .        .        .         .          .       .       .
     256        0        0      0.13    1000000       0       0
     257        0        0      0.14    1000000       0       0
     258        0        0      0.20    1000000       0       0
     259        0        0      0.14    1000000       0       0
     260        0        0      0.19    1000000       0       0
     261        0        0      0.14    1000000       0       0
     262        0        0      0.20    1000000       0       0
     263     0.35        0      0.23    1000000       0       0
     264     0.52        0      0.16    1000000       0       0
     265        0        0      0.21    1000000       0       0
     266        0        0      0.19    1000000       0       0
     267        0        0      0.18    1000000       0       0
     268        0        0      0.18    1000000       0       0
     269     0.53        0      0.09    1000000       0       0
     270     0.07        0      0.23    1000000       0       0
     271        0        0      0.17    1000000       0       0
     272        0        0      0.22    1000000       0       0
     273     1.04        0         0    1000000       0       0
*** END OF INPUT FILE 'ATMOSPH.IN' ************************************
```

Table 9.17. Input data for example 2 (input file 'GRID.IN').

```
*** BLOCK I: NODAL INFORMATION ***********************************************
      NumNP      NumEl       IJ      NumBP      NS      NObs
         66         32        2          4       0         0
   n  Code     x       z          h         Q        M   B     Axz   Bxz   Dxz     Temp
   1   -4    0.00  230.00     -55.00   0.00E+00   1   0.00  1.00  1.00  1.00    0.00
   2   -4    1.00  230.00     -55.00   0.00E+00   1   0.00  1.00  1.00  1.00    0.00
   3    0    0.00  229.00     -54.00   0.00E+00   1   0.00  1.00  1.00  1.00    0.00
   4    0    1.00  229.00     -54.00   0.00E+00   1   0.00  1.00  1.00  1.00    0.00
   5    0    0.00  228.00     -53.00   0.00E+00   1   1.00  1.00  1.00  1.00    0.00
   6    0    1.00  228.00     -53.00   0.00E+00   1   1.00  1.00  1.00  1.00    0.00
   7    0    0.00  226.00     -51.00   0.00E+00   1   1.00  1.00  1.00  1.00    0.00
   8    0    1.00  226.00     -51.00   0.00E+00   1   1.00  1.00  1.00  1.00    0.00
   9    0    0.00  224.00     -49.00   0.00E+00   1   1.00  1.00  1.00  1.00    0.00
  10    0    1.00  224.00     -49.00   0.00E+00   1   1.00  1.00  1.00  1.00    0.00
  11    0    0.00  220.00     -45.00   0.00E+00   1   1.00  1.00  1.00  1.00    0.00
  12    0    1.00  220.00     -45.00   0.00E+00   1   1.00  1.00  1.00  1.00    0.00
  13    0    0.00  215.00     -40.00   0.00E+00   1   1.00  1.00  1.00  1.00    0.00
  14    0    1.00  215.00     -40.00   0.00E+00   1   1.00  1.00  1.00  1.00    0.00
  15    0    0.00  210.00     -35.00   0.00E+00   1   1.00  1.00  1.00  1.00    0.00
  16    0    1.00  210.00     -35.00   0.00E+00   1   1.00  1.00  1.00  1.00    0.00
  17    0    0.00  205.00     -30.00   0.00E+00   1   1.00  1.00  1.00  1.00    0.00
  18    0    1.00  205.00     -30.00   0.00E+00   1   1.00  1.00  1.00  1.00    0.00
  19    0    0.00  200.00     -25.00   0.00E+00   1   1.00  1.00  1.00  1.00    0.00
  20    0    1.00  200.00     -25.00   0.00E+00   1   1.00  1.00  1.00  1.00    0.00
        .       .       .          .         .       .     .     .     .       .
        .       .       .          .         .       .     .     .     .       .
        .       .       .          .         .       .     .     .     .       .
  61    0    0.00    2.00     173.00   0.00E+00   2   0.00  1.00  1.00  1.00    0.00
  62    0    1.00    2.00     173.00   0.00E+00   2   0.00  1.00  1.00  1.00    0.00
  63    0    0.00    1.00     174.00   0.00E+00   2   0.00  1.00  1.00  1.00    0.00
  64    0    1.00    1.00     174.00   0.00E+00   2   0.00  1.00  1.00  1.00    0.00
  65   -3    0.00    0.00     175.00   0.00E+00   2   0.00  1.00  1.00  1.00    0.00
  66   -3    1.00    0.00     175.00   0.00E+00   2   0.00  1.00  1.00  1.00    0.00
*** BLOCK J: ELEMENT INFORMATION *********************************************
   e    i   j   k   l   Angle  Aniz1  Aniz2  LayNum
   1    1   3   4   2   0.00   1.00   1.00   1
   2    3   5   6   4   0.00   1.00   1.00   1
   3    5   7   8   6   0.00   1.00   1.00   1
   4    7   9  10   8   0.00   1.00   1.00   1
   5    9  11  12  10   0.00   1.00   1.00   1
   6   11  13  14  12   0.00   1.00   1.00   1
   7   13  15  16  14   0.00   1.00   1.00   1
   8   15  17  18  16   0.00   1.00   1.00   1
   9   17  19  20  18   0.00   1.00   1.00   1
  10   19  21  22  20   0.00   1.00   1.00   2
        .   .   .   .
        .   .   .   .
        .   .   .   .
  26   51  53  54  52   0.00   1.00   1.00   2
  27   53  55  56  54   0.00   1.00   1.00   2
  28   55  57  58  56   0.00   1.00   1.00   2
  29   57  59  60  58   0.00   1.00   1.00   2
  30   59  61  62  60   0.00   1.00   1.00   2
  31   61  63  64  62   0.00   1.00   1.00   2
  32   63  65  66  64   0.00   1.00   1.00   2
*** BLOCK K: BOUNDARY GEOMETRY INFORMATION ************************************
 Node number array:
       1       2       65      66
 Width array:
     0.50    0.50    0.50    0.50
 Length:
     1.00
*** END OF INPUT FILE 'GRID.IN' **********************************************
```

Table 9.18. Input data for example 3b (input file 'SELECTOR.IN').

```
*** BLOCK A: BASIC INFORMATION ***************************************************
Heading
'Example 3b - Comparison with the 2-D Analytical Solution'
LUnit  TUnit  MUnit              (indicated units are obligatory for all input data)
'm'    'days' '-'
Kat             (0:horizontal plane, 1:axisymmetric vertical flow, 2:vertical plane)
  2
MaxIt   TolTh   TolH          (maximum number of iteration and precision tolerances)
  20    .0001   .1
lWat    lChem   CheckF  ShortF  FluxF   AtmInF SeepF DrainF FreeD lTemp lWDep lEquil
f       t       f       t       f       f      t     f      f     f     f     t
*** BLOCK B: MATERIAL INFORMATION ************************************************
NMat    NLay    hTab1   hTabN   NPar
  1       1     .001    200.     9
thr     ths     tha     thm     Alfa    n       Ks      Kk      thk
 .02    .300    .02     .30     .0410   1.964   .3      .3     .30
*** BLOCK C: TIME INFORMATION ****************************************************
dt      dtMin   dtMax   DMul    DMul2   MPL
1     .0001     100.    1.3     .33     3
TPrint(1),TPrint(2),...,TPrint(MPL)                                  (print-time array)
50 100 365
*** BLOCK E: SEEPAGE INFORMATION (only if SeepF =.true.) **************************
NSeep                                                          (number of seepage faces)
  1
NSP(1),NSP(2),.......,NSP(NSeep)              (number of nodes in each seepage faces)
  15
NP(i,1),NP(i,2),.....,NP(i,NSP(i))          (nodal number array of i-th seepage faces)
301     302     303     304     305     306     307     308     309     310     311
312     313     314     315
*** BLOCK G: SOLUTE TRANSPORT INFORMATION *****************************************
Epsi    lUpW    lArtD   lTDep   cTolA   cTolR   MaxItC    PeCr
 0.5    f       f       f       0.0     0.0     1         2.
Bulk.d. DispL   DispT    Frac  (1...NMat)
 1500    1.0     0.5     1.0
Dif.w.  Dif.g. ------------------------------------------------------------ (1.solute)
 0.0     0.0
 KS      Nu     Beta Henry SnkL1 SnkS1 SnkG1 SnkL1' SnkS1' SnkG1' SnkL0 SnkS0 SnkG0 Alfa
0.0004  0.0    1.0   0.0   0.01  0.01  0.0   0.0    0.0    0.0    0.0   0.0   0.0   0.0
KodCB(1),KodCB(2),.....,KodCB(NumBP)
 1       1       1       1       1       1       1
 2       2       2       2       2       2       2       2
 2       2       2       2       2       2       2
 2       2       2       2       2       2       2       2
cTop   cBot
 1.     0.      0.      0.      0.      0.      0.      0.      0.
tPulse
 366
*** END OF INPUT FILE 'SELECTOR.IN' **********************************************
```

Table 9.19. Input data for example 3 (input file 'GRID.IN').

```
*** BLOCK I: NODAL INFORMATION **********************************************************
     NumNP      NumEl       IJ      NumBP       NS      NObs
       315        280       15         30        1         0
   n  Code     x        z          h        Q      M    B      Axz    Bxz    Dxz    Temp     Conc
   1    1     0.00     0.00       0.00  0.00E+00   1  0.00     1.00   1.00   1.00   0.00  1.00E+00
   2    1    10.00     0.00       0.00  0.00E+00   1  0.00     1.00   1.00   1.00   0.00  1.00E+00
   3    1    20.00     0.00       0.00  0.00E+00   1  0.00     1.00   1.00   1.00   0.00  1.00E+00
   4    1    30.00     0.00       0.00  0.00E+00   1  0.00     1.00   1.00   1.00   0.00  1.00E+00
   5    1    40.00     0.00       0.00  0.00E+00   1  0.00     1.00   1.00   1.00   0.00  1.00E+00
   6    1    45.00     0.00       0.00  0.00E+00   1  0.00     1.00   1.00   1.00   0.00  1.00E+00
   7    1    49.00     0.00       0.00  0.00E+00   1  0.00     1.00   1.00   1.00   0.00  1.00E+00
   8    1    51.00     0.00       0.00  0.00E+00   1  0.00     1.00   1.00   1.00   0.00  0.00E+00
   9    1    55.00     0.00       0.00  0.00E+00   1  0.00     1.00   1.00   1.00   0.00  0.00E+00
  10    1    60.00     0.00       0.00  0.00E+00   1  0.00     1.00   1.00   1.00   0.00  0.00E+00
  11    1    67.00     0.00       0.00  0.00E+00   1  0.00     1.00   1.00   1.00   0.00  0.00E+00
  12    1    75.00     0.00       0.00  0.00E+00   1  0.00     1.00   1.00   1.00   0.00  0.00E+00
  13    1    85.00     0.00       0.00  0.00E+00   1  0.00     1.00   1.00   1.00   0.00  0.00E+00
  14    1   100.00     0.00       0.00  0.00E+00   1  0.00     1.00   1.00   1.00   0.00  0.00E+00
  15    1   120.00     0.00       0.00  0.00E+00   1  0.00     1.00   1.00   1.00   0.00  0.00E+00
  16    0     0.00    -5.00       0.00  0.00E+00   1  0.00     1.00   1.00   1.00   0.00  0.00E+00
  17    0    10.00    -5.00       0.00  0.00E+00   1  0.00     1.00   1.00   1.00   0.00  0.00E+00
  18    0    20.00    -5.00       0.00  0.00E+00   1  0.00     1.00   1.00   1.00   0.00  0.00E+00
  19    0    30.00    -5.00       0.00  0.00E+00   1  0.00     1.00   1.00   1.00   0.00  0.00E+00
  20    0    40.00    -5.00       0.00  0.00E+00   1  0.00     1.00   1.00   1.00   0.00  0.00E+00
  21    0    45.00    -5.00       0.00  0.00E+00   1  0.00     1.00   1.00   1.00   0.00  0.00E+00
  22    0    49.00    -5.00       0.00  0.00E+00   1  0.00     1.00   1.00   1.00   0.00  0.00E+00
       .        .        .          .         .     .     .       .      .      .      .        .
       .        .        .          .         .     .     .       .      .      .      .        .
       .        .        .          .         .     .     .       .      .      .      .        .
 310   2    60.00  -200.00       0.00  0.00E+00   1  0.00     1.00   1.00   1.00   0.00  0.00E+00
 311   2    67.00  -200.00       0.00  0.00E+00   1  0.00     1.00   1.00   1.00   0.00  0.00E+00
 312   2    75.00  -200.00       0.00  0.00E+00   1  0.00     1.00   1.00   1.00   0.00  0.00E+00
 313   2    85.00  -200.00       0.00  0.00E+00   1  0.00     1.00   1.00   1.00   0.00  0.00E+00
 314   2   100.00  -200.00       0.00  0.00E+00   1  0.00     1.00   1.00   1.00   0.00  0.00E+00
 315   2   120.00  -200.00       0.00  0.00E+00   1  0.00     1.00   1.00   1.00   0.00  0.00E+00
*** BLOCK J: ELEMENT INFORMATION *********************************************************
   e   i   j   k   l   Angle  Aniz1  Aniz2  LayNum
   1   1  16  17   2   0.00   1.00   1.00   1
   2   2  17  18   3   0.00   1.00   1.00   1
   3   3  18  19   4   0.00   1.00   1.00   1
   4   4  19  20   5   0.00   1.00   1.00   1
   5   5  20  21   6   0.00   1.00   1.00   1
   6   6  21  22   7   0.00   1.00   1.00   1
   7   7  22  23   8   0.00   1.00   1.00   1
       .   .   .   .     .      .      .
       .   .   .   .     .      .      .
 277 296 311 312 297   0.00   1.00   1.00   1
 278 297 312 313 298   0.00   1.00   1.00   1
 279 298 313 314 299   0.00   1.00   1.00   1
 280 299 314 315 300   0.00   1.00   1.00   1
*** BLOCK K: BOUNDARY GEOMETRY INFORMATION ***********************************************
 Node number array:
         1         2         3         4         5         6         7
         8         9        10        11        12        13        14
        15       301       302       303       304       305       306
       307       308       309       310       311       312       313
       314       315
 Width array:
      5.00     10.00     10.00     10.00      7.50      4.50      3.00
      3.00      4.50      6.00      7.50      9.00     12.50     17.50
     10.00      5.00     10.00     10.00     10.00      7.50      4.50
      3.00      3.00      4.50      6.00      7.50      9.00     12.50
     17.50     10.00
 Length:
      0.00
*** END OF INPUT FILE 'GRID.IN' **********************************************************
```

Table 9.19. Input data for example 4 (input file 'SELECTOR.IN').

```
*** BLOCK A: BASIC INFORMATION ************************************************
Heading
'Example 4 - Solute Transport with Nitrification Chain'
LUnit  TUnit  MUnit              (indicated units are obligatory for all input data)
'm'    'days' '-'
Kat             (0:horizontal plane, 1:axisymmetric vertical flow, 2:vertical plane)
  2
MaxIt   TolTh    TolH          (maximum number of iterations and precision tolerance)
  20    .0001    .01
lWat    lChem   CheckF  ShortF  FluxF   AtmInF SeepF DrainF FreeD lTemp lWDep lEquil
f       t       f       t       f       f      t     f      f     f     f     t
*** BLOCK B: MATERIAL INFORMATION *********************************************
NMat    NLay    hTab1   hTabN   NPar
  1      1      .001    200.     9
thr     ths     tha     thm     Alfa    n       Ks      Kk      thk
 .0     1.0     .0      1.0     .05     2.0     1.0     1.0     1.0
*** BLOCK C: TIME INFORMATION *************************************************
dt      dtMin   dtMax   DMul    DMul2   MPL
1       .0001    100.   1.3     .33     3
TPrint(1),TPrint(2),...,TPrint(MPL)                              (print-time array)
50 100 200
*** BLOCK E: SEEPAGE INFORMATION (only if SeepF =.true.) ***********************
NSeep                                                          (number of seepage faces)
  1
NSP(1),NSP(2),.......,NSP(NSeep)                        (number of nodes in each s.f.)
  2
NP(i,1),NP(i,2),.....,NP(i,NSP(i))                   (nodal number array of i-th s.f.)
  401   402
*** BLOCK G: SOLUTE TRANSPORT INFORMATION *************************************
Epsi    lUpW    lArtD   lTDep   cTolA  cTolR   MaxItC   PeCr
 0.5    f       f       f       0.0    0.0     1        10
Bulk.d. DispL  DispT  Frac  (1...NMat)
 1000    0.0    0.0   1.0
Dif.w.  Dif.g. ---------------------------------------------------------- (1.solute)
 0.18    0.0
 KS     Nu   Beta Henry SnkL1 SnkS1 SnkG1 SnkL1' SnkS1' SnkG1' SnkL0 SnkS0 SnkG0 Alfa
0.001  0.0  1.0   0.0   0.0   0.0   0.0   0.005  0.005   0.0    0.0   0.0   0.0   0.0
Dif.w.  Dif.g. ---------------------------------------------------------- (2.solute)
 0.18    0.0
 KS     Nu   Beta Henry SnkL1 SnkS1 SnkG1 SnkL1' SnkS1' SnkG1' SnkL0 SnkS0 SnkG0 Alfa
 0.0   0.0  1.0   0.0   0.0   0.0   0.0   0.1    0.0     0.0    0.0   0.0   0.0   0.0
Dif.w.  Dif.g. ---------------------------------------------------------- (3.solute)
 0.18    0.0
 KS     Nu   Beta Henry SnkL1 SnkS1 SnkG1 SnkL1' SnkS1' SnkG1' SnkL0 SnkS0 SnkG0 Alfa
 0.0   0.0  1.0   0.0   0.0   0.0   0.0   0.0    0.0     0.0    0.0   0.0   0.0   0.0
KodCB(1),KodCB(2),.....,KodCB(NumBP)
-1      -1      -2      -2
cTop    cBot
 1.      0.      0.      0.      0.      0.      0.      0.
 0.      0.      0.      0.      0.      0.      0.      0.
 0.      0.      0.      0.      0.      0.      0.      0.
tPulse
 366
*** END OF INPUT FILE 'SELECTOR.IN' *******************************************
```

Table 9.21. Input data for example 4 (input file 'GRID.IN').

```
*** BLOCK I: NODAL INFORMATION ***********************************************************************************
      NumNP       NumEl         IJ       NumBP         NS      NObs
        402         200          2           4          3         0
  n  Code    x        z        h        Q        M    B      Axz    Bxz    Dxz     Temp     Conc1      Conc2      Conc3
  1    1   0.00     0.00     0.00  0.00E+00    1  0.00     1.00   1.00   1.00     0.00  0.000E+00  0.000E+00  0.000E+00
  2    1   1.00     0.00     0.00  0.00E+00    1  0.00     1.00   1.00   1.00     0.00  0.000E+00  0.000E+00  0.000E+00
  3    0   0.00    -1.00     0.00  0.00E+00    1  0.00     1.00   1.00   1.00     0.00  0.000E+00  0.000E+00  0.000E+00
  4    0   1.00    -1.00     0.00  0.00E+00    1  0.00     1.00   1.00   1.00     0.00  0.000E+00  0.000E+00  0.000E+00
  5    0   0.00    -2.00     0.00  0.00E+00    1  0.00     1.00   1.00   1.00     0.00  0.000E+00  0.000E+00  0.000E+00
  6    0   1.00    -2.00     0.00  0.00E+00    1  0.00     1.00   1.00   1.00     0.00  0.000E+00  0.000E+00  0.000E+00
  7    0   0.00    -3.00     0.00  0.00E+00    1  0.00     1.00   1.00   1.00     0.00  0.000E+00  0.000E+00  0.000E+00
  8    0   1.00    -3.00     0.00  0.00E+00    1  0.00     1.00   1.00   1.00     0.00  0.000E+00  0.000E+00  0.000E+00
  9    0   0.00    -4.00     0.00  0.00E+00    1  0.00     1.00   1.00   1.00     0.00  0.000E+00  0.000E+00  0.000E+00
 10    0   1.00    -4.00     0.00  0.00E+00    1  0.00     1.00   1.00   1.00     0.00  0.000E+00  0.000E+00  0.000E+00
 11    0   0.00    -5.00     0.00  0.00E+00    1  0.00     1.00   1.00   1.00     0.00  0.000E+00  0.000E+00  0.000E+00
 12    0   1.00    -5.00     0.00  0.00E+00    1  0.00     1.00   1.00   1.00     0.00  0.000E+00  0.000E+00  0.000E+00
 13    0   0.00    -6.00     0.00  0.00E+00    1  0.00     1.00   1.00   1.00     0.00  0.000E+00  0.000E+00  0.000E+00
 14    0   1.00    -6.00     0.00  0.00E+00    1  0.00     1.00   1.00   1.00     0.00  0.000E+00  0.000E+00  0.000E+00
          .        .        .        .        .    .        .      .      .        .        .          .          .
          .        .        .        .        .    .        .      .      .        .        .          .          .
          .        .        .        .        .    .        .      .      .        .        .          .          .
395    0   0.00  -197.00     0.00  0.00E+00    1  0.00     1.00   1.00   1.00     0.00  0.000E+00  0.000E+00  0.000E+00
396    0   1.00  -197.00     0.00  0.00E+00    1  0.00     1.00   1.00   1.00     0.00  0.000E+00  0.000E+00  0.000E+00
397    0   0.00  -198.00     0.00  0.00E+00    1  0.00     1.00   1.00   1.00     0.00  0.000E+00  0.000E+00  0.000E+00
398    0   1.00  -198.00     0.00  0.00E+00    1  0.00     1.00   1.00   1.00     0.00  0.000E+00  0.000E+00  0.000E+00
399    0   0.00  -199.00     0.00  0.00E+00    1  0.00     1.00   1.00   1.00     0.00  0.000E+00  0.000E+00  0.000E+00
400    0   1.00  -199.00     0.00  0.00E+00    1  0.00     1.00   1.00   1.00     0.00  0.000E+00  0.000E+00  0.000E+00
401    2   0.00  -200.00     0.00  0.00E+00    1  0.00     1.00   1.00   1.00     0.00  0.000E+00  0.000E+00  0.000E+00
402    2   1.00  -200.00     0.00  0.00E+00    1  0.00     1.00   1.00   1.00     0.00  0.000E+00  0.000E+00  0.000E+00
*** BLOCK J: ELEMENT INFORMATION *********************************************************************************
    e    i    j    k    l  Angle  Aniz1  Aniz2 LayNum
    1    1    3    4    2   0.00   1.00   1.00   1
    2    3    5    6    4   0.00   1.00   1.00   1
    3    5    7    8    6   0.00   1.00   1.00   1
    4    7    9   10    8   0.00   1.00   1.00   1
    5    9   11   12   10   0.00   1.00   1.00   1
    6   11   13   14   12   0.00   1.00   1.00   1
    7   13   15   16   14   0.00   1.00   1.00   1
    8   15   17   18   16   0.00   1.00   1.00   1
    9   17   19   20   18   0.00   1.00   1.00   1
   10   19   21   22   20   0.00   1.00   1.00   1
          .    .    .    .      .      .      .
          .    .    .    .      .      .      .
          .    .    .    .      .      .      .
  190  379  381  382  380   0.00   1.00   1.00   1
  191  381  383  384  382   0.00   1.00   1.00   1
  192  383  385  386  384   0.00   1.00   1.00   1
  193  385  387  388  386   0.00   1.00   1.00   1
  194  387  389  390  388   0.00   1.00   1.00   1
  195  389  391  392  390   0.00   1.00   1.00   1
  196  391  393  394  392   0.00   1.00   1.00   1
  197  393  395  396  394   0.00   1.00   1.00   1
  198  395  397  398  396   0.00   1.00   1.00   1
  199  397  399  400  398   0.00   1.00   1.00   1
  200  399  401  402  400   0.00   1.00   1.00   1
*** BLOCK K: BOUNDARY GEOMETRY INFORMATION ************************************************************************
 Node number array:
        1        2      401      402
 Width array:
     0.50     0.50     0.50     0.50
 Length:
     0.00
*** END OF INPUT FILE 'GRID.IN' **********************************************************************************
```

Table 9.22. Input data for example 5 (input file 'SELECTOR.IN').

```
*** BLOCK A: BASIC INFORMATION ***********************************************************
Heading
'Example 5 - Solute Transport with Nonlinear Cation Adsorption - Freundlich isoterm'
LUnit  TUnit  MUnit                (indicated units are obligatory for all input data)
'cm'   'day' '-'
Kat              (0:horizontal plane, 1:axisymmetric vertical flow, 2:vertical plane)
  2
MaxIt   TolTh    TolH          (maximum number of iterations and precision tolerances)
  20    .0001     .01
lWat    lChem   CheckF  ShortF  FluxF   AtmInF  SeepF  DrainF FreeD lTemp lWDep lEquil
f       t       f       t       f       f       t      f      f     f     f     t
*** BLOCK B: MATERIAL INFORMATION ********************************************************
NMat    NLay    hTab1   hTabN   NPar
  1      1      .001    200.     9
thr     ths     tha     thm     Alfa    n       Ks      Kk      thk
 .0     0.633    .0     0.633   .01     2.0     6.495   6.495   0.633
*** BLOCK C: TIME INFORMATION ************************************************************
dt      dtMin   dtMax   DMul    DMul2   MPL
.002     .002     1     1.3     .33     5
TPrint(1),TPrint(2),...,TPrint(MPL)                                  (print-time array)
5 10 15 20 25
*** BLOCK E: SEEPAGE INFORMATION (only if SeepF =.true.) *****************************
NSeep                                                          (number of seepage faces)
  1
NSP(1),NSP(2),.......,NSP(NSeep)                          (number of nodes in each s.f.)
  2
NP(i,1),NP(i,2),.....,NP(i,NSP(i))                     (nodal number array of i-th s.f.)
  87   88
*** BLOCK G: SOLUTE TRANSPORT INFORMATION *********************************************
Epsi    lUpW    lArtD   lTDep   cTolA  cTolR   MaxItC   PeCr
 0.5    f       f       f       .0001  .0001   20       2.
Bulk.d. DispL  DispT   Frac  (1...NMat)
 .884   2.727   0.0     1.0
Dif.w.  Dif.g. ------------------------------------------------------------ (1.solute)
 0.0     0.0
 KS      Nu     Beta Henry SnkL1 SnkS1 SnkG1 SnkL1' SnkS1' SnkG1' SnkL0 SnkS0 SnkG0 Alfa
1.687    0.0  1.6151 0.0    0.0   0.0   0.0   0.0    0.0    0.0    0.0   0.0   0.0   0.0
KodCB(1),KodCB(2),.....,KodCB(NumBP)
 1       1       -2      -2
cTop    cBot
 10.     0.      0.      0.      0.      0.      0.      0.      0.
tPulse
 14.919
*** END OF INPUT FILE 'SELECTOR.IN' ******************************************************
```

Table 9.23. Input data for example 5 (input file 'GRID.IN').

```
*** BLOCK I: NODAL INFORMATION ***********************************************************
      NumNP      NumEl       IJ      NumBP       NS      NObs
         88         43        2          4        1         1
   n  Code     x       z          h        Q        M   B     Axz   Bxz   Dxz     Temp     Conc1
   1    1   0.00    0.00       0.00  0.00E+00   1   0.00  1.00  1.00  1.00     0.00  0.000E+00
   2    1   1.00    0.00       0.00  0.00E+00   1   0.00  1.00  1.00  1.00     0.00  0.000E+00
   3    0   0.00   -0.25       0.00  0.00E+00   1   0.00  1.00  1.00  1.00     0.00  0.000E+00
   4    0   1.00   -0.25       0.00  0.00E+00   1   0.00  1.00  1.00  1.00     0.00  0.000E+00
   5    0   0.00   -0.50       0.00  0.00E+00   1   0.00  1.00  1.00  1.00     0.00  0.000E+00
   6    0   1.00   -0.50       0.00  0.00E+00   1   0.00  1.00  1.00  1.00     0.00  0.000E+00
   7    0   0.00   -0.75       0.00  0.00E+00   1   0.00  1.00  1.00  1.00     0.00  0.000E+00
   8    0   1.00   -0.75       0.00  0.00E+00   1   0.00  1.00  1.00  1.00     0.00  0.000E+00
   9    0   0.00   -1.00       0.00  0.00E+00   1   0.00  1.00  1.00  1.00     0.00  0.000E+00
  10    0   1.00   -1.00       0.00  0.00E+00   1   0.00  1.00  1.00  1.00     0.00  0.000E+00
  11    0   0.00   -1.25       0.00  0.00E+00   1   0.00  1.00  1.00  1.00     0.00  0.000E+00
  12    0   1.00   -1.25       0.00  0.00E+00   1   0.00  1.00  1.00  1.00     0.00  0.000E+00
  13    0   0.00   -1.50       0.00  0.00E+00   1   0.00  1.00  1.00  1.00     0.00  0.000E+00
  14    0   1.00   -1.50       0.00  0.00E+00   1   0.00  1.00  1.00  1.00     0.00  0.000E+00
  15    0   0.00   -1.75       0.00  0.00E+00   1   0.00  1.00  1.00  1.00     0.00  0.000E+00
        .      .       .        .        .      .     .     .     .     .        .
        .      .       .        .        .      .     .     .     .     .        .
        .      .       .        .        .      .     .     .     .     .        .
  81    0   0.00  -10.00       0.00  0.00E+00   1   0.00  1.00  1.00  1.00     0.00  0.000E+00
  82    0   1.00  -10.00       0.00  0.00E+00   1   0.00  1.00  1.00  1.00     0.00  0.000E+00
  83    0   0.00  -10.25       0.00  0.00E+00   1   0.00  1.00  1.00  1.00     0.00  0.000E+00
  84    0   1.00  -10.25       0.00  0.00E+00   1   0.00  1.00  1.00  1.00     0.00  0.000E+00
  85    0   0.00  -10.50       0.00  0.00E+00   1   0.00  1.00  1.00  1.00     0.00  0.000E+00
  86    0   1.00  -10.50       0.00  0.00E+00   1   0.00  1.00  1.00  1.00     0.00  0.000E+00
  87    2   0.00  -10.75       0.00  0.00E+00   1   0.00  1.00  1.00  1.00     0.00  0.000E+00
  88    2   1.00  -10.75       0.00  0.00E+00   1   0.00  1.00  1.00  1.00     0.00  0.000E+00
*** BLOCK J: ELEMENT INFORMATION *********************************************************
    e    i    j    k    l  Angle  Aniz1  Aniz2 LayNum
    1    1    3    4    2   0.00   1.00   1.00   1
    2    3    5    6    4   0.00   1.00   1.00   1
    3    5    7    8    6   0.00   1.00   1.00   1
    4    7    9   10    8   0.00   1.00   1.00   1
    5    9   11   12   10   0.00   1.00   1.00   1
    6   11   13   14   12   0.00   1.00   1.00   1
    7   13   15   16   14   0.00   1.00   1.00   1
    8   15   17   18   16   0.00   1.00   1.00   1
    9   17   19   20   18   0.00   1.00   1.00   1
   10   19   21   22   20   0.00   1.00   1.00   1
        .    .    .    .      .      .      .
        .    .    .    .      .      .      .
        .    .    .    .      .      .      .
   35   69   71   72   70   0.00   1.00   1.00   1
   36   71   73   74   72   0.00   1.00   1.00   1
   37   73   75   76   74   0.00   1.00   1.00   1
   38   75   77   78   76   0.00   1.00   1.00   1
   39   77   79   80   78   0.00   1.00   1.00   1
   40   79   81   82   80   0.00   1.00   1.00   1
   41   81   83   84   82   0.00   1.00   1.00   1
   42   83   85   86   84   0.00   1.00   1.00   1
   43   85   87   88   86   0.00   1.00   1.00   1
*** BLOCK K: BOUNDARY GEOMETRY INFORMATION ***********************************************
 Node number array:
        1        2       87       88
 Width array:
     0.50     0.50     0.50     0.50
 Length:
     0.00
 Observation Nodes (1,..,Nobs):
 87
*** END OF INPUT FILE 'GRID.IN' **********************************************************
```

Table 9.24. Input data for example 6 (input file 'SELECTOR.IN').

```
*** BLOCK A: BASIC INFORMATION ************************************************
Heading
'Example 6 - Solute Transport with Kinetic Linear Cation Adsorption'
LUnit  TUnit  MUnit                (indicated units are obligatory for all input data)
'cm'   'day' '-'
Kat              (0:horizontal plane, 1:axisymmetric vertical flow, 2:vertical plane)
  2
MaxIt   TolTh    TolH          (maximum number of iterations and precision tolerances)
  20    .0001     .01
lWat    lChem   CheckF  ShortF  FluxF   AtmInF  SeepF  DrainF FreeD lTemp lWDep lEquil
f       t       f       t       f       f       t      f      f     f     f     f
*** BLOCK B: MATERIAL INFORMATION *********************************************
NMat    NLay    hTab1   hTabN   NPar
  1      1      .001    200.     9
thr     ths     tha     thm     Alfa      n        Ks       Kk       thk
.0      0.445   .0      0.445   .01       2.0      17.12    17.12    0.445
*** BLOCK C: TIME INFORMATION *************************************************
dt      dtMin   dtMax   DMul    DMul2   MPL
.01      .002     1     1.3     .33     7
TPrint(1),TPrint(2),...,TPrint(MPL)                                (print-time array)
0.5 1 2.5 5 7 10 20
*** BLOCK E: SEEPAGE INFORMATION (only if SeepF =.true.) ***********************
NSeep                                                        (number of seepage faces)
  1
NSP(1),NSP(2),.......,NSP(NSeep)                          (number of nodes in each s.f.)
  2
NP(i,1),NP(i,2),.....,NP(i,NSP(i))                      (nodal number array of i-th s.f.)
  31 32
*** BLOCK G: SOLUTE TRANSPORT INFORMATION *************************************
Epsi    lUpW    lArtD   lTDep cTolA   cTolR   MaxItC  PeCr
 0.5    f       f       f      .0001   .0001   10      2.
Bulk.d. DispL   DispT Fract   (1...NMat)
1.222    0.0    0.0   0.47
Dif.w.  Dif.g.     ------------------------------------------------------ (1.solute)
49.0     0.0
 KS     Nu     Beta Henry SnkL1 SnkS1 SnkG1 SnkL1' SnkS1' SnkG1' SnkL0 SnkS0 SnkG0 Alfa
 1.14   0.0    1.0  0.0    0.0   0.0   0.0   0.0    0.0    0.0    0.0   0.0   0.0  0.320
KodCB(1),KodCB(2),.....,KodCB(NumBP)
 -1      -1      -2      -2
cTop    cBot
 20.    0.      0.      0.      0.      0.      0.      0.      0.
tPulse
 5.060
*** END OF INPUT FILE 'SELECTOR.IN' *******************************************
```

Table 9.25. Input data for example 6 (input file 'GRID.IN').

```
*** BLOCK I: NODAL INFORMATION ***************************************************************************
     NumNP      NumEl         IJ      NumBP         NS       NObs
        32         15          2          4          1          1
   n  Code      x         z          h          Q    M     B     Axz   Bxz   Dxz     Temp     Conc1     Sorb1
   1     1   0.00       .00        .00   .00E+00    1   .00    1.00  1.00  1.00    20.00  .000E+00  .000E+00
   2     1   1.00       .00        .00   .00E+00    1   .00    1.00  1.00  1.00    20.00  .000E+00  .000E+00
   3     0   0.00     -2.00        .00   .00E+00    1   .00    1.00  1.00  1.00    20.00  .000E+00  .000E+00
   4     0   1.00     -2.00        .00   .00E+00    1   .00    1.00  1.00  1.00    20.00  .000E+00  .000E+00
   5     0   0.00     -4.00        .00   .00E+00    1   .00    1.00  1.00  1.00    20.00  .000E+00  .000E+00
   6     0   1.00     -4.00        .00   .00E+00    1   .00    1.00  1.00  1.00    20.00  .000E+00  .000E+00
   7     0   0.00     -6.00        .00   .00E+00    1   .00    1.00  1.00  1.00    20.00  .000E+00  .000E+00
   8     0   1.00     -6.00        .00   .00E+00    1   .00    1.00  1.00  1.00    20.00  .000E+00  .000E+00
   9     0   0.00     -8.00        .00   .00E+00    1   .00    1.00  1.00  1.00    20.00  .000E+00  .000E+00
  10     0   1.00     -8.00        .00   .00E+00    1   .00    1.00  1.00  1.00    20.00  .000E+00  .000E+00
  11     0   0.00    -10.00        .00   .00E+00    1   .00    1.00  1.00  1.00    20.00  .000E+00  .000E+00
  12     0   1.00    -10.00        .00   .00E+00    1   .00    1.00  1.00  1.00    20.00  .000E+00  .000E+00
  13     0   0.00    -12.00        .00   .00E+00    1   .00    1.00  1.00  1.00    20.00  .000E+00  .000E+00
  14     0   1.00    -12.00        .00   .00E+00    1   .00    1.00  1.00  1.00    20.00  .000E+00  .000E+00
  15     0   0.00    -14.00        .00   .00E+00    1   .00    1.00  1.00  1.00    20.00  .000E+00  .000E+00
  16     0   1.00    -14.00        .00   .00E+00    1   .00    1.00  1.00  1.00    20.00  .000E+00  .000E+00
  17     0   0.00    -16.00        .00   .00E+00    1   .00    1.00  1.00  1.00    20.00  .000E+00  .000E+00
  18     0   1.00    -16.00        .00   .00E+00    1   .00    1.00  1.00  1.00    20.00  .000E+00  .000E+00
  19     0   0.00    -18.00        .00   .00E+00    1   .00    1.00  1.00  1.00    20.00  .000E+00  .000E+00
  20     0   1.00    -18.00        .00   .00E+00    1   .00    1.00  1.00  1.00    20.00  .000E+00  .000E+00
  21     0   0.00    -20.00        .00   .00E+00    1   .00    1.00  1.00  1.00    20.00  .000E+00  .000E+00
  22     0   1.00    -20.00        .00   .00E+00    1   .00    1.00  1.00  1.00    20.00  .000E+00  .000E+00
  23     0   0.00    -22.00        .00   .00E+00    1   .00    1.00  1.00  1.00    20.00  .000E+00  .000E+00
  24     0   1.00    -22.00        .00   .00E+00    1   .00    1.00  1.00  1.00    20.00  .000E+00  .000E+00
  25     0   0.00    -24.00        .00   .00E+00    1   .00    1.00  1.00  1.00    20.00  .000E+00  .000E+00
  26     0   1.00    -24.00        .00   .00E+00    1   .00    1.00  1.00  1.00    20.00  .000E+00  .000E+00
  27     0   0.00    -26.00        .00   .00E+00    1   .00    1.00  1.00  1.00    20.00  .000E+00  .000E+00
  28     0   1.00    -26.00        .00   .00E+00    1   .00    1.00  1.00  1.00    20.00  .000E+00  .000E+00
  29     0   0.00    -28.00        .00   .00E+00    1   .00    1.00  1.00  1.00    20.00  .000E+00  .000E+00
  30     0   1.00    -28.00        .00   .00E+00    1   .00    1.00  1.00  1.00    20.00  .000E+00  .000E+00
  31     2   0.00    -30.00        .00   .00E+00    1   .00    1.00  1.00  1.00    20.00  .000E+00  .000E+00
  32     2   1.00    -30.00        .00   .00E+00    1   .00    1.00  1.00  1.00    20.00  .000E+00  .000E+00
*** BLOCK J: ELEMENT INFORMATION ***************************************************************************
    e    i    j    k    l  Angle  Aniz1  Aniz2 LayNum
    1    1    3    4    2    .00   1.00   1.00   1
    2    3    5    6    4    .00   1.00   1.00   1
    3    5    7    8    6    .00   1.00   1.00   1
    4    7    9   10    8    .00   1.00   1.00   1
    5    9   11   12   10    .00   1.00   1.00   1
    6   11   13   14   12    .00   1.00   1.00   1
    7   13   15   16   14    .00   1.00   1.00   1
    8   15   17   18   16    .00   1.00   1.00   1
    9   17   19   20   18    .00   1.00   1.00   1
   10   19   21   22   20    .00   1.00   1.00   1
   11   21   23   24   22    .00   1.00   1.00   1
   12   23   25   26   24    .00   1.00   1.00   1
   13   25   27   28   26    .00   1.00   1.00   1
   14   27   29   30   28    .00   1.00   1.00   1
   15   29   31   32   30    .00   1.00   1.00   1
*** BLOCK K: BOUNDARY GEOMETRY INFORMATION *****************************************************************
 Node number array:
         1          2         31         32
 Width array:
       .50        .50        .50        .50
 Length:
      0.00
 Observation Nodes (2,..,NObs):
 31
*** END OF INPUT FILE GRID.IN ******************************************************************************
```

Table 9.26. Input data for example 7 (input file 'SELECTOR.IN').

```
*** BLOCK A: BASIC INFORMATION **********************************************************
Heading
'Example 7 - Water and Solute Infiltration Test '
LUnit  TUnit  MUnit                  (indicated units are obligatory for all input data)
'cm'   'min'  '-'
Kat               (0:horizontal plane, 1:axisymmetric vertical flow, 2:vertical plane)
1
MaxIt   TolTh    TolH           (maximum number of iterations and precision tolerances)
20      .0001    .1
lWat    lChem   CheckF  ShortF  FluxF   AtmInF  SeepF  DrainF  FreeD lTemp lWDep lEquil
t       t       f       t       f       f       f      f       f     t     f     t
*** BLOCK B: MATERIAL INFORMATION *******************************************************
NMat    NLay    hTab1   hTabN   NPar
  2       2     .001    200.    9
thr     ths     tha     thm     Alfa    n       Ks      Kk      thk
.0001   .399    .0001   .399    .0174   1.3757  .0207   .0207   .399
.0001   .339    .0001   .339    .0139   1.6024  .0315   .0315   .339
*** BLOCK C: TIME INFORMATION ***********************************************************
dt      dtMin   dtMax   DMul    DMul2   MPL
.1      .001    1000.   1.33    .33     6
TPrint(1),TPrint(2),...,TPrint(MPL)                                    (print-time array)
720 1440 3600 7200 10800 14400
*** BLOCK G: SOLUTE TRANSPORT INFORMATION ************************************************
Epsi    lUpW    lArtD   lTDep   cTolA   cTolR   MaxItC  PeCr
0.5     t       f       t       0.0     0.0     1       2.
Bulk.d. DispL   DispT   Frac  (1...NMat)
 1.30    0.5     0.1     1.0
 1.30    0.5     0.1     1.0
Dif.w.  Dif.g. ------------------------------------------------------------ (1.solute)
 0.026   3.0
 KS      Nu   Beta Henry   SnkL1 SnkS1 SnkG1 SnkL1' SnkS1' SnkG1' SnkL0 SnkS0 SnkG0 Alfa
 0.1     0.0  1.0 1.33e-7 1.39e-4 0.0   0.0  2.5e-4  0.0    0.0    0.0   0.0   0.0   0.0
 0.1     0.0  1.0 1.33e-7 1.39e-4 0.0   0.0  2.5e-4  0.0    0.0    0.0   0.0   0.0   0.0
Dif.w.  Dif.g. ------------------------------------------------------------ (2.solute)
 0.026   3.0
 KS      Nu   Beta Henry   SnkL1 SnkS1 SnkG1 SnkL1' SnkS1' SnkG1' SnkL0 SnkS0 SnkG0 Alfa
 0.05    0.0  1.0  0.0    6.94e-6 0.0   0.0  1.67e-5 0.0    0.0    0.0   0.0   0.0   0.0
 0.05    0.0  1.0  0.0    6.94e-6 0.0   0.0  1.67e-5 0.0    0.0    0.0   0.0   0.0   0.0
Dif.w.  Dif.g. ------------------------------------------------------------ (3.solute)
 0.026   3.0
 KS      Nu   Beta Henry   SnkL1 SnkS1 SnkG1 SnkL1' SnkS1' SnkG1' SnkL0 SnkS0 SnkG0 Alfa
 0.2     0.0  1.0 1.33e-3 3.47e-6 0.0   0.0 1.67e-6 0.0    0.0    0.0   0.0   0.0   0.0
 0.2     0.0  1.0 1.33e-3 3.47e-6 0.0   0.0 1.67e-6 0.0    0.0    0.0   0.0   0.0   0.0
Temperature dependence
Dif.w.  Dif.g. ------------------------------------------------------------ (1.solute)
 0.0     0.0
 KS      Nu    Beta Henry SnkL1 SnkS1 SnkG1 SnkL1' SnkS1' SnkG1' SnkL0  SnkS0 SnkG0 Alfa
 0.0     0.0   0.0   0.0  51213. 0.0   0.0  81171   0.0    0.0    0.0    0.0   0.0   0.0
Dif.w.  Dif.g. ------------------------------------------------------------ (2.solute)
 0.0     0.0
 KS      Nu    Beta Henry SnkL1 SnkS1 SnkG1 SnkL1' SnkS1' SnkG1' SnkL0  SnkS0 SnkG0 Alfa
 0.0     0.0   0.0   0.0  51213. 0.0   0.0  81171   0.0    0.0    0.0    0.0   0.0   0.0
Dif.w.  Dif.g. ------------------------------------------------------------ (3.solute)
 0.0     0.0
 KS      Nu    Beta Henry SnkL1 SnkS1 SnkG1 SnkL1' SnkS1' SnkG1' SnkL0  SnkS0 SnkG0 Alfa
 0.0     0.0   0.0   0.0  51213. 0.0   0.0  81171   0.0    0.0    0.0    0.0   0.0   0.0
KodCB(1),KodCB(2),.....,KodCB(NumBP)
-1      -1      -1      -1      -1      -7      -7      -7      -7      -7
-7      -7      -7      -7      -7      -7      -7      -7      -7      -7
2       2
cTop    cBot
1.      0.      0.      0.      0.      0.      0.      0.      0.5
0.      0.      0.      0.      0.      0.      0.      0.      0.5
0.      0.      0.      0.      0.      0.      0.      0.      0.5
tPulse
7200
```

Table 9.26. (continued)

```
*** BLOCK H: HEAT TRANSPORT INFORMATION ************************************************
Qn      Qo    Th. Disper.    B1       B2       B3       Cn       Co       Cw
0.600  0.001  0.5   0.1  5.25e+6  8.45e+6 3.313e+7 6.912e+7 9.036e+7 1.505e+8
0.660  0.001  0.5   0.1  5.25e+6  8.45e+6 3.313e+7 6.912e+7 9.036e+7 1.505e+8
KodTB(1),KodTB(2),.....,KodTB(NumBP)
-1      -1      -1      -1      -1      -2      -2      -2      -2      -2
-2      -2      -2      -2      -2      -2      -2      -2      -2      -2
-3      -3
TBound(1),TBound(2),.....,TBound(6)
30.      0.      0.      0.      0.      0.
Amplitude tPeriod
0.        3600.
*** END OF INPUT FILE 'SELECTOR.IN' ****************************************************
```

Table 9.27. Input data for example 7 (input file 'GRID.IN').

```
*** BLOCK I: NODAL INFORMATION ************************************************************************
     NumNP      NumEl         IJ      NumBP         NS      NObs
       380        342         19         22          3         0
  n Code    x       z          h          Q          M    B   Axz  Bxz  Dxz   Temp    Conc1      Conc2      Conc3
  1   1   0.00  230.00       0.00  0.000E+00  1  0.0  1.0  1.0  1.0  20.0  0.000E+00  0.000E+00  0.000E+00
  2   0   0.00  228.00    -145.50  0.000E+00  1  0.0  1.0  1.0  1.0  20.0  0.000E+00  0.000E+00  0.000E+00
  3   0   0.00  226.00    -143.40  0.000E+00  1  0.0  1.0  1.0  1.0  20.0  0.000E+00  0.000E+00  0.000E+00
  4   0   0.00  224.00    -141.00  0.000E+00  1  0.0  1.0  1.0  1.0  20.0  0.000E+00  0.000E+00  0.000E+00
  5   0   0.00  220.00    -135.60  0.000E+00  1  0.0  1.0  1.0  1.0  20.0  0.000E+00  0.000E+00  0.000E+00
  6   0   0.00  215.00    -127.70  0.000E+00  1  0.0  1.0  1.0  1.0  20.0  0.000E+00  0.000E+00  0.000E+00
  7   0   0.00  210.00    -119.00  0.000E+00  1  0.0  1.0  1.0  1.0  20.0  0.000E+00  0.000E+00  0.000E+00
  8   0   0.00  205.00    -109.90  0.000E+00  1  0.0  1.0  1.0  1.0  20.0  0.000E+00  0.000E+00  0.000E+00
  9   0   0.00  200.00    -100.50  0.000E+00  1  0.0  1.0  1.0  1.0  20.0  0.000E+00  0.000E+00  0.000E+00
 10   0   0.00  190.00     -82.80  0.000E+00  2  0.0  1.0  1.0  1.0  20.0  0.000E+00  0.000E+00  0.000E+00
 11   0   0.00  180.00     -71.00  0.000E+00  2  0.0  1.0  1.0  1.0  20.0  0.000E+00  0.000E+00  0.000E+00
 12   0   0.00  170.00     -60.30  0.000E+00  2  0.0  1.0  1.0  1.0  20.0  0.000E+00  0.000E+00  0.000E+00
 13   0   0.00  160.00     -49.80  0.000E+00  2  0.0  1.0  1.0  1.0  20.0  0.000E+00  0.000E+00  0.000E+00
 14   0   0.00  150.00     -39.60  0.000E+00  2  0.0  1.0  1.0  1.0  20.0  0.000E+00  0.000E+00  0.000E+00
 15   0   0.00  140.00     -29.50  0.000E+00  2  0.0  1.0  1.0  1.0  20.0  0.000E+00  0.000E+00  0.000E+00
 16   0   0.00  130.00     -19.40  0.000E+00  2  0.0  1.0  1.0  1.0  20.0  0.000E+00  0.000E+00  0.000E+00
 17   0   0.00  120.00      -9.40  0.000E+00  2  0.0  1.0  1.0  1.0  20.0  0.000E+00  0.000E+00  0.000E+00
 18   0   0.00  110.00       0.60  0.000E+00  2  0.0  1.0  1.0  1.0  20.0  0.000E+00  0.000E+00  0.000E+00
 19   0   0.00  100.00      10.20  0.000E+00  2  0.0  1.0  1.0  1.0  20.0  0.000E+00  0.000E+00  0.000E+00
 20   1   5.00  230.00       0.00  0.000E+00  1  0.0  1.0  1.0  1.0  20.0  0.000E+00  0.000E+00  0.000E+00
 21   0   5.00  228.00    -145.50  0.000E+00  1  0.0  1.0  1.0  1.0  20.0  0.000E+00  0.000E+00  0.000E+00
          .       .          .          .     .    .    .    .    .     .          .          .
          .       .          .          .     .    .    .    .    .     .          .          .
          .       .          .          .     .    .    .    .    .     .          .          .
373   0 125.00  170.00     -60.30  0.000E+00  2  0.0  1.0  1.0  1.0  20.0  0.000E+00  0.000E+00  0.000E+00
374   0 125.00  160.00     -49.80  0.000E+00  2  0.0  1.0  1.0  1.0  20.0  0.000E+00  0.000E+00  0.000E+00
375   0 125.00  150.00     -39.60  0.000E+00  2  0.0  1.0  1.0  1.0  20.0  0.000E+00  0.000E+00  0.000E+00
376   0 125.00  140.00     -29.50  0.000E+00  2  0.0  1.0  1.0  1.0  20.0  0.000E+00  0.000E+00  0.000E+00
377   0 125.00  130.00     -19.40  0.000E+00  2  0.0  1.0  1.0  1.0  20.0  0.000E+00  0.000E+00  0.000E+00
378   0 125.00  120.00      -9.40  0.000E+00  2  0.0  1.0  1.0  1.0  20.0  0.000E+00  0.000E+00  0.000E+00
379   5 125.00  110.00       0.60  0.000E+00  2  0.0  1.0  1.0  1.0  20.0  0.000E+00  0.000E+00  0.000E+00
380   5 125.00  100.00      10.20  0.000E+00  2  0.0  1.0  1.0  1.0  20.0  0.000E+00  0.000E+00  0.000E+00
*** BLOCK J: ELEMENT INFORMATION **********************************************************************
    e    i    j    k    l  Angle  Aniz1  Aniz2 LayNum
    1    2   21   20    1   0.00   1.00   1.00   1
    2    3   22   21    2   0.00   1.00   1.00   1
    3    4   23   22    3   0.00   1.00   1.00   1
    4    5   24   23    4   0.00   1.00   1.00   1
    5    6   25   24    5   0.00   1.00   1.00   1
    6    7   26   25    6   0.00   1.00   1.00   1
    7    8   27   26    7   0.00   1.00   1.00   1
         .    .    .    .      .      .
         .    .    .    .      .      .
  336  355  374  373  354   0.00   1.00   1.00   2
  337  356  375  374  355   0.00   1.00   1.00   2
  338  357  376  375  356   0.00   1.00   1.00   2
  339  358  377  376  357   0.00   1.00   1.00   2
  340  359  378  377  358   0.00   1.00   1.00   2
  341  360  379  378  359   0.00   1.00   1.00   2
  342  361  380  379  360   0.00   1.00   1.00   2
*** BLOCK K: BOUNDARY GEOMETRY INFORMATION ************************************************************
 Node number array:
        1       20       39       58       77       96      115
      134      153      172      191      210      229      248
      267      286      305      324      343      362      379
      380
 Width array:
    26.18   157.08   273.32   300.55   261.80   238.76   263.89
   366.52   579.10   857.66  1221.04  1688.09  2277.66  3008.61
  3899.77  4970.01  6238.17  7723.10  9443.65  5292.55  7853.98
  3926.99
 Length:
     0.00
*** END OF INPUT FILE 'GRID.IN' ***********************************************************************
```

10. OUTPUT DATA

The program output consists of $17+(n_s\text{-}1)$ output files organized into 3 groups:

T-level information
- H_MEAN.OUT
- V_MEAN.OUT
- CUM_Q.OUT
- RUN_INF.OUT
- SOLUTE.OUT
- OBSNOD.OUT

P-level information
- H.OUT
- TH.OUT
- CONC.OUT
- TEMP.OUT
- Q.OUT
- VX.OUT
- VZ.OUT
- BOUNDARY.OUT
- BALANCE.OUT

A-level information
- A_LEVEL.OUT

In addition, some of the input data are printed to file CHECK.OUT. A separate output file SOLUTE.OUT is created for each solute. All output files are directed to subdirectory CHAIN_2D.OUT, which must be created by the user prior to program execution. The various output files are described in detail in Section 10.1. Section 10.2 lists selected output files for examples 1 through 7 (see Section 8). The input files for these examples were discussed in Section 9.2.

10.1. *Description of Data Output Files*

The file CHECK.OUT contains a complete description of the finite element mesh, the boundary code of each node, and the hydraulic and transport properties of each soil material. Finite element mesh data are printed only when the logical variable *CheckF* in

input Block A (Table 9.1) is set equal to .true..

T-level information - This group of output files contains information which is printed at the end of each time step. Printing can be suppressed by setting the logical variable *ShortF* in input Block A equal to .true.; the information is then printed only at selected print times. Output files printed at the T-level are described in Tables 10.1 through 10.5. Output file OBSNOD.OUT brings the information about the time change of the pressure head, water content, temperature, and solution and sorbed concentrations, in specified observation nodes.

P-level information - P-level information is printed only at prescribed print times. The following output files are printed at the P-level:

H.OUT	Nodal values of the pressure head
TH.OUT	Nodal values of the water content
CONC.OUT	Nodal values of the solution and sorbed concentrations
TEMP.OUT	Nodal values of the temperature
Q.OUT	Discharge/recharge rates assigned to boundary or internal sink/source nodes
VX.OUT	Nodal values of the x-components of the Darcian flux vector
VZ.OUT	Nodal values of the z-components of the Darcian flux vector
BOUNDARY.OUT	This file contains information about each boundary node, n, for which $Kode(n) \neq 0$, including the discharge/recharge rate, $Q(n)$, the boundary flux, $q(n)$, the pressure head $h(n)$, the water content $\theta(n)$, the temperature $Temp(n)$, and the concentration $Conc(n_s, n)$.
BALANCE.OUT	This file gives the total amount of water, heat and solute inside each specified subregion, the inflow/outflow rates to/from that subregion, together with the mean pressure head (*hMean*), mean temperature (*TMean*) and the mean concentration (*cMean*) over each subregion (see Table 10.6). Absolute and relative errors in the water and solute mass balances are also printed to this file.

The output files H.OUT, TH.OUT, CONC.OUT, TEMP.OUT, Q.OUT, VZ.OUT and VX.OUT provide printed tables of the specific variables. To better identify the output, each printed line starts with the nodal number and spatial coordinates of the first node on that line for which information is printed. Users can easily reprogram the original

subroutines to restructure the output for their specific needs.

A-level information - A-level information is printed each time a time-dependent boundary condition is specified. The information is directed to output file A_LEVEL.OUT (Table 10.7).

Table 10.1. H_MEAN.OUT - mean pressure heads.

hAtm	Mean valuee of the pressure head calculated over a set of nodes for which $Kode(n) = \pm 4$ (i.e., along part of a boundary controlled by atmospheric conditions) [L].
hRoot	Mean value of the pressure head over a region for which $Beta(n) > 0$ (i.e., within the root zone) [L].
*hKode*3	Mean value of the pressure head calculated over a set of nodes for which $Kode(n) = \pm 3$ (i.e., along part of a boundary where the groundwater level, the bottom flux, or other time-dependent pressure head and/or flux is imposed) [L].
*hKode*1	Mean value of the pressure head calculated over a set of nodes for which $Kode(n) = \pm 1$ (i.e., along part of a boundary where time-independent pressure heads and/or fluxes are imposed) [L].
hSeep	Mean value of the pressure head calculated over a set of nodes for which $Kode(n) = \pm 2$ (i.e., along seepage faces) [L].
*hKode*5	Mean value of the pressure head calculated over a set of nodes for which $Kode(n) = \pm 5$ [L].
.	.
.	.
.	.
hKodeN	Mean value of the pressure head calculated over a set of nodes for which $Kode(n) = \pm NumKD$ [L].

Table 10.2. V_MEAN.OUT - mean and total water fluxes.‡

rAtm	Potential surface flux per unit atmospheric boundary (*Kode(n)* = ±4) [LT^{-1}].
rRoot	Potential transpiration rate, T_p [LT^{-1}].
vAtm	Mean value of actual surface flux per unit atmospheric boundary (*Kode(n)* = ±4) [LT^{-1}].
vRoot	Actual transpiration rate, T_a [LT^{-1}].
vKode3	Total value of the bottom or other flux across part of a boundary where the groundwater level, the bottom flux, or other time-dependent pressure head and/or flux is imposed (*Kode(n)* = ±3), [L^2T^{-1}] or [L^3T^{-1}]†.
vKode1	Total value of the boundary flux across part of a boundary where time-independent pressure heads and/or fluxes are imposed, including internal sinks/sources (*Kode(n)* = ±1), [L^2T^{-1}] or [L^3T^{-1}].
vSeep	Total value of the boundary flux across a potential seepage face (*Kode(n)* = ±2), [L^2T^{-1}] or [L^3T^{-1}].
vKode5	Total value of the flux across a boundary containing nodes for which *Kode(n)* = ±5, [L^2T^{-1}] or [L^3T^{-1}].
.	.
.	.
.	.
vKodeN	Total value of the flux across a boundary containing nodes for which *Kode(n)* = ±*NumKD*, [L^2T^{-1}] or [L^3T^{-1}].

† For plane and axisymmetric flow, respectively
‡ Boundary fluxes are positive when water is removed from the system.

Table 10.3. CUM_Q.OUT - total cumulative water fluxes.‡

CumQAP	Cumulative total potential surface flux across the atmospheric boundary (*Kode(n)* = ±4), [L^2] or [L^3]†.
CumQRP	Cumulative total potential transpiration rate, [L^2] or [L^3]†.
CumQA	Cumulative total actual surface flux across the atmospheric boundary (*Kode(n)* = ±4), [L^2] or [L^3]†.
CumQR	Cumulative total actual transpiration rate, [L^2] or [L^3]†.
CumQ3	Cumulative total value of the bottom or other boundary flux across part of a boundary where the groundwater level, the bottom flux, or other time-dependent pressure head and/or flux is imposed (*Kode*(*n*) = ±3), [L^2] or [L^3]†.
CumQ1	Cumulative total value of the flux across part of a boundary along which time-independent pressure heads and/or fluxes are imposed, including internal sinks/sources (*Kode*(*n*) = ±1), [L^2] or [L^3]†.
CumQS	Cumulative total value of the flux across a potential seepage faces (*Kode*(*n*) = ±2), [L^2] or [L^3]†.
CumQ5	Cumulative total value of the flux across a boundary containing nodes for which *Kode*(*n*) = ±5, [L^2] or [L^3]†.
.	.
.	.
.	.
CumQN	Cumulative total value of the flux across a boundary containing nodes for which *Kode*(*n*) = ±*NumKD*, [L^2] or [L^3]†.

† For plane and axisymmetric flow, respectively
‡ Boundary fluxes are positive when water is removed from the system.

Table 10.4. RUN_INF.OUT - time and iteration information.

TLevel	Time-level (current time-step number) [-].
Time	Time, t, at current time-level [T].
dt	Time step, Δt [T].
IterW	Number of iterations for water flow [-].
IterC	Number of iterations for solute transport [-].
ItCum	Cumulative number of iterations [-].
Peclet	Maximum local Peclet number [-].
Courant	Maximum local Courant number [-].

Table 10.5. SOLUTE.OUT - actual and cumulative concentration fluxes.‡

*CumCh*0	Cumulative amount of solute removed from the flow region by zero-order reactions (positive when removed from the system), [ML^{-1}] or [M]†.
*CumCh*1	Cumulative amount of solute removed from the flow region by first-order reactions, [ML^{-1}] or [M]†.
CumChR	Cumulative amount of solute removed from the flow region by root water uptake S, [ML^{-1}] or [M]†.
*ChemS*1	Cumulative solute flux across part of a boundary along which time-independent pressure heads and/or fluxes are imposed (*Kode*(n) = ±1), [ML^{-1}] or [M]†.
*ChemS*2	Cumulative solute flux across a potential seepage faces (*Kode*(n) = ±2), [ML^{-1}] or [M]†.
*ChemS*3	Cumulative solute flux across part of a boundary along which the groundwater level, the bottom flux, or other time-dependent pressure head and/or flux is imposed (*Kode*(n) = ±3), [ML^{-1}] or [M]†.
*ChemS*4	Cumulative total solute flux across the atmospheric boundary (*Kode*(n) = ±4), [ML^{-1}] or [M]†.
*ChemS*5	Cumulative total solute flux across an internal or external boundary containing nodes for which *Kode*(n) = ±5, [ML^{-1}] or [M]†.
.	.
.	.
.	.
ChemSN	Cumulative total solute flux across an internal or external boundary containing nodes for which *Kode*(n) = ±*NumKD*, [ML^{-1}] or [M]†.
*qc*1	Total solute flux across part of a boundary along which time-independent pressure heads and/or fluxes are imposed (*Kode*(n) = ±1), [$ML^{-1}T^{-1}$] or [MT^{-1}]†.
*qc*2	Total solute flux across a potential seepage face (*Kode*(n) = ±2), [$ML^{-1}T^{-1}$] or [MT^{-1}]†.
*qc*3	Total solute flux calculated across a boundary containing nodes for which *Kode*(n) = ±3 (i.e., along part of a boundary where the groundwater level, the bottom flux, or other time-dependent pressure head and/or flux is specified), [$ML^{-1}T^{-1}$] or [MT^{-1}]†.
*qc*4	Total solute flux across the atmospheric boundary (*Kode*(n) = ±4), [$ML^{-1}T^{-1}$] or [MT^{-1}]†.
*qc*5	Total solute flux across an internal or external boundary containing nodes for which *Kode*(n) = ±5, [$ML^{-1}T^{-1}$] or [MT^{-1}]†.
.	.
.	.
.	.
qcN	Total solute flux across an internal or external boundary containing nodes for which *Kode*(n) = ±*NumKD*, [$ML^{-1}T^{-1}$] or [MT^{-1}]†.

† For plane and axisymmetric flow, respectively

‡ Same output file is created for each solute from 1 to NS. Values of the solute flux and the cumulative solute flux are positive when solute is removed from the system.

Table 10.6. BALANCE.OUT - mass balance variables.

Area	Area of the entire flow domain or a specified subregion, $[L^2]$ or $[L^3]^\dagger$.
Volume	Volume of water in the entire flow domain or in a specified subregion, $[L^2]$ or $[L^3]^\dagger$.
InFlow	Inflow/Outflow to/from the entire flow domain or to/from a specified subregion, $[L^2T^{-1}]$ or $[L^3T^{-1}]^\dagger$.
hMean	Mean pressure head in the entire flow domain or in a specified subregion [L].
TVol	Amount of heat in the entire flow domain or in a specified subregion, $[MLT^{-2}]$ or $[ML^2T^{-2}]^\dagger$.
TMean	Mean temperature in the entire flow domain or in a specified subregion [K].
ConcVol	Amount of solute in the entire flow domain or in a specified subregion. This variable is given for all solutes from 1 to *NS*, $[ML^{-1}]$ or $[M]^\dagger$.
cMean	Mean concentration in the entire flow domain or in a specified subregion. This variable is given for all solutes from 1 to *NS* $[ML^{-3}]$.
WatBalT	Absolute error in the water mass balance of the entire flow domain, $[L^2]$ or $[L^3]^\dagger$.
WatBalR	Relative error in the water mass balance of the entire flow domain [%].
CncBalT	Absolute error in the solute mass balance of the entire flow domain. This variable is given for all solutes from 1 to *NS*, $[ML^{-1}]$ or $[M]^\dagger$.
CncBalR	Relative error in the solute mass balance of the entire flow domain. This variable is given for all solutes from 1 to *NS* [%].

† For plane and axisymmetric flow, respectively

Table 10.7. A_LEVEL.OUT - mean pressure heads and total cumulative fluxes.‡

CumQAP	Cumulative total potential flux across the atmospheric boundary (*Kode(n)* = ±4), [L^2] or [L^3]†.
CumQRP	Cumulative total potential transpiration rate, [L^2] or [L^3]†.
CumQA	Cumulative total actual flux across the atmospheric boundary (*Kode(n)* = ±4), [L^2] or [L^3]†.
CumQR	Cumulative total actual transpiration rate, [L^2] or [L^3]†.
CumQ3	Cumulative total bottom or other flux across a boundary along which the groundwater level, the bottom flux, or other time-dependent pressure head and/or flux is imposed (*Kode(n)* = ±3), [L^2] or [L^3]†.
hAtm	Mean value of the pressure head calculated over a set of nodes for which *Kode(n)* = ±4 [L].
hRoot	Mean value of the pressure head over a region for which *Beta(n)* > 0 (i.e., the root zone) [L].
hKode3	Mean value of the pressure head over a set of nodes for which *Kode(n)* = ±3 [L].

† For plane and axisymmetric flow, respectively
‡ Boundary fluxes are positive when water is removed from the system.

Table 10.8. Output data for example 1 (part of output file 'H.OUT').

Time *** 5400.0000 ***

n	x(n)	z(n)	h(n)	h(n+1) ...
1	0.0	61.0	0.8	0.8
3	0.0	60.8	0.6	0.6
5	0.0	60.5	0.4	0.4
7	0.0	60.3	0.3	0.3
9	0.0	60.0	0.1	0.1
11	0.0	59.5	-0.2	-0.2
13	0.0	59.0	-0.5	-0.5
15	0.0	58.0	-1.2	-1.2
17	0.0	57.0	-1.8	-1.8
19	0.0	56.0	-2.5	-2.5
21	0.0	55.0	-3.1	-3.1
23	0.0	54.0	-3.7	-3.7
25	0.0	53.0	-4.4	-4.4
27	0.0	52.0	-5.0	-5.0
29	0.0	51.0	-5.7	-5.7
31	0.0	50.0	-6.3	-6.3
33	0.0	49.0	-7.0	-7.0
35	0.0	48.0	-7.6	-7.6
37	0.0	47.0	-8.3	-8.3
39	0.0	46.0	-8.9	-8.9
41	0.0	45.0	-9.5	-9.5
43	0.0	44.0	-10.1	-10.1
45	0.0	43.0	-10.8	-10.8
47	0.0	42.0	-11.4	-11.4
49	0.0	41.0	-12.0	-12.0
51	0.0	40.0	-12.6	-12.6
53	0.0	39.0	-13.2	-13.2
55	0.0	38.0	-13.7	-13.7
57	0.0	37.0	-14.3	-14.3
59	0.0	36.0	-14.9	-14.9
61	0.0	35.0	-15.4	-15.4
63	0.0	34.0	-16.0	-16.0
65	0.0	33.0	-16.5	-16.5
67	0.0	32.0	-17.0	-17.0
69	0.0	31.0	-17.6	-17.6
71	0.0	30.0	-18.1	-18.1
73	0.0	29.0	-18.8	-18.8
75	0.0	28.0	-19.5	-19.5
77	0.0	27.0	-20.3	-20.3
79	0.0	26.0	-21.3	-21.3
81	0.0	25.0	-22.5	-22.5
83	0.0	24.0	-23.9	-23.9
85	0.0	23.0	-25.6	-25.6
87	0.0	22.0	-27.8	-27.9
89	0.0	21.0	-30.8	-30.8
91	0.0	20.0	-34.8	-34.9
93	0.0	18.0	-48.7	-48.6
95	0.0	16.0	-81.9	-80.2
97	0.0	14.0	-137.1	-134.4
99	0.0	12.0	-149.5	-149.4
101	0.0	10.0	-150.0	-150.0
103	0.0	8.0	-150.0	-150.0
105	0.0	6.0	-149.9	-149.9
107	0.0	4.0	-149.7	-149.7
109	0.0	2.0	-149.0	-149.0
111	0.0	0.0	-147.4	-147.5

Table 10.9. Output data for example 1 (output file 'CUM_Q.OUT').

Example 1 - Column Test

Program CHAIN_2D
Time independent boundary conditions
Vertical plane flow, V = L*L
Units: L = cm , T = sec , M = -
All cumulative fluxes (CumQ) are positive out of the region

Time [T]	CumQAP [V]	CumQRP [V]	CumQA [V]	CumQR [V]	CumQ3 [V]	CumQ1 [V]	CumQS [V]	CumQ5 [V]	CumQ6.. [V]
60.0000	0.000E+00	0.000E+00	0.000E+00	0.000E+00	0.000E+00	-0.796E+00	0.000E+00	0.000E+00	0.000E+00
900.0000	0.000E+00	0.000E+00	0.000E+00	0.000E+00	0.000E+00	-0.340E+01	0.000E+00	0.000E+00	0.000E+00
1800.0000	0.000E+00	0.000E+00	0.000E+00	0.000E+00	0.000E+00	-0.505E+01	0.000E+00	0.000E+00	0.000E+00
2700.0000	0.000E+00	0.000E+00	0.000E+00	0.000E+00	0.000E+00	-0.643E+01	0.000E+00	0.000E+00	0.000E+00
3600.0000	0.000E+00	0.000E+00	0.000E+00	0.000E+00	0.000E+00	-0.767E+01	0.000E+00	0.000E+00	0.000E+00
5400.0000	0.000E+00	0.000E+00	0.000E+00	0.000E+00	0.000E+00	-0.991E+01	0.000E+00	0.000E+00	0.000E+00

Table 10.10. Output data for example 2 (output file 'RUN_INF.OUT').

TLevel	Time	dt	Iter	ItCum
70	.120E+03	.500E+00	2	166
132	.151E+03	.500E+00	3	335
192	.181E+03	.500E+00	3	522
254	.212E+03	.500E+00	3	673
328	.243E+03	.500E+00	2	912
388	.273E+03	.500E+00	6	1067

Table 10.11. Output data for example 2 (part of output file 'A_LEVEL.OUT').

```
Program CHAIN_2D
Time dependent boundary conditions
Vertical plane flow, V = L*L
Units: L = cm    , T = day   , M = -
All cumulative fluxes (CumQ) are positive out of the region
```

Time [T]	CumQAP [V]	CumQRP [V]	CumQA [V]	CumQR [V]	CumQ3 [V]	hAtm [L]	hRoot [L]	hKode3 [L]	A-level
91.0000	.000E+00	.160E+00	.000E+00	.160E+00	.373E-01	-58.2	-37.1	171.9	1
92.0000	-.700E-01	.340E+00	-.700E-01	.340E+00	.722E-01	-59.5	-39.0	169.4	2
93.0000	-.900E-01	.470E+00	-.900E-01	.470E+00	.105E+00	-62.3	-40.9	167.4	3
94.0000	-.900E-01	.670E+00	-.900E-01	.670E+00	.136E+00	-66.3	-43.8	164.3	4
95.0000	-.900E-01	.950E+00	-.900E-01	.950E+00	.164E+00	-71.2	-47.9	160.3	5
96.0000	-.160E+00	.113E+01	-.160E+00	.113E+01	.190E+00	-71.2	-50.8	158.0	6
97.0000	-.450E+00	.121E+01	-.450E+00	.121E+01	.215E+00	-63.6	-49.7	159.0	7
98.0000	-.890E+00	.135E+01	-.890E+00	.135E+01	.240E+00	-57.8	-46.1	162.1	8
99.0000	-.109E+01	.146E+01	-.109E+01	.146E+01	.268E+00	-60.9	-44.1	164.0	9
100.0000	-.138E+01	.157E+01	-.138E+01	.157E+01	.298E+00	-57.8	-42.6	166.0	10
101.0000	-.170E+01	.168E+01	-.170E+01	.168E+01	.329E+00	-55.1	-40.2	168.6	11
102.0000	-.219E+01	.179E+01	-.219E+01	.179E+01	.362E+00	-48.8	-36.2	173.7	12
103.0000	-.220E+01	.195E+01	-.220E+01	.195E+01	.400E+00	-57.2	-35.3	172.4	13
104.0000	-.220E+01	.212E+01	-.220E+01	.212E+01	.435E+00	-60.8	-38.6	169.4	14
105.0000	-.220E+01	.234E+01	-.220E+01	.234E+01	.468E+00	-64.8	-42.1	165.8	15
106.0000	-.220E+01	.255E+01	-.220E+01	.255E+01	.497E+00	-68.4	-45.8	162.5	16
107.0000	-.220E+01	.278E+01	-.220E+01	.278E+01	.524E+00	-72.3	-49.4	159.1	17
108.0000	-.220E+01	.301E+01	-.220E+01	.301E+01	.549E+00	-76.0	-53.0	155.9	18
109.0000	-.220E+01	.325E+01	-.220E+01	.325E+01	.572E+00	-79.7	-56.5	152.7	19
110.0000	-.220E+01	.343E+01	-.220E+01	.343E+01	.593E+00	-82.1	-59.5	150.1	20
111.0000	-.220E+01	.358E+01	-.220E+01	.358E+01	.613E+00	-84.1	-61.7	148.0	21
112.0000	-.220E+01	.377E+01	-.220E+01	.377E+01	.631E+00	-87.0	-64.2	145.7	22
113.0000	-.221E+01	.392E+01	-.221E+01	.392E+01	.649E+00	-88.4	-66.3	143.7	23
114.0000	-.222E+01	.414E+01	-.222E+01	.414E+01	.665E+00	-91.7	-68.8	141.5	24
115.0000	-.222E+01	.437E+01	-.222E+01	.437E+01	.681E+00	-95.6	-71.8	139.0	25
116.0000	-.224E+01	.457E+01	-.224E+01	.457E+01	.695E+00	-97.0	-74.4	136.8	26
117.0000	-.224E+01	.474E+01	-.224E+01	.474E+01	.709E+00	-99.6	-76.4	134.9	27
118.0000	-.226E+01	.488E+01	-.226E+01	.488E+01	.722E+00	-99.7	-77.9	133.2	28
119.0000	-.252E+01	.501E+01	-.252E+01	.501E+01	.735E+00	-86.9	-76.1	132.6	29
120.0000	-.276E+01	.512E+01	-.276E+01	.512E+01	.747E+00	-84.2	-73.1	133.2	30
121.0000	-.337E+01	.520E+01	-.337E+01	.520E+01	.760E+00	-68.2	-67.1	135.9	31
122.0000	-.337E+01	.541E+01	-.337E+01	.541E+01	.774E+00	-89.2	-67.4	137.2	32
123.0000	-.356E+01	.555E+01	-.356E+01	.555E+01	.788E+00	-84.3	-70.1	137.4	33
124.0000	-.373E+01	.576E+01	-.373E+01	.576E+01	.802E+00	-85.9	-70.3	137.1	34
125.0000	-.451E+01	.583E+01	-.451E+01	.583E+01	.816E+00	-62.0	-63.5	140.5	35
126.0000	-.569E+01	.593E+01	-.569E+01	.593E+01	.833E+00	-48.2	-51.0	151.4	36
127.0000	-.637E+01	.603E+01	-.637E+01	.603E+01	.855E+00	-51.3	-43.6	162.7	37
128.0000	-.637E+01	.619E+01	-.637E+01	.619E+01	.884E+00	-65.3	-43.4	163.8	38
129.0000	-.637E+01	.645E+01	-.637E+01	.645E+01	.912E+00	-70.7	-47.5	160.5	39
130.0000	-.637E+01	.671E+01	-.637E+01	.671E+01	.938E+00	-75.0	-51.7	156.9	40
.	.	.	.	.	.	.	.	.	.	.
.	.	.	.	.	.	.	.	.	.	.
.	.	.	.	.	.	.	.	.	.	.
259.0000	-.229E+02	.420E+02	-.229E+02	.419E+02	.149E+01	-336.3	-272.9	18.8	169
260.0000	-.229E+02	.422E+02	-.229E+02	.421E+02	.149E+01	-346.2	-277.6	18.1	170
261.0000	-.229E+02	.423E+02	-.229E+02	.423E+02	.149E+01	-350.5	-282.0	17.4	171
262.0000	-.229E+02	.425E+02	-.229E+02	.425E+02	.149E+01	-361.6	-287.1	16.7	172
263.0000	-.233E+02	.427E+02	-.233E+02	.427E+02	.149E+01	-216.3	-278.6	16.0	173
264.0000	-.238E+02	.429E+02	-.238E+02	.429E+02	.149E+01	-156.9	-246.6	15.3	174
265.0000	-.238E+02	.431E+02	-.238E+02	.431E+02	.149E+01	-228.3	-229.7	14.6	175
266.0000	-.238E+02	.433E+02	-.238E+02	.433E+02	.149E+01	-257.4	-237.0	13.9	176
267.0000	-.238E+02	.435E+02	-.238E+02	.434E+02	.149E+01	-276.8	-245.1	13.2	177
268.0000	-.238E+02	.437E+02	-.238E+02	.436E+02	.149E+01	-293.1	-252.9	12.6	178
269.0000	-.243E+02	.438E+02	-.243E+02	.437E+02	.149E+01	-157.4	-236.4	12.0	179
270.0000	-.244E+02	.440E+02	-.244E+02	.439E+02	.149E+01	-206.6	-219.2	11.4	180
271.0000	-.244E+02	.442E+02	-.244E+02	.441E+02	.149E+01	-240.3	-225.3	10.8	181
272.0000	-.244E+02	.444E+02	-.244E+02	.443E+02	.149E+01	-264.1	-234.5	10.3	182
273.0000	-.254E+02	.444E+02	-.254E+02	.443E+02	.149E+01	-103.1	-203.9	9.8	183

TABLE 10.12. Output data for example 3b (part of output file 'CONC.OUT'†).

Time *** 365.0000 *** Species 1

n	x(n)	z(n)	Conc(n)		Conc(n+1)		...										
1	.0	.0	1.000	1.000	1.000	1.000	1.000	1.000	1.000	.000	.000	.000	.000	.000	.000	.000	.000
16	.0	-5.0	.864	.864	.864	.864	.867	.847	.650	.226	-.009	.001	.000	.000	.000	.000	.000
31	.0	-10.0	.747	.747	.747	.748	.750	.704	.491	.265	.020	-.002	.000	.000	.000	.000	.000
46	.0	-15.0	.646	.646	.645	.647	.646	.585	.398	.253	.044	-.002	.000	.000	.000	.000	.000
61	.0	-20.0	.559	.558	.558	.560	.554	.488	.333	.228	.059	.000	.000	.000	.000	.000	.000
76	.0	-25.0	.483	.482	.482	.485	.475	.409	.282	.202	.066	.004	-.001	.000	.000	.000	.000
91	.0	-30.0	.417	.417	.417	.419	.406	.345	.240	.177	.067	.007	-.001	.000	.000	.000	.000
106	.0	-35.0	.361	.360	.360	.363	.348	.291	.205	.155	.066	.010	-.001	.000	.000	.000	.000
121	.0	-40.0	.312	.311	.312	.314	.297	.247	.176	.135	.062	.012	-.001	.000	.000	.000	.000
136	.0	-45.0	.270	.269	.269	.271	.254	.210	.151	.118	.058	.013	.000	.000	.000	.000	.000
151	.0	-50.0	.233	.232	.233	.234	.217	.178	.130	.102	.053	.014	.000	.000	.000	.000	.000
166	.0	-55.0	.204	.201	.202	.203	.186	.153	.112	.089	.048	.014	.000	.000	.000	.000	.000
181	.0	-60.0	.170	.172	.173	.173	.157	.128	.095	.076	.043	.014	.001	.000	.000	.000	.000
196	.0	-70.0	.132	.130	.131	.130	.116	.095	.071	.058	.034	.013	.001	.000	.000	.000	.000
211	.0	-80.0	.095	.097	.096	.095	.084	.069	.052	.043	.027	.011	.002	.000	.000	.000	.000
226	.0	-90.0	.085	.078	.078	.074	.064	.053	.041	.034	.022	.010	.002	.000	.000	.000	.000
241	.0	-100.0	.043	.048	.046	.044	.040	.032	.025	.021	.014	.007	.002	.000	.000	.000	.000
256	.0	-125.0	.010	.012	.013	.012	.012	.010	.007	.006	.004	.002	.001	.000	.000	.000	.000
271	.0	-150.0	.002	.002	.003	.003	.003	.002	.002	.001	.001	.001	.000	.000	.000	.000	.000
286	.0	-175.0	.000	.000	.000	.001	.001	.000	.000	.000	.000	.000	.000	.000	.000	.000	.000
301	.0	-200.0	.000	.000	.000	.000	.000	.000	.000	.000	.000	.000	.000	.000	.000	.000	.000

† This output file has different formatting than the original output file 'CONC.OUT'.

TABLE 10.13. Output data for example 4 (output files 'SOLUTE1.OUT, SOLUTE2.OUT, AND SOLUTE3.OUT').

All solute fluxes (SMean) and cumulative solute fluxes (ChemS) are positive out of the region

Time	CumCh0	Cumch1	CumChR	ChemS(i),i=1,NumKD						SMean(j),j=1,NumKD				
[T]	[VM/L3]	[VM/L3]	[VM/L3]	[VM/L3]						[VM/T/L3]				
50.00	0.000E+00	0.565E+01	0.000E+00	-0.500E+02	0.000E+00	0.000E+00	0.000E+00	0.000E+00	0.000E+00	-0.100E+01	0.000E+00	0.000E+00	0.000E+00	0.000E+00	0.000E+00
100.00	0.000E+00	0.211E+02	0.000E+00	-0.100E+03	0.000E+00	0.000E+00	0.000E+00	0.000E+00	0.000E+00	-0.100E+01	0.000E+00	0.000E+00	0.000E+00	0.000E+00	0.000E+00
200.00	0.000E+00	0.733E+02	0.000E+00	-0.200E+03	0.402E-29	0.000E+00	0.000E+00	0.000E+00	0.000E+00	-0.100E+01	0.203E-29	0.000E+00	0.000E+00	0.000E+00	0.000E+00

All solute fluxes (SMean) and cumulative solute fluxes (ChemS) are positive out of the region

Time	CumCh0	Cumch1	CumChR	ChemS(i),i=1,NumKD						SMean(j),j=1,NumKD				
[T]	[VM/L3]	[VM/L3]	[VM/L3]	[VM/L3]						[VM/T/L3]				
50.00	-0.576E+01	0.386E+01	0.000E+00	0.000E+00	0.000E+00	0.000E+00	0.000E+00	0.000E+00	0.000E+00	0.000E+00	0.000E+00	0.000E+00	0.000E+00	0.000E+00	0.000E+00
100.00	-0.213E+02	0.175E+02	0.000E+00	0.000E+00	0.389E-35	0.000E+00	0.000E+00	0.000E+00	0.000E+00	0.000E+00	0.268E-35	0.000E+00	0.000E+00	0.000E+00	0.000E+00
200.00	-0.736E+02	0.671E+02	0.000E+00	0.000E+00	0.296E-08	0.000E+00	0.000E+00	0.000E+00	0.000E+00	0.000E+00	0.458E-09	0.000E+00	0.000E+00	0.000E+00	0.000E+00

All solute fluxes (SMean) and cumulative solute fluxes (ChemS) are positive out of the region

Time	CumCh0	Cumch1	CumChR	ChemS(i),i=1,NumKD						SMean(j),j=1,NumKD				
[T]	[VM/L3]	[VM/L3]	[VM/L3]	[VM/L3]						[VM/T/L3]				
50.00	-0.395E+01	0.000E+00	0.000E+00	0.000E+00	0.000E+00	0.000E+00	0.000E+00	0.000E+00	0.000E+00	0.000E+00	0.000E+00	0.000E+00	0.000E+00	0.000E+00	0.000E+00
100.00	-0.177E+02	0.000E+00	0.000E+00	0.000E+00	0.505E-29	0.000E+00	0.000E+00	0.000E+00	0.000E+00	0.000E+00	0.360E-29	0.000E+00	0.000E+00	0.000E+00	0.000E+00
200.00	-0.674E+02	0.000E+00	0.000E+00	0.000E+00	0.166E+00	0.000E+00	0.000E+00	0.000E+00	0.000E+00	0.000E+00	0.280E-01	0.000E+00	0.000E+00	0.000E+00	0.000E+00

TABLE 10.14. Output data for example 5 (output file 'CHECK.OUT').

```
Example 5 - One-Dimensional Solute Transport with Nonlinear Cation Adsorption

Program CHAIN_2D
Time independent boundary conditions
Vertical plane flow, V = L*L
Units: L = cm   , T = day  , M = -

Max. number of iterations            20
Absolute water content tolerance [-]  .00010
Absolute pressure head tolerance [L]  .01000

MatNum        thR     thS     tha     thm      alpha        n          Ks          Kk          thk

   1          .000    .633    .000    .633    .100E-01    .200E+01    .649E+01    .649E+01    .633E+00

MatNum         Qe      Q        h         C         K

   1          1.000   .633      .000   .00E+00   .649E+01
   1           .990   .627   -14.249   .88E-03   .477E+01
   1           .900   .570   -48.432   .22E-02   .196E+01
   1           .850   .538   -61.974   .24E-02   .134E+01
   1           .750   .475   -88.192   .24E-02   .645E+00
   1           .650   .411  -116.913   .20E-02   .302E+00
   1           .500   .317  -173.205   .14E-02   .824E-01
   1           .350   .222  -267.643   .73E-03   .154E-01
   1           .200   .127  -489.898   .25E-03   .119E-02
   1           .100   .063  -994.987   .63E-04   .516E-04

Solute transport information
============================

Galerkin finite-element method

Number of species in the chain :  1

Mat.     Bulk.D.    DispL     DispT    Fraction
  1        .8840    2.7270     .0000    1.0000

   Dif.w.      Dif.g.   ------------------------------------------------ ( 1.solute)
  .000E+00    .000E+00
Mat.    KS     Nu    Beta    Henry   SinkL1  SinkS1  SinkG1  SinkL1'  SinkS1'  SinkG1'  SinkL0  SinkS0  SinkG0  Alfa
  1   .17E+01  .0   .16E+01    .0       .0      .0      .0       .0       .0       .0       .0      .0      .0     .0

Freundlich nonlinear adsorption isotherm for material  1

  Conc1     Conc2     Conc3     Conc4     cSink     cWell     Conc7     gAtm          d
 .100E+02  .000E+00  .000E+00  .000E+00  .000E+00  .000E+00  .000E+00  .000E+00     .0000

tPulse =            14.919
```

TABLE 10.15. Output data for example 5 (part of output file 'CONC.OUT').

Time *** 25.0000 *** Species 1

n	x(n)	z(n)	Conc(n)	Conc(n+1)	...
1	0.0	0.0	0.000E+00	0.000E+00	
3	0.0	-0.3	0.154E-01	0.144E-01	
5	0.0	-0.5	0.322E-01	0.302E-01	
7	0.0	-0.8	0.506E-01	0.475E-01	
9	0.0	-1.0	0.706E-01	0.663E-01	
11	0.0	-1.3	0.925E-01	0.869E-01	
13	0.0	-1.5	0.116E+00	0.109E+00	
15	0.0	-1.8	0.142E+00	0.134E+00	
17	0.0	-2.0	0.170E+00	0.160E+00	
19	0.0	-2.3	0.200E+00	0.189E+00	
21	0.0	-2.5	0.233E+00	0.220E+00	
23	0.0	-2.8	0.269E+00	0.253E+00	
25	0.0	-3.0	0.307E+00	0.289E+00	
27	0.0	-3.3	0.348E+00	0.328E+00	
29	0.0	-3.5	0.391E+00	0.370E+00	
31	0.0	-3.8	0.438E+00	0.414E+00	
33	0.0	-4.0	0.488E+00	0.462E+00	
35	0.0	-4.3	0.541E+00	0.513E+00	
37	0.0	-4.5	0.598E+00	0.567E+00	
39	0.0	-4.8	0.658E+00	0.624E+00	
41	0.0	-5.0	0.721E+00	0.684E+00	
43	0.0	-5.3	0.787E+00	0.747E+00	
45	0.0	-5.5	0.856E+00	0.814E+00	
47	0.0	-5.8	0.929E+00	0.884E+00	
49	0.0	-6.0	0.100E+01	0.956E+00	
51	0.0	-6.3	0.108E+01	0.103E+01	
53	0.0	-6.5	0.116E+01	0.111E+01	
55	0.0	-6.8	0.124E+01	0.119E+01	
57	0.0	-7.0	0.133E+01	0.127E+01	
59	0.0	-7.3	0.141E+01	0.135E+01	
61	0.0	-7.5	0.150E+01	0.144E+01	
63	0.0	-7.8	0.158E+01	0.152E+01	
65	0.0	-8.0	0.167E+01	0.160E+01	
67	0.0	-8.3	0.175E+01	0.168E+01	
69	0.0	-8.5	0.183E+01	0.176E+01	
71	0.0	-8.8	0.191E+01	0.184E+01	
73	0.0	-9.0	0.198E+01	0.191E+01	
75	0.0	-9.3	0.205E+01	0.198E+01	
77	0.0	-9.5	0.211E+01	0.204E+01	
79	0.0	-9.8	0.216E+01	0.209E+01	
81	0.0	-10.0	0.220E+01	0.213E+01	
83	0.0	-10.3	0.223E+01	0.217E+01	
85	0.0	-10.5	0.225E+01	0.219E+01	
87	0.0	-10.8	0.225E+01	0.220E+01	

TABLE 10.16. Output data for example 6 (part of output file 'OBSNOD.OUT').

Node(31)

time	hNew	theta	Temp	Conc	Sorb
.000	.000	.4450	20.000	.000E+00	.000E+00
.010	.000	.4450	20.000	.755E-21	.726E-24
.023	.000	.4450	20.000	.313E-18	.391E-21
.040	.000	.4450	20.000	.784E-16	.129E-18
.062	.000	.4450	20.000	.981E-14	.210E-16
.091	.000	.4450	20.000	.109E-11	.311E-14
.128	.000	.4450	20.000	.677E-10	.248E-12
.175	.000	.4450	20.000	.271E-08	.126E-10
.240	.000	.4450	20.000	.142E-06	.908E-09
.327	.000	.4450	20.000	.513E-05	.443E-07
.413	.000	.4450	20.000	.537E-04	.529E-06
.500	.000	.4450	20.000	.343E-03	.380E-05
.625	.000	.4450	20.000	.317E-02	.453E-04
.750	.000	.4450	20.000	.170E-01	.282E-03
.875	.000	.4450	20.000	.648E-01	.124E-02
.937	.000	.4450	20.000	.116E+00	.230E-02
1.000	.000	.4450	20.000	.195E+00	.411E-02
1.125	.000	.4450	20.000	.471E+00	.118E-01
1.250	.000	.4450	20.000	.979E+00	.285E-01
1.375	.000	.4450	20.000	.178E+01	.600E-01
1.500	.000	.4450	20.000	.287E+01	.113E+00
1.625	.000	.4450	20.000	.422E+01	.192E+00
1.750	.000	.4450	20.000	.573E+01	.303E+00
1.874	.000	.4450	20.000	.727E+01	.445E+00
1.999	.000	.4450	20.000	.875E+01	.617E+00
2.124	.000	.4450	20.000	.101E+02	.815E+00
2.249	.000	.4450	20.000	.112E+02	.104E+01
.		.		.	
.		.		.	
.		.		.	
16.496	.000	.4450	20.000	.425E+00	.968E+00
16.621	.000	.4450	20.000	.411E+00	.940E+00
16.746	.000	.4450	20.000	.398E+00	.913E+00
16.871	.000	.4450	20.000	.385E+00	.887E+00
16.996	.000	.4450	20.000	.373E+00	.861E+00
17.121	.000	.4450	20.000	.361E+00	.836E+00
17.246	.000	.4450	20.000	.349E+00	.811E+00
17.371	.000	.4450	20.000	.338E+00	.788E+00
17.496	.000	.4450	20.000	.327E+00	.765E+00
17.621	.000	.4450	20.000	.317E+00	.742E+00
17.746	.000	.4450	20.000	.306E+00	.721E+00
17.870	.000	.4450	20.000	.297E+00	.700E+00
17.995	.000	.4450	20.000	.287E+00	.679E+00
18.120	.000	.4450	20.000	.278E+00	.659E+00
18.245	.000	.4450	20.000	.269E+00	.640E+00
18.370	.000	.4450	20.000	.260E+00	.621E+00
18.495	.000	.4450	20.000	.252E+00	.603E+00
18.620	.000	.4450	20.000	.244E+00	.585E+00
18.745	.000	.4450	20.000	.236E+00	.568E+00
18.870	.000	.4450	20.000	.228E+00	.551E+00
18.995	.000	.4450	20.000	.221E+00	.535E+00
19.120	.000	.4450	20.000	.214E+00	.519E+00
19.245	.000	.4450	20.000	.207E+00	.504E+00
19.370	.000	.4450	20.000	.200E+00	.489E+00
19.494	.000	.4450	20.000	.194E+00	.474E+00
19.619	.000	.4450	20.000	.187E+00	.460E+00
19.744	.000	.4450	20.000	.181E+00	.446E+00
19.869	.000	.4450	20.000	.175E+00	.433E+00
19.935	.000	.4450	20.000	.172E+00	.426E+00
20.000	.000	.4450	20.000	.169E+00	.420E+00

end

TABLE 10.17. Output data for example 7 (output files 'SOLUTE1.OUT, SOLUTE2.OUT, AND SOLUTE3.OUT').

All solute fluxes (SMean) and cumulative solute fluxes (ChemS) are positive out of the region

Time [T]	CumCh0 [VM/L3]	CumCh1 [VM/L3]	CumChR [VM/L3]	ChemS(i),i=1,NumKD [VM/L3]						SMean(j),j=1,NumKD [VM/T/L3]					
720.00	.000E+00	.325E+04	.000E+00	-.223E+05	.000E+00	.000E+00	.000E+00	.000E+00	.564E+00	-.280E+02	.000E+00	.000E+00	.000E+00	.000E+00	.119E-02
1440.00	.000E+00	.109E+05	.000E+00	-.423E+05	.000E+00	.000E+00	.000E+00	.000E+00	.160E+01	-.277E+02	.000E+00	.000E+00	.000E+00	.000E+00	.163E-02
3600.00	.000E+00	.487E+05	.000E+00	-.102E+06	.000E+00	.000E+00	.000E+00	.000E+00	.579E+01	-.276E+02	.000E+00	.000E+00	.000E+00	.000E+00	.213E-02
7200.00	.000E+00	.135E+06	.000E+00	-.201E+06	.000E+00	.000E+00	.000E+00	.000E+00	.138E+02	-.275E+02	.000E+00	.000E+00	.000E+00	.000E+00	.228E-02
10800.00	.000E+00	.180E+06	.000E+00	-.201E+06	.000E+00	.000E+00	.000E+00	.000E+00	.169E+02	.000E+00	.000E+00	.000E+00	.000E+00	.000E+00	.297E-03
14400.00	.000E+00	.192E+06	.000E+00	-.201E+06	.000E+00	.000E+00	.000E+00	.000E+00	.175E+02	.000E+00	.000E+00	.000E+00	.000E+00	.000E+00	.642E-04

All solute fluxes (SMean) and cumulative solute fluxes (ChemS) are positive out of the region

Time [T]	CumCh0 [VM/L3]	CumCh1 [VM/L3]	CumChR [VM/L3]	ChemS(i),i=1,NumKD [VM/L3]						SMean(j),j=1,NumKD [VM/T/L3]					
720.00	-.224E+04	.160E+02	.000E+00	.000E+00	.000E+00	.000E+00	.000E+00	.000E+00	.000E+00	.000E+00	.000E+00	.000E+00	.000E+00	.000E+00	.000E+00
1440.00	-.744E+04	.105E+03	.000E+00	.000E+00	.000E+00	.000E+00	.000E+00	.000E+00	.000E+00	.000E+00	.000E+00	.000E+00	.000E+00	.000E+00	.000E+00
3600.00	-.332E+05	.115E+04	.000E+00	.000E+00	.000E+00	.000E+00	.000E+00	.000E+00	.000E+00	.000E+00	.000E+00	.000E+00	.000E+00	.000E+00	.000E+00
7200.00	-.915E+05	.635E+04	.000E+00	.000E+00	.000E+00	.000E+00	.000E+00	.000E+00	.000E+00	.000E+00	.000E+00	.000E+00	.000E+00	.000E+00	.000E+00
10800.00	-.122E+06	.149E+05	.000E+00	.000E+00	.000E+00	.000E+00	.000E+00	.000E+00	.000E+00	.000E+00	.000E+00	.000E+00	.000E+00	.000E+00	.000E+00
14400.00	-.130E+06	.237E+05	.000E+00	.000E+00	.000E+00	.000E+00	.000E+00	.000E+00	.000E+00	.000E+00	.000E+00	.000E+00	.000E+00	.000E+00	.000E+00

All solute fluxes (SMean) and cumulative solute fluxes (ChemS) are positive out of the region

Time [T]	CumCh0 [VM/L3]	CumCh1 [VM/L3]	CumChR [VM/L3]	ChemS(i),i=1,NumKD [VM/L3]						SMean(j),j=1,NumKD [VM/T/L3]					
720.00	-.121E+02	.867E-02	.000E+00	.000E+00	.000E+00	.000E+00	.000E+00	.000E+00	.389E+00	.000E+00	.000E+00	.000E+00	.000E+00	.000E+00	.159E-02
1440.00	-.782E+02	.110E+00	.000E+00	.000E+00	.000E+00	.000E+00	.000E+00	.000E+00	.309E+01	.000E+00	.000E+00	.000E+00	.000E+00	.000E+00	.618E-02
3600.00	-.844E+03	.286E+01	.000E+00	.000E+00	.000E+00	.000E+00	.000E+00	.000E+00	.412E+02	.000E+00	.000E+00	.000E+00	.000E+00	.000E+00	.308E-01
7200.00	-.464E+04	.310E+02	.000E+00	.000E+00	.000E+00	.000E+00	.000E+00	.000E+00	.250E+03	.000E+00	.000E+00	.000E+00	.000E+00	.000E+00	.864E-01
10800.00	-.108E+05	.115E+03	.000E+00	.000E+00	.000E+00	.000E+00	.000E+00	.000E+00	.618E+03	.000E+00	.000E+00	.000E+00	.000E+00	.000E+00	.110E+00
14400.00	-.172E+05	.263E+03	.000E+00	.000E+00	.000E+00	.000E+00	.000E+00	.000E+00	.101E+04	.000E+00	.000E+00	.000E+00	.000E+00	.000E+00	.108E+00

TABLE 10.18. Output data for example 7 (part of output file 'BALANCE.OUT').

```
Example 7 - Water and Solute Infiltration Test

Program CHAIN_2D
Time independent boundary conditions
Axisymmetric flow, V = L*L*L
Units: L = cm   , T = min   , M = -

Time [T]                    Total     Sub-region number ...

      .0000                             1          2
Area     [V]              .638E+07   .147E+07   .491E+07
Volume   [V]              .188E+07   .405E+06   .147E+07
InFlow   [V/T]             .000E+00   .000E+00   .000E+00
hMean    [L]              -.604E+02    -126.3      -40.6
HeatVol  [VM/L/T2]         .166E+18   .358E+17   .130E+18
tMean    [K]                20.000     20.000     20.000
ConcVol  [VM/L3]  1        .000E+00   .000E+00   .000E+00
cMean    [M/L3]   1        .000E+00   .000E+00   .000E+00
ConcVol  [VM/L3]  2        .000E+00   .000E+00   .000E+00
cMean    [M/L3]   2        .000E+00   .000E+00   .000E+00
ConcVol  [VM/L3]  3        .000E+00   .000E+00   .000E+00
cMean    [M/L3]   3        .000E+00   .000E+00   .000E+00
  .                .                        .          .
  .                .                        .          .
  .                .                        .          .

 14400.0000                         1          2
Area     [V]              .638E+07   .147E+07   .491E+07
Volume   [V]              .196E+07   .455E+06   .151E+07
InFlow   [V/T]            -.367E+00  -.195E+00  -.172E+00
hMean    [L]              -.450E+02    -81.3      -34.1
HeatVol  [VM/L/T2]         .170E+18   .382E+17   .132E+18
tMean    [K]                20.943     21.572     20.754
ConcVol  [VM/L3]  1        .541E+04   .115E+04   .425E+04
cMean    [M/L3]   1        .196E-02   .173E-02   .203E-02
ConcVol  [VM/L3]  2        .106E+06   .240E+05   .824E+05
cMean    [M/L3]   2        .452E-01   .425E-01   .460E-01
ConcVol  [VM/L3]  3        .159E+05   .337E+04   .125E+05
cMean    [M/L3]   3        .441E-02   .393E-02   .456E-02
WatBalT  [V]              -.394E+04
WatBalR  [%]                  .529
CncBalT  [VM/L3]  1       -.348E+04
CncBalR  [%]      1           .886
CncBalT  [VM/L3]  2        .542E+03
CncBalR  [%]      2           .353
CncBalT  [VM/L3]  3       -.231E+02
CncBalR  [%]      3           .125
```

11. PROGRAM ORGANIZATION

11.1. *Description of Program Units*

The program consists of a main program and 66 subprograms. The subprograms are organized by means of 9 source files which are stored and compiled separately and then linked together with the main program to form an executable program. Below are a list and brief descriptions of the source files and the associated subprograms.

CHAIN_2D.FOR	(Main program unit)
INPUT2.FOR	BasInf, MatIn, GenMat, TmIn, SeepIn, DrainIn, NodInf, ElemIn, GeomIn, AtmIn, SinkIn, ChemIn, TempIn
WATFLOW2.FOR	WatFlow, Reset, Dirich, Solve, Shift, SetMat, Veloc
TIME2.FOR	TmCont, SetAtm, Fgh
MATERIA2.FOR	FK, FC, FQ, FH
SINK2.FOR	SetSnk, FAlfa
OUTPUT2.FOR	TLInf, ALInf, hOut, thOut, QOut, FlxOut, SubReg, BouOut, cOut, SolInf, TOut, ObsNod
SOLUTE2.FOR	Solute, Coef, SolMat, c_Bound, Disper, SolveT, WeFact, PeCour
TEMPER2.FOR	Temper, T_Bound, DispT
ORTHOFEM.FOR	IADMake, Insert, Find, ILU, DU, ORTHOMIN, LUSolv, MatM2, SDot, SDotK, SNRM, SAXPYK, SCopy, SCopyK

Main program unit CHAIN_2D.FOR

This is the main program unit of CHAIN_2D. This unit controls execution of the program and determines which optional subroutines are necessary for a particular application.

Source file INPUT.FOR

Subroutines included in this source file are designed to read data from different input blocks. The following table summarizes from which input file and input block (described in Section 9) a particular subroutine reads.

Table 11.1. Input subroutines/files.

Subroutine	Input Block	Input File
BasInf	A. Basic Information	
MatIn	B. Material Information	
TmIn	C. Time Information	
SinkIn	D. Sink Information	SELECTOR.IN
SeepIn	E. Seepage Information	
DrainIn	F. Drainage Information	
ChemIn	G. Solute Transport Information	
TempIn	H. Heat Transport Information	
NodInf	I. Nodal Information	
ElemIn	J. Element Information	GRID.IN
GeomIn	K. Boundary Geometry Information	
AtmIn	L. Atmospheric Information	ATMOSPH.IN

Subroutine **GenMat** generates for each soil type in the flow domain a table of water contents, hydraulic conductivities, and specific water capacities from set of hydraulic parameters.

Source file WATFLOW2.FOR

Subroutine **WatFlow** is the main subroutine for simulating water flow; this subroutine controls the entire iterative procedure of solving the Richards equation.

Subroutine **Reset** constructs the global matrix equation for water flow, including the right-hand side vector.

Subroutine **Dirich** modifies the global matrix equation by incorporating prescribed pressure head nodes.

Subroutine **Solve** solves the banded symmetric matrix equation for water flow by Gaussian elimination.

Subroutine **Shift** changes atmospheric or seepage face boundary conditions from Dirichlet type to Neumann type conditions, or vice versa, as needed. Also updates boundary conditions for the variable boundary fluxes (free and deep drainage).

Subroutine **Veloc** calculates nodal water fluxes.

Subroutine **SetMat** determines the nodal values of the hydraulic properties $K(h)$, $C(h)$ and $\theta(h)$ by interpolation between intermediate values in the hydraulic property tables.

Source file TIME2.FOR

Subroutine **TmCont** adjusts the current value of the time increment Δt.

Subroutine **SetAtm** updates time variable boundary conditions.

Function **Fqh** describes the groundwater level - discharge relationship, $q(h)$, defined by equation (7.1). This function is called only from subroutine SetAtm.

Source file MATERIA2.FOR

This file includes the functions **FK, FC, FQ** and **FH** which define the unsaturated hydraulic properties $K(h)$, $C(h)$, $\theta(h)$, and $h(\theta)$, for each soil material.

Source file SINK2.FOR

This file includes subroutine **SetSnk** and function **FAlfa**. These subroutines calculate the actual root water extraction rate as a function of water stress in the soil root zone.

Source file OUTPUT2.FOR

The subroutines included in this file are designed to print data to different output files. Table 11.2 summarizes which output files are generated by a particular subroutine.

Table 11.2. Output subroutines/files.

Subroutine	Output File
TLInf	H_MEAN.OUT V_MEAN.OUT CUM_Q.OUT RUN_INF.OUT
SolInf	SOLUTE.OUT
hOut	H.OUT
thOut	TH.OUT
cOut	CONC.OUT
TOut	TEMP.OUT
QOut	Q.OUT
FlxOut	VX.OUT VZ.OUT
BouOut	BOUNDARY.OUT
SubReg	BALANCE.OUT
ALInf	A_LEVEL.OUT
ObsNod	OBSNOD.OUT

Source file SOLUTE2.FOR

Subroutine **Solute** is the main subroutine for simulating solute transport; this subroutine controls the entire iterative procedure of solving the nonlinear non-equilibrium convection-dispersion equation.

Subroutine **Coeff** calculates solute transport parameters.

Subroutine **SolMat** constructs the global matrix equation for transport, including the right-hand side vector.

Subroutine **c_Bound** determines the values of the solute transport boundary codes, *cKod(n)*, and incorporates prescribed boundary conditions in the global matrix equation for solute transport.

Subroutine **Disper** calculates nodal values of the dispersion coefficients for solute transport.

Subroutine **SolveT** solves the final asymmetric banded matrix equation for solute transport using Gaussian elimination.

Subroutine **WeFact** computes the optimum weighing factors for all sides of all elements.

Subroutine **PeCour** computes the maximum local Peclet and Courant numbers and the maximum permissible time step.

Source file TEMPER2.FOR

Subroutine **Temper** is the main subroutine for simulating heat transport; this subroutine constructs the global matrix equation for heat transport, including the right-hand side vector.

Subroutine **T_Bound** determines the values of the heat transport boundary, and incorporates prescribed boundary conditions in the global matrix equation for heat transport.

Subroutine **DispT** calculates nodal values of the apparent dispersion coefficients for heat transport.

Source file ORTHOFEM.FOR

The subroutines included in this file solve large sparse systems of linear algebraic equations by the preconditioned conjugate gradient method for symmetric matrices, and by the ORTHOMIN method for asymmetric matrices. The subroutines were adopted from *Mendoza et al.* [1991]. See *Mendoza et al.* [1991] for a detailed description of both methods.

Subroutine **IADMake** generates the adjacency matrix which determines nodal connections from the finite element incidence matrix.

Subroutine **Insert** adds node j to the adjacency list for node i.

Subroutine **Find** retrieves from the adjacency matrix the appropriate position of two global point in the coefficient matrix.

Subroutine **ILU** performs incomplete lower-upper decomposition of matrix [A].

Function **DU** searches the ith row of the upper diagonal matrix for an adjacency of node j.

Subroutine **ORTHOMIN** governs the ORTHOMIN (conjugate gradient) acceleration.

Subroutine **LUSolv** performs lower diagonal matrix inversion by forward substitution, and upper diagonal matrix inversion by backward substitution.

Subroutine **MatM2** multiplies a matrix by a vector.

Function **SDot** calculates the dot product of two vectors.

Function **SDotK** calculates the dot product of a column in matrix by a vector.

Function **SNRM** computes the maximum norm of a vector.

Subroutine **SAXPYK** multiplies a column in a matrix by a scalar, and adds the resulting value to another vector.

Subroutine **SCopy** copies a vector into another vector.

Subroutine **SCopyK** copies a column in a matrix into a vector.

11.2. *List of Significant CHAIN_2D Program Variables.*

Variables which appear in subroutines of the ORTHOFEM package are not given in the following tables. Consult the user's guide of ORTHOFEM [*Mendoza et al.*, 1991] for their definition.

Table 11.3. List of significant integer variables.

ALevel	Time level at which a time-dependent boundary condition is specified.
cKod	Code which specifies the type of boundary condition used for solute transport.
IJ	Maximum number of nodes on any transverse line (Table 9.9).
ItCum	Cumulative number of iterations (Table 10.4).
IterC	Number of iterations necessary for the solution of the solute transport equation (Table 10.4).
IterW	Number of iterations necessary for the solution of the water flow equation (Table 10.4).
Kat	Type of flow system to be analyzed (Table 9.1).
MaxAl	Number of atmospheric data records (Table 9.12).
MaxIt	Maximum number of iterations allowed during any time step for the solution of water flow equation (Table 9.1).
MaxItC	Maximum number of iterations allowed during any time step for the solution of solute transport equation (Table 9.7).
MBand	Bandwidth (half-bandwidth) of the symmetric (asymmetric) matrix A when Gaussian elimination is used. Maximum number of nodes adjacent to another node when iterative solvers are used.
MBandD	Maximum permitted bandwidth of matrix A when Gaussian elimination is used. Maximum permitted number of nodes adjacent to another node when iterative solvers are used (Table 7.7).
MPL	Number of specified print-times at which detailed information about the pressure head, the water content, flux, temperature, solute concentration, and the soil water, solute and energy balances are printed (Table 9.3).
NCorn	Number of corner nodes of a particular element.
NDr	Number of drains.
NDrD	Maximum permitted number of drains.
NLay	Number of subregions for which separate water balances are being computed (Table 9.2).
NLevel	Number of time levels at which the matrix A and vector B are assembled for solute transport.
NMat	Number of soil materials (Table 9.2).
NMatD	Maximum number of soil materials (Table 7.7).

Table 11.3. (continued)

NObs	Number of observation nodes for which the pressure head, the water content, temperature and concentration are printed at each time level
NObsD	Maximum number of observation nodes for which the pressure head, the water content, temperature and concentration are printed at each time level
NPar	Number of unsaturated soil hydraulic parameters specified for each material (Table 9.2).
NS	Number of solutes (Table 9.9).
NSD	Maximum number of solutes (Table 7.7).
NSeep	Number of seepage faces expected to develop (Table 9.5).
NSeepD	Maximum number of seepage faces (Table 7.7).
NTab	Number of entries in the internally generated tables of the hydraulic properties (see Section 5.3.11).
NTabD	Maximum number of entries in the internally generated tables of the hydraulic properties (Table 7.7).
NumBP	Number of boundary nodes for which $Kode(n) \neq 0$ (Table 9.9).
NumBPD	Maximum number of boundary nodes for which $Kode(n) \neq 0$ (Table 7.7).
NumEl	Number of elements (quadrilaterals and/or triangles) (Table 9.9).
NumElD	Maximum number of elements in finite element mesh (Table 7.7).
NumKD	Maximum number of available code number values (Table 7.7).
NumNP	Number of nodal points (Table 9.9).
NumNPD	Maximum number of nodes in finite element mesh (Table 7.7).
NumSEl	Number of subelements (triangles).
NumSPD	Maximum number of nodes along a seepage face (Table 7.7).
NUS	Number of corner nodes of a particular element (=*NCorn*).
PLevel	Print time-level (current print-time number).
TLevel	Time-level (current time-step number) (Table 10.4).

Table 11.4. List of significant real variables.

AE	Area of a triangular element, $[L^2]$ or $[L^3]^\dagger$.
Alf	1-*Epsi*, where *Epsi* is a temporal weighing coefficient [-].
Alfa	Parameter in the soil water retention function $[L^{-1}]$ (see Section 2.3).
Angle	Angle in degrees between the principal direction of K_1^A and the x-axis of the global coordinate system assigned to each element (Table 9.10).
Aqh	Parameter A_{qh} in equation (7.1) $[LT^{-1}]$ (Table 9.12).
AreaR	Area of the domain occupied by the root zone, $[L^2]$ or $[L^3]^\dagger$.
AT	Temperature scaling factor α_h^* associated with the pressure head [-].
ATot	Area of the entire flow domain, $[L^2]$ or $[L^3]^\dagger$ (*Area* in Table 10.6).
Bqh	Parameter B_{qh} in equation (7.1) $[L^{-1}]$ (Table 9.12).
BT	Temperature scaling factor α_K^* associated with the hydraulic conductivity [-].
cBalR	Relative error in the solute mass balance of the entire flow domain [%] (see equation (6.32)) (*CncBalR* in Table 10.6).
cBalT	Absolute error in the solute mass balance of the entire flow domain, $[ML^{-1}]$ or $[M]^\dagger$ (see equation (6.32)) (*CncBalT* in Table 10.6).
cBnd	Value of the boundary condition for solute transport $[ML^{-1}]$.
cE	Average concentration of an element $[ML^{-3}]$.
Change	Inflow/Outflow to/from the flow domain, $[L^2T^{-1}]$ or $[L^3T^{-1}]^\dagger$ (*InFlow* in Table 10.6).
cMid	Arithmetic mean of the concentration at the old and new time level $[ML^{-3}]$.
cNewE	Amount of solute in a particular element at the new time-level, $[ML^{-1}]$ or $[M]^\dagger$.
ConA1	First principal component, K_1^A, of the dimensionless anisotropy tensor $\mathbf{K}^A$ [-] assigned to each element (Table 9.10).
ConA2	Second principal component, K_2^A [-] (Table 9.10).
Courant	Maximum local Courant number [-] (Table 10.4).
cSink	Concentration of the sink term $[ML^{-1}]$.
cTolA	Maximum desired absolute change in the value of the concentration, c $[ML^{-3}]$, between two successive iterations for nonlinear adsorption (Table 9.7).
cTolR	Maximum desired relative change in the value of the concentration, c $[ML^{-3}]$, between two successive iterations for nonlinear adsorption (Table 9.7).
CumQrR	Cumulative total potential transpiration from the entire flow domain, $[L^2]$ or $[L^3]^\dagger$ (*CumQRP* in Tables 10.3 and 10.7).
CumQrT	Cumulative total potential flux across the atmospheric boundary, $[L^2]$ or $[L^3]^\dagger$ (*CumQAP* in Tables 10.3 and 10.7).
CumQvR	Cumulative total actual transpiration from the entire flow domain, $[L^2]$ or $[L^3]^\dagger$ (*CumQR* in Tables 10.3 and 10.7).

Table 11.4. (continued)

CumR	Amount of solute removed from the entire flow domain by root water uptake during one time step, [ML^{-1}] or [M]†.
Cum0	Amount of solute removed from the entire flow domain by zero-order reactions during one time step, [ML^{-1}] or [M]†.
Cum1	Amount of solute removed from the entire flow domain by first-order reactions during one time step, [ML^{-1}] or [M]†.
DeltC	Sum of the absolute changes in concentrations as summed over all elements, [ML^{-1}] or [M]† (see equation (6.32)).
DeltW	Sum of the absolute changes in water content as summed over all elements, [L^2] or [L^3]† (see equation (5.25)).
dHenry	Time change of the equilibrium distribution constant, k_g, within one time step [T^{-1}].
dlh	Spacing (logarithmic scale) between consecutive pressure heads in the internally generated tables of the hydraulic properties [-] (see equation (5.28)).
dMul	Dimensionless number by which Δt is multiplied if the number of iterations is less than or equal to 3 [-] (Table 9.3).
dMul2	Dimensionless number by which Δt is multiplied if the number of iterations is greater than or equal to 7 [-] (Table 9.3).
dt	Time increment, Δt [T] (Table 9.3).
dtMax	Maximum permitted time increment, Δt_{max} [T] (Table 9.3).
dtMaxC	Maximum permitted time increment, Δt_{max} for solute transport [T] (see equation (6.34)).
dtMin	Minimum permitted time increment, Δt_{min} [T] (Table 9.3).
dtOld	Old time increment [T].
dtOpt	Optimal time increment [T].
EI	Potential surface flux per unit atmospheric boundary [LT^{-1}] (=*rTop*).
Epsi	Temporal weighing coefficient [-] (Table 9.7).
EpsH	Absolute change in the nodal pressure head between two successive iterations [L].
EpsTh	Absolute change in the nodal water content between two successive iterations [-].
fExp	Adsorption isotherm coefficient, β [-] (Table 9.7).
Frac	Dimensionless fraction of the adsorption sites classified as Type-1, e.i. sites with instantaneous sorption (Table 9.7).
GamG	First-order rate constant for gaseous phase, μ_g [T^{-1}] (Table 9.7).
GamG1	Rate constant, μ_g [T^{-1}], representing first-order decay for the first solute and zero-order production for the second solute in the gaseous phase (Table 9.7).
GamL	First-order rate constant for dissolved phase, μ_w [T^{-1}] (Table 9.7).
GamL1	Rate constant, μ_w [T^{-1}], representing first-order decay for the first solute and zero-order production for the second solute in the dissolved phase (Table 9.7).

Table 11.4. (continued)

GamS	First-order rate constant for the solid phase concentration, μ_s [T^{-1}] (Table 9.7).
*GamS*1	Rate constant, μ_s [T^{-1}], representing first-order decay for the first solute and zero-order production for the second solute in the solid phase (Table 9.7).
GWL	Time-dependent prescribed head boundary condition [L] for nodes indicated by $Kode(n) = +3$ (Table 9.12).
GWL0L	Parameter in equation (7.1) [L] (Table 9.12).
hCritA	Minimum allowed pressure head at the soil surface [L] (Table 9.12).
hCritS	Maximum allowed pressure head at the soil surface [L] (Table 9.12).
hE	Mean element value of the pressure head [L].
Henry	Equilibrium distribution constant between liquid and gas phase, k_g [-] (Table 9.7).
hMeanG	Mean value of the pressure head calculated over a set of nodes for which $Kode(n) = \pm 3$ [L] (*hKode*3 in Tables 10.1 and 10.7).
hMeanR	Mean value of the pressure head within the root zone [L] (*hRoot* in Table 10.1 and 10.7).
hMeanT	Mean value of the pressure head calculated over a set of nodes for which $Kode(n) = \pm 4$ [L] (*hAtm* in Tables 10.1 and 10.7).
*hTab*1	Lower limit [L] of the pressure head interval for which tables of hydraulic properties is generated internally for each material (*ha* in Table 9.2).
hTabN	Upper limit [L] of the pressure head interval for which tables of hydraulic properties is generated internally for each material (*hb* in Table 9.2).
hTot	Mean pressure head in the entire flow domain [L] (*hMean* in Table 10.6).
Kk	Unsaturated hydraulic conductivity corresponding to θ_k [LT^{-1}] (see Section 2.3) (Table 9.2).
Ks	Saturated hydraulic conductivity [LT^{-1}] (Table 9.2).
m	Parameter in the soil water retention function [-] (see Section 2.3) (Table 9.2).
n	Parameter in the soil water retention function [-] (see Section 2.3) (Table 9.2).
Omega	Mass transfer coefficient for the nonequilibrium adsorption, ω [T^{-1}] (Table 9.7).
Peclet	Maximum local Peclet number [-] (Table 10.4).
PeCr	Stability criteria (see Section 6.3.6) (Table 9.7).
Prec	Precipitation [LT^{-1}] (Table 9.12).
P0	Value of the pressure head [L], h_1, below which roots start to extract water from the soil (Table 9.4).
P2H	Value of the limiting pressure head [L], h_3, below which the roots cannot extract water at the maximum rate (assuming a potential transpiration rate of *r2P*) (Table 9.4).
P2L	As above, but for a potential transpiration rate of *r2L* (Table 9.4).
P3	Value of the pressure head [L], h_4, below which root water uptake ceases (usually equal to the wilting point) (Table 9.4).

Table 11.4. (continued)

Qa	Parameter in the soil water retention function [-] (see Section 2.3) (Table 9.2).
Qk	Volumetric water content corresponding to K_k [-] (see Section 2.3) (Table 9.2).
Qm	Parameter in the soil water retention function [-] (see Section 2.3) (Table 9.2).
Qr	Residual soil water content [-] (Table 9.2).
Qs	Saturated soil water content [-] (Table 9.2).
R	Universal gas constant [$ML^2T^{-2}K^{-1}M^{-1}$] (8.314 kg m^2 $s^{-2}K^{-1}mol^{-1}$).
rLen	Width of soil surface associated with transpiration, [L] or [L^2]† (Table 9.11).
ρ	Bulk density of material *M* [ML^{-3}].
RootCh	Amount of solute removed from a particular subelement during one time step by root water uptake, [ML^{-1}] or [M]†.
rQWL	Time-dependent prescribed flux boundary condition [LT^{-1}] for nodes were *Kode*(*n*) = -3 (Table 9.12).
rRoot	Potential transpiration rate [LT^{-1}] (Table 9.12).
rSoil	Potential evaporation rate [LT^{-1}] (Table 9.12).
rTop	Potential surface flux per unit atmospheric boundary [LT^{-1}] (*rAtm* in Table 10.2).
r2H	Potential transpiration rate [LT^{-1}] (see Table 9.4).
r2L	Potential transpiration rate [LT^{-1}] (see Table 9.4).
t	Time, *t*, at current time-level [T].
tAtm	Time for which the *i*-th data record is provided [T] (Table 9.12).
TauG	Tortuosity factor in the gas phase [-].
TauW	Tortuosity factor in the liquid phase [-].
TE	Average temperature of an element [K].
tFix	Next time resulting from time discretizations 2 and 3 [T] (see Section 5.3.3).
tInit	Starting time of the simulation [T] (Table 9.12).
tMax	Maximum duration of the simulation [T].
TNewE	Amount of heat in a particular element, [MLT^{-2}] or [ML^2T^{-2}]†.
tOld	Previous time-level [T].
TolH	Maximum desired absolute change in the value of the pressure head, *h* [L], between two successive iterations during a particular time step (Table 9.1).
TolTh	Maximum desired absolute change in the value of the water content, θ [-], between two successive iterations during a particular time step (Table 9.1).
tPeriod	Time interval for the completion of one temperature cycle [T].
tPulse	Time duration of the concentration pulse [T] (Table 9.7).

Table 11.4. (continued)

Tr	Reference temperature 293.15 K (20°C).
TTot	Average temperature in the entire flow domain [K] (Table 10.6).
TVol	Amount of heat in the entire flow domain, [MLT^{-2}] or [ML^2T^{-2}]† (Table 10.6).
Vabs	Absolute value of the nodal Darcy fluid flux density [LT^{-1}].
vMeanR	Actual transpiration rate [LT^{-1}] (*vRoot* in Table 10.2).
vNewE	Volume of water in a particular element at the new time-level, [L^2] or [L^3]†.
vOldE	Volume of water in a particular element at the old time-level, [L^2] or [L^3]†.
Volume	Volume of water in the entire flow domain, [L^2] or [L^3]† (Table 10.6).
wBalR	Relative error in the water mass balance in the entire flow domain [%] (see equation (5.25)).
wBalT	Absolute error in the water mass balance in the entire flow domain , [L^2] or [L^3]† (see equation (5.24)).
wCumA	Sum of the absolute values of all fluxes across the flow boundaries, including those resulting from sources and sinks in the region, [L^2] or [L^3]† (see equation (5.25)).
wCumT	Sum of all cumulative fluxes across the flow boundaries, including those resulting from sources and sinks in the region, [L^2] or [L^3]† (see equation (5.24)).
wVolI	Initial volume of water in the flow domain, [L^2] or [L^3]†.
xKs	Adsorption isotherm coefficient, k_s [L^3M^{-1}] (Table 9.7).
xNu	Adsorption isotherm coefficient, η [L^3M^{-1}] (Table 9.7).
xMuG	Zero-order rate constant for the gaseous phase concentration, γ_g [$ML^{-3}T^{-1}$] (Table 9.7).
xMuL	Zero-order rate constant for the liquid phase concentration, γ_w [$ML^{-3}T^{-1}$] (Table 9.7).
xMul	Parameter which depends on the type of flow system being analyzed, [-] or [L]† (see equations (5.11) and (5.12)).
xMuS	Zero-order rate constant for the solid phase concentration, γ_s [T^{-1}] (Table 9.7).

† for plane and axisymmetric flow, respectively

Table 11.5. List of significant logical variables.

AtmInf	Logical variable indicating whether or not the input file ATMOSPH.IN is provided (Table 9.1).
CheckF	Logical variable indicating whether or not the grid input data are to be printed for checking (Table 9.1).
DrainF	Logical variable indicating whether drains are, or are not, present in the transport domain (Table 9.1); if drains are present, they are represented by an electrical resistance network analog.
Explic	Logical variable indicating whether an explicit or implicit scheme was used for solving the water flow equation.
FluxF	Logical variable indicating whether or not detailed flux information is to be printed (Table 9.1).
FreeD	Logical variable indicating whether a unit hydraulic gradient (free drainage) is, or is not, invoked at the bottom of the transport domain (Table 9.1).
ItCrit	Logical variable indicating whether or not convergence was achieved.
lArtD	Logical variable indicating whether or not an artificial dispersion is to be added in order to satisfy the stability criteria *PeCr* (see Section 6.3.6).
lChem	Logical variable indicating whether or not the solute transport equation is to be solved (Table 9.1).
lConst	Logical variable indicating whether or not there is a constant number of nodes at any transverse line.
lConv	Logical variable indicating whether or not convergence was achieved in case of nonlinear or non-equilibrium adsorption (Table 9.1).
lEquil	Logical variable indicating whether equilibrium or non-equilibrium adsorption is considered.
lLinear	Logical variable indicating whether a linear or nonlinear adsorption is considered.
lOrt	Logical variable indicating whether indirect iterative methods (the conjugate gradient method for symmetric matrices or the ORTHOMIN method for asymmetric matrices) or direct methods (Gaussian elimination for banded matrices) are used to solve the system of linear equations.
lTDep	Logical variable indicating whether or not the solute transport properties are considered to be temperature dependent.
lTemp	Logical variable indicating whether or not the heat transport equation is to be solved (Table 9.1).
lUpW	Logical variable indicating if upstream weighing or the standard Galerkin formulation is to be used (Table 9.7).
lWat	Logical variable indicating if steady-state or transient water flow is to be considered (Table 9.1).
lWDep	Logical variable indicating whether or not the soil hydraulic properties are considered to be temperature dependent.
qGWLF	Logical variable indicating whether or not the discharge-groundwater level relationship is used as bottom boundary condition (Table 9.12).

Table 11.5. (continued)

SeepF	Logical variable indicating whether or not a seepage face is to be expected (Table 9.1).
ShortF	Logical variable indicating whether or not the printing of time-level information is to be suppressed on each time level (Table 9.1).
SinkF	Logical variable indicating whether or not plant water uptake will take place (Table 9.12).

Table 11.6. List of significant arrays.

A(MBandD,NumNPD)	Coefficient matrix.
Ac(NumNPD)	Nodal values of the product θR [-].
Area(10)	Areas of the specified subregions, [L^2] or [L^3]† (Table 10.6).
Axz(NumNPD)	Nodal values of the dimensionless scaling factor α_h associated with the pressure head [-] (Table 9.9).
B(NumNPD)	Coefficient vector.
Beta(NumNPD)	Nodal values of the normalized rootwater uptake distribution, [L^{-2}] or [L^3]† (Table 9.9).
Bxz(NumNPD)	Nodal value of the scaling factor α_K associated with the saturated hydraulic conductivity [-] (Table 9.9).
Cap(NumNPD)	Nodal values of the soil water hydraulic capacity [L^{-1}].
CapTab(NTabD,NMatD)	Internal table of the soil water hydraulic capacity [L^{-1}].
cBound(NSD,9)	Values of the time independent concentration boundary condition [ML^{-3}] (Table 9.7).
cCumA(NSD)	Sum of the absolute values of all cumulative solute fluxes across the flow boundaries, including those resulting from sources and sinks in the flow domain, [ML^{-1}] or [M]† (see equation (6.32)).
cCumT(NSD)	Sum of all cumulative solute fluxes across the boundaries, including those resulting from sources and sinks in the flow domain, [ML^{-1}] or [M]† (see right hand side of equation (6.31)).
ChemS(NSD,NumKD)	Cumulative boundary solute fluxes, [ML^{-1}] or [M]† (Table 10.5).
*ChPar(NSD*16+4,NMatD)*	Parameters which describe the solute transport properties of the porous media (Table 9.7).
cht(NSD)	Time-dependent concentration for the first-type boundary condition assigned to nodes for which *Kode*(n) = +3 [ML^{-3}] (Table 9.12).
cMean(8,10)	Mean concentrations of specified subregions [ML^{-3}] (Table 10.6).
cNew(NumNPD)	Nodal values of the concentration at the new time level [ML^{-3}].
Con(NumNPD)	Nodal values of the hydraulic conductivity [LT^{-1}].
ConO(NumNPD)	Nodal values of the hydraulic conductivity at old time level [LT^{-1}].
ConAxx(NumElD)	Nodal values of the component K_{xx}^A of the anisotropy tensor $\mathbf{K}^A$ [-].
ConAxz(NumElD)	Nodal values of the component K_{xz}^A of the anisotropy tensor $\mathbf{K}^A$ [-].
ConAzz(NumElD)	Nodal values of the component K_{zz}^A of the anisotropy tensor $\mathbf{K}^A$ [-].
Conc(NSD,NumNPD)	Nodal values of the concentration [ML^{-3}] (Table 9.9).
ConSat(NMatD)	Saturated hydraulic conductivities of the material [LT^{-1}].
ConSub(8,10)	Amounts of solute in the specified subregions, [ML^{-1}] or [M]† (Table 10.6).
ConTab(NTabD,NMatD)	Internal table of the hydraulic conductivity [LT^{-1}].

Table 11.6. (continued)

ConVol(8)	Amount of solute in the entire flow domain, [ML^{-1}] or [M]† (*ConVol* in Table 10.6).
cPrec(*NSD*)	Solute concentration of rainfall water [ML^{-3}] (Table 9.12).
cPrevO(*NumNPD*)	Nodal values of the concentration of the previous solute in the decay chain at the old time-level [ML^{-3}].
crt(*NSD*)	Time-dependent concentration of the drainage flux, or some other time-dependent prescribed flux for nodes were *Kode*(n) = -3 [ML^{-3}] (Table 9.12).
cTemp(*NumNPD*)	Nodal values of the concentration at the previous iteration [ML^{-3}].
cTot(8)	Mean concentration in the flow domain [ML^{-3}] (*cMean* in Table 10.6).
*CumCh*0(*NSD*)	Cumulative amount of solute removed from the entire flow domain by zero-order reactions, [ML^{-1}] or [M]† (Table 10.5).
*CumCh*1(*NSD*)	Cumulative amount of solute removed from the entire flow domain by first-order reactions, [ML^{-1}] or [M]† (Table 10.5).
CumChR(*NSD*)	Cumulative amount of solute removed from the entire flow domain by root water uptake, [ML^{-1}] or [M]† (Table 10.5).
CumQ(*NumKD*)	Cumulative boundary fluxes, [L^2] or [L^3]† (Table 10.3).
cVolI(*NSD*)	Initial amount of solute in the entire flow domain, [ML^{-1}] or [M]†.
Dispxx(*NumNPD*)	Nodal values of the component D_{xx} of the dispersion tensor [L^2T^{-1}].
Dispxz(*NumNPD*)	Nodal values of the component D_{xz} of the dispersion tensor [L^2T^{-1}].
Dispzz(*NumNPD*)	Nodal values of the component D_{zz} of the dispersion tensor [L^2T^{-1}].
DS(*NumNPD*)	Vector $\{D\}$ in the global matrix equation for water flow, [L^2T^{-1}] or [L^3T^{-1}]† (see equation (5.9)); also used for the diagonal of the coefficient matrix $[Q]$ in the global matrix equation for solute transport, [L^2] or [L^3]† (see equation (6.5)).
Dxz(*NumNPD*)	Nodal values of the scaling factor α_θ associated with the water content (Table 9.9).
E(3,3)	Element contributions to the global matrix A for water flow [L^2] (see equation (5.5)).
EfDim(2,*NDr*)	Effective diameter of drains and side lengths of the finite element mesh representing the drain (Table 9.6).
F(*NumNPD*)	Diagonal of the coefficient matrix $[F]$ in the global matrix equation for water flow, [L^2] or [L^3]† (see equation (5.7)).
Fc(*NumNPD*)	Nodal values of the part of the parameter F (representing first-order reactions) [T^{-1}] (see equation (3.13)).
*Fc*1(*NumNPD*)	Nodal values of the parameter F [T^{-1}] (see equation (3.13)).
Gc(*NumNPD*)	Nodal values of the part of the parameter G (representing zero-order reactions) [$ML^{-3}T^{-1}$] (see equation (3.8), (3.14)).
*Gc*1(*NumNPD*)	Nodal values of the parameter G [$ML^{-3}T^{-1}$] (see equation (3.8), (3.14)).
hMean(10)	Mean values of the pressure head in specified subregions [L] (Table 10.6).
hMean(*NumKD*)	Mean values of the pressure head along a certain type of boundary [L] (Table 10.6).

Table 11.6. (continued)

hNew(NumNPD)	Nodal values of the pressure head [L] at the new time-level (Table 9.9).
hOld(NumNPD)	Nodal values of the pressure head [L] at the old time-level.
hSat(NMatD)	Air-entry values for each material [L].
hTab(NTabD)	Internal table of the pressure head [L].
hTemp(NumNPD)	Nodal values of the pressure head [L] at the previous iteration.
IU(13)	Vector which contains identification numbers of output files.
KElDr(NDr, NElD)	Global numbers of elements surrounding a particular drain (Table 9.6).
KodCB(NumBPD)	Codes which identify the type of invoked boundary conditions, and refer to the vector *cBound* for time-independent solute transport boundary conditions (Table 9.7).
Kode(NumNPD)	Codes which specify the type of invoked boundary conditions, (Table 9.9).
KodTB(NumBPD)	Codes which identify the type of invoked boundary conditions, and refer to the vector *TBound* for time-independent heat transport boundary conditions (Table 9.8).
KX(NumElD,4)	Global nodal numbers of element corner nodes (Table 9.10).
KXB(NumBPD)	Global nodal numbers of sequentially numbered boundary nodes for which $Kode(n) \neq 0$ (Table 9.11).
LayNum(NumElD)	Subregion numbers assigned to each element (Table 9.10).
ListNE(NumNPD)	Number of subelements adjacent to a particular node.
MatNum(NumNPD)	Indices for material whose hydraulic and transport properties are assigned to a particular node (Table 9.9).
ND(NDr)	Global number of a drain (Table 9.6).
NElD(NDr)	Number of elements surrounding a drain (Table 9.6).
Node(NObsD)	Observation nodes for which the pressure head, the water content, temperature and concentration are printed at each time level.
NP(NSeepD,NumSPD)	Sequential global numbers of nodes on the seepage face (Table 9.5).
NSP(NSeepD)	Numbers of nodes on seepage face (Table 9.5).
Par(10,*NMatD*)	Parameters which describe the hydraulic properties of the medium (Table 9.2).
POptm(NMatD)	Values of the pressure head [L], h_2, below which roots start to extract water at the maximum possible rate (Table 9.4).
Q(NumNPD)	Nodal values of the recharge/discharge rate, $[L^2T^{-1}]$ or $[L^3T^{-1}]^\dagger$ (Table 9.9).
Qc(NSD,NumNPD)	Nodal values of solute fluxes, $[ML^{-1}T^{-1}]$ or $[MT^{-1}]^\dagger$.
Sink(NumNPD)	Nodal values of the sink term $[T^{-1}]$ (see equation (2.3)).
SMean(NumKD)	Total solute fluxes, $[ML^{-1}T^{-1}]$ or $[MT^{-1}]^\dagger$ (Table 10.5).
SolIn(NumElD)	Element values of the initial amount of solute, $[ML^{-1}]$ or $[M]^\dagger$ (Table 10.6).

Table 11.6. (continued)

Sorb(NSD,NumNPD)	Nodal values of the sorbed concentration for type-2 sorption sites [-] (Table 9.9).
SorbN(NumNPD)	Nodal values of the sorbed concentration for type-2 sorption sites at the last iteration [-] (Table 9.9).
SubCha(10)	Inflow/outflow to/from specified subregions, $[L^2T^{-1}]$ or $[L^3T^{-1}]^\dagger$ (Table 10.6).
SubT(10)	Amount of heat in specified subregions, $[MLT^{-2}]$ or $[ML^2T^{-2}]^\dagger$ (Table 10.6).
SubVol(10)	Volume of water in specified subregions, $[L^2]$ or $[L^3]^\dagger$ (Table 10.6).
SWidth(NumKD)	Length of a boundary associated with a certain type of boundary condition, [L] or $[L^2]^\dagger$.
TBound(6)	Values of the time-independent temperature boundary condition [K] (Table 9.8).
*TDep(NSD*16+4)*	Activation energy for transport and chemical parameters $[ML^2T^{-2}M^{-1}]$ (see Section 3.4).
TempN(NumNPD)	Nodal values of the temperature at the new time level [K].
TempO(NumNPD)	Nodal values of the temperature at the old time level [K].
TheTab(NTabD,NMatD)	Internal table of the soil water content [-].
ThNew(NumNPD)	Nodal values of the water content at the new time level [-].
ThOld(NumNPD)	Nodal values of the water content at the old time level [-].
thr(NMatD)	Residual water contents for specified materials [-].
thSat(NMatD)	Saturated water contents for specified materials [-].
TMean(10)	Average temperature in a specified subregion [K].
TPar(10,*NMatD*)	Parameters which describe the heat transport properties of the porous media (Table 9.8).
TPrint(MPL)	Specified print-times [T] (Table 9.3).
vMean(NumKD)	Values of boundary fluxes across a certain type of boundary, $[L^2T^{-1}]$ or $[L^3T^{-1}]^\dagger$.
VxN(NumNPD)	Nodal values of the x-component of the Darcian velocity vector at the new time level $[LT^{-1}]$.
VxO(NumNPD)	Nodal values of the x-component of the Darcian velocity vector at the old time level $[LT^{-1}]$.
VzN(NumNPD)	Nodal values of the z-component of the Darcian velocity vector at the new time level $[LT^{-1}]$.
VzO(NumNPD)	Nodal values of the z-component of the Darcian velocity vector at the old time level $[LT^{-1}]$.
WatIn(NumElD)	Element values of the initial volume of water, $[L^2]$ or $[L^3]^\dagger$.
WeTab(3,2**NumElD*)	Weighing factors associated with the sides of subelements [-].
Width(NumBPD)	Width of the boundary associated with boundary nodes, $[L^2]$ or $[L^3]^\dagger$ (Table 9.11).

Table 11.6. (continued)

x(*NumNPD*)	*x*-coordinates [L] of the nodal points (Table 9.9).
y(*NumNPD*)	*y* or *z*-coordinates [L] of the nodal points (Table 9.9).

† for plane and axisymmetric flow, respectively

12. REFERENCES

Alexander, M., and K. M. Scow. 1989. Kinetics of biodegradation in soil, In *Reactions and Movement of Organic Chemicals in Soils*, edited by B. L. Sawhney and K. Brown, Spec. Publ. No. 22, 243-270, Soil Science Society of America, Madison, WI.

Bear, J. 1972. *Dynamics of Fluid in Porous Media*. Elsevier, New York, NY.

Behie, A., and P. Forsyth, Jr. 1983. Comparison of fast iterative methods for symmetric systems. *IMA J. of Numerical Analysis, 3,* 41-63.

Belmans, C., J. G. Wesseling and R. A. Feddes. 1983. Simulation model of the water balance of a cropped soil: SWATRE, *J. Hydrol., 63*, 271- 286.

Bromilow, R. H., and M. Leistra. 1980. Measured and simulated behavior of aldicarb and its oxidation products in fallow soils, *Pestic. Sci., 11*(4), 389-395.

Castro, C. L., and D. E. Rolston. 1977. Organic phosphate transport and hydrolysis in soil: theoretical and experimental evaluation, *Soil Sci. Soc. Am. J., 41*(6), 1085-1092.

Celia, M. A., and E. T. Bououtas, R. L. Zarba. 1990. A general mass-conservative numerical solution for the unsaturated flow equation, *Water Resour. Res., 26*, 1483-1496.

Chiou, C. T. 1989. Theoretical consideration of the partition uptake of nonionic organic compounds by soil organic matter, In *Reactions and Movement of Organic Chemicals in Soils*, edited by B. L. Sawhney and K. Brown, Spec. Publ. Number 22, 1-30, Soil Science Society of America, Madison, WI.

Chung S.-O., and R. Horton. 1987. Soil heat and water flow with a partial surface mulch, *Water Resour. Res., 23*(12), 2175-2186.

Cho, C. M. 1971. Convective transport of ammonium with nitrification in soil, *Can. Jour. Soil Sci., 51*(3), 339-350.

Christie, L. D., D. F. Griffiths, A. R. Mitchell, and O. C. Zienkiewicz. 1976. Finite element methods for second order differential equations with significant first derivatives, *Int. J. Num. Methods in Engineering, 10*, 1389-1396.

Císlerová, M. 1987. Comparison of simulated water balance for ordinary and scaled soil hydraulic characteristics, *Publ. No. 82*, Dept. of Hydraulics and Catchment Hydrology, Agricultural Univ., Wageningen, The Netherlands.

Cleary, R. W., and M. J. Ungs. 1978. Groundwater pollution and hydrology, Mathematical models and computer programs, *Research Rep. No. 78-WR-15*, Water Resour. Program, Princeton Univ. Princeton, NJ.

Constantz, J. 1982. Temperature dependence of unsaturated hydraulic conductivity of two soils. *Soil Sci. Soc. Am. J., 46*(3), 466-470.

Davis, L. A., and S. P. Neuman. 1983. Documentation and user's guide: UNSAT2 - Variably saturated flow model, *Final Rep., WWL/TM-1791-1,* Water, Waste & Land, Inc., Ft. Collins, CO.

de Marsily, G. 1986. *Quantitative Hydrogeology*, Academic Press, London.

de Vries, D. A. 1963. The thermal properties of soils, In *Physics of Plant Environment*, edited by R. W. van Wijk, pp. 210-235, North Holland, Amsterdam.

Feddes, R. A., E. Bresler, and S. P. Neuman. 1974. Field test of a modified numerical model for water uptake by root systems, *Water Resour. Res., 10*(6), 1199-1206.

Feddes, R. A., P. J. Kowalik, and H. Zaradny. 1978. *Simulation of Field Water Use and Crop Yield*, John Wiley & Sons, New York, NY.

Fipps, G., R. W. Skaggs, and J. L. Nieber. 1986. Drains as a boundary condition in finite elements, *Water Resour. Res., 22*(11), 1613-1621.

Glotfelty, D. E., and C. J. Schomburg. 1989. Volatilization of pesticides from soil, In *Reactions and Movement of Organic Chemicals in Soils*, edited by B. L. Sawhney and K. Brown, Spec. Publ. Number 22, 181-208, Soil Science Society of America, Madison, WI.

Gureghian, A. B. 1981. A two-dimensional finite-element solution for the simultaneous transport of water and multi-solutes through a nonhomogeneous aquifer under transient saturated-unsaturated flow conditions, *Sci. Total Environ., 21*, 329-337.

Gureghian, A. B., and G. Jansen. 1983. LAYFLO: A one-dimensional semianalytical model for the migration of a three-member decay chain in a multilayered geologic medium, *Tech. Rep. ONWI-466*, Office of Nuclear Waste Isolation, Battelle Memorial Institute, Columbus, OH.

Harada, M., P. L. Chambre, M. Foglia, K. Higashi, F. Iwamoto, D. Leung, T. H. Pigford, and D. Ting. 1980. Migration of radionuclides through sorbing media, analytical solutions - I, *Rep. no. LBL-10500 (UC-11)*, Lawrence Berkeley Laboratory, Univ. of California, Berkeley, CA.

Higashi, K., and T. H. Pigford. 1980. Analytical models for migration of radionuclides in geologic sorbing media, *J. Nucl. Sci. and Techn., 7*(9), 700-709.

Hopmans, J. W., and J. N. M. Stricker. 1989. Stochastic analysis of soil water regime in a watershed, *J. Hydrol., 105*, 57-84.

Huyakorn, P. S., and G. F. Pinder. 1983. *Computational Methods in Subsurface Flow*, Academic Press, London, United Kingdom.

Javandel, I., Ch. Doughty, Chin-Fu Tsang. 1984. *Groundwater Transport: Handbook of Mathematical Models*, Water Resour. Monograph No. 10, Am. Geophys. Union, Washington, D.C.

Jury, W. A., W. F. Spencer, and W. J. Farmer. 1983. Behavior assessment model for trace organics in soil, I. Model description, *J. Environ. Qual., 12*, 558-564.

Kirkham, D. 1949. Flow of ponded water into drain tubes in soil overlying an impervious layer, *Trans. Amer. Geoph. Union, 30*(3), 369-385.

Kirkham, D., and W. L. Powers. 1972. *Advanced Soil Physics*, John Wiley & Sons, New York, NY.

Kool, J. B., M. Th. van Genuchten. 1991. HYDRUS - One-dimensional variably saturated flow and transport model, including hysteresis and root water uptake, Version 3.3, Research Report No. 124, U. S. Salinity Laboratory, USDA, ARS, Riverside, CA.

Leij, F. J., T. H. Skaggs, and M. Th. van Genuchten. 1991. Analytical solutions for solute transport in three-dimensional semi-infinite porous media, *Water Resour. Res., 27*(10), 2719-2733.

Leij, F. J., and S. A. Bradford. 1994. 3DADE: A computer program for evaluating three-dimensional equilibrium solute transport in porous media, *Research Report No. 134*, U. S. Salinity Laboratory, USDA, ARS, Riverside, CA.

Lester, D. H., G. Jansen, and H. C. Burkholder. 1975. Migration of radionuclide chains through an adsorbing medium, In: *Adsorption and Ion Exchange,* Am. Inst. Chem. Eng., Symp. Series no. 152, 71, 202-213.

Letniowski, F. W. 1989. An overview of preconditioned iterative methods for sparse matrix equations. *Research Report CS-89-26,* Faculty of Mathematics, Univ. of Waterloo, Waterloo, Ontario, Canada.

Luckner, L., M. Th. van Genuchten, and D. R. Nielsen. 1989. A consistent set of parametric models for the two-phase flow of immiscible fluids in the subsurface. *Water Resour. Res., 25*(10), 2187-2193.

Lynch, D. 1984. Mass conservation in finite element groundwater models. *Adv. Water Resour., 7*, 67-75.

McCord, J. T. 1991. Application of second-type boundaries in unsaturated flow modeling. *Water Resour. Res., 27*(12), 3257-3260.

Meijerink, J. A. , and H. A. van der Vorst. 1977. An iterative solution method for linear systems of which the coefficient matrix is a symmetric M-matrix. *Math. of Comp., 31*(137), 148-162.

Mendoza, C. A., R. Therrien, and E. A. Sudicky. 1991. *ORTHOFEM User's Guide, Version 1.02.* Waterloo Centre for Groundwater Research, Univ. of Waterloo, Waterloo, Ontario, Canada.

Miller, E. E., and R. D. Miller. 1956. Physical theory for capillary flow phenomena, *J. Appl. Phys., 27*, 324-332.

Millington, R. J., and J. M. Quirk. 1961. Permeability of porous solids, *Trans. Faraday Soc., 57*, 1200-1207.

Misra, C., D. R. Nielsen, J. W. Biggar. 1974. Nitrogen transformations in soil during leaching: I. Theoretical considerations, *Soil Sci. Soc. Am. Proc., 38*(2), 289-293.

Mls, J. 1982. Formulation and solution of fundamental problems of vertical infiltration, *Vodohosp. Čas., 30*, 304-313 (in Czech).

Mohammad, F. S., and R. W. Skaggs. 1983. Drain tube opening effects on drain inflow, *J. Irrig. Drain. Div., Am. Soc. Civ. Eng., 109*(4), 393-404.

Mualem, Y. 1976. A new model for predicting the hydraulic conductivity of unsaturated porous media, *Water Resour. Res., 12*(3), 513-522.

Neuman, S. P. 1972. Finite element computer programs for flow in saturated-unsaturated porous media, *Second Annual Report, Project No. A10-SWC-77*, Hydraulic Engineering Lab., Technion, Haifa, Israel.

Neuman, S. P. 1973. Saturated-unsaturated seepage by finite elements, *J. Hydraul. Div.*, ASCE, 99 (HY12), 2233-2250.

Neuman, S. P., R. A. Feddes, and E. Bresler. 1974. Finite element simulation of flow in saturated-unsaturated soils considering water uptake by plants, *Third Annual Report, Project No. A10-SWC-77*, Hydraulic Engineering Lab., Technion, Haifa, Israel.

Neuman, S. P. 1975. Galerkin approach to saturated-unsaturated flow in porous media, Chapter 10 in *Finite Elements in Fluids, Vol. I, Viscous Flow and Hydrodynamics*, edited by R. H. Gallagher, J. T. Oden, C. Taylor, and O.C. Zienkiewicz, John Wiley & Sons, London, pp. 201-217.

Ou, L. T., P. S. C. Rao, K. S. V. Edvardson, R. E. Jessup, A. G. Hornsby, and R. L. Jones. 1988. Aldicarb degradation in sandy soils from different depths, *Pesticide Sci., 23*, 1-12.

Perrochet, P., and D. Berod. 1993. Stability of the standard Crank-Nicolson-Galerkin scheme applied to the diffusion-convection equation: some new insights, *Water Resour. Res., 29*(9), 3291-3297.

Philip, J. R., and D. A. de Vries. 1957. Moisture movement in porous media under temperature gradients, *Eos Trans. AGU, 38*(2), 222-232.

Pignatello, J. J. 1989. Sorption dynamics of organic compounds in soils and sediments, In *Reactions and Movement of Organic Chemicals in Soils*, edited by B. L. Sawhney and K. Brown, Spec. Publ. Number 22, 45-80, Soil Science Society of America, Madison, WI.

Pinder, G. F., W. G. Gray. 1977. *Finite Element Simulation in Surface and Subsurface Hydrology*, Academic Press, New York, N.Y.

Rogers, V. C. 1978. Migration of radionuclide chains in groundwater, *Nucl. Techn.,* 40(3), 315-320.

Rogers, J. S., J. L. Fouss. 1989. Hydraulic conductivity determination from vertical and horizontal drains in layered soil profiles, *Transaction of the ASAE, 32*(2), 589-595.

Selim, H. M., R. Schulin, H. Flühler. 1987. Transport and ion exchange of calcium and magnesium in an aggregated soil, *Soil Sci. Soc. Am. J., 51*(4), 876-884.

Simmons, C. S., D. R. Nielsen, J. W. Biggar. 1980. Scaling of field-measured soil water properties, *Hilgardia, 47*, 101-122.

Šimůnek, J., T. Vogel and M. Th. van Genuchten. 1992. The SWMS_2D code for simulating water flow and solute transport in two-dimensional variably saturated media, Version 1.1., *Research Report No. 126*, U. S. Salinity Laboratory, USDA, ARS, Riverside, CA.

Šimůnek, J., and D. L. Suarez. 1993a. Modeling of carbon dioxide transport and production in soil: 1. Model development, *Water Resour. Res.*, *29*(2), 487-497.

Šimůnek, J., and D. L. Suarez. 1993b. UNSATCHEM-2D code for simulating two-dimensional variably saturated water flow, heat transport, carbon dioxide production and transport, and multicomponent solute transport with major ion equilibrium and kinetic chemistry, Version 1.1., *Research Report No. 128*, U. S. Salinity Laboratory, USDA, ARS, Riverside, CA.

Šimůnek, J., T. Vogel and M. Th. van Genuchten. 1994. The SWMS_2D code for simulating water flow and solute transport in two-dimensional variably saturated media, Version 1.1., *Research Report No. 132*, U. S. Salinity Laboratory, USDA, ARS, Riverside, CA.

Šír, M., T. Vogel, and M. Číslerová. 1985. Analytical expression of the retention curve and hydraulic conductivity for porous material, *Vodohosp. Čas., 33*(1), 74-85 (in Czech).

Sisson, J. B. 1987. Drainage from layered field soils: Fixed gradient models, *Water Resour. Res., 23*(11), 2071-2075.

Skaggs, R. W., E. J. Monke, and L. F. Huggins. 1970. An approximate method for determining the hydraulic conductivity function of an unsaturated soil, *Techn. Rep. No. 11*, Water Resour. Res. Center, Purdue University, Lafayette, IN.

Sophocleous, M. 1979. Analysis of water and heat flow in unsaturated-saturated porous media, *Water Resour. Res., 15*(5), 1195-1206.

Spencer, W. F. 1991. Volatilization of pesticides from soil: processes and measurement, *Pesticide Res. J., 3*(1), 1-14.

Sposito, G. 1981. *The Thermodynamics of Soil Solutions*. Oxford University Press, New York, NY.

Stumm, W., and J. J. Morgan. 1981. *Aquatic Chemistry: An Introduction Emphasizing Chemical Equilibria in Natural Waters*, John Wiley & Sons, New York, NY.

Sudicky, E. A., and P. S. Huyakorn. 1991. Contaminant migration in imperfectly known heterogeneous groundwater systems, *Review of Geophysics*, Supplement, U. S. National Rep. to Inter. Union of Geodesy and Geophysics 1987-1990, 240-253.

Tillotson, W. R., C. W. Robbins, R. J. Wagenet, R. J. Hanks. 1980. Soil water, solute and plant growth simulation, *Bulletin 502,* Utah Agricultural Experiment Station, 53 p.

Toride, N., F. J. Leij, and M. Th. van Genuchten. 1993. A comprehensive set of analytical solutions for nonequilibrium solute transport with first-order decay and zero-order production, *Water Resour. Res., 29*(7), 2167-2182.

van Genuchten, M. Th. 1976. On the accuracy and efficiency of several numerical schemes for solving the convective-dispersive equation, in *Finite Elements in Water Resources*, edited by W. G. Gray et al., Pentech Press, London, pp. 1.71-1.90.

van Genuchten, M. Th. 1978. Mass transport in saturated-unsaturated media: one-dimensional solutions, *Research Rep. No. 78-WR-11*, Water Resources Program, Princeton Univ., Princeton, NJ.

van Genuchten, M. Th. 1980. A closed-form equation for predicting the hydraulic conductivity of unsaturated soils, *Soil Sci. Soc. Am. J., 44*, 892-898.

van Genuchten, M. Th. 1981. Non-equilibrium transport parameters from miscible displacement experiments. *Research Report No. 119*, U.S. Salinity Laboratory, Riverside, CA.

van Genuchten, M. Th. 1985. Convective-dispersive transport of solutes involved in sequential first-order decay reactions, *Computers & Geosciences, 11*(2), 129-147.

van Genuchten, M. Th., and J. Parker. 1984. Boundary conditions for displacement experiment through short laboratory soil columns, *Soil Sci. Soc. Am. J., 48*, 703-708.

van Genuchten, M. Th., and R. J. Wagenet. 1989. Two-site/two-region models for pesticide transport and degradation: Theoretical development and analytical solutions, *Soil Sci. Soc. Am. J., 53*, 1303-1310.

Vimoke, B. S., and G. S. Taylor. 1962. Simulating water flow in soil with an electric resistance network, *Report No. 41-65*, 51 p., Soil and Water Conserv. Res. Div., U. S. Agric. Res. Serv., Columbus, OH.

Vimoke, B. S., T. D. Tura, T. J. Thiel, and G. S. Taylor. 1963. Improvements in construction and use of resistance networks for studying drainage problems, *Soil Sci. Soc. Am. Proc., 26*(2), 203-207.

Vogel, T. 1987. SWMII - Numerical model of two-dimensional flow in a variably saturated porous medium, *Research Rep. No. 87*, Dept. of Hydraulics and Catchment Hydrology, Agricultural Univ., Wageningen, The Netherlands.

Vogel, T., M. Císlerová. 1988. On the reliability of unsaturated hydraulic conductivity calculated from the moisture retention curve, *Transport in Porous Media, 3*, 1-15.

Vogel, T., M. Císlerová, and J. W. Hopmans. 1991. Porous media with linearly variable hydraulic properties, *Water Resour. Res., 27*(10), 2735-2741.

Wagenet, R. J., J. W. Biggar, and D. R. Nielsen. 1976. Analytical solutions of miscible displacement equations describing the sequential microbiological transformations of urea, ammonium and nitrate, *Research Rep. no 6001,* Dept. of Water Science and Engineering, Univ. California, Davis, CA.

Wagenet R. J., and J. L. Hutson. 1987. LEACHM: Leaching Estimation And CHemistry Model, A process-based model of water and solute movement, transformations, plant uptake and chemical reactions in the unsaturated zone, *Continuum 2*, Dept. of Agronomy, Cornell University, Ithaca, New York, NY.

Wesseling, J. G., and T. Brandyk. 1985. Introduction of the occurrence of high groundwater levels and surface water storage in computer program SWATRE, *Nota 1636*, Institute for Land and Water Management Research (ICW), Wageningen, The Netherlands.

Yeh, G. T., and V. S. Tripathi. 1990. HYDROGEOCHEM: A coupled model of HYDROlogic transport and GEOCHEMical equilibria in reactive multicomponent systems, *Environs Sci. Div., Publ. No. 3170.*, Oak Ridge National Lab., Oak Ridge, TN.

Zienkiewicz, O.C. 1977. *The Finite Element Method*, 3rd ed., McGraw-Hill, London, United Kingdom.

APPENDIX - MESH GENERATOR

To overcome potential problems with the correct definition and numbering of finite elements and their corner nodes in input file GRID.IN, we provided a separate finite element generator, GENER2 which produces the nodes and elements for a quadrilateral domain.

The mesh generator assumes that the initial pressure heads, concentrations and temperatures, as well as the recharge, the material number, the root water uptake distribution, and the scaling factors for the hydraulic property functions are all constant in each horizontal layer. The initial conditions, root distribution, recharge, material number and related parameters should, in general, be given for each horizontal layer. However, a short-cut is possible when two horizontal layers (e.g., n_1 and n_2), not adjacent to each other, are located such that n_2 is greater than n_1+1. The program will automatically generate layers between n_1 and n_2, provided all of the following conditions are met simultaneously: (1) all horizontal layers between layers n_1 and n_2 are spaced at equal intervals, (2) values of the input variables *hNew*(n), *Beta*(n), *Axz*(n), *Bxz*(n), *Dxz*(n), *Temp*(n), and *Conc*(1,n) through *Conc*(*NS*,n) vary linearly between layers n_1 and n_2, and (3) the values of *Kode*(n), $Q(n)$ and *MatNum*(n) are the same for all $n = n_1, n_1+1,..., n_2-1$ (see also Table A.1).

Table A.1 gives a description of an input file for the finite element mesh generator GENER2. The input file GENER2.IN must be placed in directory CHAIN_2D.IN. The resulting file GRID.IN can then be modified using any word- or data-processing software. The input files for example problems 1 through 7 are given in Tables A.2 through A.8. The input files GRID.IN, generated with GENER2 for example problems 1 through 6, can be used directly as input files for CHAIN_2D without further modification. The GRID.IN file for example 7 needs additional modifications involving the boundary conditions.

Table A.1. Input file 'GENER2.IN' for finite element mesh generator.

Record	Type	Variable	Description
1,2	-	-	Comment lines.
3	Logical	*lAxisym*	Set equal to .true. if axisymmetrical flow domain is to be analyzed.
4	-	-	Comment line.
5	Real	*Angle*	Angle in degrees between K_1^A and the x-coordinate axis assigned to all elements.
5	Real	*ConA*1	First principal component, K_1^A, of the dimensionless tensor $\mathbf{K}^A$ which describes the local anisotropy of the hydraulic conductivity assigned to all elements.
5	Real	*ConA*2	Second principal component, K_2^A.
6	-	-	Comment line.
7	Integer	*NS*	Number of solutes in a chain reaction.
7	Logical	*lEquil*	**.true.** if equilibrium or no adsorption is considered for solute transport. **.false.** if nonequilibrium adsorption is considered for at least one solute species. If *lEquil*=**.false.**, then initial values of the sorbed concentration for type-2 sorption sites must be specified.
8	-	-	Comment line.
9	Integer	*NColX*	Number of nodal points in the direction of the horizontal axes, x.
9	Integer	*NLinZ*	Number of nodal points in the direction of the vertical axes, z.
10	-	-	Comment line.
11	Real	$x(1)$	x-coordinate of the left-most node [L].
11	Real	$z(NLinZ)$	z-coordinate of the bottom node [L].
12,13	-	-	Comment lines.
14	Real	$dx(i)$	Array of Δx increments [L], i = 1, 2,..., (*NColX*-1). Input subsequently from left to the right.
15	-	-	Comment lines.
16	Real	$dz(i)$	Array of Δz increments [L], i = 1, 2,..., (*NLinZ*-1). Input subsequently from top to the bottom.
17,18	-	-	Comment lines.
19	Integer	n	Number of the horizontal layer starting at the upper boundary and continuing down to the bottom.
19	Integer	$Kode(n)$	Code specifying the type of boundary condition applied to nodes of a particular horizontal layer n. Permissible values are 0, ±1, ±2, ±3, ±4,..., ±*NumKD* (see Section 8.3).

Table A.1. (continued)

Record	Type	Variable	Description
19	Real	*hOld*(*n*)	Initial value of the pressure head assigned to nodes of a particular horizontal layer *n* [L].
19	Real	*Q*(*n*)	Prescribed recharge/discharge rates assigned to nodes of a horizontal layer *n*, [L^2T^{-1}]. *Q*(*n*) is negative when directed out of the system. When no value for *Q*(*n*) is needed, set *Q*(*n*) equal to zero.
19	Int	*MatNum*(*n*)	Material number assigned to nodes of a particular horizontal layer *n*.
19	Real	*Beta*(*n*)	Value of the water uptake distribution, $b(x,z)$, in the soil root zone assigned to nodes of a particular horizontal layer *n* [L^{-2}]. Set *Beta*(*n*) equal to zero if horizontal layer *n* lies outside the root zone.
19	Real	*Axz*(*n*)	Nodal value of the dimensionless scaling factor α_h associated with the pressure head assigned to nodes of a particular horizontal layer *n* [-].
19	Real	*Bxz*(*n*)	Nodal value of the dimensionless scaling factor α_K associated with the saturated hydraulic conductivity assigned to nodes of a particular horizontal layer *n* [-].
19	Real	*Dxz*(*n*)	Nodal value of the dimensionless scaling factor α_θ associated with the water content assigned to nodes of a particular horizontal layer *n* [-].
19	Real	*Temp*(*n*)	Initial value of the temperature assigned to nodes of a particular horizontal layer *n* [°C].
19	Real	*Conc*(1,*n*)	Initial value of the concentration of the first solute assigned to nodes of a particular horizontal layer *n* [ML^{-3}]. This variable does not need to be specified if *NS* = 0.
19	Real	*Conc*(2,*n*)	Initial value of the concentration of the second solute assigned to nodes of a particular horizontal layer *n* [ML^{-3}]. This variable does not need to be specified if *NS* < 2.
.	.	.	.
.	.	.	.
.	.	.	.
19	Real	*Conc*(*NS*,*n*)	Initial value of the concentration of the last solute assigned to nodes of a particular horizontal layer *n* [ML^{-3}].
19	Real	*Sorb*(1,*n*)	Initial value of the sorbed concentration of the first solute for type-2 sorption sites assigned to nodes of a particular horizontal layer *n* [ML^{-3}]. This variable does not need to be specified if *NS* = 0 or *lEquil* = **.true.**
19	Real	*Sorb*(2,*n*)	Initial value of the sorbed concentration of the second solute for type-2 sorption sites assigned to nodes of a particular horizontal layer *n* [ML^{-3}]. This variable does not need to be specified if *NS* < 2 or *lEquil* = **.true.**
.	.	.	.
.	.	.	.
.	.	.	.
19	Real	*Sorb*(*NS*,*n*)	Initial value of the sorbed concentration of the last solute for type-2 sorption sites assigned to nodes of a particular horizontal layer *n* [ML^{-3}].

Table A.1. (continued)

Record	Type	Variable	Description
			In general, record 19 information is required for each horizontal layer n, starting with $n=1$ and continuing sequentially until $n=NLinZ$. Record 19 information for certain horizontal layers may be skipped if several conditions are satisfied (see beginning of this section).

Table A.2. Input file 'GENER2.IN' for the first example.

```
*** INPUT FILE 'GENER2.IN' ************************************************
AxisymmetricFlow                                  (Type of flow being analyzed)
  f
Angle  Aniz1  Aniz2                                    (Anisotropy Information)
  0.     1.     1.
NS     lEquil      (number of solutes and equilibrium or nonequilibrium)
0        f
NCol   NLin       (number of nodes in horizontal and vertical direction)
  2     56
x(1)   z(NLin)                      (x, z-coordinate of left bottom node)
  0      0
*** SPACE INCREMENTS ******************************************************
dx-array                                          (number of items is NCol-1)
  1
dz-array                                          (number of items is NLin-1)
  4*.25  2*.5  39*1  10*2
*** LINE ATTRIBUTES *******************************************************
LineNumber  Code  hInit    Q  MatNum Beta  Axz  Bxz  Dxz  Temp
  1          1     .75    0.   1     0.    1.   1.   1.   0.
  2          0    -150    0.   1     0.    1.   1.   1.   0.
  55         0    -150    0.   1     0.    1.   1.   1.   0.
  56        -2    -150    0.   1     0.    1.   1.   1.   0.
*** END OF FILE 'GENER2.IN' ************************************************
```

Table A.3. Input file 'GENER2.IN' for the second example.

```
*** INPUT FILE 'GENER2.IN' ********************************************
AxisymetricFlow                                  (Type of flow being analyzed)
  f
Angle  Aniz1  Aniz2                                (Anisotropy Information)
  0.     1.     1.
NS     lEquil      (number of solutes and equilibrium or nonequilibrium)
0        f
NCol   NLin       (number of nodes in horizontal and vertical direction)
  2     33
x(1)   z(NLin)                     (x, z-coordinate of left bottom node)
  0      0
*** SPACE INCREMENTS **************************************************
dx-array                                         (number of items is NCol-1)
  1
dz-array                                         (number of items is NLin-1)
  2*1 2*2 4 4*5 19*10 5 3 2*1
*** LINE ATTRIBUTES ***************************************************
LineNumber  Code  hInit    Q  MatNum Beta  Axz  Bxz  Dxz  Temp
  1          -4    -55.    0.   1     0.    1.   1.   1.   0.
  2           0    -54.    0.   1     0.    1.   1.   1.   0.
  3           0    -53.    0.   1     1.    1.   1.   1.   0.
 10           0    -25.    0.   1     1.    1.   1.   1.   0.
 11           0    -15.    0.   1     0.    1.   1.   1.   0.
 12           0     -5.    0.   2     0.    1.   1.   1.   0.
 32           0    174.    0.   2     0.    1.   1.   1.   0.
 33          -3    175.    0.   2     0.    1.   1.   1.   0.
*** END OF FILE 'GENER2.IN' *******************************************
```

Table A.4. Input file 'GENER2.IN' for the third example.

```
*** INPUT FILE 'GENER2.IN' ********************************************
AxisymetricFlow                                  (Type of flow being analyzed)
  f
Angle  Aniz1  Aniz2                                (Anisotropy Information)
  0.     1.     1.
NS     lEquil      (number of solutes and equilibrium or nonequilibrium)
1        t
NCol   NLin       (number of nodes in horizontal and vertical direction)
 15     21
x(1)   z(NLin)                    (x, z-coordinate of left bottom node)
  0     -200
*** SPACE INCREMENTS ***************************************************
dx-array                                         (number of items is NCol-1)
  4*10 5 2 4 2*5 7 8 10 15 20
dz-array                                         (number of items is NLin-1)
  12*5 4*10 4*25
*** LINE ATTRIBUTES ****************************************************
LineNumber  Code  hInit    Q  MatNum Beta  Axz  Bxz  Dxz  Temp  Conc
  1          1      0.    0.   1     0.    1.   1.   1.   0.    0.
  2          0      0.    0.   1     0.    1.   1.   1.   0.    0.
 20          0      0.    0.   1     0.    1.   1.   1.   0.    0.
 21          2      0.    0.   1     0.    1.   1.   1.   0.    0.
*** END OF FILE 'GENER2.IN' ********************************************
```

Table A.5. Input file 'GENER2.IN' for the forth example.

```
*** INPUT FILE 'GENER2.IN' ********************************************
AxisymetricFlow                                  (Type of flow being analyzed)
  f
Angle  Aniz1  Aniz2                                (Anisotropy Information)
  0.     1.     1.
NS     lEquil      (number of solutes and equilibrium or nonequilibrium)
3        t
NCol   NLin       (number of nodes in horizontal and vertical direction)
 2     201
x(1)   z(NLin)                    (x, z-coordinate of left bottom node)
  0     -200
*** SPACE INCREMENTS **************************************************
dx-array                                         (number of items is NCol-1)
 1
dz-array                                         (number of items is NLin-1)
 200*1
*** LINE ATTRIBUTES ***************************************************
LineN Code hInit  Q    MatNum  Beta  Axz  Bxz  Dxz Temp Conc1 Conc2 Conc3
  1    1    0.0   0.    1     0.     1.   1.   1.  0.    0.    0.    0.
  2    0    0.0   0.    1     0.     1.   1.   1.  0.    0.    0.    0.
200    0    0.0   0.    1     0.     1.   1.   1.  0.    0.    0.    0.
201    2    0.0   0.    1     0.     1.   1.   1.  0.    0.    0.    0.
*** END OF FILE 'GENER2.IN' *******************************************
```

Table A.6. Input file 'GENER2.IN' for the fifth example.

```
*** INPUT FILE 'GENER2.IN' ********************************************
AxisymetricFlow                                  (Type of flow being analyzed)
  f
Angle  Aniz1  Aniz2                                (Anisotropy Information)
  0.     1.     1.
NS     lEquil      (number of solutes and equilibrium or nonequilibrium)
1        t
NCol   NLin       (number of nodes in horizontal and vertical direction)
 2      44
x(1)   z(NLin)                    (x, z-coordinate of left bottom node)
  0     -10.75
*** SPACE INCREMENTS ***************************************************
dx-array                                         (number of items is NCol-1)
 1
dz-array                                         (number of items is NLin-1)
 43*.25
*** LINE ATTRIBUTES ****************************************************
LineN Code  hInit    Q   MatNum  Beta  Axz  Bxz  Dxz  Temp Conc
  1    1     0.0    0.    1     0.    1.   1.   1.   0.    0.
  2    0     0.0    0.    1     0.    1.   1.   1.   0.    0.
 43    0     0.0    0.    1     0.    1.   1.   1.   0.    0.
 44    2     0.0    0.    1     0.    1.   1.   1.   0.    0.
*** END OF FILE 'GENER2.IN' ********************************************
```

Table A.7. Input file 'GENER2.IN' for the sixth example.

```
*** INPUT FILE 'GENER2.IN' ************************************************
AxisymetricFlow                                  (Type of flow being analyzed)
  f
Angle  Aniz1  Aniz2                                 (Anisotropy Information)
  0.     1.     1.
NS     lEquil      (number of solutes and equilibrium or nonequilibrium)
1        f
NCol   NLin       (number of nodes in horizontal and vertical direction)
 2      16
x(1)   z(NLin)                     (x, z-coordinate of left bottom node)
  0     -30.
*** SPACE INCREMENTS *****************************************************
dx-array                                         (number of items is NCol-1)
 1
dz-array                                         (number of items is NLin-1)
 15*2
*** LINE ATTRIBUTES ******************************************************
LineN Code  hInit    Q   MatNum  Beta  Axz  Bxz  Dxz  Temp Conc  Sorb
  1    1     0.0    0.    1     0.    1.   1.   1.   0.   0.   0.
  2    0     0.0    0.    1     0.    1.   1.   1.   0.   0.   0.
 15    0     0.0    0.    1     0.    1.   1.   1.   0.   0.   0.
 16    2     0.0    0.    1     0.    1.   1.   1.   0.   0.   0.
*** END OF FILE 'GENER2.IN' ***********************************************
```

Table A.8. Input file 'GENER2.IN' for the seventh example.

```
*** INPUT FILE 'GENER2.IN' ************************************************
AxisymetricFlow                                  (Type of flow being analyzed)
  t
Angle  Aniz1  Aniz2                                (Anisotropy Information)
  0.     1.     1.
NS     lEquil      (number of solutes and equilibrium or nonequilibrium)
3        t
NCol   NLin       (number of nodes in horizontal and vertical direction)
 20     19
x(1)   z(NLin)                    (x, z-coordinate of left bottom node)
  0     100
*** SPACE INCREMENTS ***************************************************
dx-array                                         (number of items is NCol-1)
  5 5 4 3 2 2 2 3 4 5 6 7 8 9 10 11 12 13 14
dz-array                                         (number of items is NLin-1)
  3*2 4 4*5 10*10
*** LINE ATTRIBUTES ****************************************************
LineN Code  hInit   Q  MatNum Beta Axz  Bxz  Dxz  Temp Conc1 Conc2 Conc3
  1   -6   -147.4  0.   1     0.   1.   1.   1.   20.  0.0   0.0   0.0
  2    0   -145.5  0.   1     0.   1.   1.   1.   20.  0.0   0.0   0.0
  3    0   -143.4  0.   1     0.   1.   1.   1.   20.  0.0   0.0   0.0
  4    0   -141.0  0.   1     0.   1.   1.   1.   20.  0.0   0.0   0.0
  5    0   -135.6  0.   1     0.   1.   1.   1.   20.  0.0   0.0   0.0
  6    0   -127.7  0.   1     0.   1.   1.   1.   20.  0.0   0.0   0.0
  7    0   -119.0  0.   1     0.   1.   1.   1.   20.  0.0   0.0   0.0
  8    0   -109.9  0.   1     0.   1.   1.   1.   20.  0.0   0.0   0.0
  9    0   -100.5  0.   1     0.   1.   1.   1.   20.  0.0   0.0   0.0
 10    0    -82.8  0.   2     0.   1.   1.   1.   20.  0.0   0.0   0.0
 11    0    -71.0  0.   2     0.   1.   1.   1.   20.  0.0   0.0   0.0
 12    0    -60.3  0.   2     0.   1.   1.   1.   20.  0.0   0.0   0.0
 13    0    -49.8  0.   2     0.   1.   1.   1.   20.  0.0   0.0   0.0
 14    0    -39.6  0.   2     0.   1.   1.   1.   20.  0.0   0.0   0.0
 15    0    -29.5  0.   2     0.   1.   1.   1.   20.  0.0   0.0   0.0
 16    0    -19.4  0.   2     0.   1.   1.   1.   20.  0.0   0.0   0.0
 17    0     -9.4  0.   2     0.   1.   1.   1.   20.  0.0   0.0   0.0
 18    0      0.6  0.   2     0.   1.   1.   1.   20.  0.0   0.0   0.0
 19    0     10.2  0.   2     0.   1.   1.   1.   20.  0.0   0.0   0.0
*** END OF FILE 'GENER2.IN' ********************************************
```